

*LoFTIS*



TECHNICAL REPORT H-76-3

## B. EVERETT JORDAN LAKE WATER-QUALITY STUDY

by

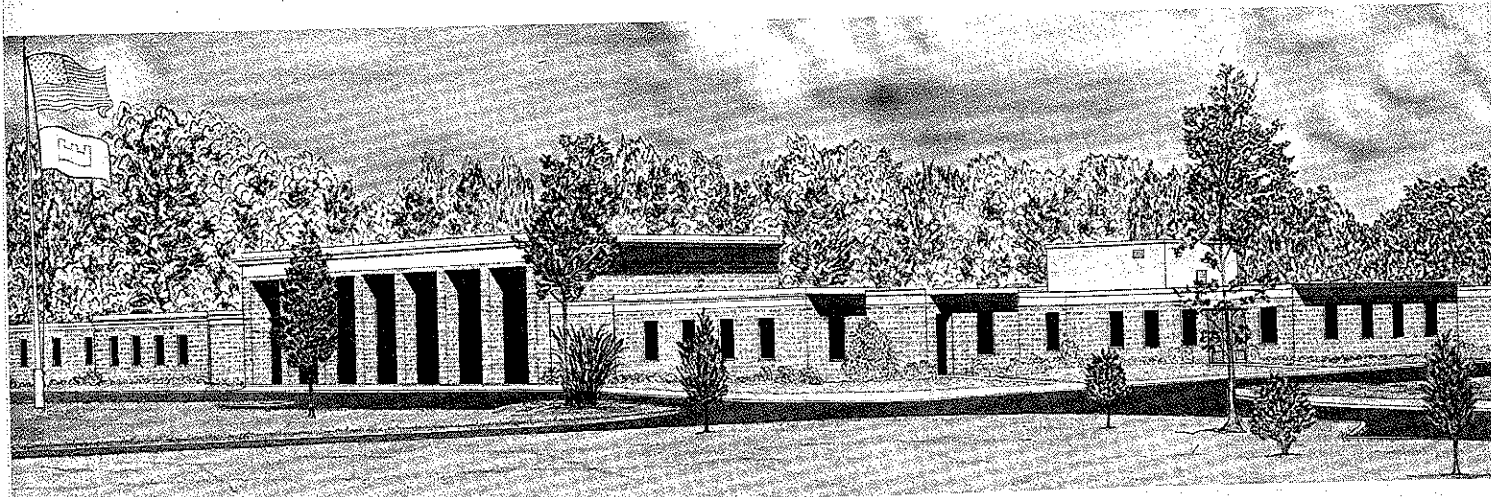
Bruce Loftis, Peter E. Saunders, John L. Grace, Jr.

Hydraulics Laboratory  
U. S. Army Engineer Waterways Experiment Station  
P. O. Box 631, Vicksburg, Miss. 39180

February 1976

Final Report

Approved For Public Release; Distribution Unlimited



Prepared for U. S. Army Engineer District, Wilmington  
Wilmington, North Carolina 28401

Unclassified

---

SECURITY CLASSIFICATION OF THIS PAGE (When Data Entered)

**DD FORM 1 JAN 73 1473 EDITION OF 1 NOV 65 IS OBSOLETE**

Unclassified SECURITY CLASSIFICATION OF THIS PAGE (When Data Entered)

Unclassified

SECURITY CLASSIFICATION OF THIS PAGE(When Data Entered)

20. ABSTRACT (Continued).

essentially divide the New Hope arm of the lake into three pools. The lower pool is influenced primarily by the Haw River, and the upper pool is influenced only by the New Hope River. The results of the numerical simulations indicate that the multilevel outlet works can be operated such that downstream temperature and D.O. objectives can be satisfied.

Unclassified

SECURITY CLASSIFICATION OF THIS PAGE(When Data Entered)

## PREFACE

The physical and mathematical model studies of B. Everett Jordan Lake reported herein were authorized by the Office, Chief of Engineers, U. S. Army, on 26 March 1975 at the request of the U. S. Army Engineer District, Wilmington.

The investigation was conducted during the period March-August 1975 in the Hydraulics Laboratory of the U. S. Army Engineer Waterways Experiment Station (WES), under the direction of Mr. H. B. Simmons, Chief of the Hydraulics Laboratory (HL), and Mr. J. L. Grace, Jr., Chief of the Structures Division, and under the supervision of Mr. J. P. Bohan, Chief of the Spillways and Channels Branch, and Mr. F. A. Herrmann, Assistant Chief of HL. The study was conducted by Messrs. B. Loftis and P. E. Saunders, with assistance from Messrs. C. H. Tate, Jr., and S. T. Maynard. This report was prepared by Messrs. Loftis, Saunders, and Grace, with assistance from Mr. D. G. Fontane.

During the course of this study, Ms. C. E. Correale of the Wilmington District visited WES to discuss the program of numerical simulations, observe tests of the physical hydraulic model, and aid in preparation of input data for the mathematical model.

Director of WES during this study was COL G. H. Hilt, CE. Technical Director was Mr. F. R. Brown.

## CONTENTS

	<u>Page</u>
PREFACE . . . . .	1
CONVERSION FACTORS, U. S. CUSTOMARY TO METRIC (SI) UNITS OF MEASUREMENT . . . . .	4
PART I: INTRODUCTION . . . . .	5
Purpose and Scope of Study . . . . .	5
Project Description . . . . .	6
PART II: MATHEMATICAL MODEL DESCRIPTION . . . . .	8
Fundamental Assumptions . . . . .	8
Surface Heat Exchange . . . . .	10
Inflow . . . . .	11
Internal Dispersion . . . . .	12
Outflow . . . . .	12
Lake Regulation . . . . .	13
Oxygen . . . . .	13
PART III: DEVELOPMENT AND ACQUISITION OF DATA . . . . .	18
Study Years . . . . .	18
Data Requirements . . . . .	18
PART IV: INITIAL SIMULATIONS . . . . .	25
Model Calibration . . . . .	25
Numerical Representation of Outlet Structure . . . . .	26
PART V: THE PHYSICAL MODEL . . . . .	28
Purpose . . . . .	28
Description . . . . .	28
Scale Relations . . . . .	29
Test Results . . . . .	30
PART VI: NUMERICAL MODIFICATIONS . . . . .	34
Objective Temperature . . . . .	35
Minimum Release Temperature . . . . .	35
Maximum Release Temperature . . . . .	35
PART VII: REAERATION . . . . .	37
PART VIII: DISCUSSION . . . . .	39
REFERENCES . . . . .	41
TABLE 1	
PLATES 1-13	
APPENDIX A: SIMULATIONS OF B. EVERETT JORDAN LAKE ABOVE SR 1008 . . . . .	A1
Purpose . . . . .	A1

## CONTENTS

	<u>Page</u>
Description . . . . .	A1
Input Data . . . . .	A1
D. O. Saturation Depth Sensitivity Analysis . . . . .	A2
Discussion . . . . .	A3
PLATE A1	
APPENDIX B: RESULTS OF INITIAL SIMULATIONS . . . . .	B1
PLATES B1-B8	
APPENDIX C: NOTATION . . . . .	C1

CONVERSION FACTORS, U. S. CUSTOMARY TO METRIC (SI)  
UNITS OF MEASUREMENT

U. S. customary units of measurement used in this report can be converted to metric (SI) units as follows:

<u>Multiply</u>	<u>By</u>	<u>To Obtain</u>
feet	0.3048	metres
miles (U. S. statute)	1.609	kilometres
square feet	0.092903	square metres
square miles	2.58999	square kilometres
acres	2.471	hectares
acre-feet	1233.482	cubic metres
cubic feet per second	0.02832	cubic metres per second
BTU	1055.056	joules
Fahrenheit degrees	5/9	Celsius degrees or Kelvins*

---

\* To obtain Celsius (C) temperature readings from Fahrenheit (F) readings, use the following formula:  $C = (5/9)(F - 32)$ . To obtain Kelvin (K) readings, use:  $K = (5/9)(F - 32) + 273.15$ .

B. EVERETT JORDAN LAKE WATER-QUALITY STUDY

Hydraulic and Mathematical Model Investigation

PART I: INTRODUCTION

Purpose and Scope of Study

1. This study was conducted to investigate the structure of temperature and dissolved oxygen (D.O.) within B. Everett Jordan Lake, and to determine an operational plan that would best satisfy downstream water-quality objectives. The study required (a) investigation and description of the large-scale hydrodynamic phenomena in the impoundment, (b) description of the temperature and D.O. profiles of the impoundment, (c) description of temperature and D.O. content of releases from the multilevel intake structure, and (d) estimation of reaeration expected as the release flow passes through the intake structure and the stilling basin.

2. A physical hydrodynamic model and a numerical simulation model were used in the study. The physical model provided information relative to the response of the prototype lake for various flow rates and stratification conditions. The numerical model provided the capability for assessing the effect of historical data on the lake for year-long periods.

3. The primary concern for this B. Everett Jordan Lake investigation was the D.O. content within the lake and in the downstream release. In any lake, the inflow placement, withdrawal, and internal mixing of D.O. are determined by the density structure of the lake. It is important, then, to obtain an accurate description of density, especially the effects on density of lake hydrodynamics and temperature, and then to assess the effects on the D.O. structure as the lake responds to the processes of inflow, outflow, mixing, and heat exchange.

### Project Description

4. B. Everett Jordan Lake is located at the confluence of the Haw and New Hope Rivers approximately 20 miles\* south of Chapel Hill, North Carolina, and just northeast of the town of Haywood, North Carolina (Figure 1). The damsite is in the upper part of the Cape Fear River

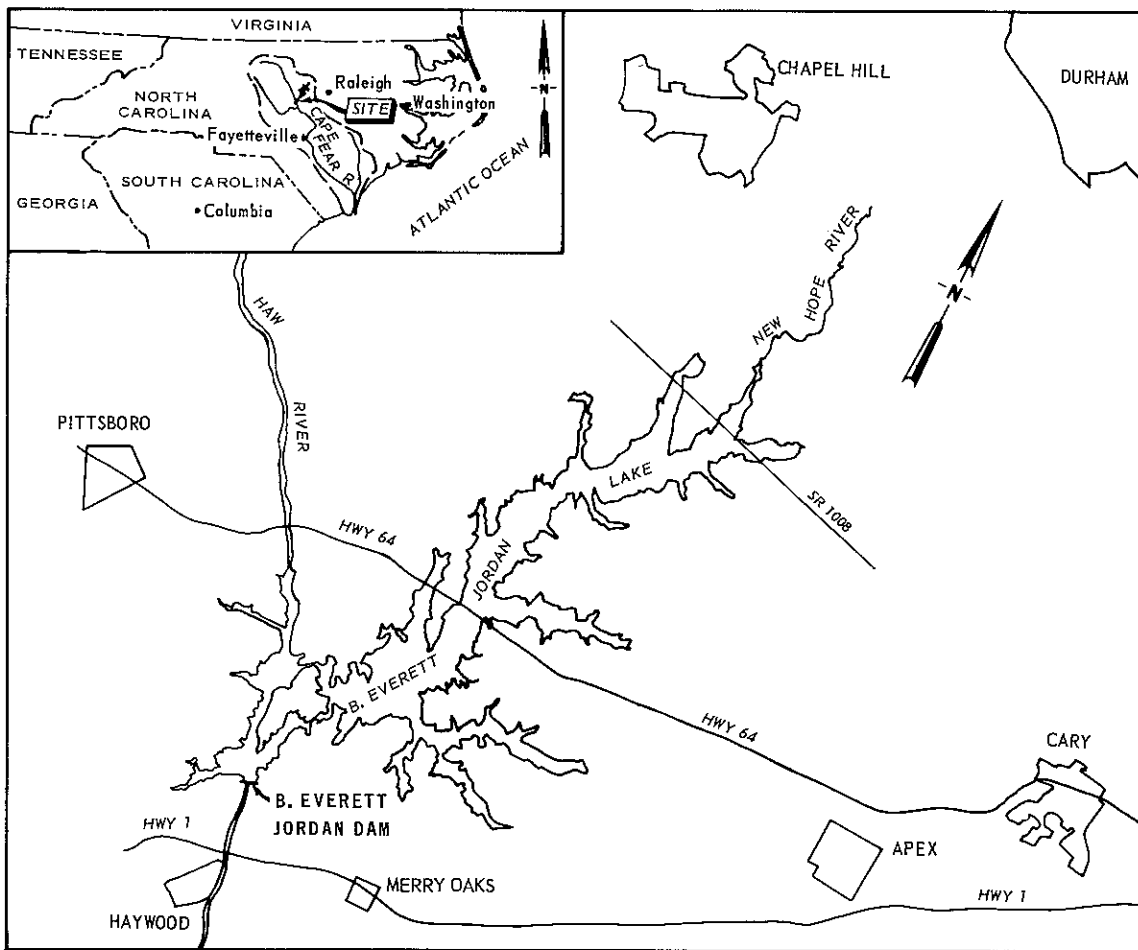


Figure 1. Vicinity map, B. Everett Jordan Lake, North Carolina

Basin, 17 $\frac{1}{4}$  miles above the mouth. The drainage area at the site is 1690 square miles and represents approximately 20 percent of the total

---

\* A table of factors for converting U. S. customary units of measurement to metric (SI) units is given on page 3.

Cape Fear River Basin. A 1300-ft-long earth-fill dam will impound water for flood control, low-flow augmentation, municipal and industrial water supply, general recreation, and fish and wildlife conservation.

5. The lake will have a flood-control storage capacity of 778,075 acre-feet and a conservation storage capacity of 183,012 acre-feet (Plate 1). The maximum pool depth at the top of conservation pool will be 58 ft. A multilevel intake tower is located at the upstream face of the dam to control the quality of low-flow releases.

6. The outlet works include an intake structure with provisions for making multilevel releases up to 2700 cfs through two wet wells. Each wet well has three 8- by 8-ft intakes with inverts at el 209, 207 205, 203, 201, and 197 ft\* and one 6- by 6-ft intake with inverts at el 188 and 181. Control of flood flows is provided by a 9.0- by 19.0-ft flood-control passage connected to each wet well with inverts at el 150.0.<sup>1</sup>

---

\* All elevations (el) cited herein are in feet referred to mean sea level.

## PART III: MATHEMATICAL MODEL DESCRIPTION

### Fundamental Assumptions

7. The downstream release characteristics and the internal structure of temperature and D.O. for B. Everett Jordan Lake were predicted using a numerical simulation model. The model (WESTEX) used in conjunction with this investigation was developed at the U. S. Army Engineer Waterways Experiment Station (WES) based upon the results of Clay and Fruh,<sup>2</sup> Edinger and Geyer,<sup>3</sup> Dake and Harleman,<sup>4</sup> and others. A simplified flow chart of the WESTEX simulation procedure is presented in Figure 2.

8. The WESTEX model provides a procedure for examining the balance of thermal energy imposed on an impoundment. This energy balance and lake hydrodynamic phenomena are used to map vertical profiles of temperature and D.O. in the time domain. The model includes computational methods for simulating heat transfer at the air-water interface, advective heat due to inflow and outflow, and the internal dispersion of thermal energy. The model is conceptually based on the division of the impoundment into discrete horizontal layers. Fundamental assumptions include the following:

- a. Isotherms are parallel to the water surface both laterally and longitudinally.
- b. The water in each discrete layer is isotropic and physically homogeneous.
- c. Internal advection and heat transfer occur only in the vertical direction.
- d. External advection (inflow and outflow) occurs as a uniform distribution within each layer.
- e. Internal dispersion (between layers) of thermal energy is accomplished by a diffusion mechanism which combines the effects of molecular diffusion, turbulent diffusion, and thermal convection.

9. The surface heat exchange, internal mixing, inflow, and outflow processes are simulated separately and their effects are introduced sequentially at daily intervals.

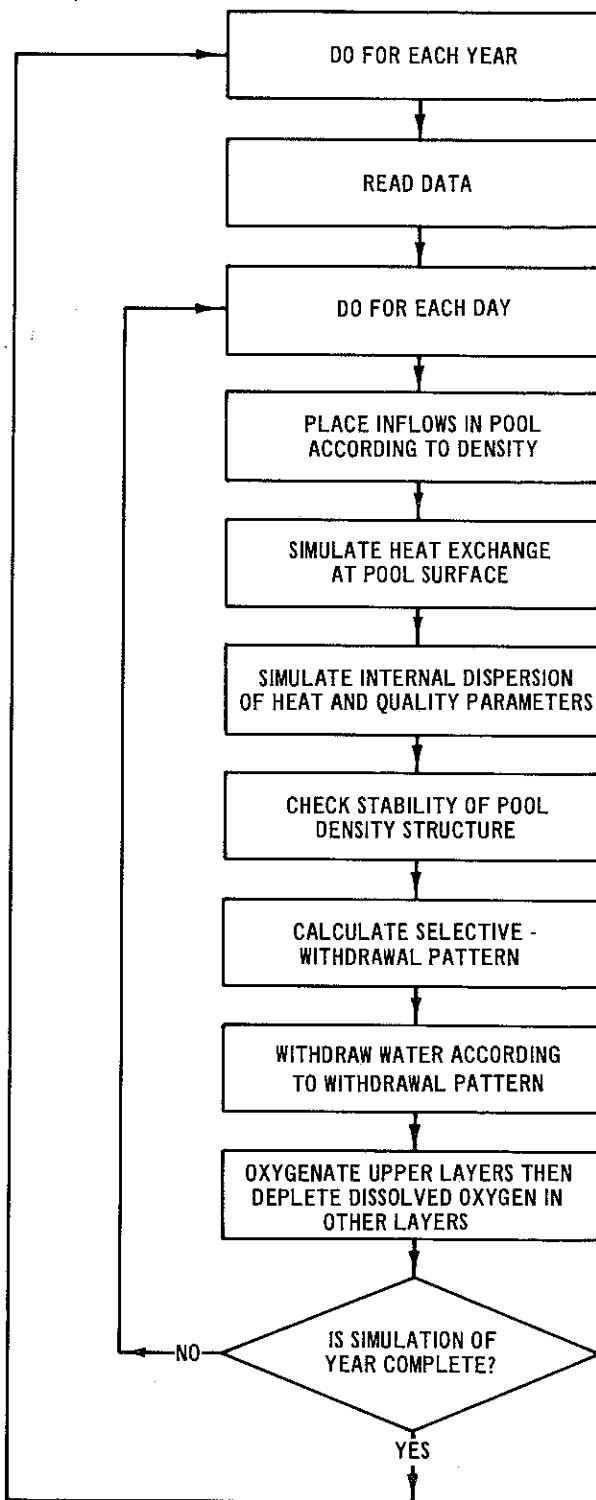


Figure 2. Simplified flow chart  
of the WESTEX simulation

### Surface Heat Exchange

10. The WESTEX model employs an approach to the evaluation of surface heat transfer developed by Edinger and Geyer.<sup>3</sup> This method formulates equilibrium temperatures and coefficients of surface heat exchange. Equilibrium temperature is defined as that temperature at which the net rate of heat exchange between the water surface and the atmosphere is zero. The coefficient of surface heat exchange is the rate at which the heat transfer process will occur. The equation describing this relationship is:

$$H = K(E - \theta) \quad (1)$$

where

$H$  = net rate of surface heat transfer,  $\text{Btu}/\text{ft}^2/\text{day}$

$K$  = coefficient of surface heat exchange,  $\text{Btu}/\text{ft}^2/\text{day}/{}^\circ\text{F}$

$E$  = equilibrium temperature,  ${}^\circ\text{F}$

$\theta$  = surface temperature,  ${}^\circ\text{F}$

The computation of equilibrium temperature and heat exchange coefficient is based solely on meteorological data as outlined by Edinger, Duttweiler, and Geyer.<sup>5</sup>

11. The net heat exchange at the surface is composed of seven heat exchange processes:

- a. Shortwave solar radiation.
- b. Reflected shortwave radiation.
- c. Long-wave atmospheric radiation.
- d. Reflected long-wave radiation.
- e. Heat transfer due to conduction.
- f. Back radiation from the water surface.
- g. Heat loss due to evaporation.

For every day of meteorological data, the seven heat exchange terms can be evaluated and the net heat exchange expressed in terms of an equilibrium temperature and an exchange coefficient.

12. All of the surface heat exchange processes, with the

exception of shortwave radiation, affect only approximately the top few feet of the lake. Shortwave radiation penetrates the water surface and increases the temperature at greater depths. Based on laboratory investigations, Dake and Harleman<sup>4</sup> have suggested an exponential decay with depth for describing the heat flux due to shortwave penetration.

13. The surface heat exchange concepts are implemented in the WESTEX model by the exponential penetration of a percentage of the incoming shortwave radiation and the placement of the effect of all other sources of surface heat exchange into the surface layer. This procedure can be expressed mathematically by the following two equations:

$$H_s = K(E - \theta) - (1 - \beta)S \quad (2)$$

$$H_i = (1 - \beta)Se^{-\lambda z_i} \quad (3)$$

where

$H_s$  = heat transfer rate into or out of surface layer, Btu/ft<sup>2</sup>/day

$\beta$  = shortwave radiation absorbed in the surface layer, percent

$S$  = total incoming shortwave radiation rate, Btu/ft<sup>2</sup>/day

$H_i$  = rate of heat absorbed in layer (i), Btu/ft<sup>2</sup>/day

$e$  = natural logarithmic base (2.7183)

$\lambda$  = heat absorption coefficient, ft<sup>-1</sup>

$z_i$  = depth below surface, ft

#### Inflow

14. The process of inflow into a lake is simulated in WESTEX by the placement of inflow quantity and quality at that layer in which the density of the lake corresponds most nearly to the density of the inflow. Research efforts and physical model studies at WES have indicated the existence of entrainment-induced density currents which flow upstream along the surface into the turbulent mixing zone caused by the inflow.

Entrainment is implemented in the model by augmenting the inflow quantity with a volume from the surface layer. Characteristics of inflow and the entrained flow are averaged, and mixed values of density, temperature, and other water-quality parameters are determined. The mixed density is used to determine placement of the total quantity and mixed quality. Simulation of the inflow process displaces upward a volume equal to the total inflow quantity. This upward displacement is reflected in the model by an increase in the water surface. A corresponding decrease in water surface occurs as a result of the outflow simulation process.

15. The volume of the entrained current is generally expressed as a percentage of the inflow quantity. Prior flume studies at WES indicated that this percentage ranges from 25 to nearly 200. The percentage is thought to be a function of slope, width, flow quantity, density of inflow, and density within the lake, but analytical relationships have not been determined. Thus, a physical model is of significant benefit in the evaluation of entrainment.

#### Internal Dispersion

16. The internal dispersion process is represented by an internal mixing scheme based on a simple diffusion analogy. Internal mixing transfers heat and other water-quality constituents between adjacent layers. The magnitude of the transfer between two layers is a percentage of the total transfer required to completely mix the two layers. This percentage is a mixing coefficient which is defined for every layer. Data input includes values of the mixing coefficient at the top and at the bottom of the lake. An exponential fit between the two extreme values is used to determine the appropriate coefficient at each layer.

#### Outflow

17. The outflow component of the model incorporates the

selective-withdrawal techniques developed at WES.<sup>6</sup> Transcendental equations defining the zero-velocity limits of the withdrawal zone are solved with a half-interval search method. With knowledge of the withdrawal limits, the velocity profile due to outflow can be determined. The flow from each layer is then the product of the velocity in the layer and the width and thickness of the layer. A flow-weighted average is applied to water-quality profiles to determine the value of the release content of each parameter for each time step.

#### Lake Regulation

18. The lake regulation algorithms have been developed to realistically simulate operation of a selective-withdrawal system. The selective-withdrawal system is assumed to be configured with an arbitrary number of selective-withdrawal intakes located in each of two wet wells with a separate floodgate. Maximum and minimum flows from each intake and from the floodgate must be specified. Also, the maximum flow for the selective-withdrawal system must be specified. The algorithms attempt to numerically withdraw water at or near the objective temperature. Withdrawal will be from either one intake level, two adjacent intake levels, and/or the flood-control intake, depending upon the objective temperature, the temperature profile, the intake capacities, and the amount of flow to be released.

#### Oxygen

19. The D.O. content of the lake at any time is a function of the sources and sinks of oxygen. The sources of D.O. in lakes include photosynthesis in the euphotic zone, atmospheric reaeration, and inflows. D.O. sinks include respiration of plants and animals, atmospheric exchange under conditions of supersaturation, inflow B.O.D., organic and inorganic benthic demand, organic and inorganic sediment in the hypolimnion, and outflows. Figure 3 is a schematic representation of these D.O. sources and sinks in a typical impoundment.

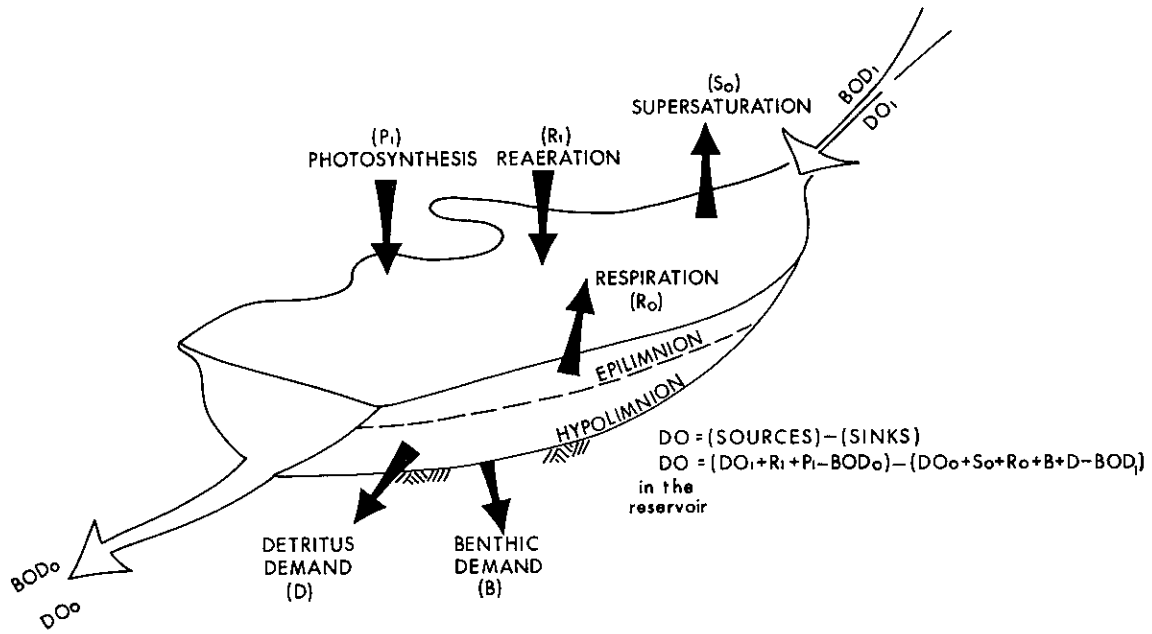


Figure 3. Schematic of dissolved oxygen sources and sinks in a typical impoundment

20. Observations of actual D.O. profiles in Hartwell and Clark Hill Reservoirs<sup>7</sup> and the work of Bella<sup>8</sup> and Carroll and Fruh<sup>9</sup> indicate that a portion of a lake below the surface can experience temperature-dependent saturated D.O. conditions. Data from Hartwell and Clark Hill Reservoirs indicate the saturation condition extends from the surface down to the depth at which a 1°C temperature difference exists from the water surface. For depths below this saturation zone, the net effect of all D.O. sources and sinks can be represented by a total D.O. depletion term.

21. The WESTEX model contains a simple method for routing D.O. and B.O.D. based on work done by Markofsky and Harleman<sup>10</sup> and Fontane and Bohan.<sup>7</sup> The D.O. and B.O.D. are routed in a manner similar to that for temperature. Processes simulated in the model that influence D.O. content of the lake are advection, surface saturation, internal dispersion, and oxygen depletion.

22. Total oxygen depletion rates for the hypolimnia of lakes are determined by plotting D.O. versus time for a particular elevation. The total depletion rate is a function of all the processes which influence

the D.O. content of the lake. Since the WESTEX model is a budget model, it inherently accounts for the hydrodynamic processes; therefore the oxygen depletion technique used in the WESTEX model represents only the oxygen processes not influenced by the hydrodynamics. The results of the modeling effort should be reasonable if the D.O. profiles predicted by the model are reasonable, and the total depletion rates are in the range of observed total depletion rate data on similar (in terms of hydrodynamics and oxygen demand) lakes.

#### Advection

23. The D.O. and B.O.D. content of the inflow and the outflow is evaluated and used to adjust profiles within the lake. The net D.O. contributed by the inflow is the inflowing D.O. content decreased by an amount which represents D.O. depletion due to travel time within the lake.

$$D.O._{net} = D.O._{in} - K_D(T)\psi L_{in} \quad (4)$$

where

$D.O._{net}$  = net D.O. content due to inflow, mg/l; applied to D.O. profile at dam

$D.O._{in}$  = D.O. content of inflowing stream, mg/l

$K_D(T)$  = temperature-dependent deoxygenation coefficient, day<sup>-1</sup>

$\psi$  = travel time, or time required for the inflow current to reach the outlet structure, days

$L_{in}$  = B.O.D. content of the inflowing stream, mg/l

The temperature-dependent deoxygenation coefficient has been approximated in the literature by several forms. The relation used for this investigation is the following:<sup>11</sup>

$$K_D(T) = K_D(20) \times 1.047^{T-20} \quad (5)$$

where

$$K_D(T) = \text{temperature-dependent deoxygenation coefficient, day}^{-1}$$

$$K_D(20) = \text{deoxygenation coefficient at } 20^\circ\text{C, day}^{-1}$$

$$T = \text{temperature, } ^\circ\text{C}$$

The travel time  $\psi$  can best be determined by field measurement or physical-model observation. In addition to advection due to inflow, advection of outflow also contributes to the total D.O. and B.O.D. budgets. As a flow volume is removed from the lake, D.O. and B.O.D. are also released.

#### Surface saturation

24. As indicated previously, observed data at Hartwell and Clark Hill Reservoirs show a saturation zone from the surface down to a  $1^\circ\text{C}$  temperature difference. Many factors influence the characteristics of this saturation zone. Considerable analysis of many lake profiles is needed for a general determination of saturation zone thickness and percentage of D.O. saturation within this zone. The values used for a given project study should be based on observed data from similar lakes.

#### Internal mixing

25. Bella<sup>8</sup> indicated the need to describe the diffusive D.O. transport from the surface layers to greater depths in the pool. He suggested this be accomplished through the use of the vertical-dispersion coefficient in the one-dimensional model. As discussed previously, the internal mixing scheme used in the WESTEX model describes the internal dispersion process; therefore the same internal mixing scheme was used to describe the diffusive D.O. transport.

#### Oxygen depletion

26. Oxygen depletion terms for D.O. and B.O.D. are applied to every layer below the saturation zone. The D.O. depletion rate is of the form

$$\Delta D = K_D(T)L \quad (6)$$

where

$$\Delta D = \text{D.O. depletion rate, mg/l/day}$$

$$K_D(T) = \text{temperature-dependent deoxygenation coefficient, day}^{-1}$$

$$L = \text{existing B.O.D., mg/l}$$

The B.O.D. depletion rate has the form

$$\Delta B = K_b L \quad (7)$$

where

$$\Delta B = \text{B.O.D. depletion rate, mg/l/day}$$

$$K_b = \text{B.O.D. decay coefficient, day}^{-1}$$

Subtracting the D.O. and B.O.D. depletions from the existing D.O. and B.O.D. in each layer yields the final D.O. and B.O.D. content in every layer for the time step.

### PART III: DEVELOPMENT AND ACQUISITION OF DATA

#### Study Years

27. For the selection of study years, statistical analyses of mean monthly streamflow and mean monthly dry bulb temperature were conducted for the period of record, 1950 through 1971. Plots of mean monthly dry bulb temperatures and mass curves of runoff are presented in Plate 2. Study years were limited to this period due to the lack of adequate meteorological data prior to 1950 and streamflow after 1971. Only records from March through October were considered in the selection of study years. Experience has shown that this is the period of greatest density stratification in a lake. Emphasis was given to the characteristics of the spring months due to the particular importance of these months in fish reproductive cycles.

28. Combinations of above average, average, and below average hydrologic and meteorologic conditions were considered in the selection of study years. The six years discussed below were selected for the B. Everett Jordan Lake water-quality investigation.

1950: Normal temperatures and below normal flow.

1952: Hot during summer months; normal temperatures otherwise. Flow higher than average during the spring; average after April.

1959: Average temperature; flow much higher than average, especially in the spring.

1960: Average temperature except for a very cold March; average flow throughout the year.

1961: Temperatures colder than normal, especially during spring and early summer; flow higher than average throughout the year.

1968: Average temperatures except for a cold May; normal flows.

#### Data Requirements

#### Meteorology

29. Meteorological data from the Raleigh Weather Station, located

20 miles northeast of the damssite, were used for this study. The required data consisted of dry bulb temperature, dew point temperature, wind speed, and cloud cover. These data were obtained from the National Climatic Center, Asheville, North Carolina. Eight observations were furnished for each day. Daily average values were computed and used to determine equilibrium temperatures, surface heat exchange coefficients, and daily average net solar radiation quantities for the 1-yr periods.

#### Hydrology

30. Mean daily flow into the lake was obtained by adjusting the Haw River and New Hope River streamflow records. The Haw River gaging station is at Bynum, North Carolina, 7 miles above the damssite. The drainage area of the Haw River at the gaging station is 1310 square miles. The New Hope River gaging station is 8 miles above the dam, near New Hill, North Carolina. Drainage area at this location is 285 square miles. The total drainage area at the dam for both rivers is 1690 square miles. Thus, streamflow records at each gaging station were increased by a factor of the drainage area ratio 1.0596. Hydraulic routings were conducted by Wilmington District (SAW) to produce daily average outflow quantities for the simulations. Inflow and outflow quantities are shown in Plate 3.

#### Stream temperature

31. Stream temperature records for each of the five study years were not available. Stream temperature measurements from the two gaging stations described previously do exist for the years 1956-1967. These data were used in the development of a regression equation for each river, relating equilibrium temperature and flow quantity to observed stream temperatures. The following regression equation was used.

$$\theta_t = \alpha + \beta_1 Q_t + \beta_2 E_t + \beta_3 E_{t-1} + \beta_4 E_{t-2} \quad (8)$$

where

$\theta$  = stream temperature, °F

t = Julian day

Q = mean daily streamflow, cfs

E = mean daily equilibrium temperature, °F

$\alpha$  and  $\beta$  are regression coefficients as follows:

	Haw River	New Hope River
$\alpha$	5.03	8.81
$\beta_1$	-7.52E-4	1.32E-4
$\beta_2$	0.358	0.240
$\beta_3$	0.121	0.464
$\beta_4$	0.406	0.359

Standard errors for the regression analyses are 4.34°F for the Haw River and 4.11°F for the New Hope River. The regression equations were used to generate lake inflow temperatures for the two inflow points during the period of record. For the simulations, however, computed inflow temperatures were used only for the years in which observed stream temperatures were not available.

#### Objective temperature

32. Although no specific temperature objective was established for the B. Everett Jordan Lake project, the numerical model used in this study requires an objective temperature for simulation purposes. The objective used was based on an average natural stream temperature variation. Temperature downstream of the confluence of the two rivers was computed as a flow-weighted average of the inflow temperatures. That is,

$$\theta = \frac{Q_1 T_1 + Q_2 T_2}{Q_1 + Q_2} \quad (9)$$

where  $\theta$  is the downstream temperature and  $Q_1$ ,  $T_1$ ,  $Q_2$ ,  $T_2$  are the flow quantity and stream temperature of the two rivers. A least squares analysis was used to fit a harmonic curve to the full record of predicted downstream temperatures. The harmonic curve represents the average natural stream temperature variation to be expected during a year. The following regression equation was used.

$$\theta_t = A \sin (Bt + C) + D \quad (10)$$

where

$\theta$  = average stream temperature, °F

t = Julian day

The coefficient B is a unit conversion from days to radians. The coefficients A, C, D were determined by solution of Equation 10 with the Newton-Raphson technique and were computed to be the following:

$$A = -19.20, \text{ } ^\circ\text{F}$$

$$B = 1.721 \times 10^{-2}, \text{ day}^{-1}$$

$$C = 1.281$$

$$D = 59.20, \text{ } ^\circ\text{F}$$

The standard error for the harmonic regression of downstream temperatures is 4.53°F. Equation 10 was used to define the downstream temperature objective.

33. Additionally, the entire record of predicted downstream temperatures was scanned for the maximum stream temperature for each day of the year. These 365 maximum temperatures were then fit by a sine curve of the general form described by Equation 10. A similar sine curve was determined for the minimum temperatures to be expected each day of the year over the period of record. The coefficients for these curves are as follows:

	Maximum	Minimum
A	-16.81	-20.27
B	$1.721 \times 10^{-2}$	$1.721 \times 10^{-2}$
C	1.175	1.175
D	68.54	50.03

These curves of maximum and minimum predicted downstream temperatures indicate the variation of natural stream temperatures from the smooth harmonic curve used as an objective temperature.

34. Inflow temperatures of both rivers for the period of record are plotted in Plate 4. For the period 1956-1966, the plots reflect observed data; otherwise, predicted stream temperatures are plotted.

The maximum and minimum stream temperatures (sine curves discussed above) are plotted also.

#### Oxygen data

35. A 5-yr record of daily inflow D.O. and 5-day B.O.D. was furnished by SAW. The record was developed by linear interpolation of data collected by Weiss<sup>12,13,14</sup> for the years 1968-1973. Future 5-day B.O.D. loadings were predicted based on waste load projections and effluent limitations.<sup>15,16</sup> The estimated changes of B.O.D. (in percent) from 1973 are shown below.

	<u>1980</u>	<u>1990</u>	<u>2010</u>
New Hope inflow	-28	-10	+11
Haw inflow	-47	-40	-18

36. For the purpose of this study, the depth of the saturation zone was determined by a 1°C temperature difference from the water-surface temperature. Average monthly values of the percentages of saturation in this zone were furnished by SAW based on John Kerr Lake data for 1956-1974. The values used in the simulations were:

Average D.O., % Saturation												
Jan	Feb	Mar	Apr	May	Jun	Jul	Aug	Sep	Oct	Nov	Dec	
87	84	87	90	94	94	93	87	74	73	76	86	

37. Descriptions of the variation of the D.O. regime of an impoundment with time have shown linear total oxygen depletion for the hypolimnia of selected impoundments.<sup>9</sup> By plotting elevation on a D.O.-versus-time coordinate system, annual total D.O. depletion rates of various layers of a particular lake can be determined. In the absence of prototype data for the B. Everett Jordan Lake, D.O. profiles observed for the period 1954-1973 in John H. Kerr Lake were examined and used to determine annual total oxygen depletion rates. For 1959, 1960, 1961, and 1968 the observed D.O. profiles are shown in Plate 5. The B. Everett Jordan Lake project is subject to meteorological phenomena and wastewater influx similar to those at nearby John H. Kerr Lake. Annual total depletion rates may change significantly from year to year, depending on stratification stability, density currents, and changes in wastewater inflow.<sup>9</sup> Annual hypolimnetic total D.O. depletion rates

for John H. Kerr Lake are listed below.

<u>Year</u>	<u>Rate</u>	<u>Year</u>	<u>Rate</u>
1954	0.056	1964	0.127
1955	0.066	1965	0.107
1956	0.073	1966	0.099
1957	0.096	1967	0.114
1958	0.081	1968	0.109
1959	0.099	1969	0.135
1960	0.059	1970	0.145
1961	0.150	1971	0.107
1962	0.088	1972	0.095
1963	0.089	1973	0.085
	Max	0.150	
	Min	0.056	
	Mean	0.099	

These observations from John H. Kerr Lake indicate a mean total oxygen depletion rate of 0.1 mg/l/day.

38. Investigation of D.O. depletion in the lower 14 ft of the hypolimnion of John H. Kerr Lake often showed a greater depletion rate than that in the upper hypolimnion. These annual total depletion rates (in mg/l/day) are listed below.

<u>Year</u>	<u>Rate</u>	<u>Year</u>	<u>Rate</u>
1954	0.041	1965	0.157
1955	0.067	1966	0.098
1956	0.076	1967	0.152
1962	0.106	1968	0.168
1963	0.096	1970	0.162
1964	0.110	1971	0.167
1957	0.089	1972	0.236
1958	0.096	1973	0.143
1959	0.114		
	Max	0.236	
	Min	0.041	
	Mean	0.122	

39. Initially, the deoxygenation coefficient  $K_D$  (20) and the B.O.D. decay coefficient  $K_b$  were assumed equal and set to a value of  $0.1 \text{ day}^{-1}$ . Although typical B.O.D. decay coefficients for streams in the vicinity of B. Everett Jordan Lake range from 0.29 to  $0.79 \text{ day}^{-1}$ ,<sup>15,16</sup> the value of  $0.1 \text{ day}^{-1}$  is referenced in the literature.<sup>11,17,18</sup> While the values of 0.1, 0.29, and  $0.79 \text{ day}^{-1}$  are perhaps reasonable in a stream environment, Markofsky and Harleman<sup>10</sup> suggest they may be inappropriate for use in a lake. A 5-day B.O.D. value will not be a good estimate of the ultimate B.O.D. in a lake, and the decay process may proceed at a slower rate than in a stream. Markofsky and Harleman suggest using a B.O.D. decay coefficient on the order of  $0.01 \text{ day}^{-1}$  and increasing the B.O.D. values to represent a larger ultimate demand. However, accurate estimation of ultimate B.O.D. in B. Everett Jordan Lake is not possible with existing data.

40. To evaluate the effect of the inflow B.O.D. loadings on the D.O. predictions, the decay coefficient for B.O.D. was set to  $0.01 \text{ day}^{-1}$ , while the deoxygenation coefficient was set at  $0.1 \text{ day}^{-1}$ . While this is not a realistic condition, i.e. that D.O. depletes faster than B.O.D., it has the mathematical effect of maintaining levels of B.O.D. in the lake longer than if the decay coefficient was  $0.1 \text{ day}^{-1}$ . This procedure is also representative of increasing the inflow B.O.D.

41. For the B. Everett Jordan Lake simulations, a temperature-dependent deoxygenation coefficient  $K_D(T)$  of  $0.1 \text{ day}^{-1}$  was used except in the lower 14 ft of the hypolimnion where a value of  $0.15 \text{ day}^{-1}$  was used. A value of  $0.01 \text{ day}^{-1}$  was used as the B.O.D. decay coefficient  $K_b$ . As indicated previously, these coefficients are only related to the oxygen processes and are independent of the hydrodynamic phenomena which also influence the oxygen budget. Simulation with these oxygen coefficients in conjunction with the hydrodynamic aspects of the oxygen budget resulted in D.O. profiles which were similar to profiles observed at John H. Kerr Lake. The computed profiles exhibited a total oxygen depletion rate of approximately  $0.1 \text{ mg/l/day}$ . Simulations with  $K_b = 0.1 \text{ day}^{-1}$  are presented in Appendix B, Plate B4.

#### PART IV: INITIAL SIMULATIONS

42. Although a physical model of a lake under investigation can provide considerable insight into the hydrodynamics and the resulting effects on water-quality parameters, initial numerical simulations of B. Everett Jordan Lake were conducted without the benefit of physical model observations. This procedure was used (a) to allow determination of proper values of coefficients to be used in subsequent simulations in order to provide the most reliable results possible from the simulations, and (b) to permit comparison of initial simulation results with results from simulations with physical model input, thereby providing some assessment of the benefit of the physical model investigation.

##### Model Calibration

43. As discussed previously, the WESTEX model requires the determination of coefficients of surface heat exchange distribution and internal mixing. For B. Everett Jordan Lake, these coefficients were determined by conducting a simulation with 1968 hydrologic and meteorologic data. Coefficients were adjusted and the simulation was repeated until the predicted temperature profiles at the B. Everett Jordan Dam corresponded in shape and range to those observed during 1968 in nearby John H. Kerr Lake (Plate 5). The following coefficients were determined from this analysis:

$$\beta = 0.6$$

$$\lambda = 0.2$$

$$\alpha_1 = 0.3$$

$$\alpha_2 = 0.3$$

where

$\beta$  = incoming shortwave radiation absorbed in the surface layer, percent

$\lambda$  = absorption coefficient

$\alpha_1$  = mixing coefficient at surface

$\alpha_2$  = mixing coefficient at bottom

44. Results of the initial simulations are presented in Appendix B in the form of profiles and release plots of temperature and D.O. for all of the study years. Comparison of Plate 5 with the results in Appendix B reveals that predicted temperature and D.O. profiles for B. Everett Jordan Lake are of the same general shape as the observed profiles at John H. Kerr Lake. This comparison indicates that an acceptable calibration was achieved. A discussion of the benefit of the physical model is presented in Appendix B.

#### Numerical Representation of Outlet Structure

45. The WESTEX model is incapable of simulating exactly the unique configuration of the intake structure existing at B. Everett Jordan Dam. The model requires that flood flows be released through a floodgate external to two wet wells containing selective-withdrawal intakes. The existing intake structure has two flood-control passages with a wet well connected to each. Flow is allowed to pass only through the selective-withdrawal intakes of a wet well or through the floodgate to which the wet well is connected. Simultaneous operation for flood control and selective withdrawal through one wet well and connected floodgate is not permitted due to the possibility of adverse flow conditions.<sup>1</sup> To adapt the existing WESTEX to the B. Everett Jordan Lake outlet works, the intake structure was represented as one wet well with the eight selective-withdrawal intakes at their respective elevations and a separate floodgate with a capacity of 15,000 cfs. Therefore, in the model, flow can be withdrawn from a single selective-withdrawal intake or from a selective-withdrawal intake and a floodgate if blending is required. But blending between two or more selective-withdrawal ports is not permissible due to model constraints. The prototype can be operated according to this representation with one exception. For

very large flood flows, the prototype must release only through the floodgates. The model will allow one selective-withdrawal intake to remain open even for large flows. The inaccuracy incurred for this condition is considered minor. Otherwise, the representation is a realistic one, and operation of the prototype with blending can exhibit better control of the releases of temperature and D.O. than indicated by the WESTEX model.

## PART V: THE PHYSICAL MODEL

### Purpose

46. The physical model study of B. Everett Jordan Lake was conducted to determine if significant hydrodynamic effects existed which should be accounted for in the numerical simulation model. It was felt significant effects might exist due to the unusual topography. The greater portion of the storage volume of the B. Everett Jordan Lake is in the New Hope River Basin and is separated from the dam by a narrow valley. Of the total inflow, 70 to 90 percent comes from the Haw River.

47. The hydrodynamic effects of particular interest were the large-scale circulation patterns, the possible mixing occurring in the region of the dam, the relative amount of lake water entrained by the inflows, and the time of travel required for the inflows to reach the intake structure. Circulation, mixing, and entrainment can significantly affect the density and quality structure within the lake. Inflow travel times are required to evaluate the D.O. and B.O.D. depletion that will occur within the lake.

### Description

48. The physical model of B. Everett Jordan Lake (Figure 4) was constructed to a distorted, linear scale ratio of 1:100 vertically and 1:2500 horizontally. The model represented a surface area of 17,000 acres and a volume of 297,000 acre-feet, from the base of the dam at el 154 to 220. The seasonal pool is to be located at el 216. The model was constructed of plastic, with a urethane foam section shaped to represent the topography in the vicinity of the dam. No attempt was made to scale topography in the New Hope arm of the model. However, the model simulated the overall slope, storage volume, and surface area of the New Hope arm of the lake. A layer of dyed saline water below a freshwater layer was used to simulate various density differences typical of expected thermal stratification conditions. Dyed saline waters were

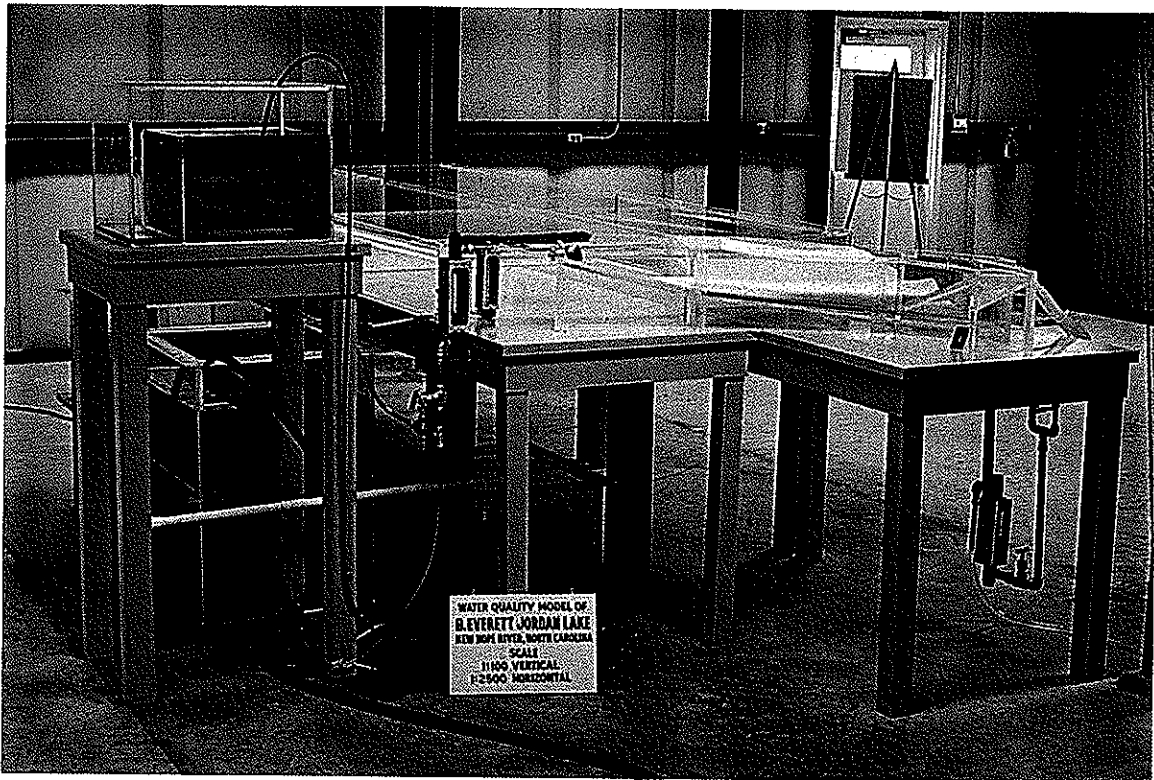


Figure 4. Overall view of physical model

used to represent the relative densities of inflows.

49. Water used in the model was supplied by pumps. Entrance and exit discharges were measured with rotameters. Water-surface elevations were measured with staff gages. Velocity profiles and flow patterns were observed through the use of dye particles.

#### Scale Relations

50. The predominant forces affecting density-stratified flows in lakes are inertia and gravity. Hydraulic similarity between a model and prototype system requires that the ratio of inertial to gravitational forces, defined as the Froude number of flow, be the same in both the model and the prototype. Therefore, the accepted equations of hydraulic similitude based on the Froudian criteria, were used to express the mathematical relations between the dimensions and hydraulic quantities

of the model and prototype. The general relations are as follows:

Dimension	Ratio	Scale Relation
Length in vertical direction	$L_r = L_y$	1:100
Length in horizontal direction	$L_r = L_x$	1:2,500
Area in vertical plane	$A_r = L_x L_y$	1:250,000
Area in horizontal plane	$A_r^2 = L_x^2$	1:6,250,000
Time	$T_r = L_x / L_y^{1/2}$	1:250
Discharge	$Q_r = L_x^3 L_y^{3/2}$	1:2,500,000

Measurements of discharge, water-surface elevations, and travel time can be transferred quantitatively from the model to the prototype by means of the scale relations above.

#### Test Results

51. The Haw River arm of B. Everett Jordan Lake is short, has a steep slope and a narrow cross section, and contributes most of the inflow to the lake. The physical model indicated that flow patterns in the vicinity of the dam are affected significantly by the Haw River inflow.

#### Low flows

52. Flow patterns with low discharges (440 cfs) were controlled by the vertical position of the Haw River inflow current relative to that of the outflow released through the intakes. Intakes releasing flow above the level of the inflow current withdrew approximately 60 percent from the Haw arm and 40 percent from the New Hope arm. The Haw inflow current, however, moved upstream on the New Hope arm without encroaching on the dam. Ports opened at the same level as the Haw inflow current withdrew almost exclusively from the Haw arm. Some of the excess inflow moved up the New Hope arm into storage after coming quite close to the dam (Figure 5). Ports lower than the inflow current withdrew mainly from the Haw arm. Some withdrawal was obtained from the New Hope arm due to the relatively strong countercurrent developed in

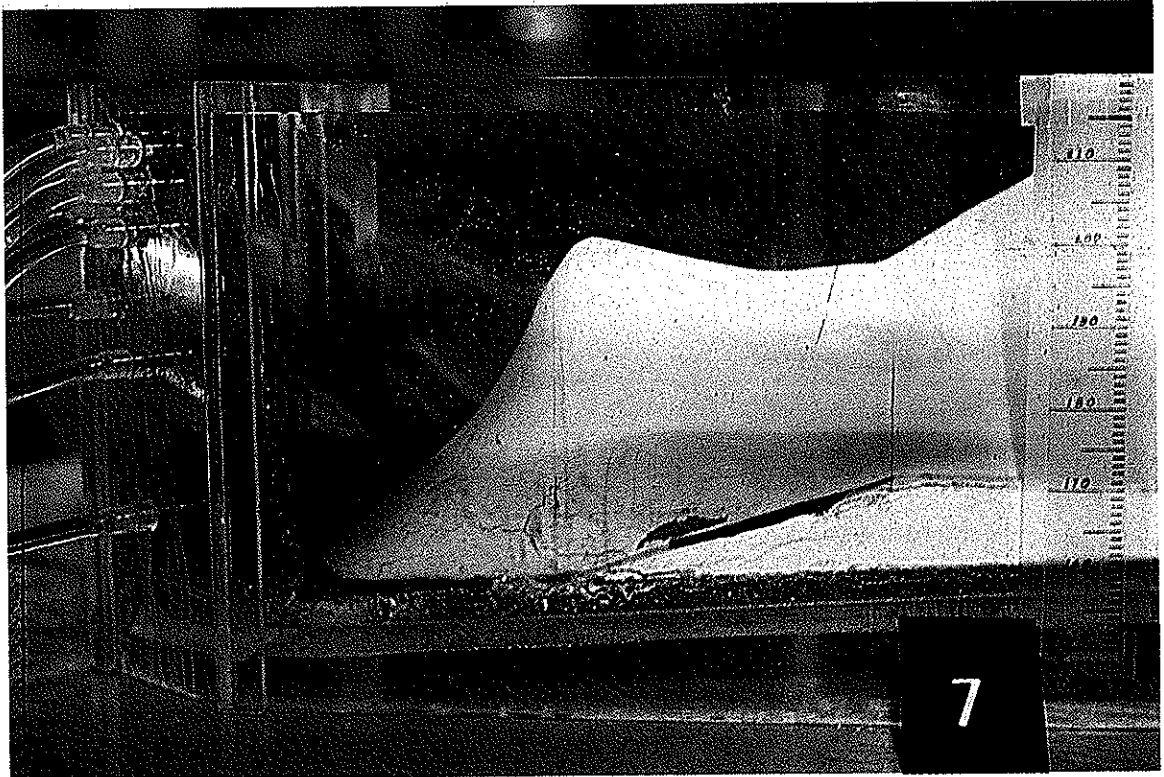


Figure 5. Flow moving upstream (blue) in the  
New Hope arm of the lake

the hypolimnion due to excess Haw inflow moving into storage.

#### Intermediate flows

53. Flow patterns at intermediate discharges were essentially identical with those observed with the lower discharges (Figure 6). Haw River inflows above 2000 cfs had sufficient turbulence and momentum to induce considerable mixing or destratification within the vicinity of the dam and created a strong upstream current within the New Hope arm as excess inflows moved into storage. The effect of flood flows was to create essentially isothermal or homogeneous conditions.

#### Entrainment

54. Visual observation of the flow along the Haw River arm of the B. Everett Jordan Lake model indicated that the Haw River inflow entrained a volume of surface water from the lake equal to the inflow quantity. This observation was interpreted as an entrainment coefficient of 1.

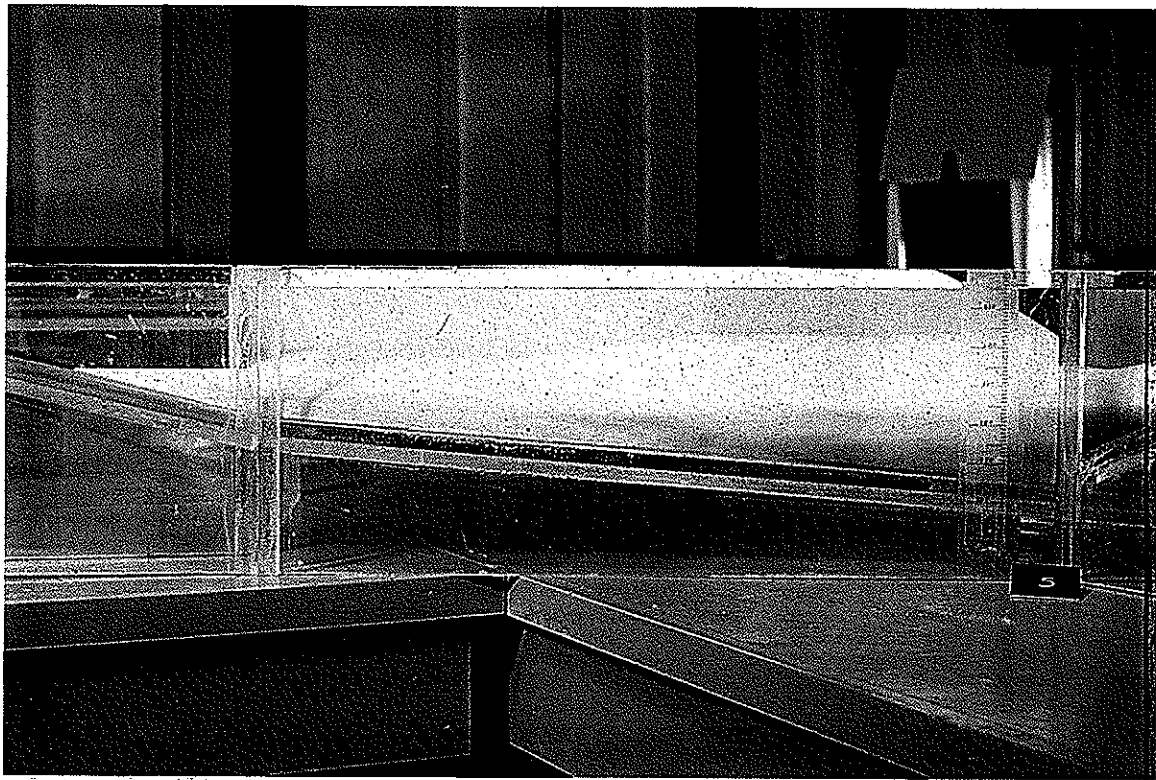


Figure 6. Inflow (blue) in the Haw arm of the lake

#### New Hope River

55. The New Hope River inflow accounts for a small percentage (10 to 30) of the total inflow, enters at a very gradual slope, and must pass through almost all the storage area of the lake. The New Hope River inflow had no observable effect on flow patterns in the vicinity of the dam.

56. Two highways (U. S. 64 and SR 1008) cross the New Hope arm of the lake. They consist of earth embankments across most of the lake, with only a narrow bridged waterway provided in each. The physical model indicated that water entering the lake from the New Hope River will be largely retained by the highway embankments (Figure 7). In fact, it appears that there will be essentially three separate pools within the lake. The first pool, upstream of the most northerly highway embankment, will consist of the New Hope River inflow. The second pool,

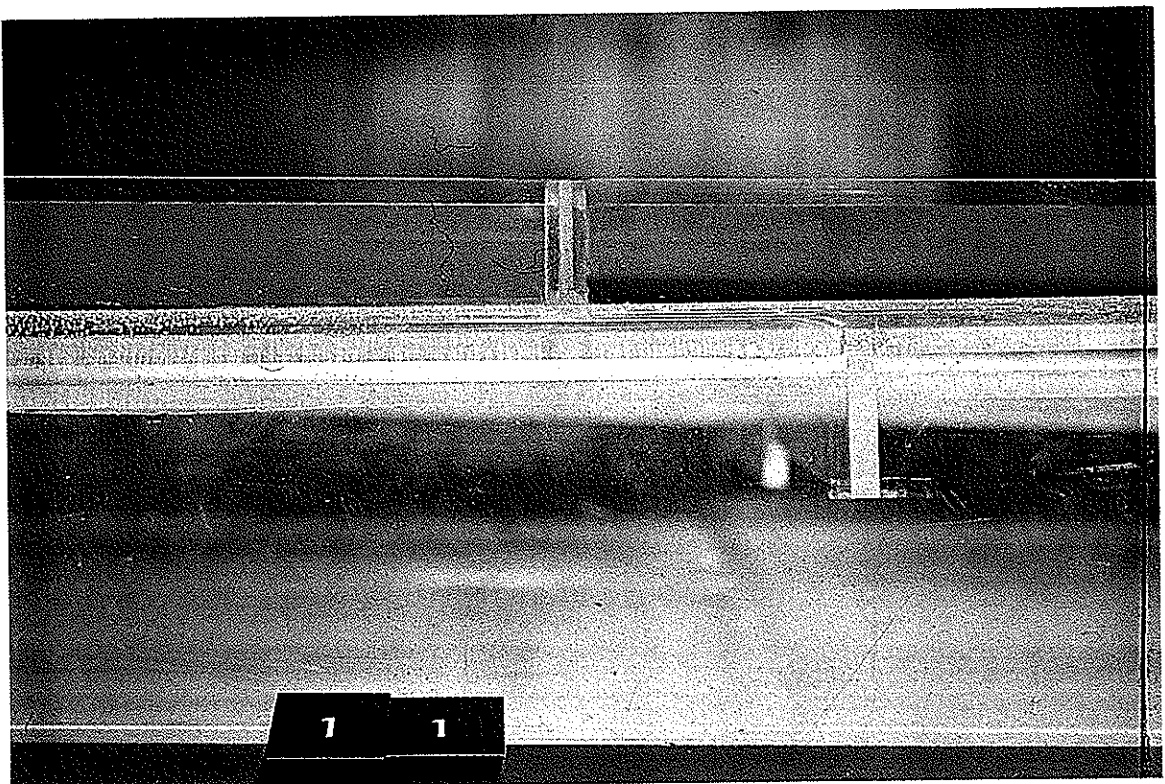


Figure 7. New Hope inflow (green) being retained by highway embankment for SR 1008

between the two highway embankments, will contain a mixture of New Hope and Haw inflows. The third pool, downstream of both highway embankments, will contain primarily Haw River inflow.

#### Travel time

57. The Haw River inflow took less than one day to travel to the outlet structure under all flow conditions. However, inflow may be stored, depending on flow conditions, and therefore travel time is not indicative of the residence time of a particular volume of water in the lake. The New Hope inflow did not reach the outlet structure in the physical model during a test duration simulating 120 days. After reaching the second pool in the simulated 60-day period, there was virtually no movement for another 60 days of operation. The model simulation was ended at this point since it appeared that the New Hope inflow would not reach the dam prior to turnover.

## PART VI: NUMERICAL MODIFICATIONS

58. Based on results of physical model tests, several modifications were made to the WESTEX model to allow a better representation of temperature and D.O. profiles in the vicinity of the B. Everett Jordan Dam. The physical model indicated no effect on the profiles at the dam by the New Hope River inflow. Also, the New Hope arm above the U. S. Highway 64 Bridge was not used for storage by Haw River inflow. The modified WESTEX model includes:

- a. Computations with available volume only in the Haw arm and in the New Hope arm up to the U. S. Highway 64 embankment.
- b. One inflow point with Haw River inflow qualities and total inflow quantity to maintain the water budget.

59. A second observation in the physical model concerns the extent of inflow mixing in the Haw arm. Inflows during and after a storm are expected to be of increased density due to a larger sediment load. The condition of storm magnitude with high inflow density was simulated in the physical model. For a flow of approximately 2000 cfs, the bottom half of the Haw River arm from the inflow point to the dam appeared well mixed; for larger flows, the amount of mixing increased. A flow of 6000 cfs appeared to completely mix the Haw River arm. This mixing condition is simulated in the WESTEX model by the placement of all flows greater than 2000 cfs in the lowest layer. This causes numerically a density instability, especially in the spring when inflow temperatures are usually warmer than temperatures in the lake. The model forces mixing until a stable density profile is achieved. This procedure reproduces numerically the observations of the physical model. For flows of 2000 cfs, about half of the profile is mixed. For flows in excess of 6000 cfs, stratification is completely destroyed, and the water-quality parameters are constant from top to bottom.

60. Several types of operation schedules were simulated. Each was run with the inflow mixing modification. The first type involved operation of the intake structure to obtain objective temperatures. Second, all flow was released through the flood-control gates to achieve

minimum release temperatures. Third, flow was passed from the highest possible intake to obtain maximum release temperatures.

#### Objective Temperature

61. For operation to meet the objective temperature, the release temperatures are well within the temperature band for all of the study years. Each study year was subject to low flows in late August. During this time of year the temperature objective requires that flow be released as low as possible. This would result in the release of low D.O. water.\* The low-flow year of 1960 is especially indicative of this phenomenon. D.O. release levels for other parts of the year are acceptable. Plate 6 shows temperature and D.O. profiles resulting from operations for achieving objective temperatures. Plate 7 shows the corresponding temperature and D.O. release plots.

#### Minimum Release Temperature

62. For operations to release flows of minimum temperature, the release temperatures remained within the band between average minimum and average maximum objective temperatures. Release D.O. is of approximately the same quality as that resulting from operations for objective temperatures. During the low-flow periods of August, the bottom of the lake became anaerobic and D.O. contents of releases drop to less than 1.0 mg/l. Resulting profiles from operations to obtain minimum release temperature are presented in Plate 8. Corresponding release plots are shown in Plate 9.

#### Maximum Release Temperature

63. The most promising operational schedule is the release of

---

\* North Carolina Water Quality Standards for dissolved oxygen in non-trout waters for Classes A-II, B, and C requires a daily average of 5.0 mg/l and a minimum of not less than 4.0 mg/l.

flow from the highest possible intake. The release temperatures are within the release temperature band (average minimum to average maximum temperatures) except for a few scattered days. D.O. contents of releases remain above 8 mg/l for all of the study years except for a few points corresponding to high-flow requirements during the summer months. Plate 10 shows the profiles resulting from this operation. The corresponding release plots are presented in Plate 11.

## PART VII: REAERATION

64. The WESTEX model predicts D.O. profiles upstream of the dam and the D.O. content of the withdrawal as it enters the intake structure. However, the predicted D.O. content of the flow entering the intake structure is not necessarily a reasonable estimate of the D.O. content of the flow released downstream. Reaeration can occur as flow discharges through the regulating gate, outlet conduit, and stilling basin. Although it is not possible to predict the amount of reaeration which will occur as flow passes through the B. Everett Jordan Lake outlet works, an attempt was made to quantify the reaeration which occurs in the release from several existing lakes.

65. Data from four existing impoundments in northern Mississippi were readily available. These observed data from Sardis, Enid, Grenada, and Arkabutla Lakes included temperature and D.O. profiles near the intake structure and measurements of temperature and D.O. immediately downstream of the stilling basin. To predict the temperature and D.O. content of the flow entering the intake structure, the WES selective-withdrawal technique<sup>6</sup> was applied to the temperature and D.O. profiles. It was assumed that the temperature of the flow entering the intake structure predicted by selective withdrawal should correspond to the downstream temperature. The WES selective-withdrawal technique requires various input data including effective width at the withdrawal control section, effective intake elevation, and type of withdrawal device (orifice or submerged weir). For some of the existing lakes, the initial data input did not yield the required temperature validation. For these lakes, minor modifications of the input data were made to achieve the desired predicted temperature. In general, the predicted temperature was within 1°C of the observed downstream temperature. With the temperature validation achieved, it was then assumed that the difference in D.O. from the predicted value at the intake to the measured value downstream was entirely a result of reaeration through the outlet works and stilling basin.

66. Plate 12 contains the results of the reaeration analysis.

The D.O. content of flow entering the intake structure is plotted as an initial percentage of saturated D.O. content versus the change in percentage of saturated D.O. content as flow passes through the outlet works and stilling basin. The saturated D.O. content was determined for each set of available from tables<sup>19</sup> as a function of the release temperature. For any of the points shown in Plate 12, the estimated downstream percent D.O. saturation is the sum of the ordinate and the abscissa. These results indicate the D.O. content of the downstream flow can be expected to be 80-90 percent of the saturation value for releases through similar outlet works.

67. The similarity of outlet works of the four Mississippi lakes to the outlet works of B. Everett Jordan Lake is illustrated in Plate 13. The results of the reaeration analysis are not included in the plots of computed release D.O. It was not felt that reaeration data from only four Mississippi impoundments were sufficient for accurate prediction of D.O. content in the downstream release from B. Everett Jordan Lake. However, Plates 12 and 13 indicate that 80-90 percent D.O. saturation will be a realistic estimate of D.O. content downstream of B. Everett Jordan Lake.

## PART VIII: DISCUSSION

68. This study was conducted to investigate the structure of temperature and D.O. within and downstream of B. Everett Jordan Lake. Initial simulations were conducted, and predicted profiles of temperature and D.O. at B. Everett Jordan Lake were compared with observed profiles at John H. Kerr Lake. Appropriate heat exchange coefficients were determined, and temperature calibration was achieved. D.O. calibration required the use of a B.O.D. decay rate which was smaller than the deoxygenation rate. Simulations with equal decay coefficients for D.O. and B.O.D. indicated that the B.O.D. in each layer depletes faster than the inflow process can replenish it. By referring to Equations 6 and 7, it can be recognized that as the B.O.D. approaches zero, the oxygen depletion must also approach zero. When the oxygen depletion becomes zero, the only oxygen sink remaining in the model is advection. The equations in the WESTEX model used to predict D.O. and B.O.D. content exhibit a form of numerical instability when equal D.O. and B.O.D. decay coefficients are used. Resulting profiles (Appendix B) consistently indicate more oxygen than profiles at John H. Kerr Lake. It is apparent that a zero oxygen depletion is not realistic in a lake. A residual oxygen demand will exist due to oxygen sinks such as respiration and detrital and benthic demand. The use of a B.O.D. decay rate smaller than the deoxygenation rate insures that a residual oxygen demand will be retained. The use of a lower B.O.D. decay coefficient combined with the hydrodynamic effects on the oxygen budget resulted in predicted D.O. profiles for B. Everett Jordan Lake which compared favorably to observed profiles at John H. Kerr Lake.

69. A physical model of B. Everett Jordan Lake was used to investigate the expected hydrodynamic response of the prototype to various flow rates and stratification conditions. The model indicated that temperature and D.O. conditions in the vicinity of the prototype dam will be controlled by the Haw River inflow. The flow patterns near the dam were observed to be dependent on the quantity of inflow, the vertical location of the inflow current, and the withdrawal location.

In most cases, the Haw River inflow current moved down the Haw River and, not impinging on the dam, up the New Hope arm through a narrow valley and into storage. The two highway embankments essentially divide the New Hope arm of the lake into three pools. The lowest pool provides storage for Haw River inflows. The upstream pool above SR 1008 is influenced only by New Hope River flow. Simulations for the upstream pool are presented in Appendix A. It was observed that flow from the New Hope River did not travel past the middle pool for any of the physical model simulations. The Haw River inflow traveled to the dam in less than a day for all conditions. However, since the inflow current moved past the dam and up the New Hope arm into storage, it was not possible to accurately estimate time of residence for the Haw River flow from the time it enters the lake until it is released through the outlet structure.

70. The simulation results for various modes of operating the multilevel intake structure to achieve a minimum, average, or maximum temperature objective indicated that release temperatures are within the band of observed natural stream temperature variation. Whether downstream D.O. objectives can be satisfied depends on the amount of reaeration obtained as release flows pass through the outlet works.

71. Although an exact estimate of the amount of reaeration to be expected through the B. Everett Jordan Lake outlet works could not be made, data on similar outlet works indicated that at least 80 percent saturation of D.O. could be expected downstream. Assuming that 80 percent saturation would occur, the minimum value of downstream release D.O. for all study years and conditions would be greater than 6 mg/l.

## REFERENCES

1. Melsheimer, E. S. and Oswalt, N. R., "Outlet Works for New Hope Reservoir, Cape Fear River Basin., N. C.; Hydraulic Model Investigation," Technical Report H-69-14, Oct 1969, U. S. Army Engineer Waterways Experiment Station.
2. Clay, H. M., Jr., and Fruh, E. G., "Selective Withdrawal at Lake Livingston; An Impoundment Water Quality Model Emphasizing Selective Withdrawal," Progress Report EHE 70-18 (CRWR 66), Nov 1970, Environmental Health Engineering Research Laboratory, University of Texas, Austin, Tex.
3. Edinger, J. E. and Geyer, J. C., "Heat Exchange in the Environment," Publication No. 65-902, Jun 1965, Edison Electric Institute, New York, N. Y.
4. Dake, J. M. K. and Harleman, D. R. F., "An Analytical and Experimental Investigation of Thermal Stratification in Lakes and Ponds," Technical Report No. 99, Sep 1966, Massachusetts Institute of Technology Hydrodynamics Laboratory, Cambridge, Mass.
5. Edinger, J. E., Duttweiler, D. W., and Geyer, J. C., "The Response of Water Temperature to Meteorological Conditions," Water Resources Research, Vol 4, No. 5, Oct 1968, pp 1137-1143.
6. Bohan, J. P. and Grace, J. L., Jr., "Selective Withdrawal from Man-Made Lakes; Hydraulic Laboratory Investigation," Technical Report H-73-4, Mar 1973, U. S. Army Engineer Waterways Experiment Station, CE, Vicksburg, Miss.
7. Fontane, D. G. and Bohan, J. P., "Richard B. Russell Lake Water Quality Investigation; Hydraulic Laboratory Investigation," Technical Report H-74-14, Dec 1974, U. S. Army Engineer Waterways Experiment Station, CE, Vicksburg, Miss.
8. Bella, D. A., "Dissolved Oxygen Variations in Stratified Lakes," Journal, Sanitary Engineering Division, American Society of Civil Engineers, Vol 96, No. SA5, Paper No. 7628, Oct 1970, pp 1129-1146.
9. Fruh, E. G. et al., "Limnological Investigations of Texas Impoundments for Water Quality Management Purposes," Final Report EHE 72-6 (CRWR 87), Feb 1972, University of Texas, Austin, Tex.
10. Markofsky, M. and Harleman, D. R. F., "A Predictive Model for Thermal Stratification and Water Quality in Reservoirs," Report No. 134, Jan 1971, Department of Civil Engineering, Massachusetts Institute of Technology, Cambridge, Mass.
11. Velz, C. J., Applied Stream Sanitation, John Wiley and Sons, Inc., 1970, New York, N. Y.
12. Weiss, C. M., "Long Term Trends in Water Quality, Lower Haw and New Hope Rivers, 1966-1973," Report No. 101, Oct 1974, Water Resources

Research Institute of the University of North Carolina, Raleigh,  
N. C.

13. Weiss, C. M., "Water Quality Characteristics of the New Hope and Lower Haw Rivers, July 1966-February 1970 with Estimates of the Probable Quality of New Hope Lake," Report No. 48, Jan 1971, Water Resources Research Institute of the University of North Carolina, Raleigh, N. C.
14. Weiss, C. M., Yocom, T. W., and Minogua, J. E., "Further Characterization of the New Hope and Lower Haw Rivers, Including Benthic Macroinvertebrate Diversity and Trace Metal Analyses," Report No. 73, Nov 1972, Water Resources Research Institute of the University of North Carolina, Raleigh, N. C.
15. Environmental Management Commission, "Water Quality Management Plan, Cape Fear River Basin, Sub Basin 05," Draft Report, Raleigh, N. C.
16. \_\_\_\_\_, "Water Quality Management Plan, Cape Fear River Basin, Sub Basin 06," Draft Report, Raleigh, N. C.
17. Linsley, Ray K. and Franzini, J. B., Water-Resources Engineering, McGraw-Hill, Inc., 1972.
18. Wastewater Engineering, Metcalf and Eddy, Inc., McGraw-Hill, Inc., 1972.
19. Fair, G. M. and Geyer, J. C., Elements of Water Supply and Waste-Water Disposal, John Wiley & Sons, Inc., 1963.

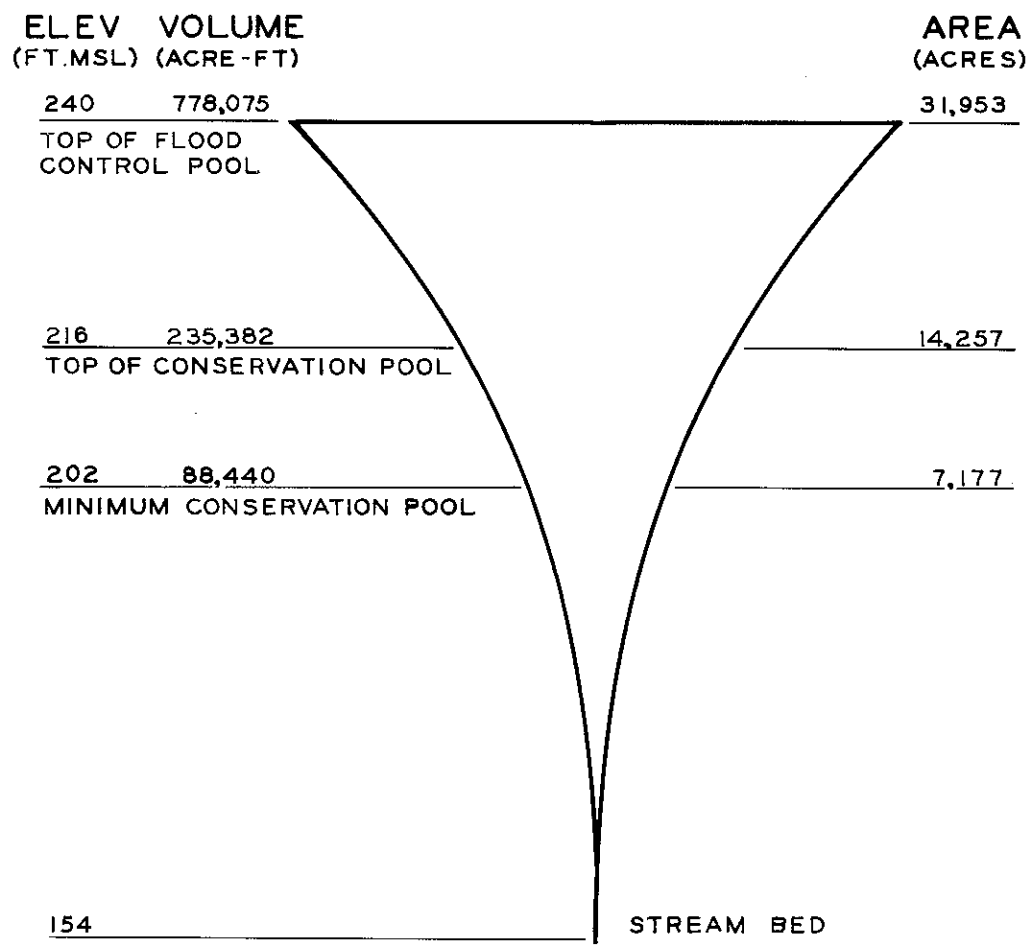
Table 1  
Reaeration Data

Discharge cfs	Initial Temp °C	Initial D.O. ppm	Final Temp °C	Final D.O. ppm	Condition
<u>Sardis</u>					
4480	20.2	8.0	20.2	9.5	Isothermal
545	10.4	9.8	12.9	8.9	Isothermal
2680	7.3	10.5	10.1	10.4	Isothermal
4200	5.9	11.3	5.9	12.7	Isothermal
2730	7.6	11.1	8.4	1.5	Isothermal
2890	9.4	10.5	9.7	12.2	Isothermal
2650	16.3	8.4	16.8	9.7	Isothermal
3180	18.4	8.1	18.4	9.4	Isothermal
344	12.1	9.8	12.1	10.5	Isothermal
1900	10.2	10.0	10.5	11.1	Isothermal
150	2.5	12.7	7.8	10.4	Isothermal
2660	4.1	12.0	4.3	13.0	Isothermal
536	9.9	10.9	10.1	10.7	Isothermal
271	19.4	6.8	19.7	7.4	Isothermal
2240	13.4	9.0	13.5	10.3	Isothermal
2510	24.2	6.3	23.5	7.0	Isothermal
4110	21.6	4.2	21.8	8.1	Stratified
2000	26.5	4.5	26.7	7.7	Stratified
4040	23.2	4.9	23.8	7.6	Stratified
4570	21.3	3.85	21.6	8.1	Stratified
4070	21.9	5.8	21.2	8.2	Stratified
3620	26.1	3.5	26.5	7.9	Stratified
3250	25.6	5.45	25.9	7.8	Stratified
3740	20.3	5.3	20.8	8.7	Stratified
3570	21.5	6.9	21.9	7.9	Stratified
3490	23.6	1.7	25.2	7.6	Stratified
4090	26.4	5.6	27.1	7.6	Stratified
1030	17.5	7.5	19.0	9.0	Stratified
2910	20.7	5.9	22.0	8.4	Stratified
2450	25.2	4.1	25.3	7.7	Stratified
<u>Enid</u>					
1140	23.0	7.0	23.0	8.4	Isothermal
662	3.7	11.7	4.0	12.8	Isothermal
312	6.2	11.0	6.2	11.9	Isothermal
133	15.8	8.3	15.5	9.1	Isothermal
1470	22.9	6.3	23.2	7.4	Isothermal

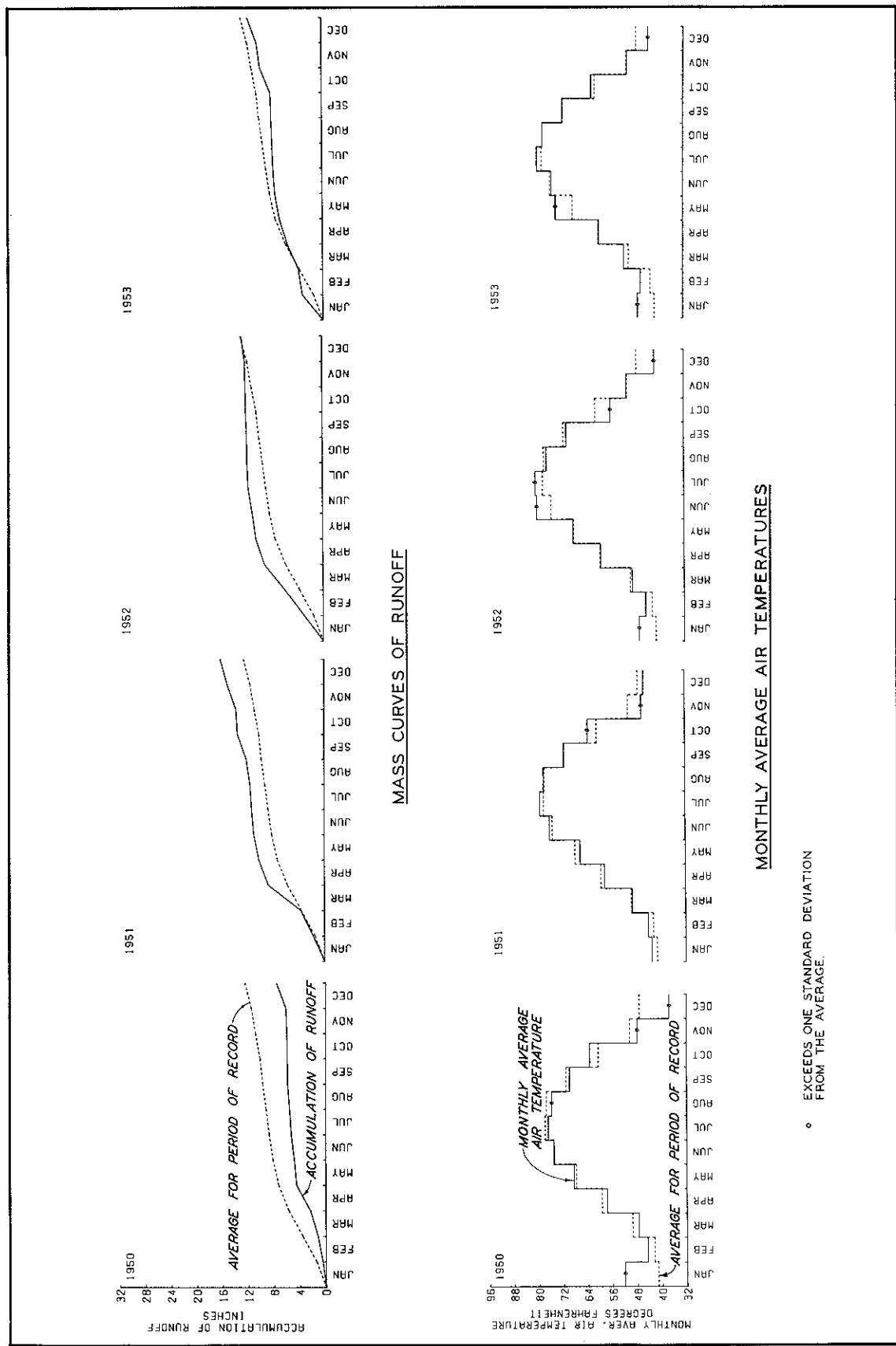
(Continued)

Table 1 (Concluded)

Discharge cfs	Initial Temp °C	Initial D.O. ppm	Final Temp °C	Final D.O. ppm	Condition
<u>Enid (Continued)</u>					
124	20.2	6.4	20.5	7.4	Isothermal
293	8.9	10.9	9.1	10.8	Isothermal
736	13.1	9.15	13.5	9.5	Isothermal
950	28.2	4.95	28.1	7.9	Stratified
684	25.0	2.1	25.7	6.8	Stratified
1370	23.2	0.9	24.1	7.9	Stratified
<u>Grenada</u>					
1050	4.2	6.7	5.3	6.7	Isothermal
900	16.6	8.8	14.9	9.8	Isothermal
2300	5.5	11.4	5.6	12.2	Isothermal
600	18.5	7.6	19.8	8.7	Isothermal
1100	10.7	9.8	11.0	10.9	Isothermal
300	24.5	6.1	25.0	7.1	Isothermal
2300	18.9	6.8	21.2	8.8	Isothermal
2650	26.2	4.6	26.3	7.6	Stratified
2400	26.0	3.1	28.2	7.7	Stratified
3400	27.4	5.5	27.9	6.8	Stratified
2600	27.4	3.5	27.6	6.9	Stratified
<u>Arkabutla</u>					
2550	3.0	10.8	2.3	13.1	Isothermal
600	10.6	10.85	11.0	11.6	Isothermal
1600	26.5	5.35	27.0	6.7	Isothermal
150	12.5	9.4	14.4	9.2	Isothermal
2250	13.6	8.95	14.2	10.2	Isothermal
1050	22.6	7.2	22.7	8.1	Isothermal
1100	27.6	1.9	28.3	6.9	Stratified
1400	26.3	3.65	26.3	6.9	Stratified
600	27.3	5.95	27.1	6.6	Stratified
600	26.4	5.35	27.1	6.6	Stratified
600	29.0	3.4	28.7	7.1	Stratified



**MORPHOLOGIC DATA**  
**B. EVERETT JORDAN LAKE**



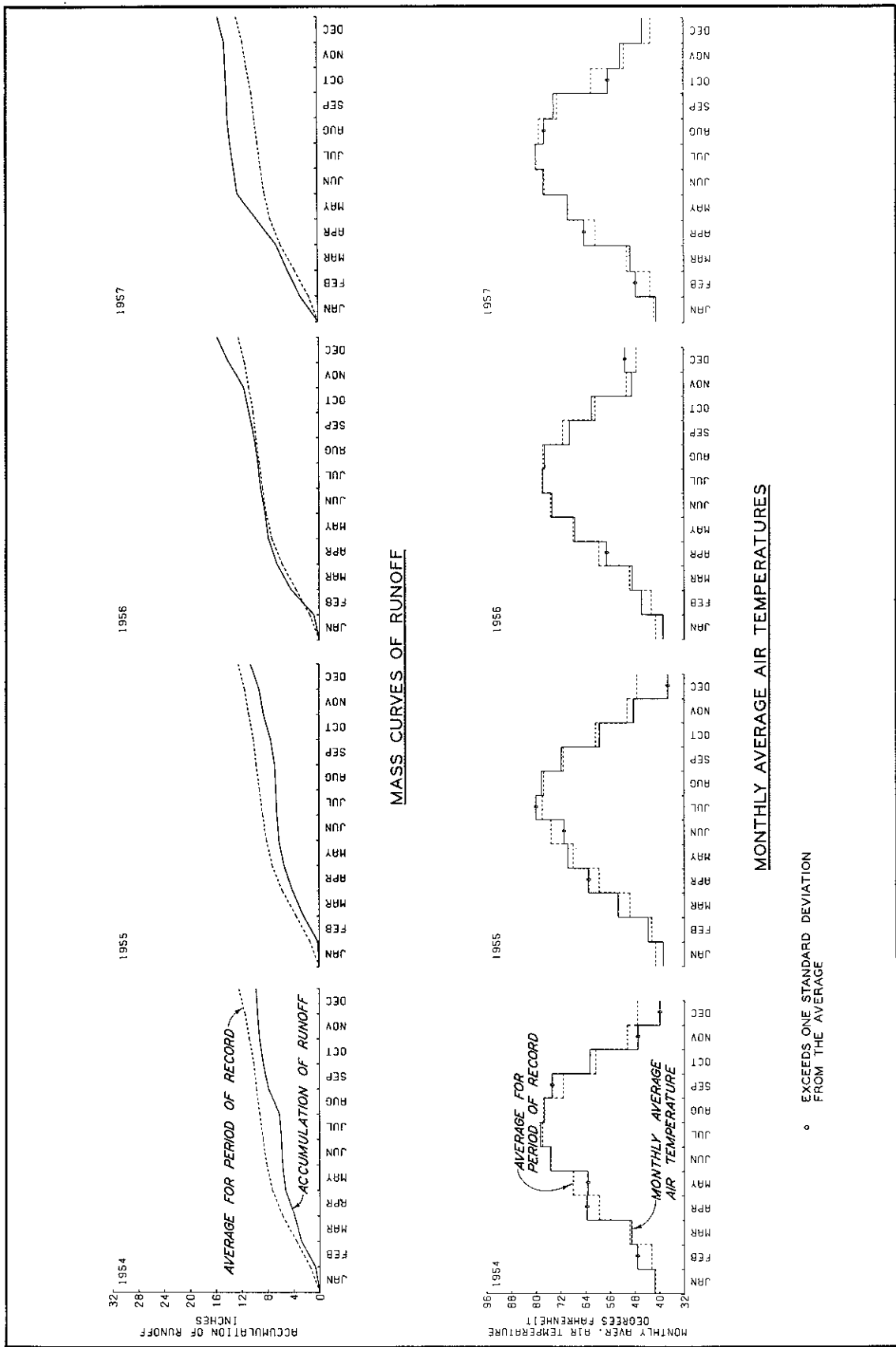


PLATE 2 (SHEET 2 OF 6)

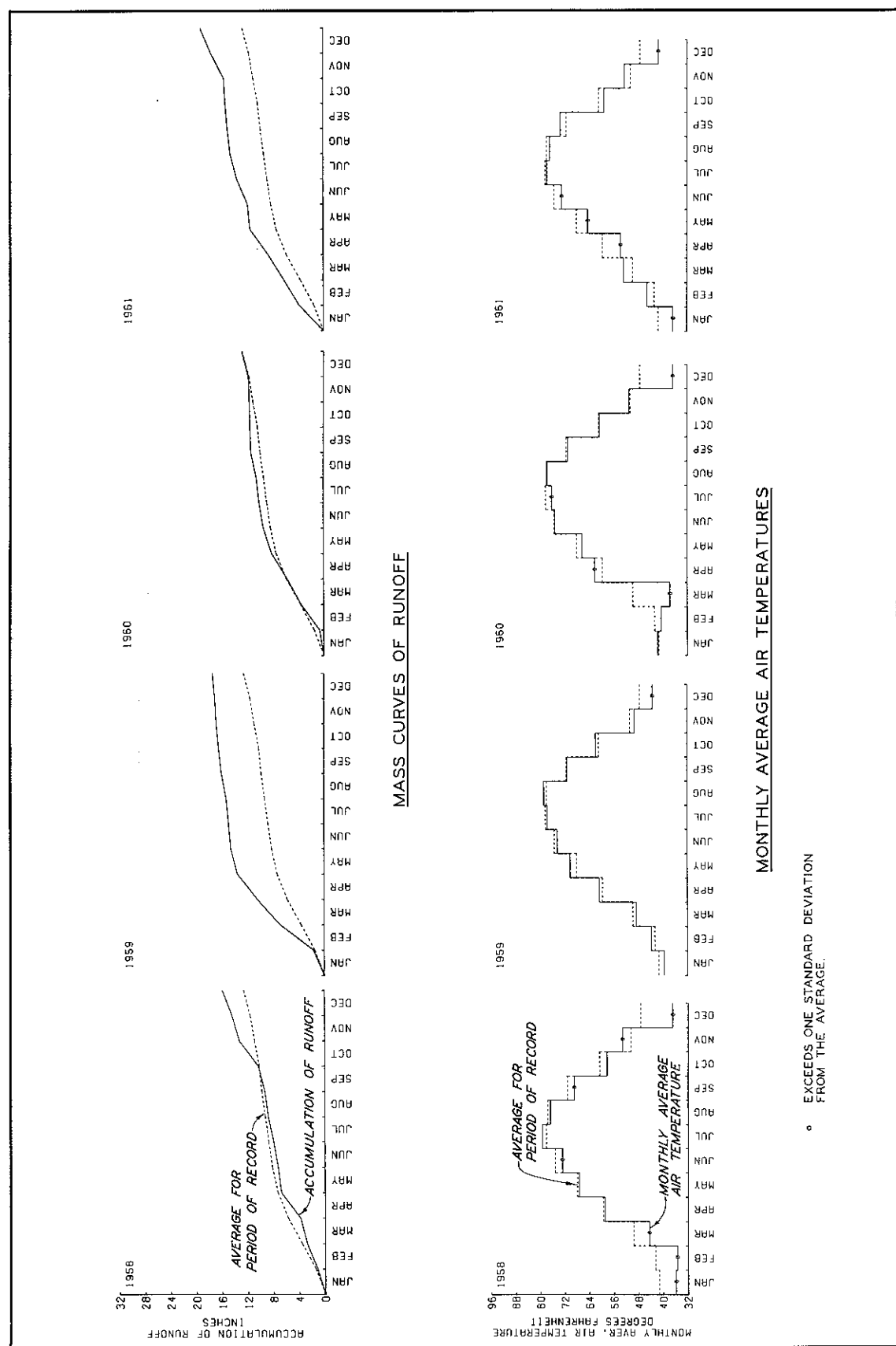
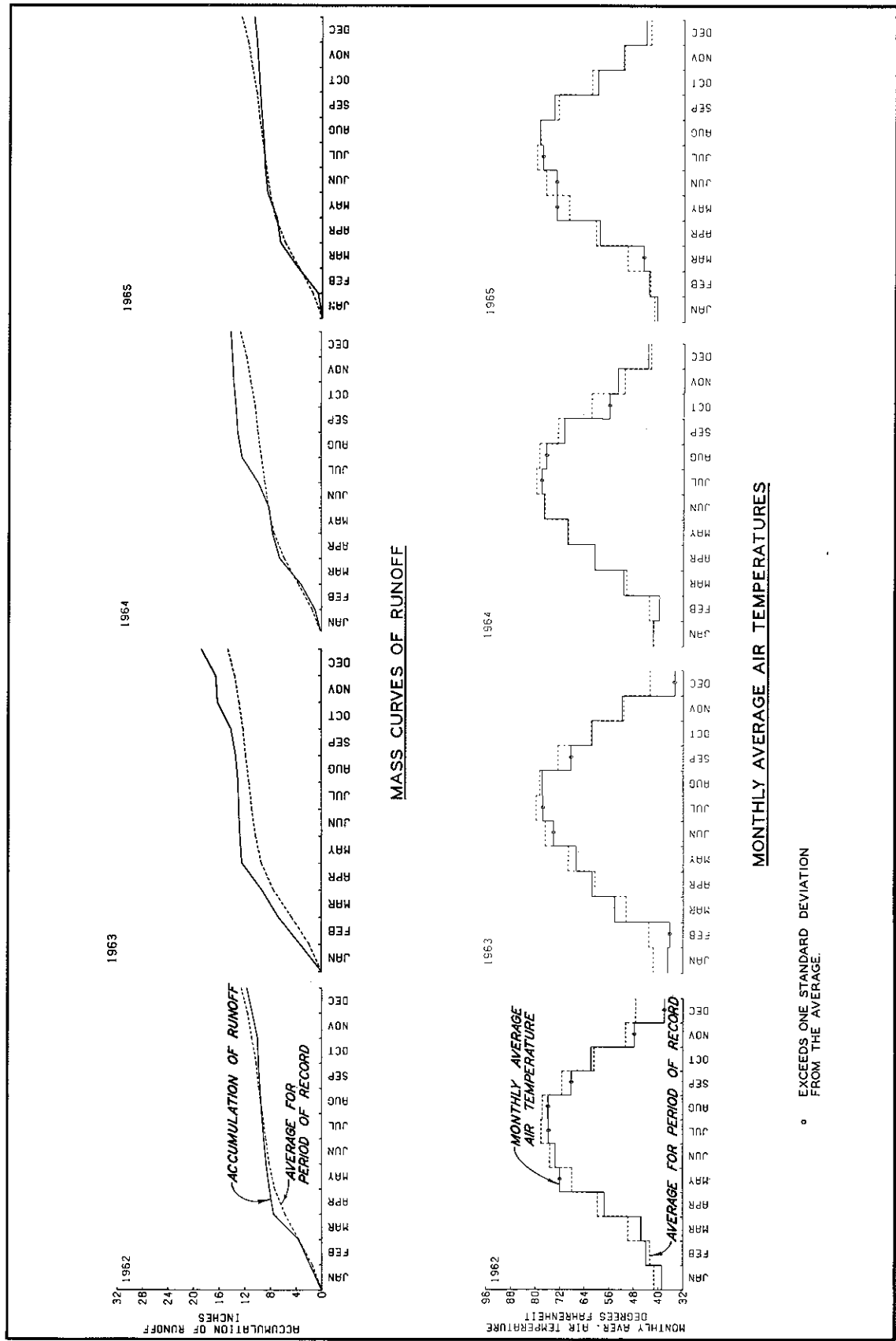


PLATE 2 (SHEET 3 OF 6)



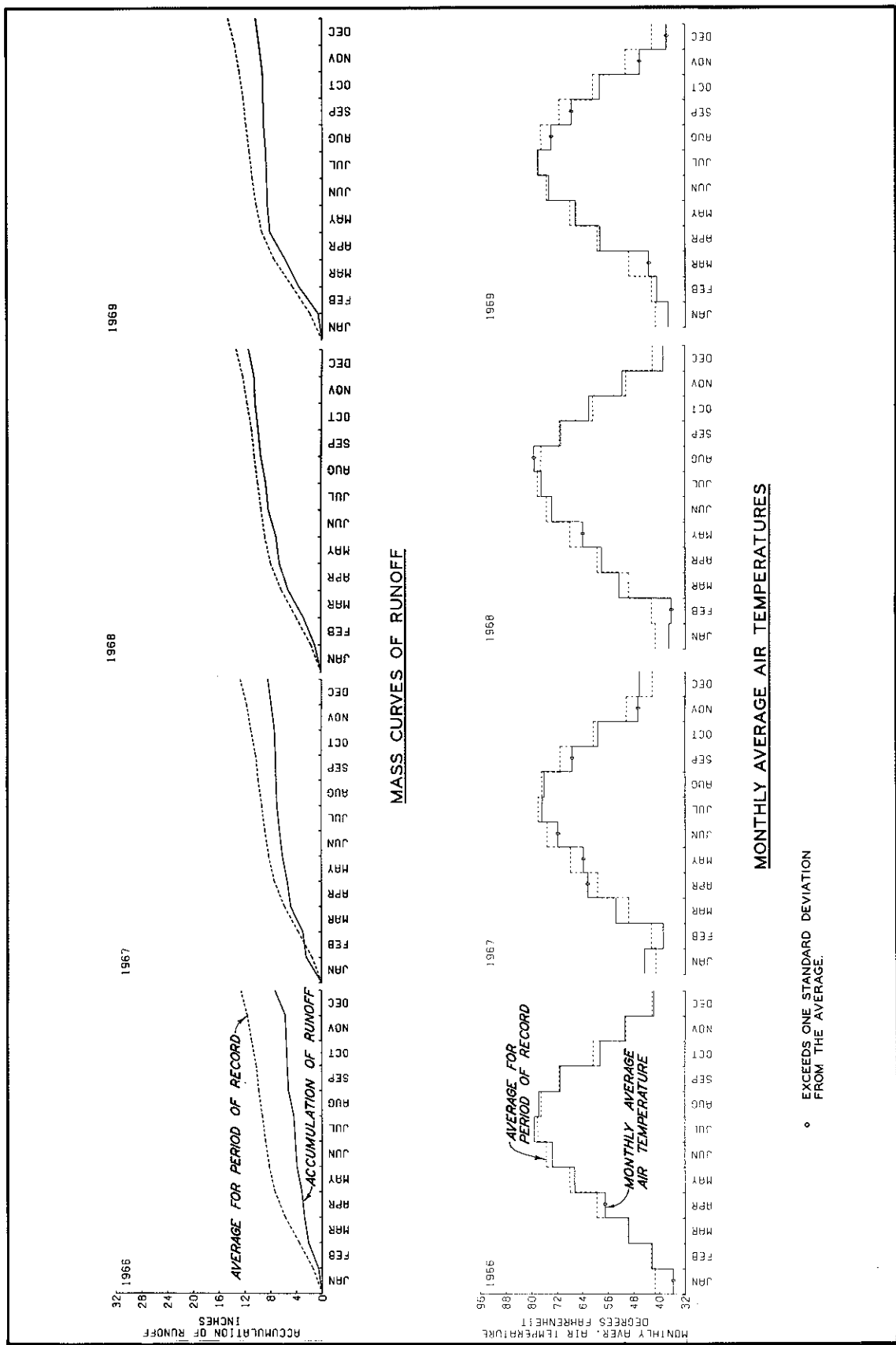
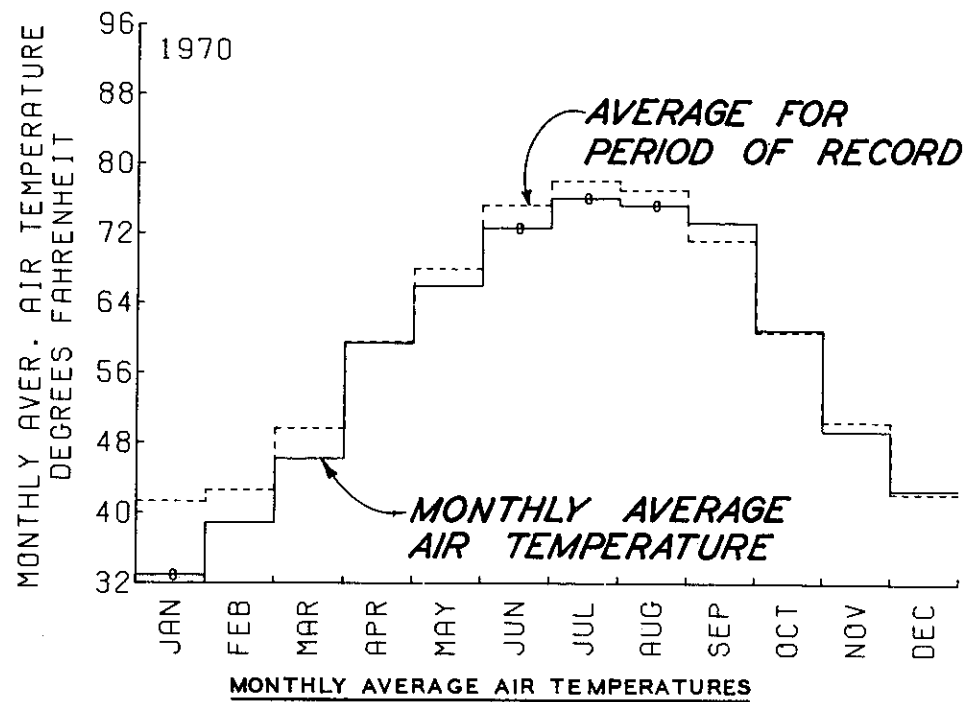
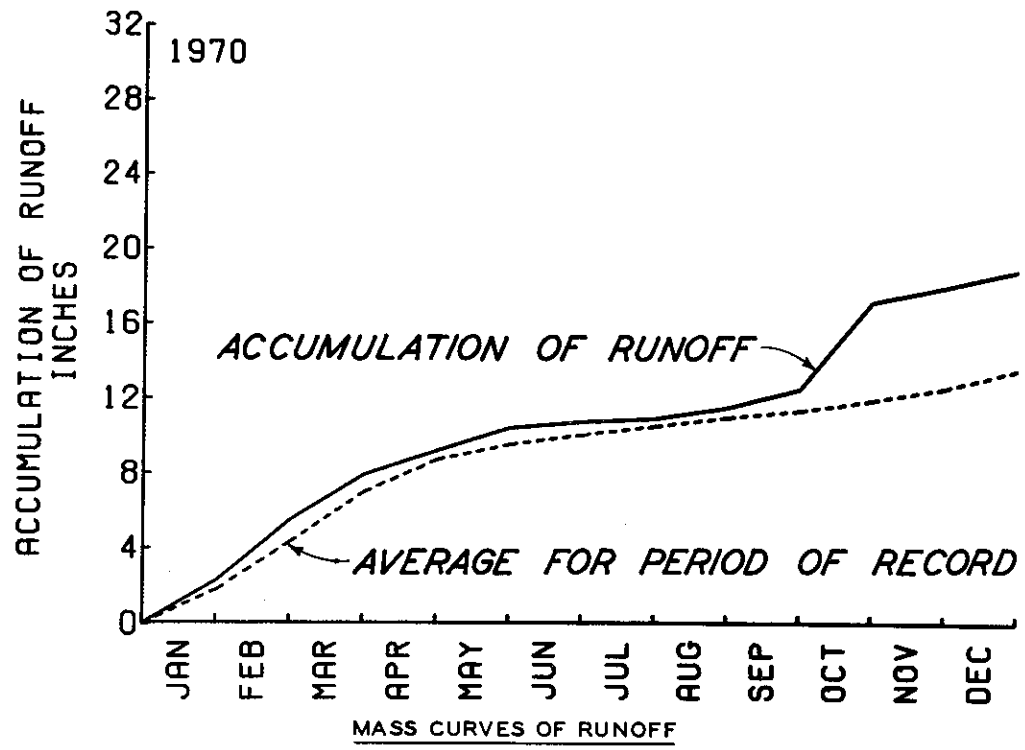
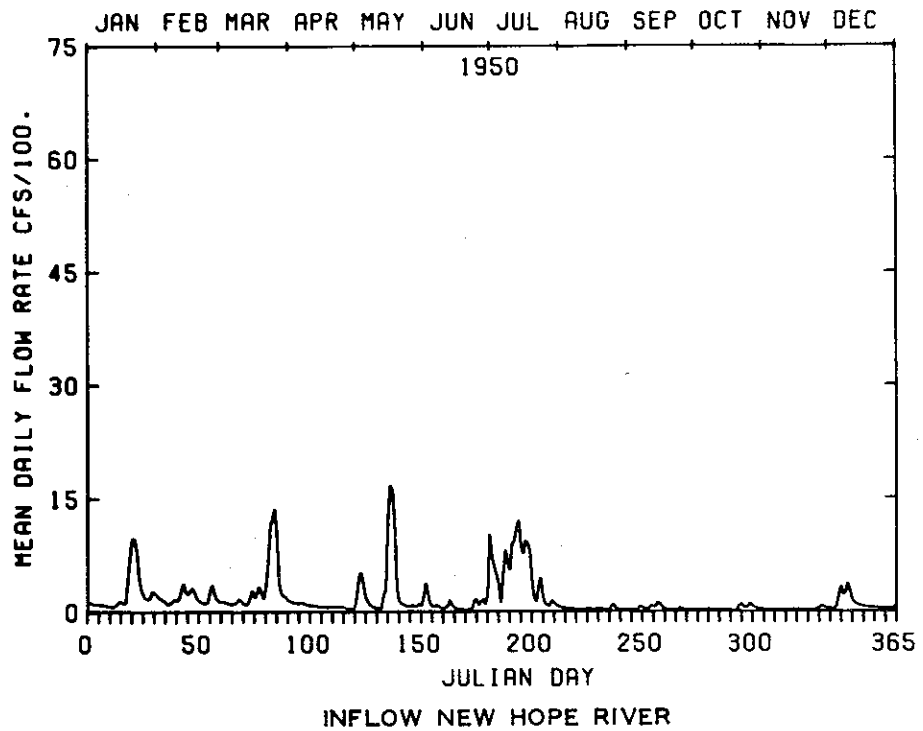
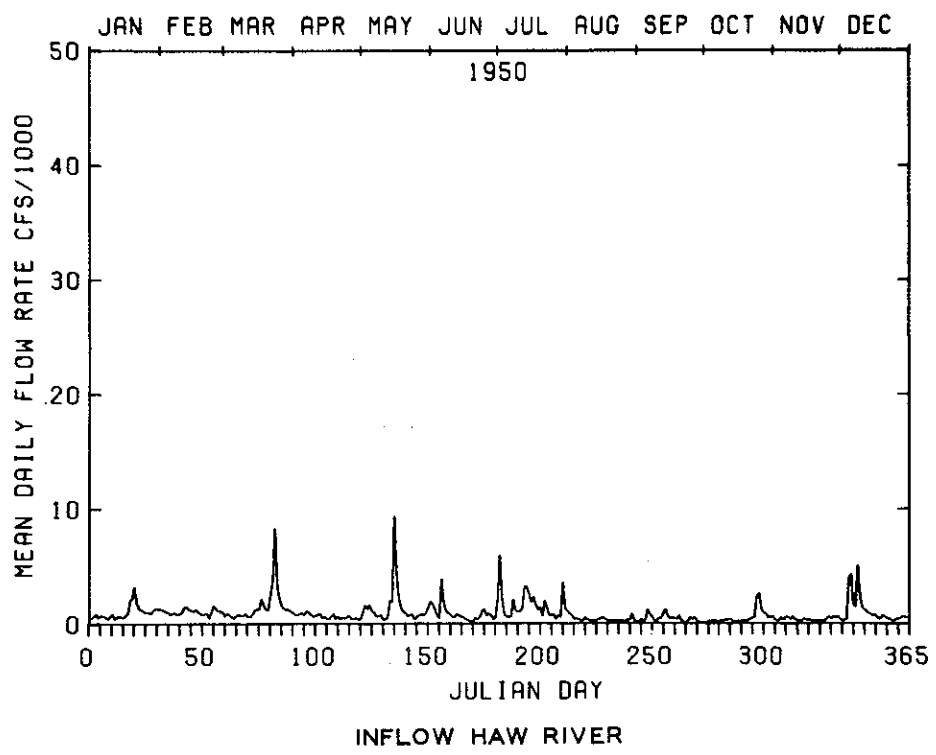


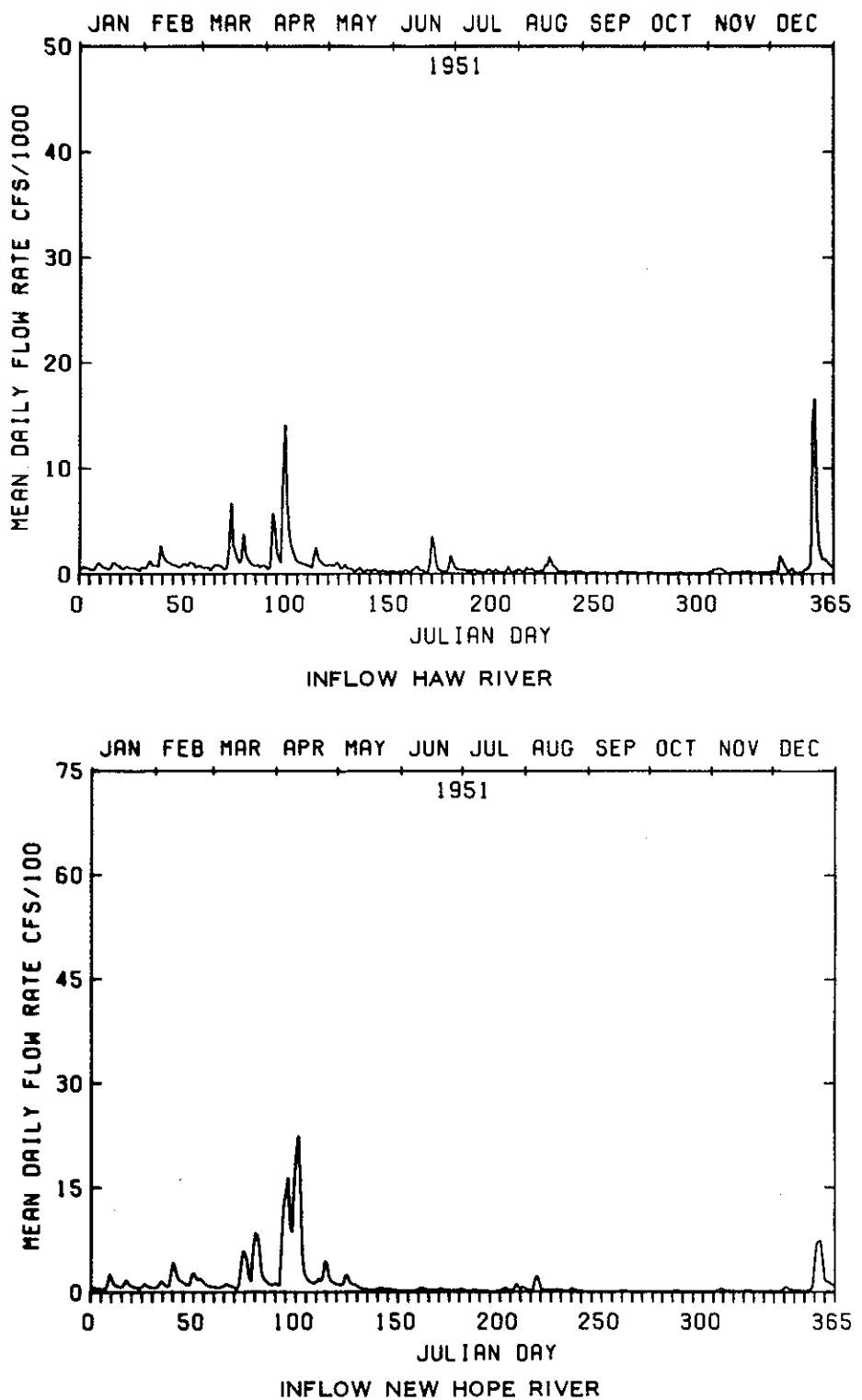
PLATE 2 (SHEET 5 OF 6)



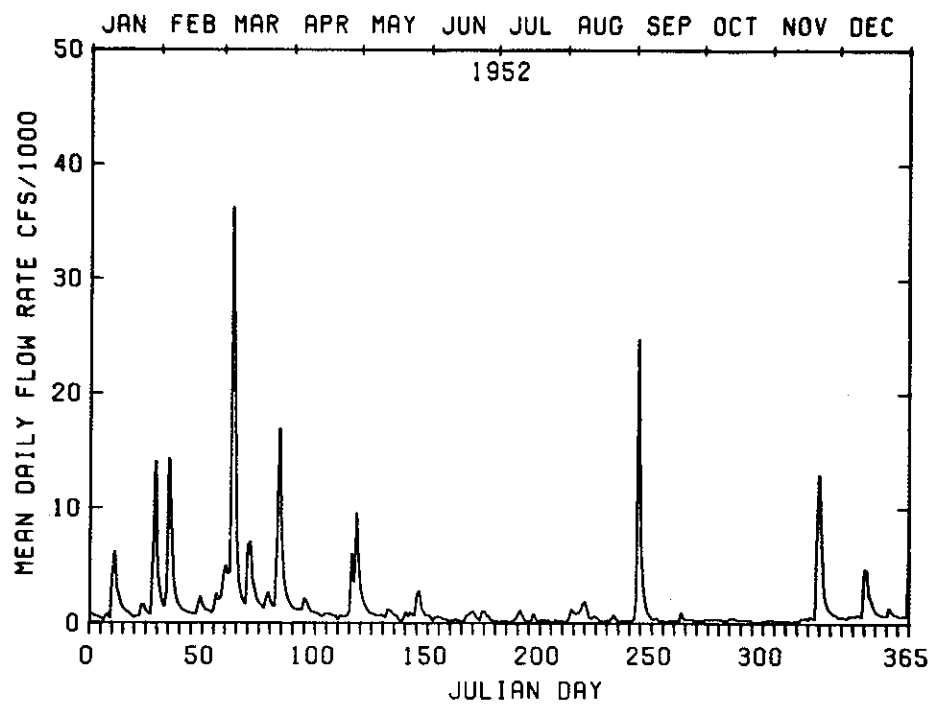
○ EXCEEDS ONE STANDARD DEVIATION FROM THE AVERAGE.



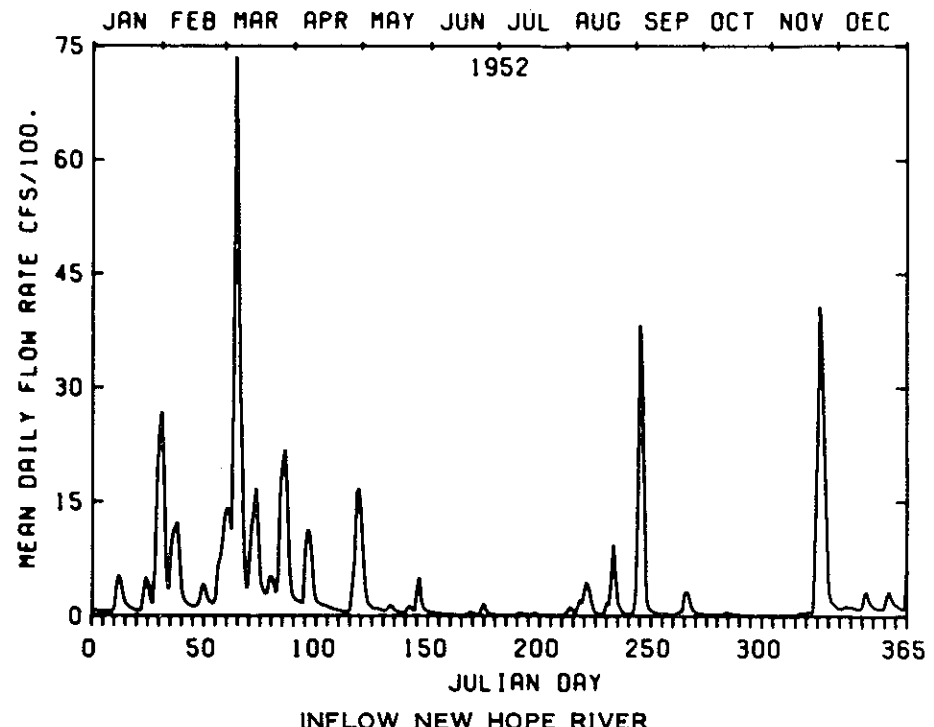
FLOW HYDROGRAPHS  
1950



FLOW HYDROGRAPHS  
1951

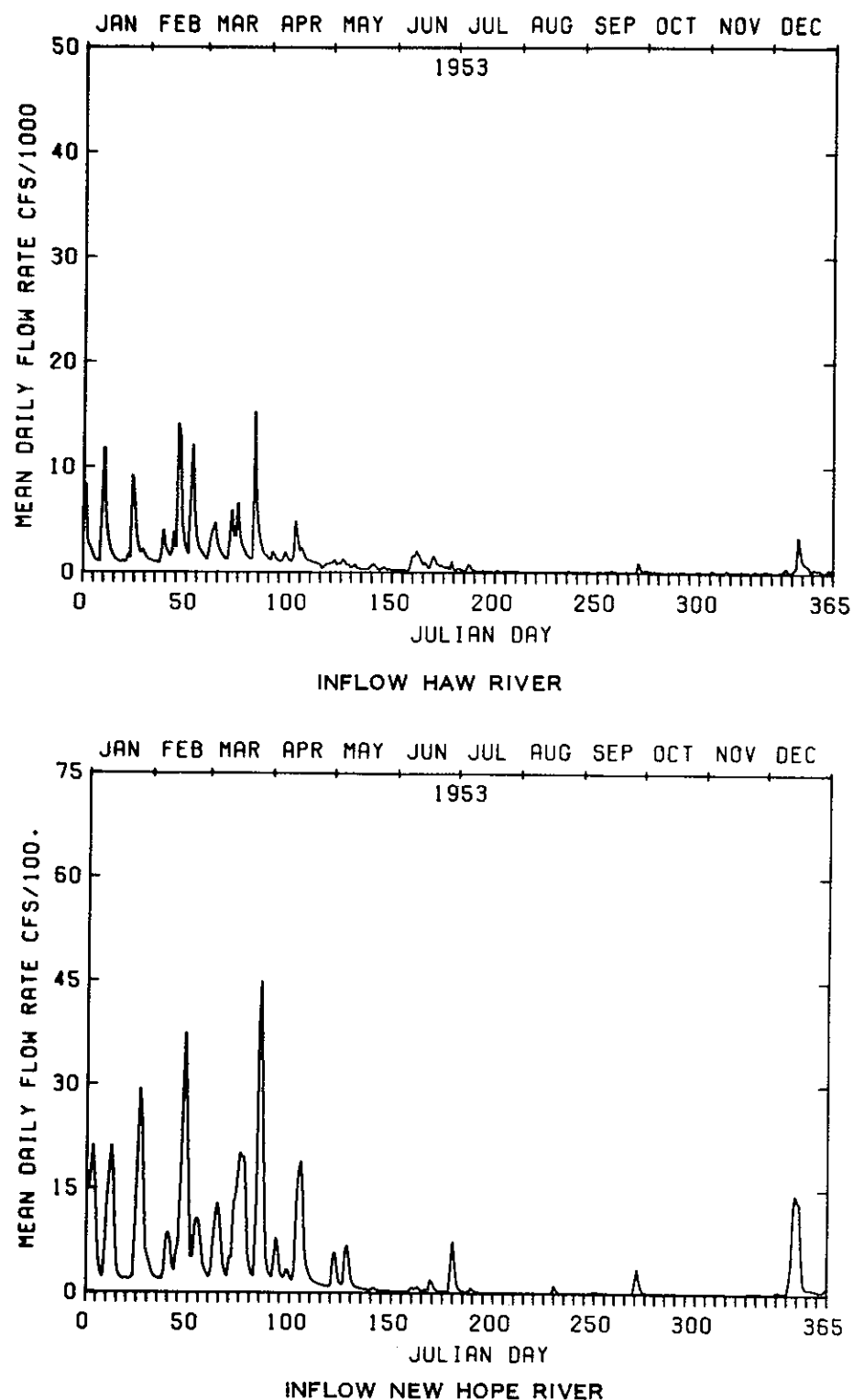


INFLOW HAW RIVER

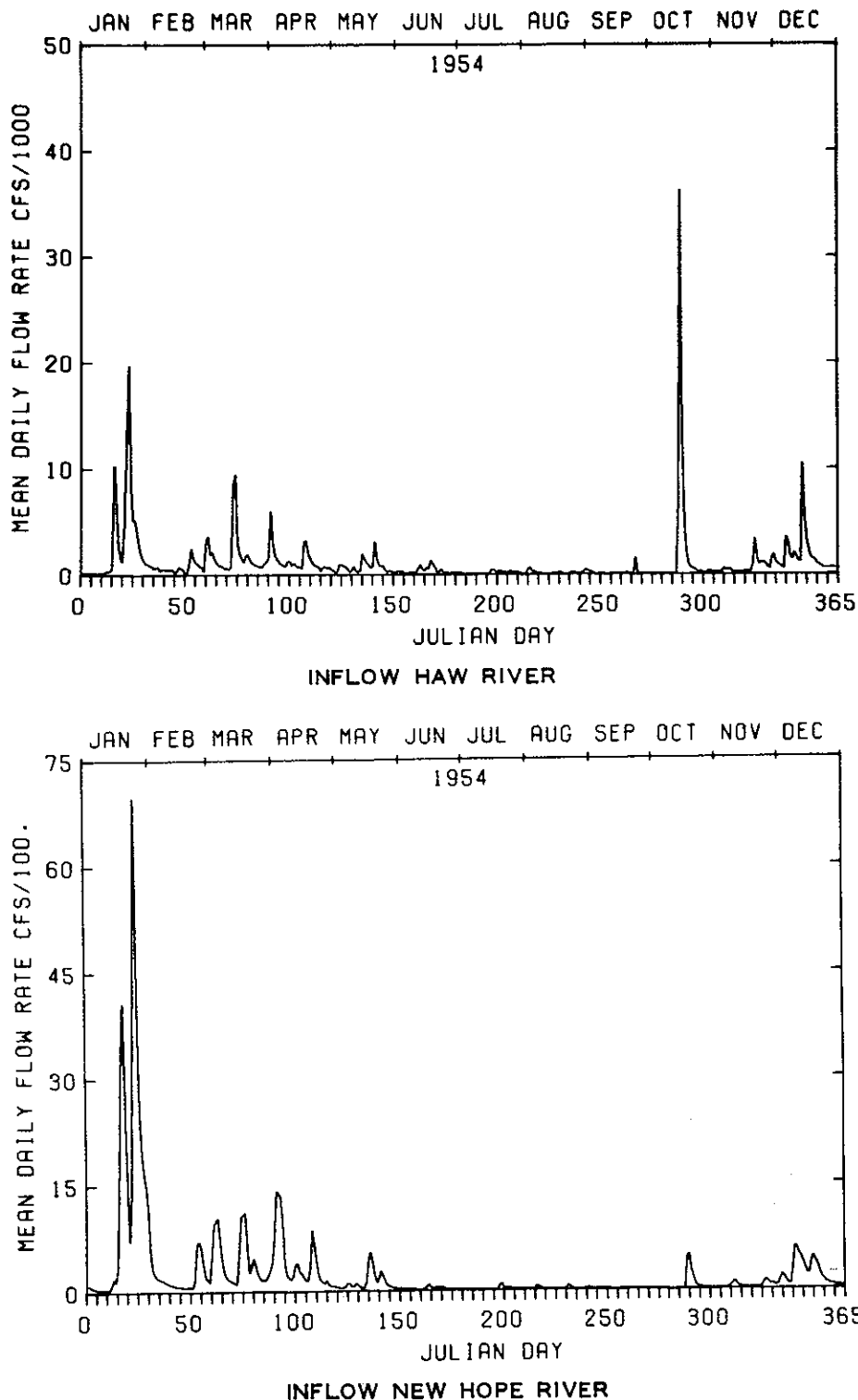


INFLOW NEW HOPE RIVER

FLOW HYDROGRAPHS  
1952

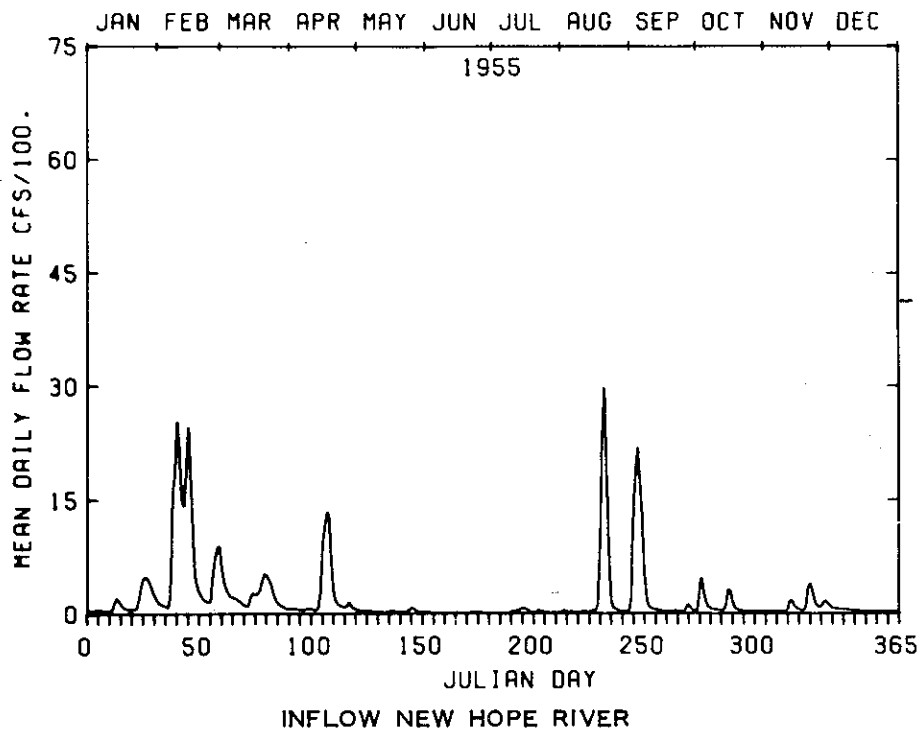
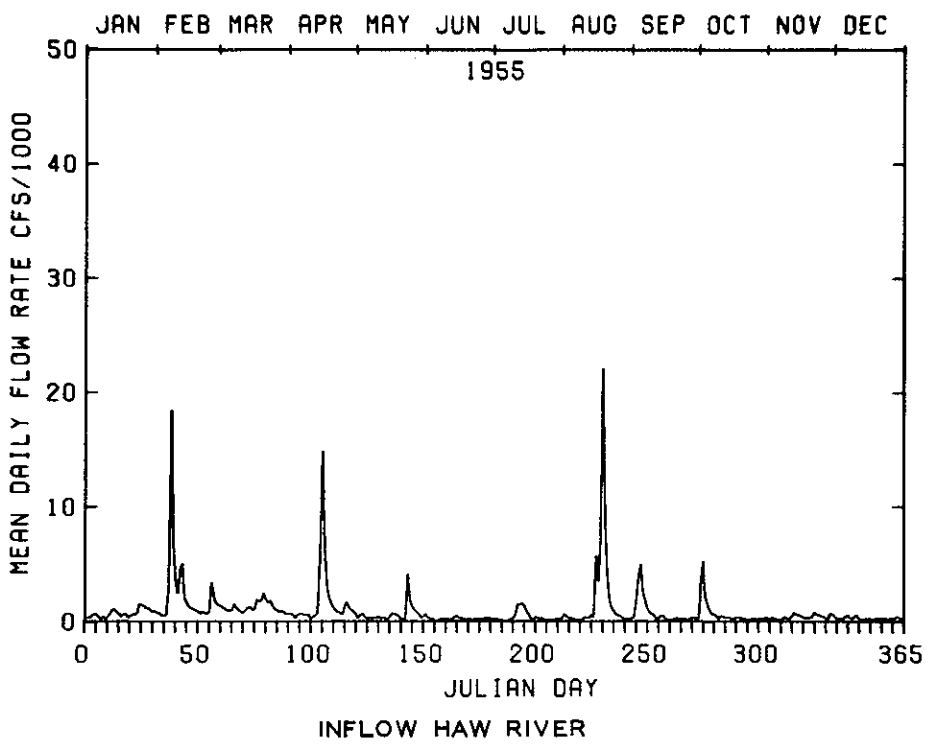


FLOW HYDROGRAPHS  
1953

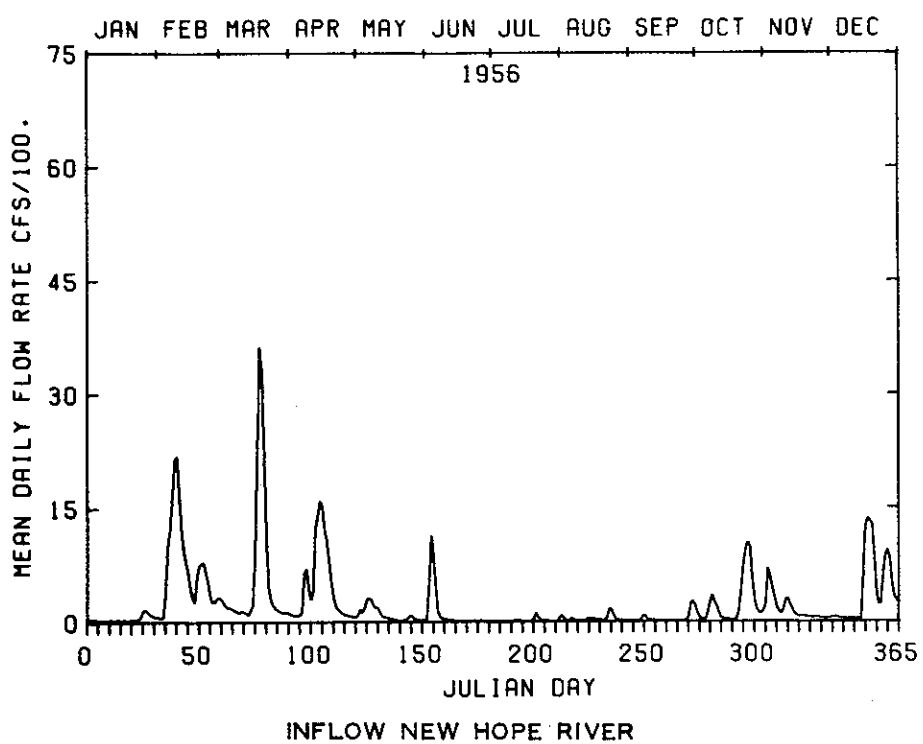
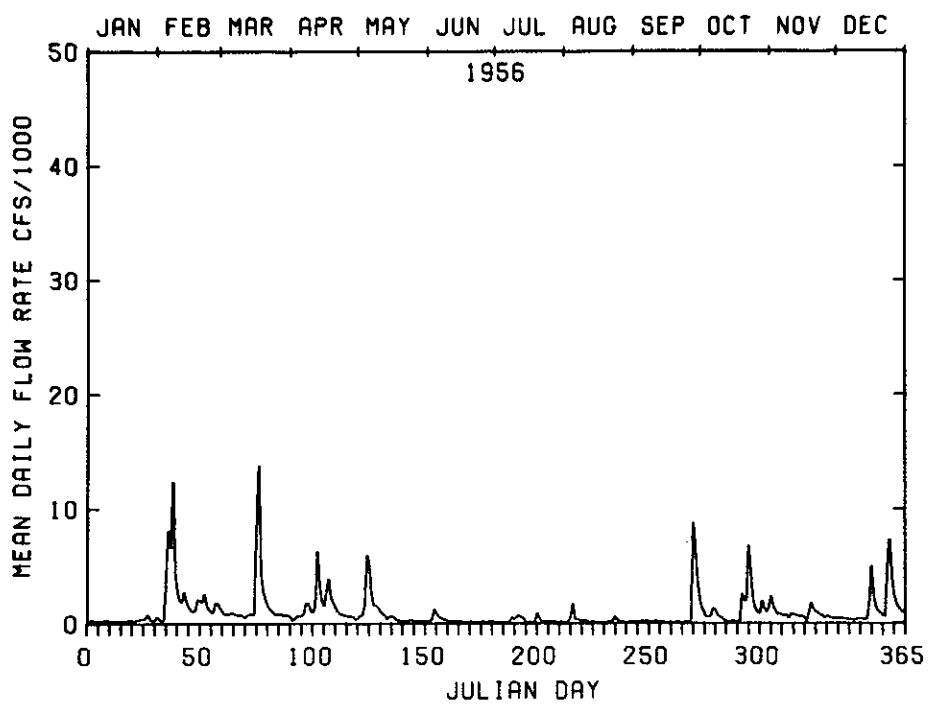


**FLOW HYDROGRAPHS**

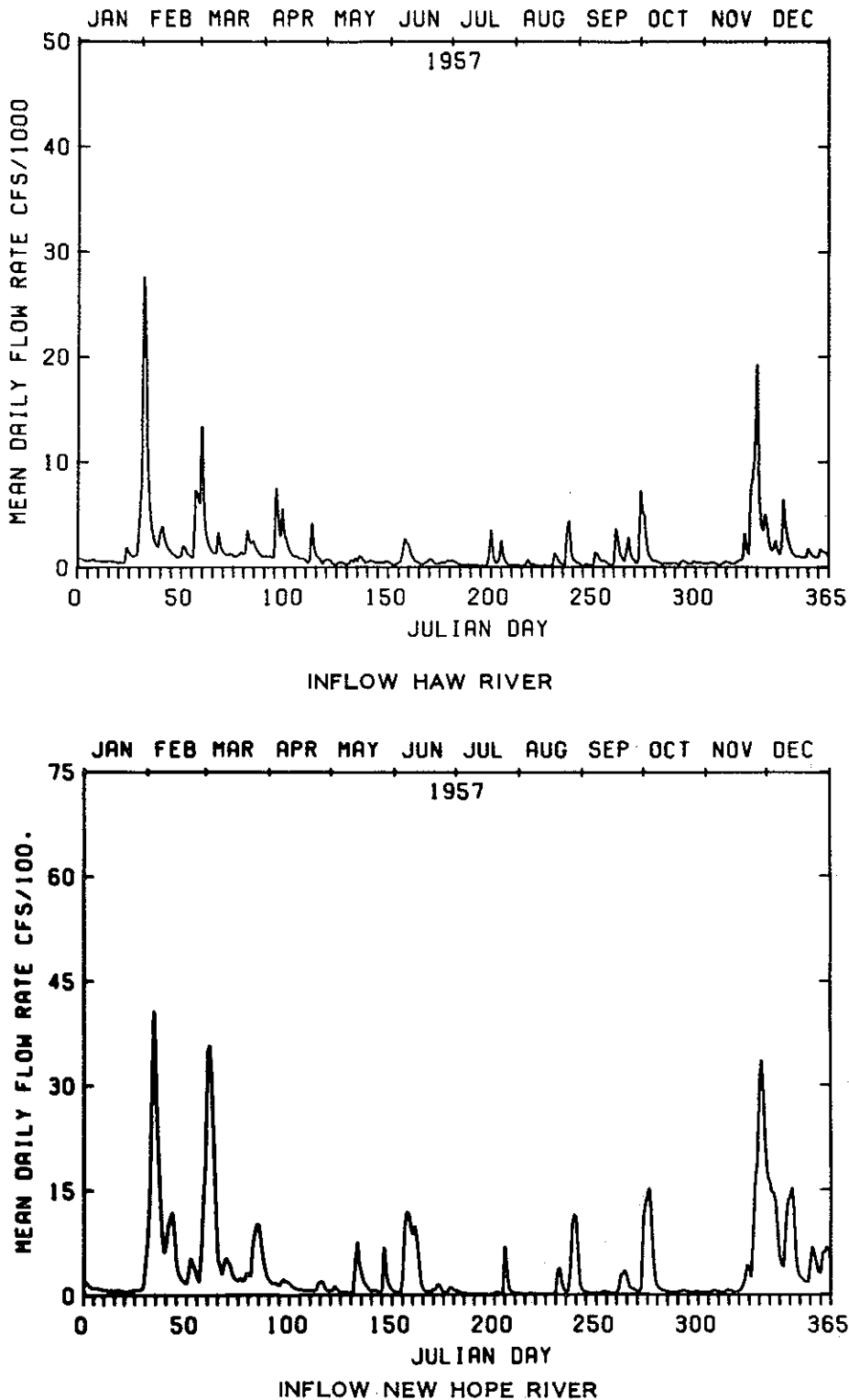
1954



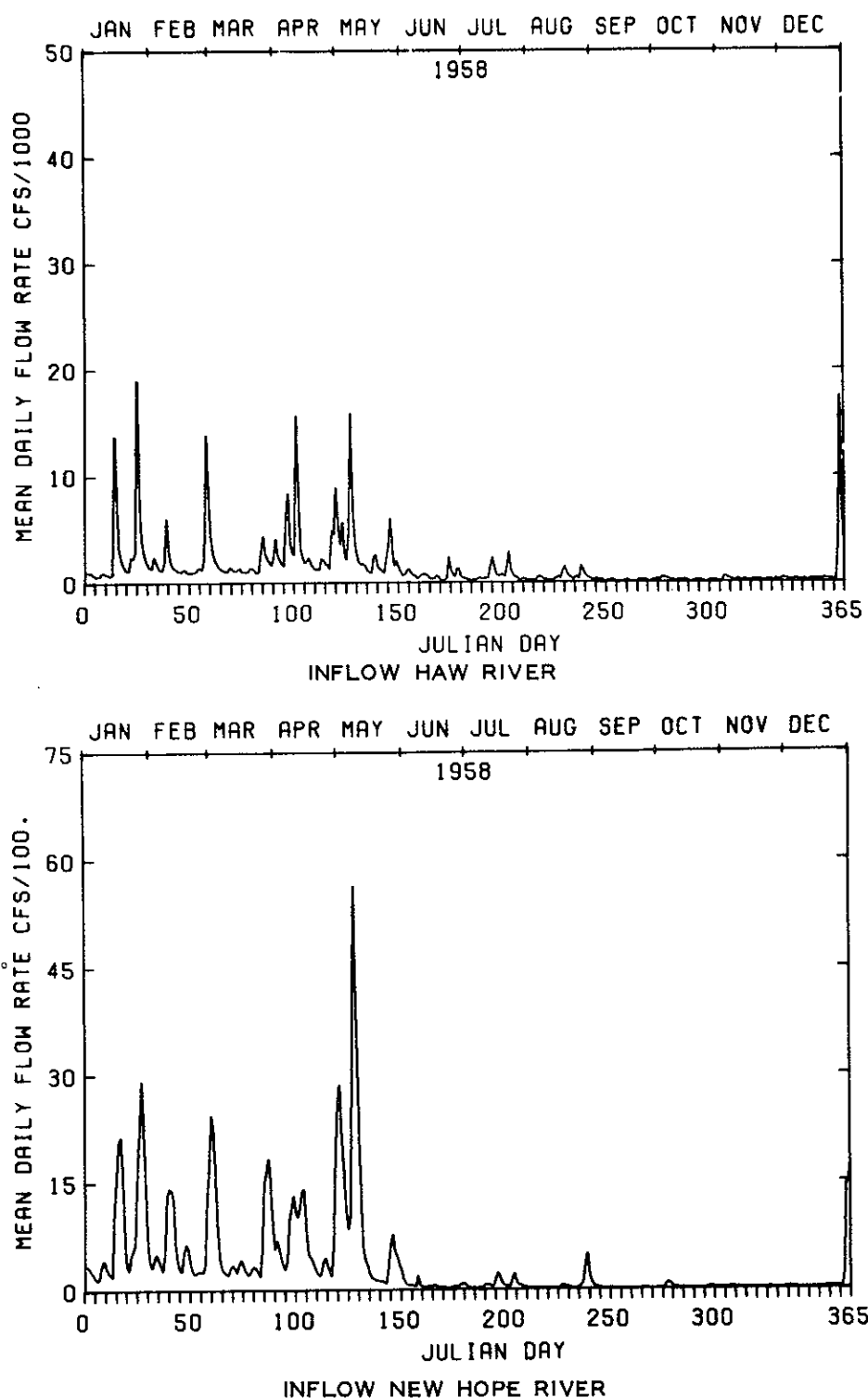
FLOW HYDROGRAPHS  
1955



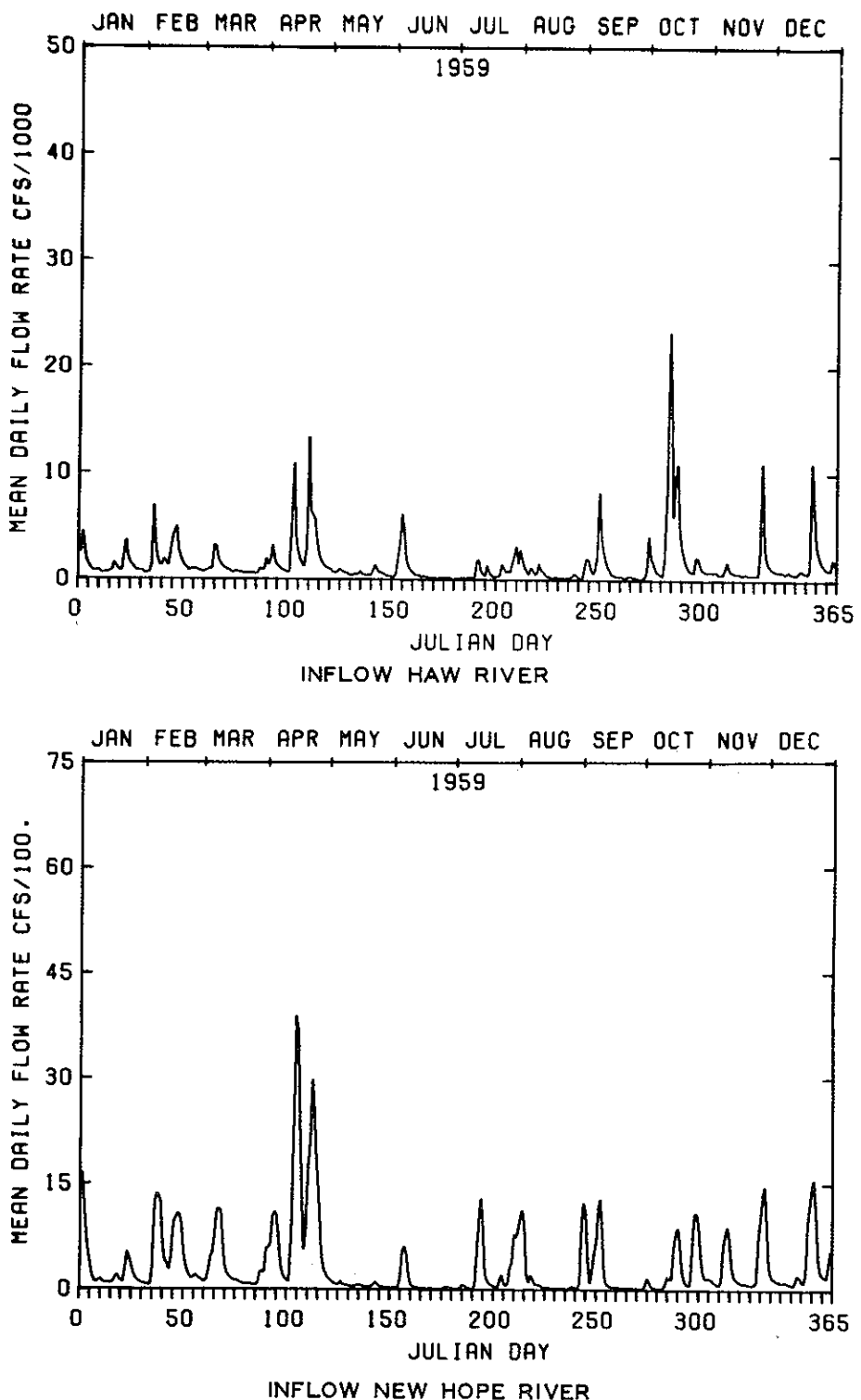
FLOW HYDROGRAPHS  
1956



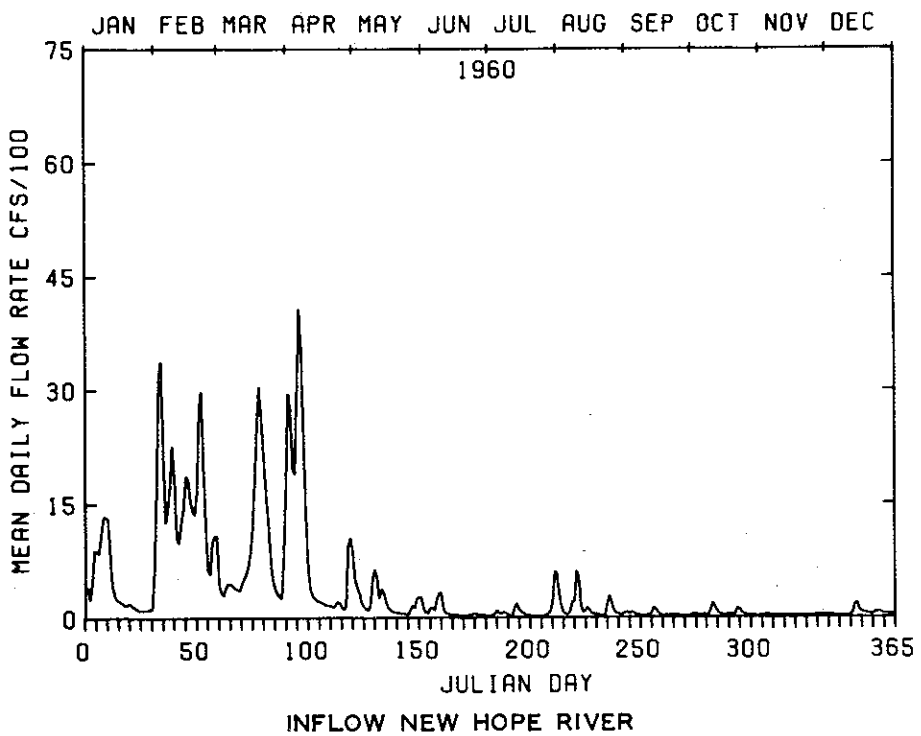
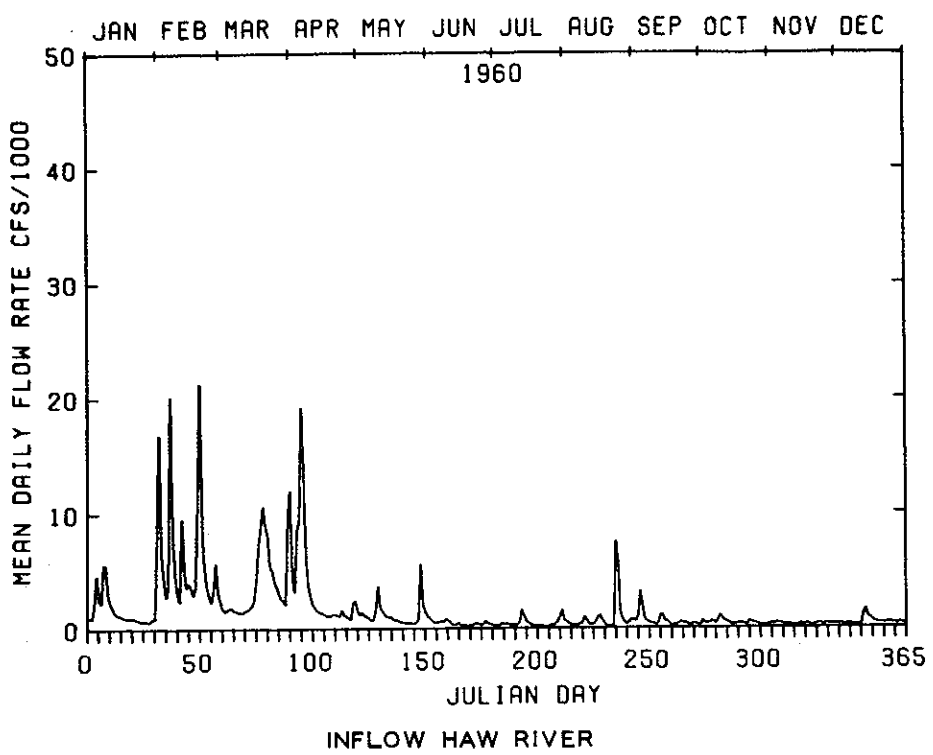
FLOW HYDROGRAPHS  
1957



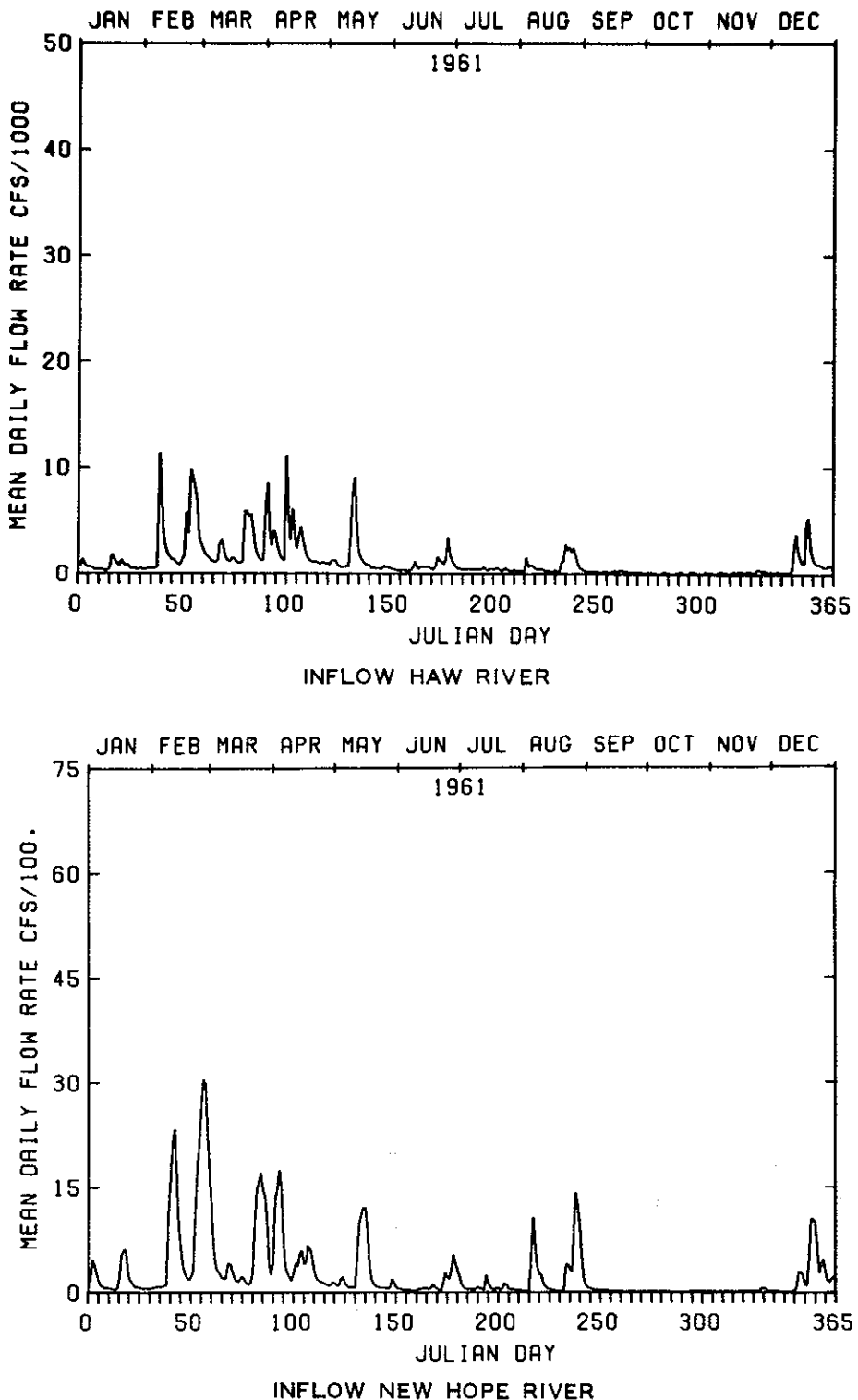
FLOW HYDROGRAPHS  
1958



FLOW HYDROGRAPHS  
1959

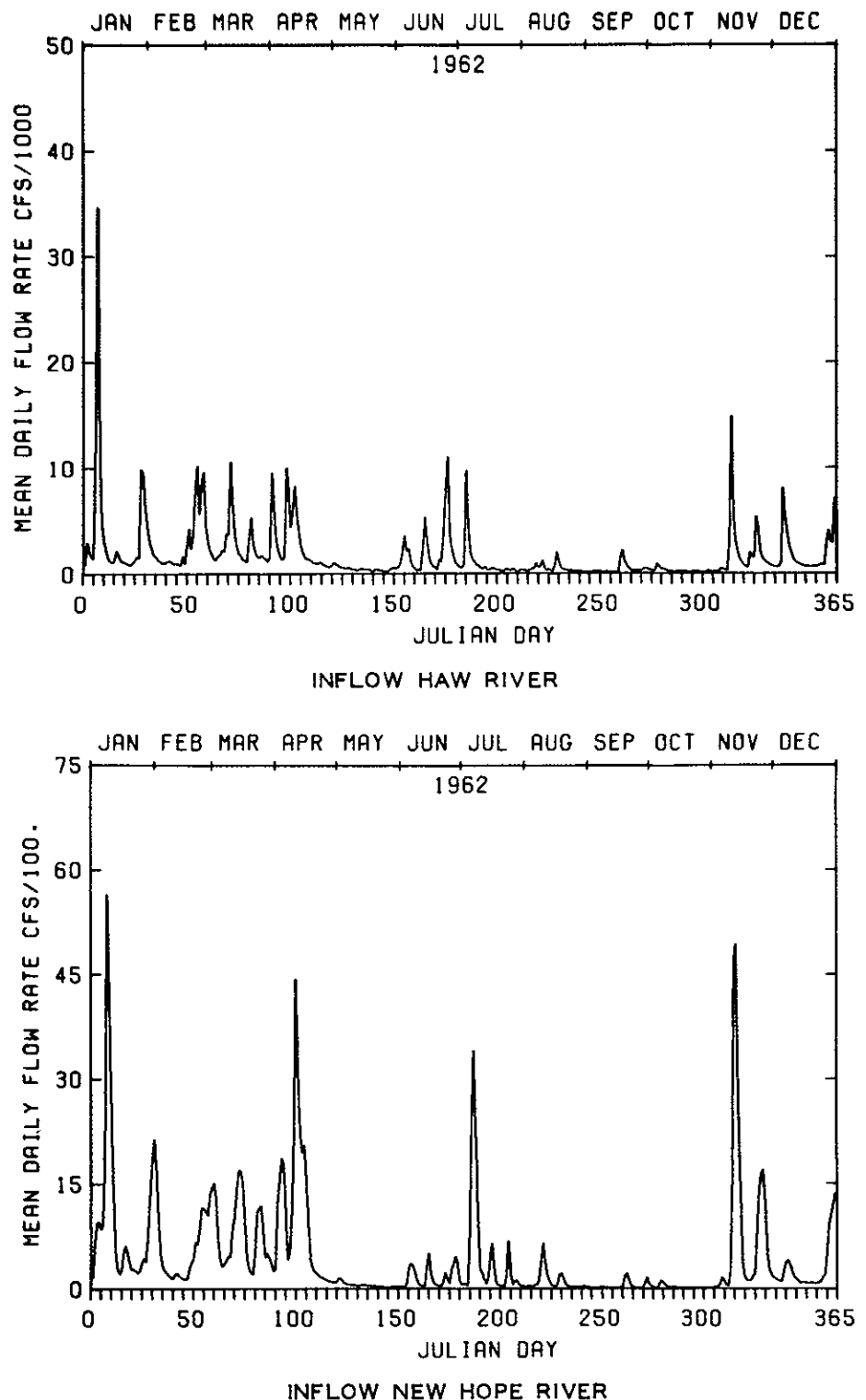


FLOW HYDROGRAPHS  
1960



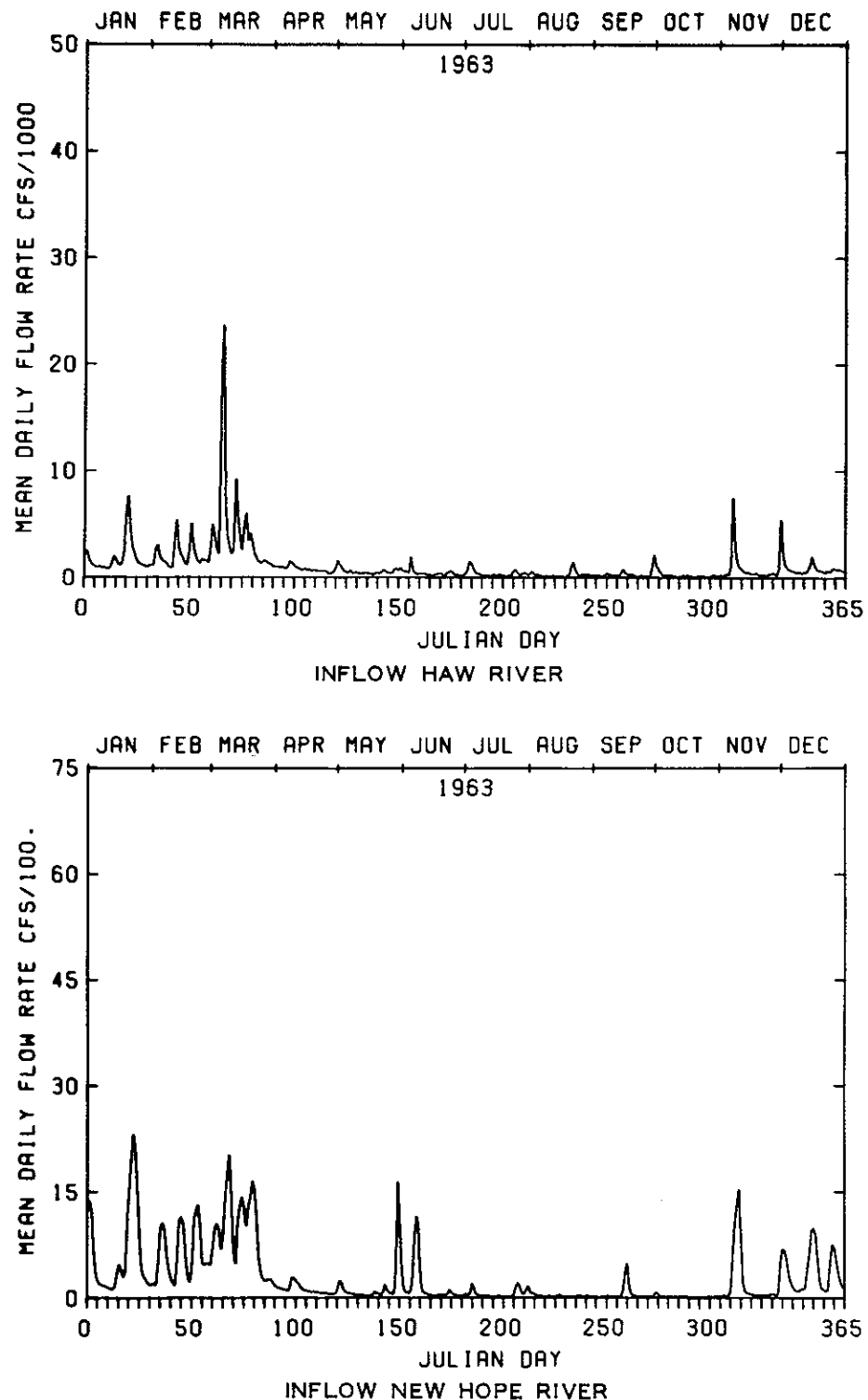
FLOW HYDROGRAPHS

1961

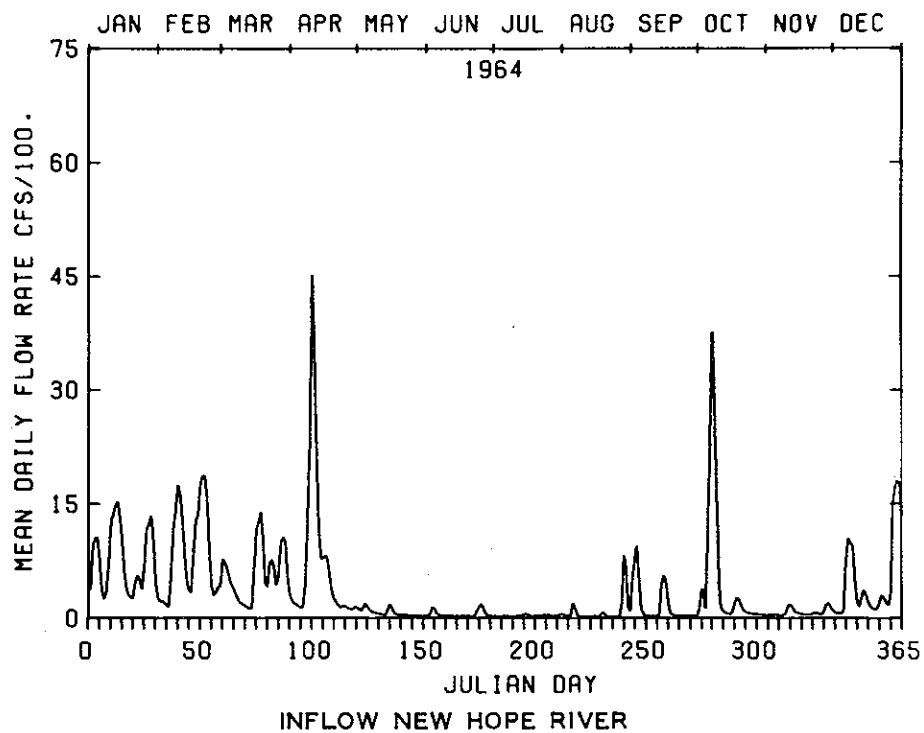
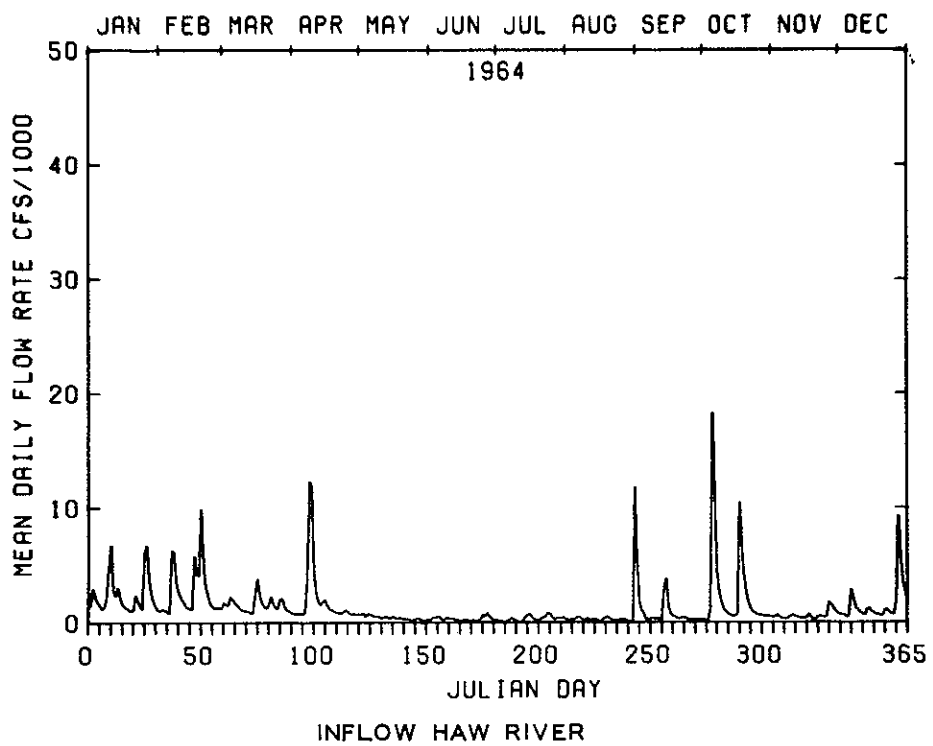


### FLOW HYDROGRAPHS

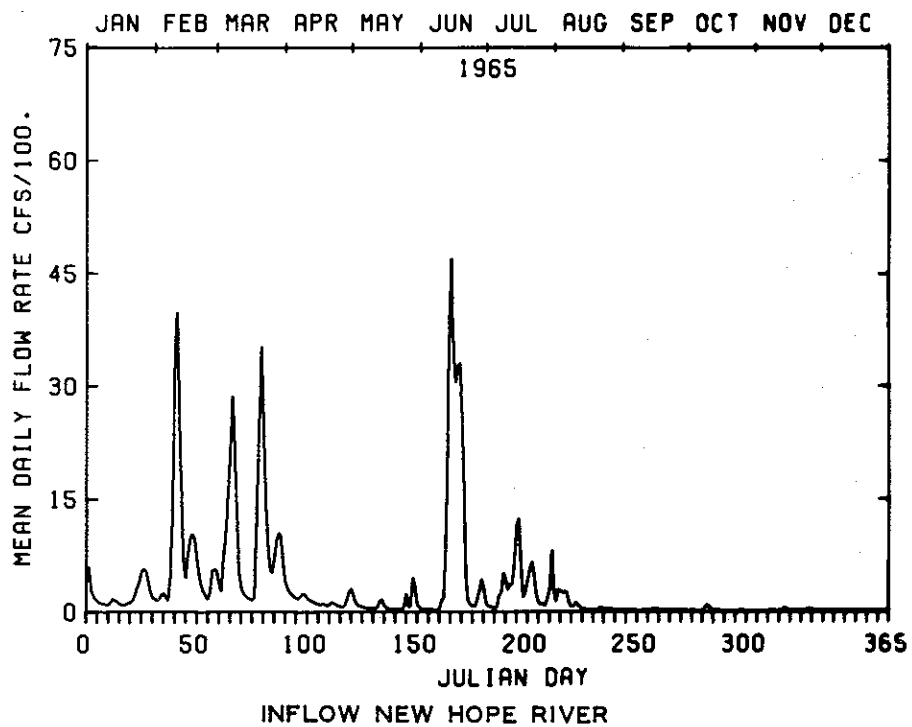
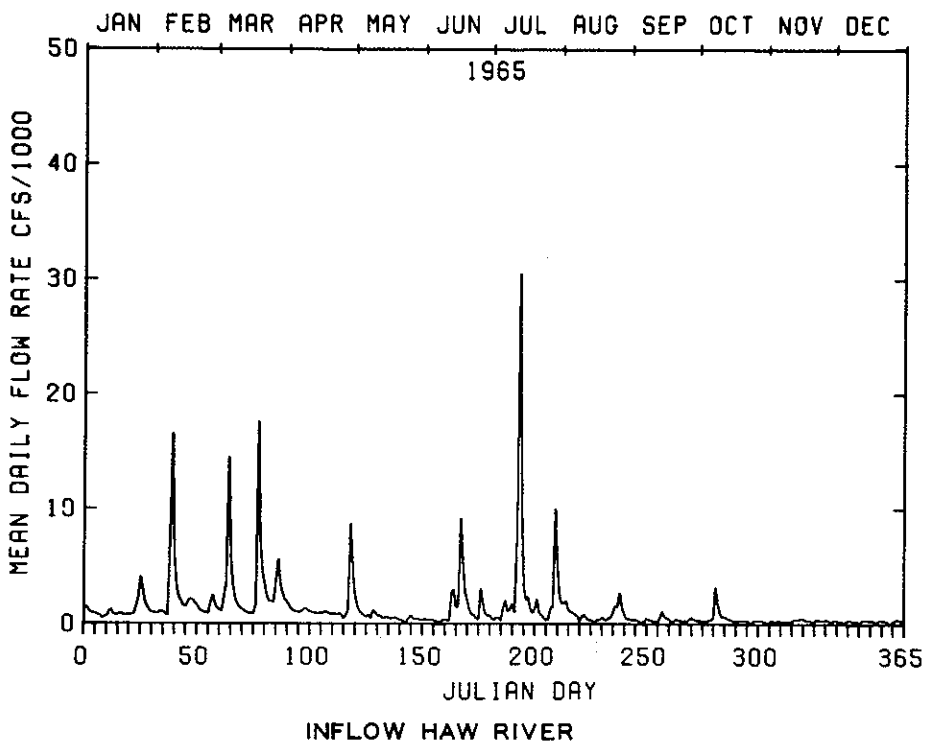
1962



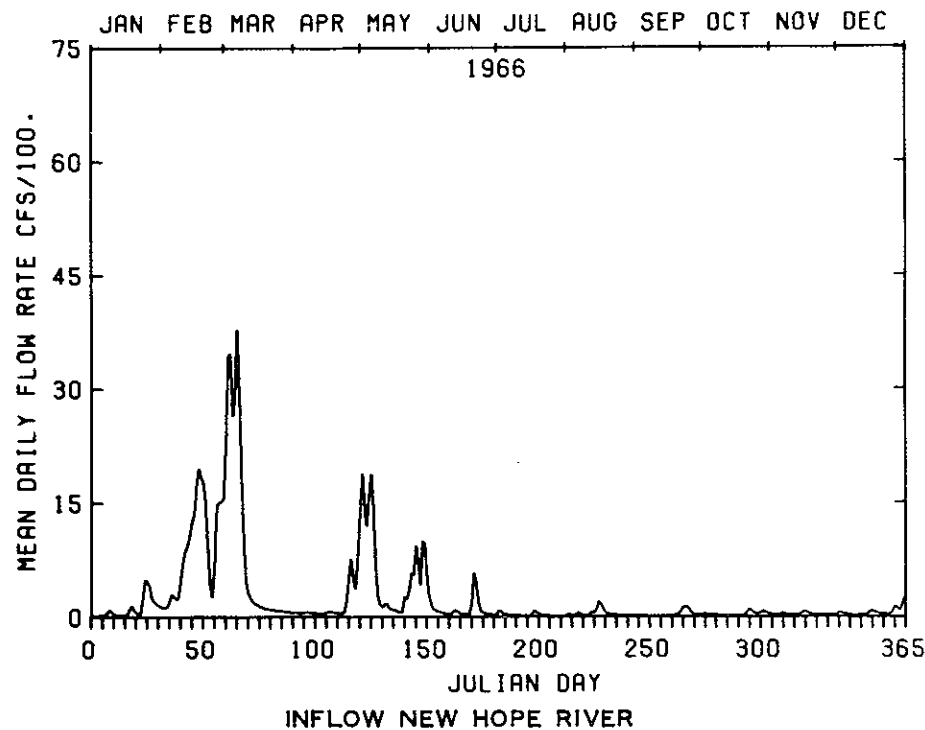
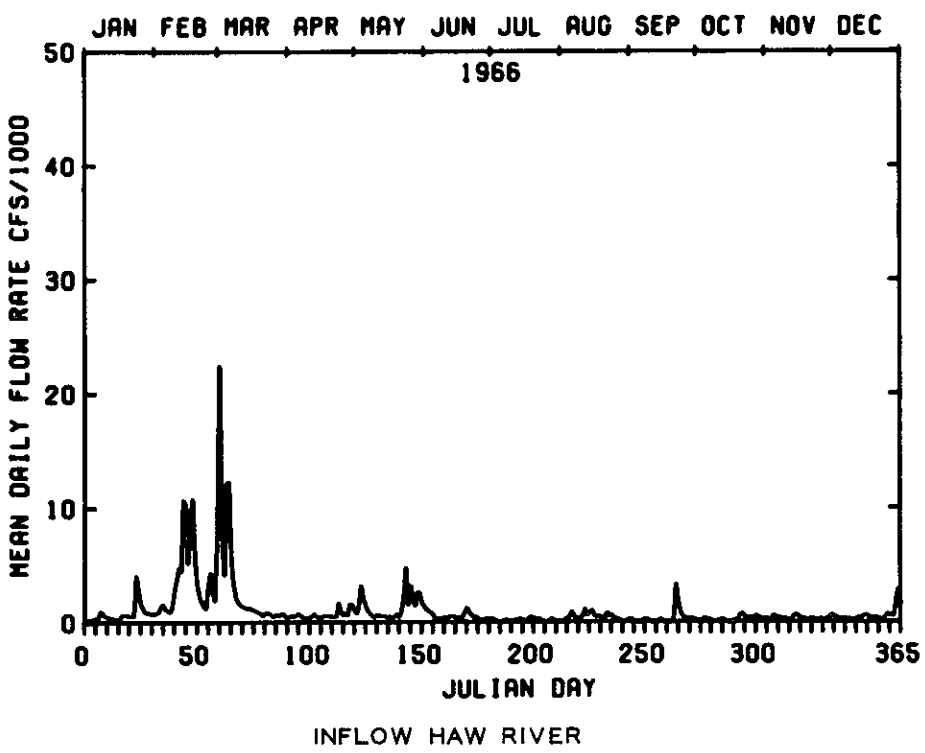
FLOW HYDROGRAPHS  
1963



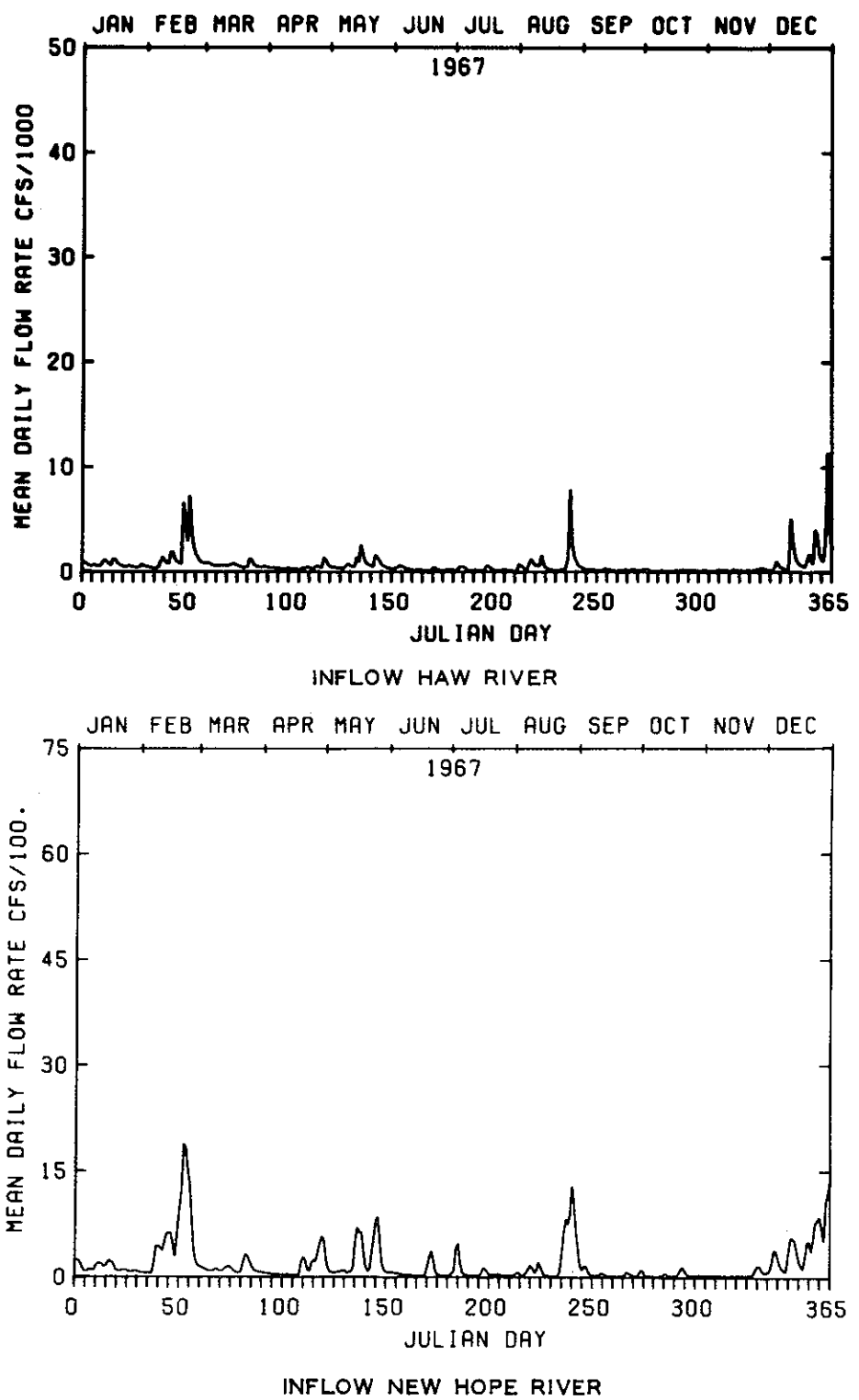
FLOW HYDROGRAPHS  
1964



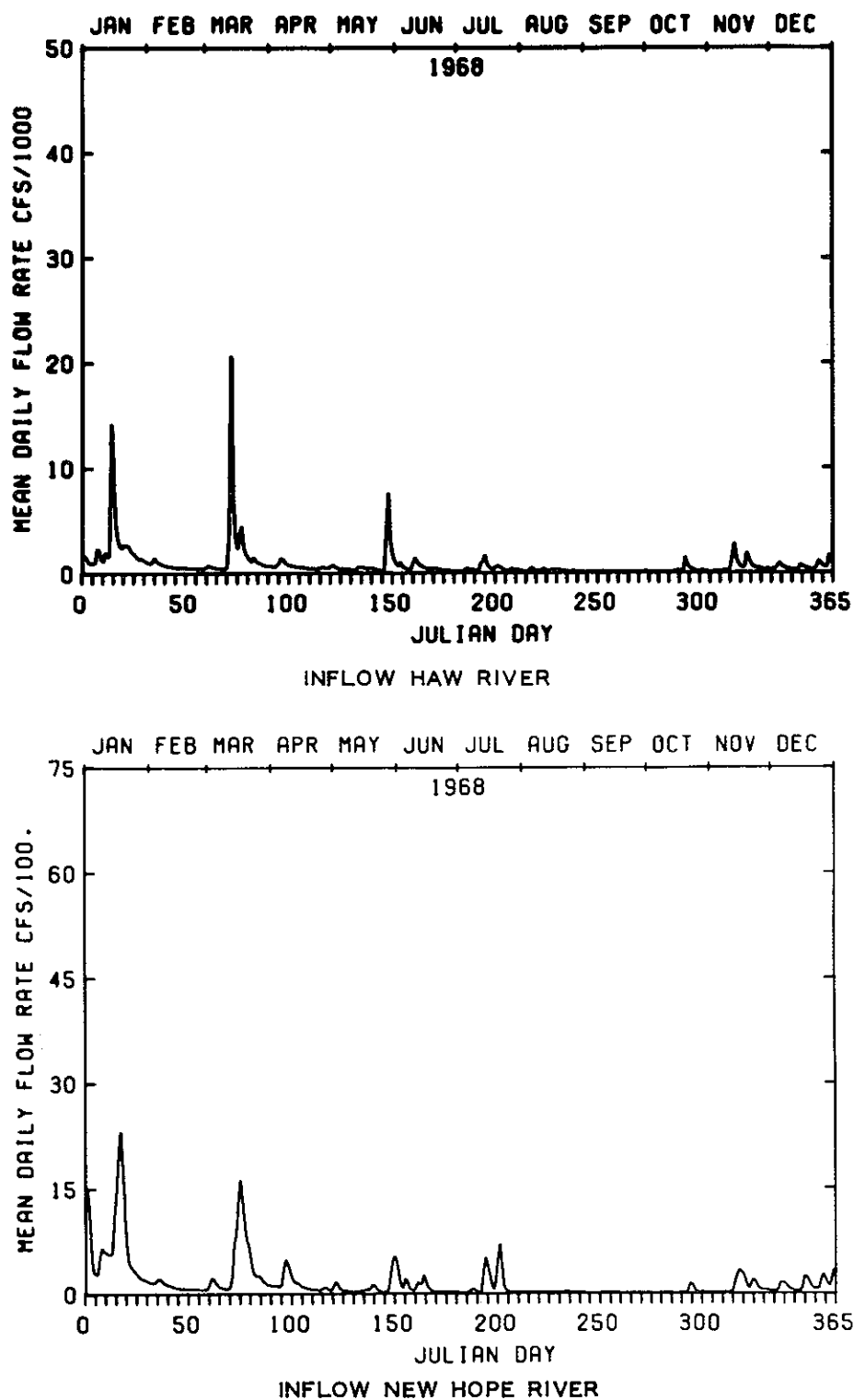
FLOW HYDROGRAPHS  
1965



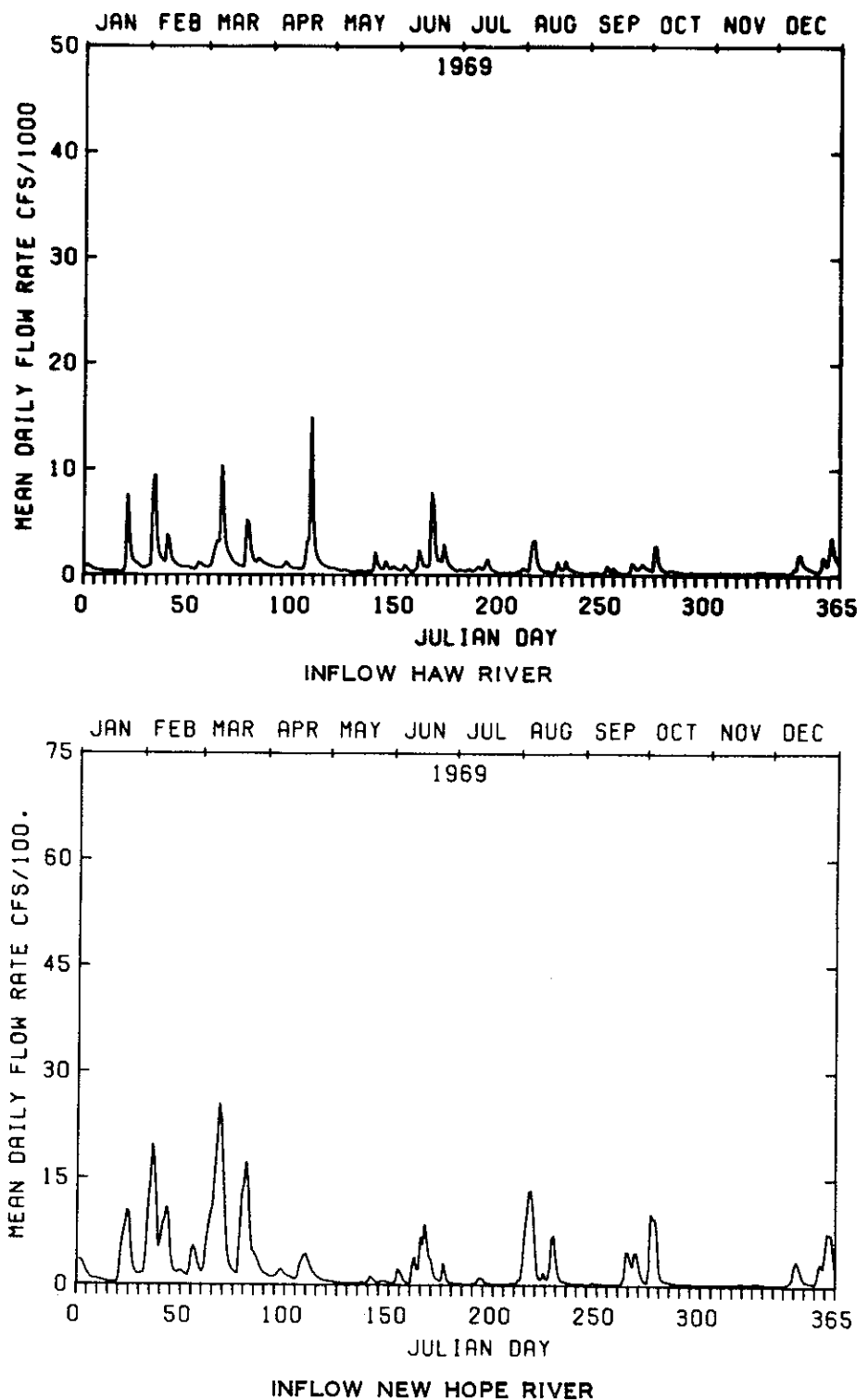
FLOW HYDROGRAPHS  
1966



FLOW HYDROGRAPHS  
1967

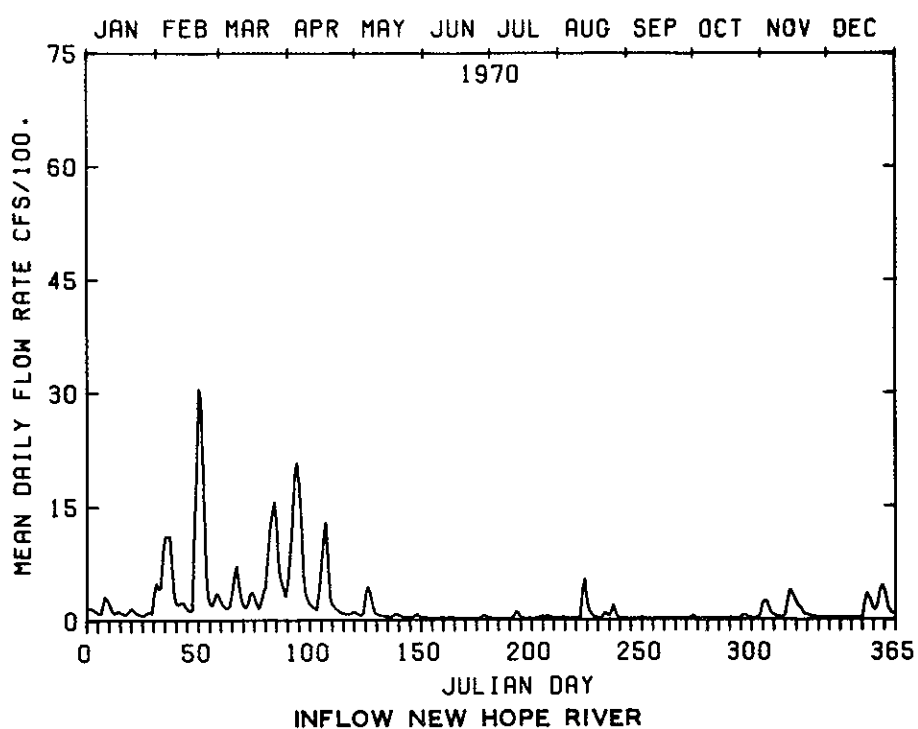
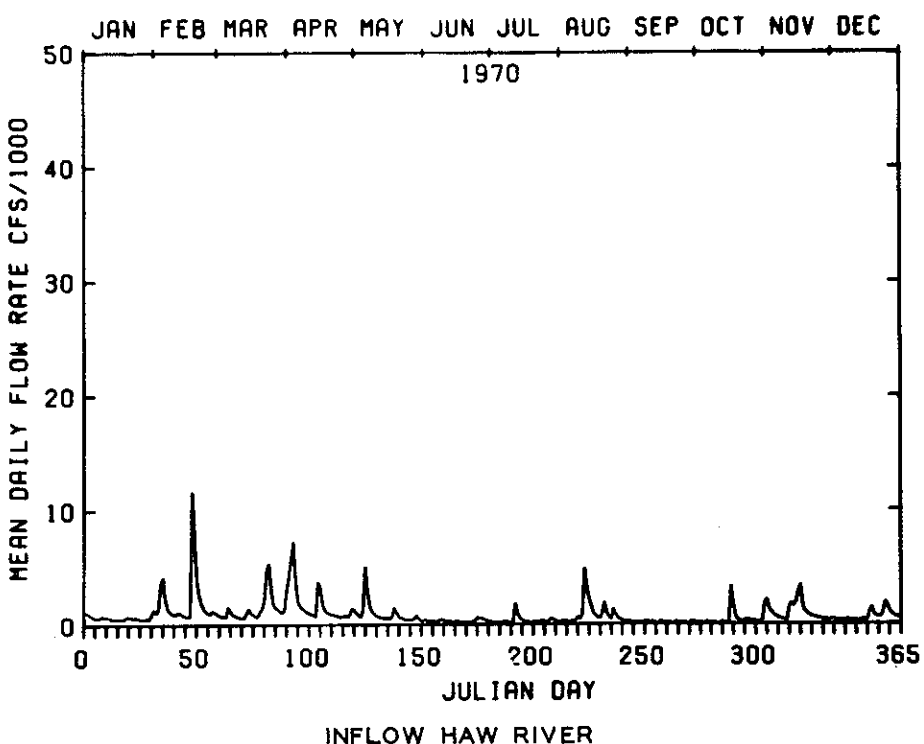


FLOW HYDROGRAPHS  
1968

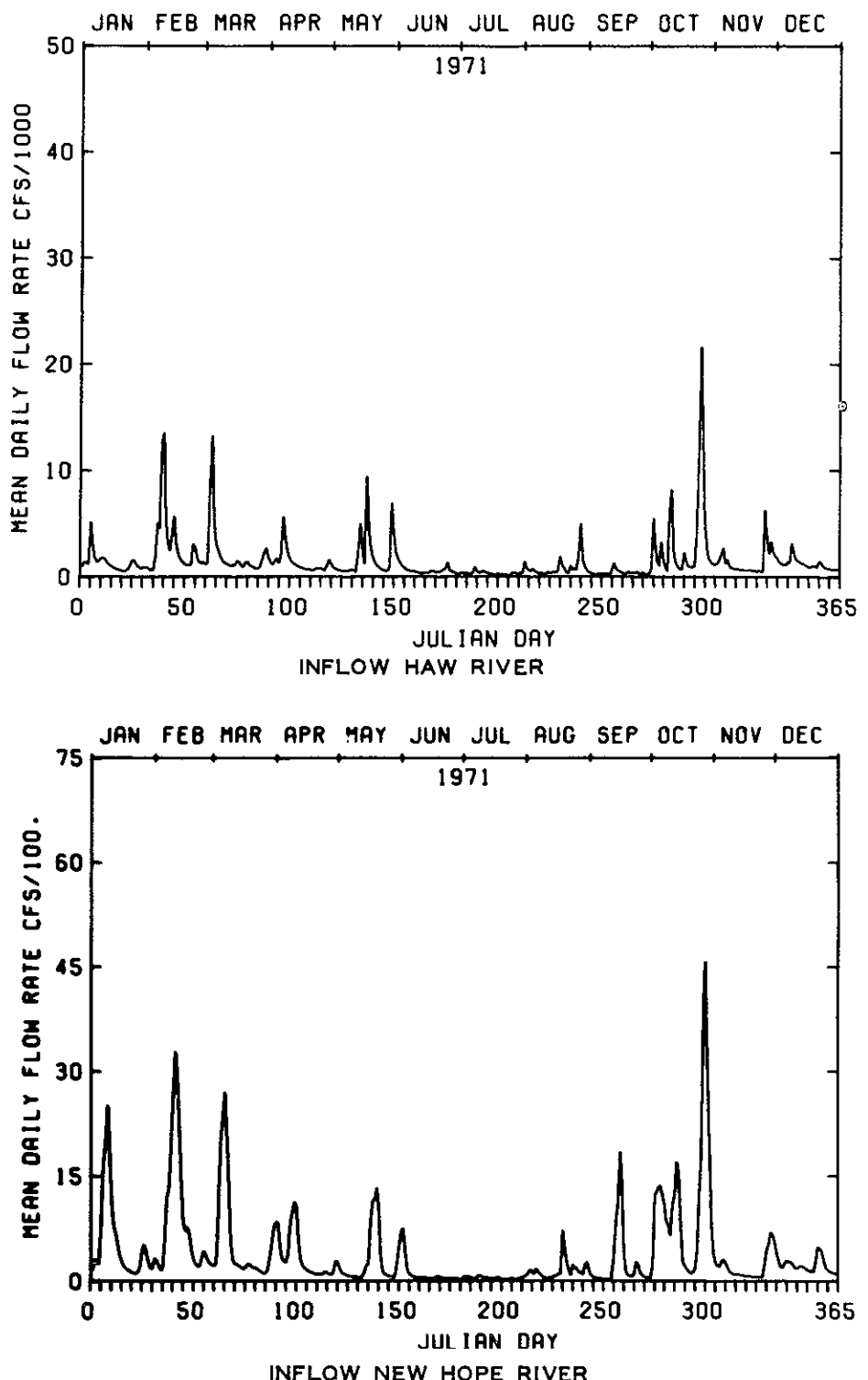


### FLOW HYDROGRAPHS

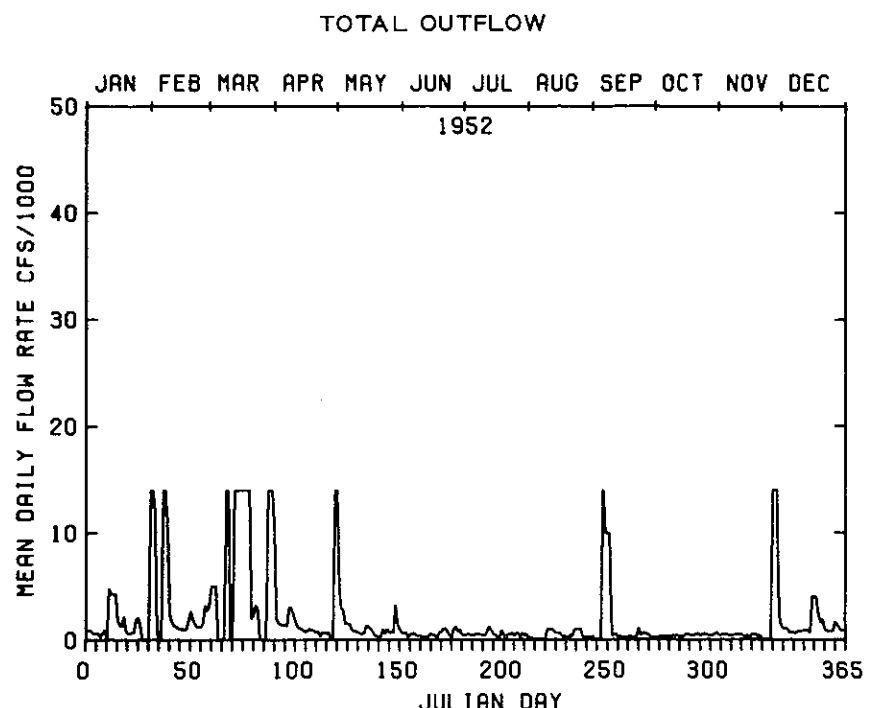
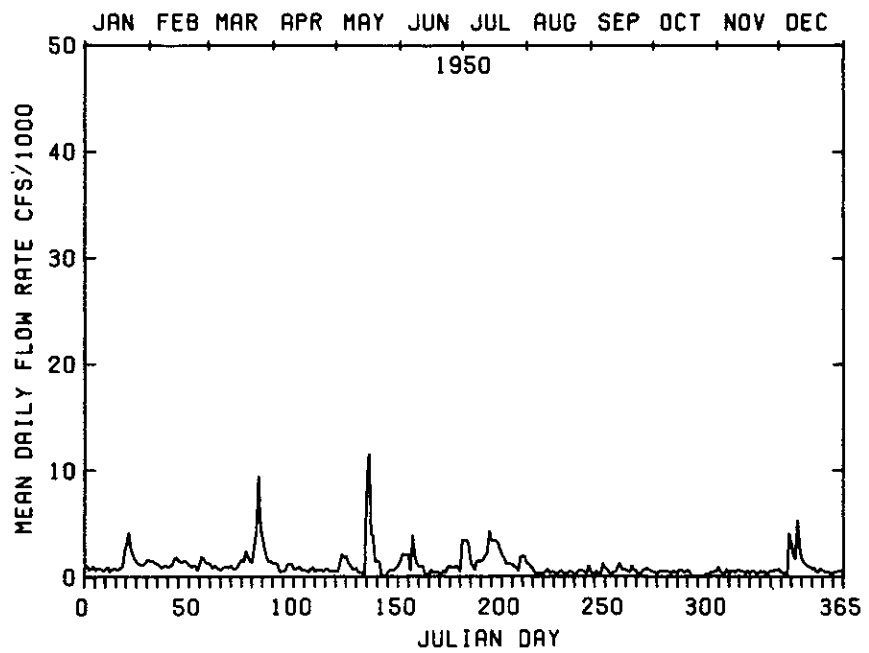
1969



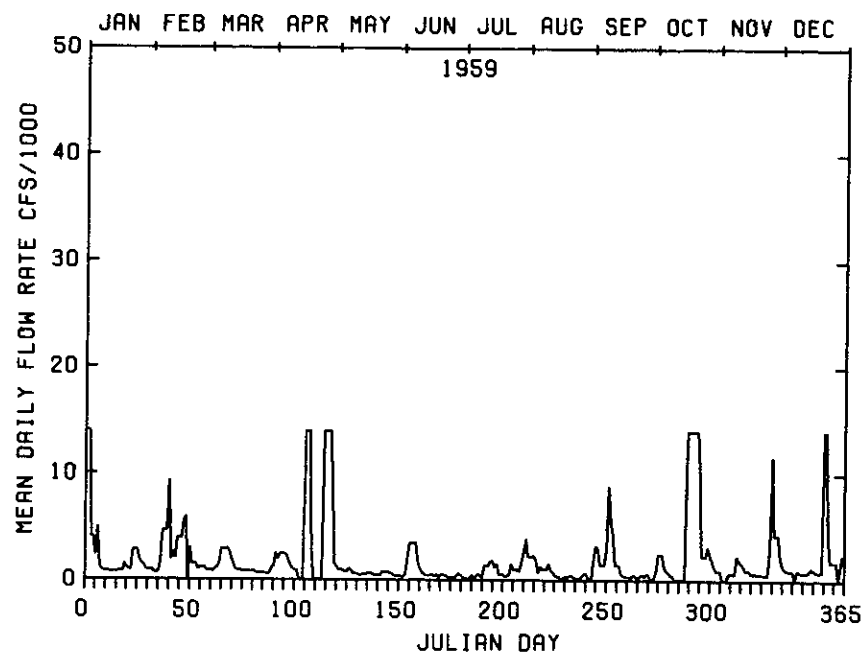
FLOW HYDROGRAPHS  
1970



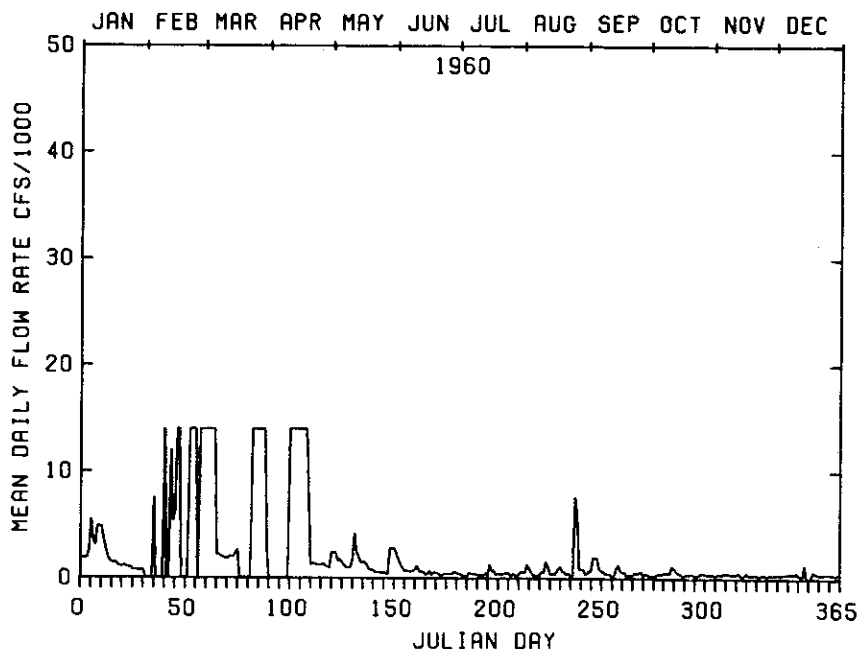
FLOW HYDROGRAPHS  
1971



B. EVERETT JORDAN LAKE  
FLOW HYDROGRAPHS  
1950-1952

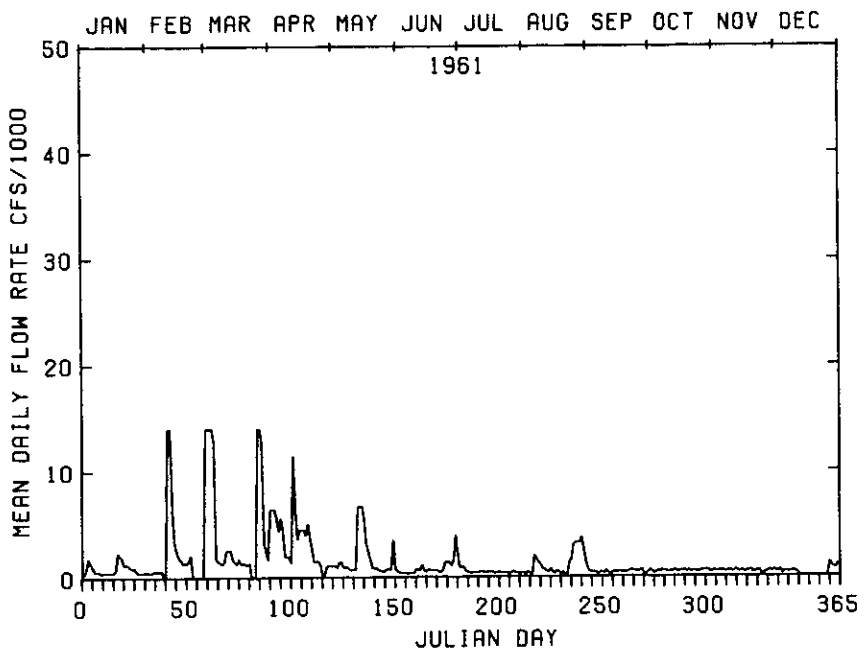


TOTAL OUTFLOW

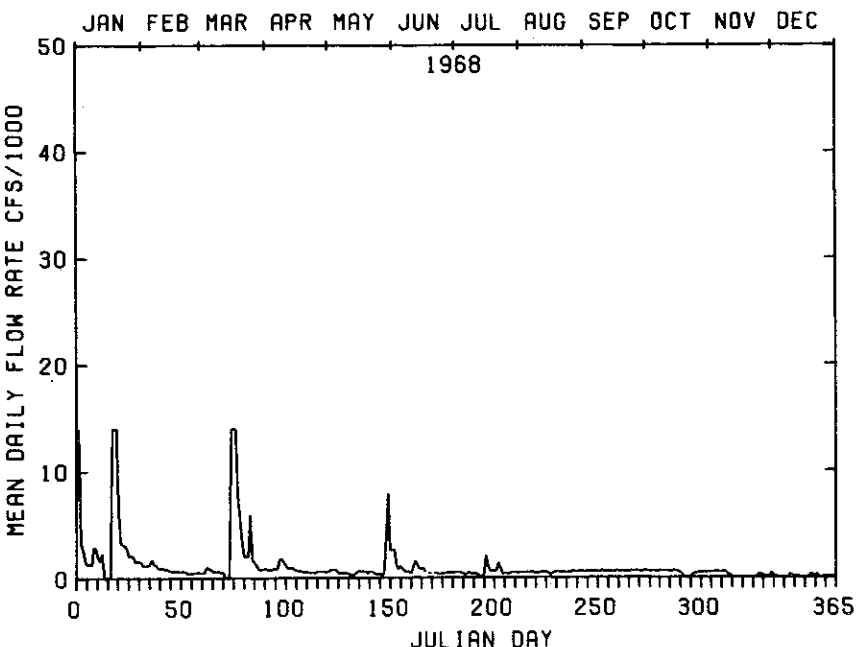


TOTAL OUTFLOW

B. EVERETT JORDAN LAKE  
FLOW HYDROGRAPHS  
1959 - 1960

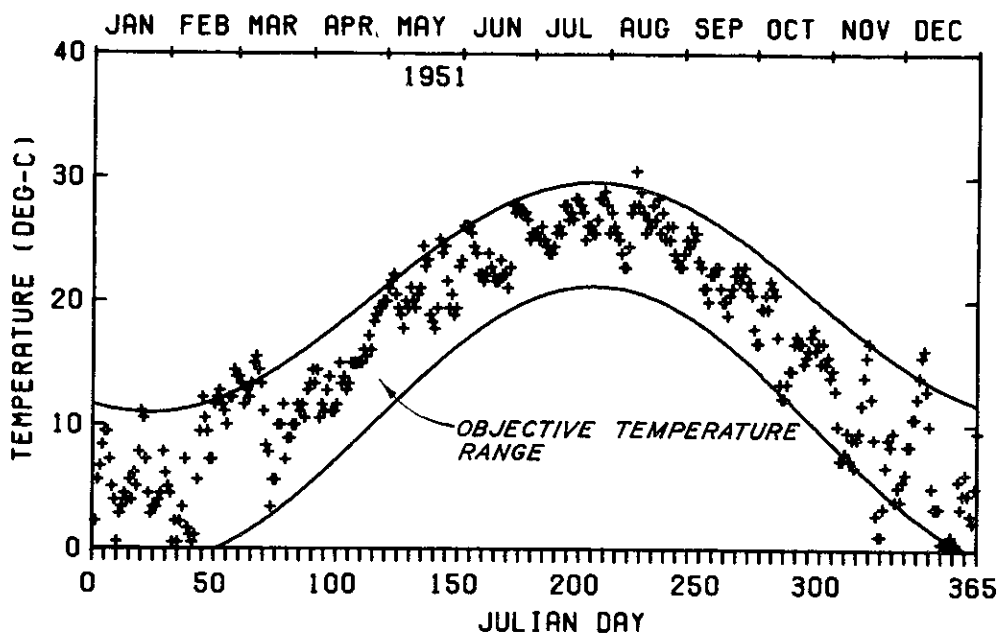
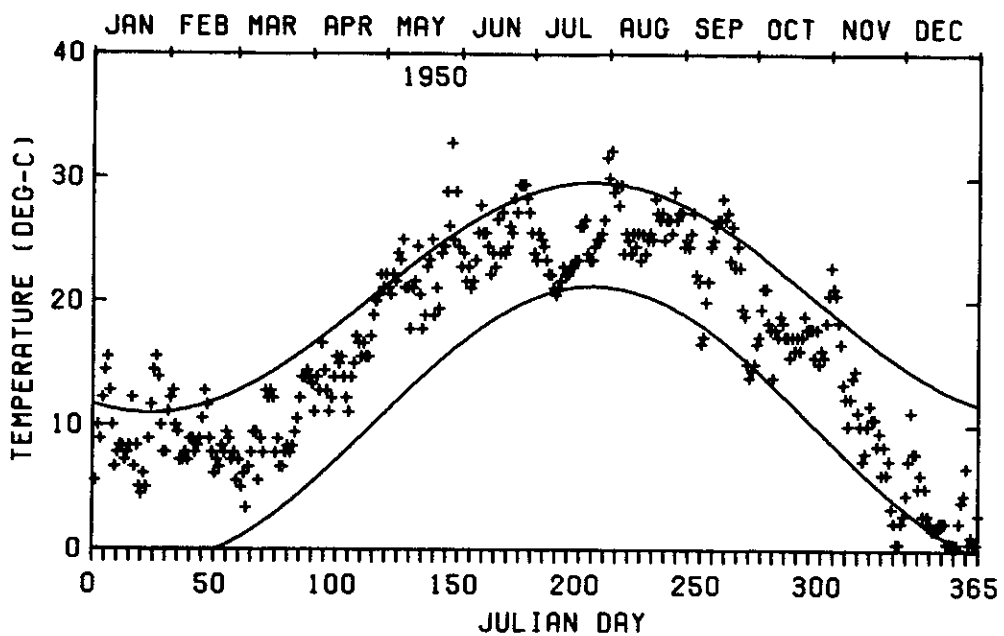


TOTAL OUTFLOW

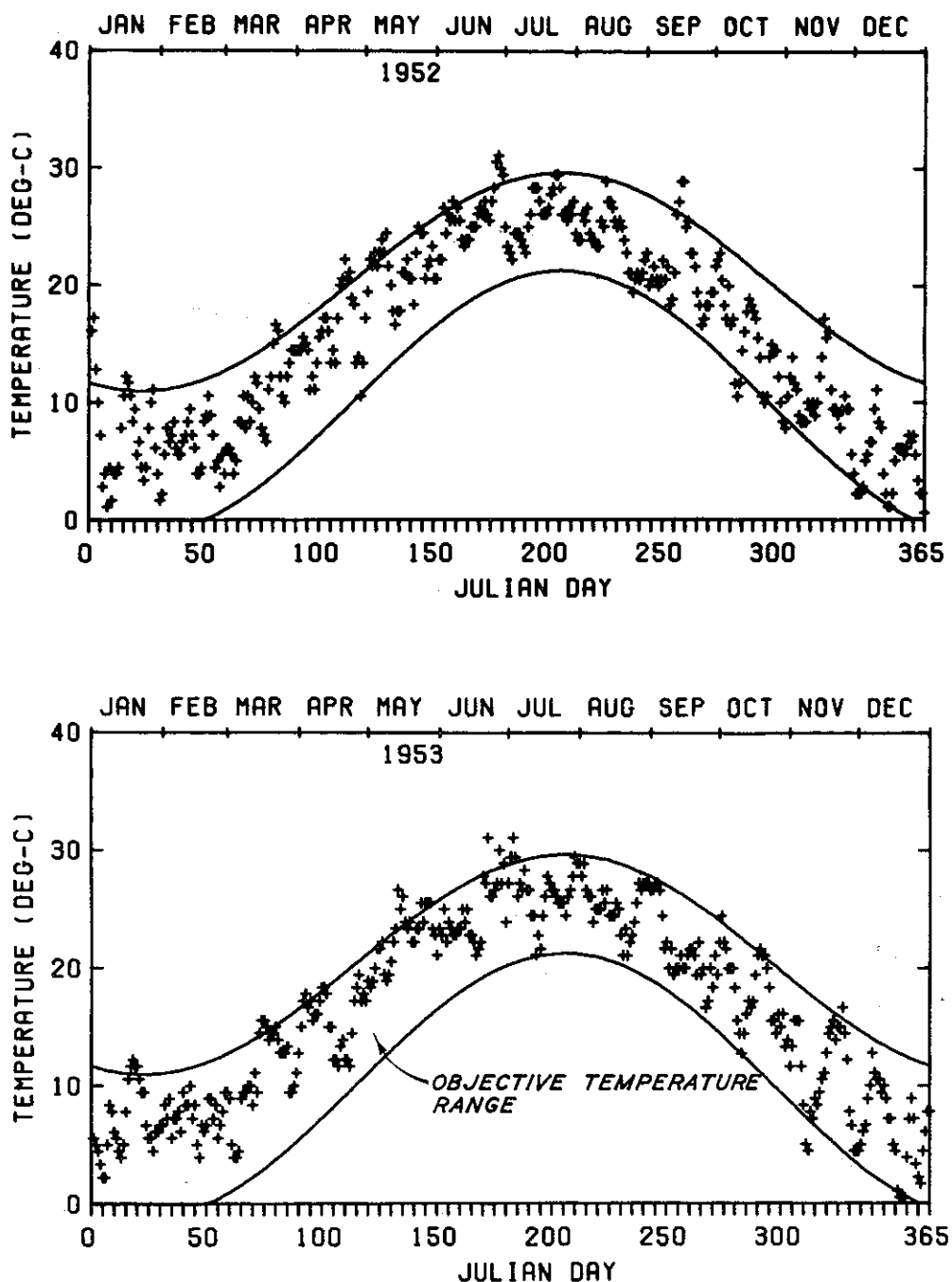


TOTAL OUTFLOW

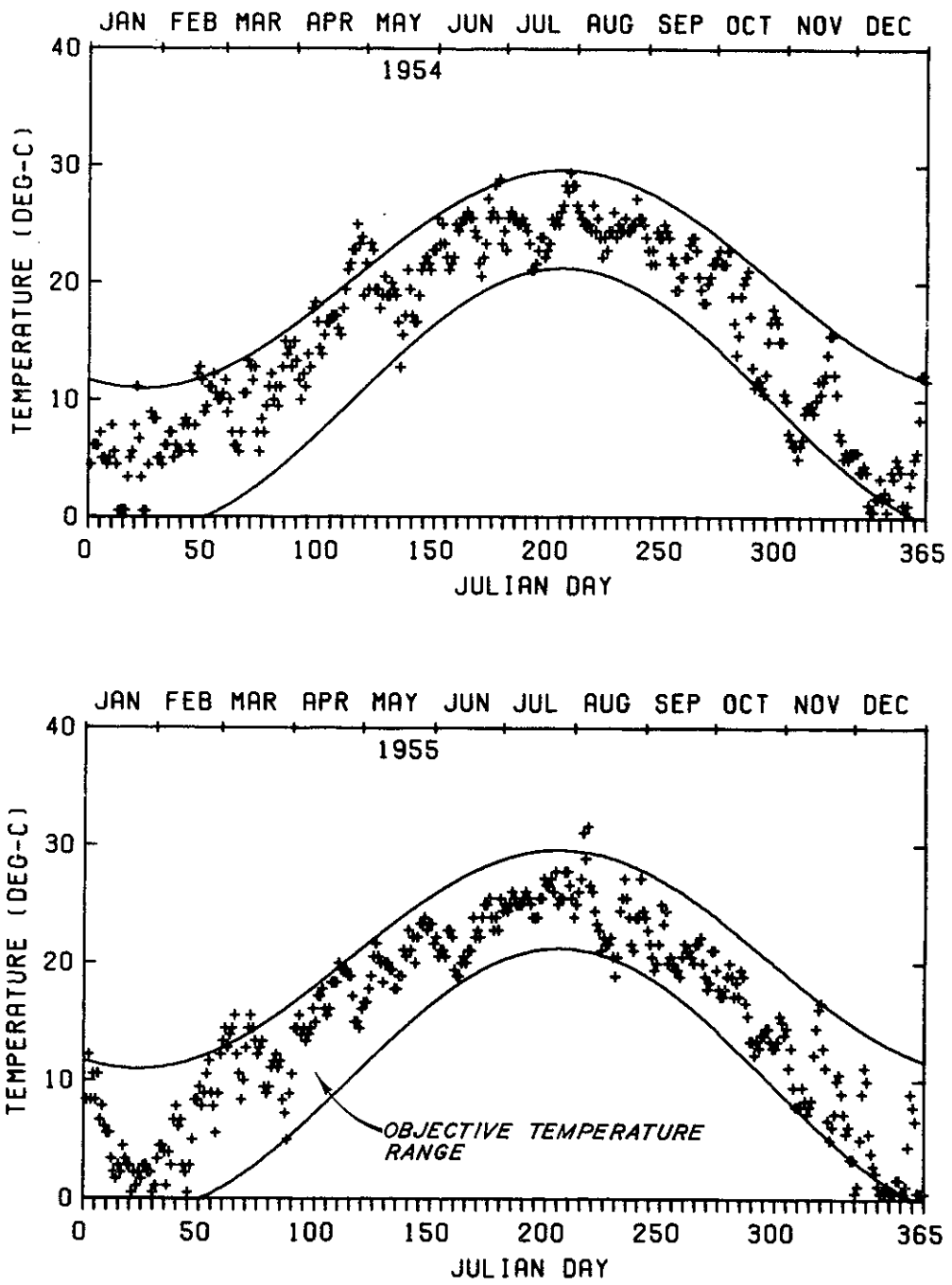
B. EVERETT JORDAN LAKE  
FLOW HYDROGRAPHS  
1961 - 1968



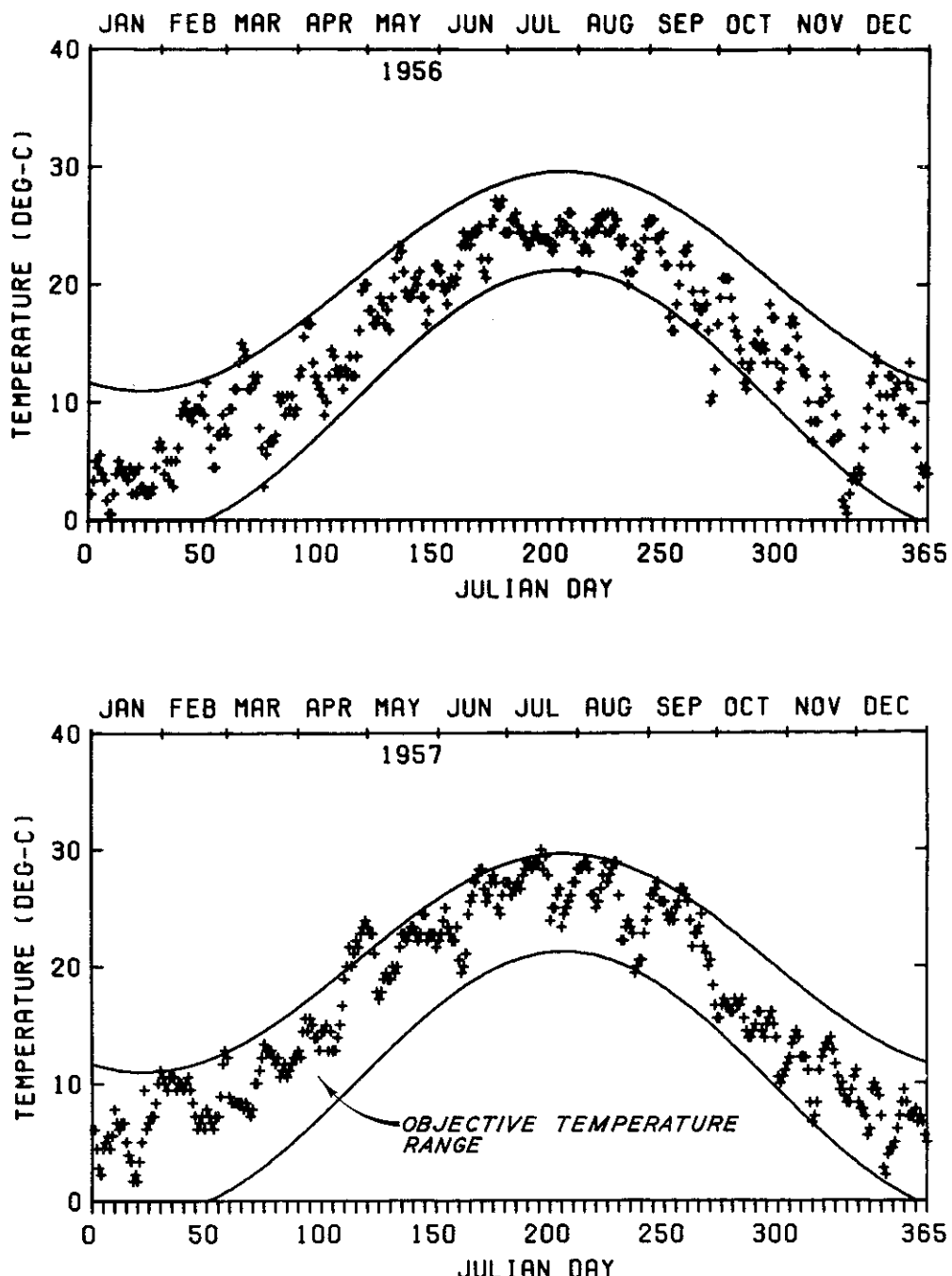
B. EVERETT JORDAN LAKE  
COMPUTED STREAM TEMPERATURE  
1950 - 1951



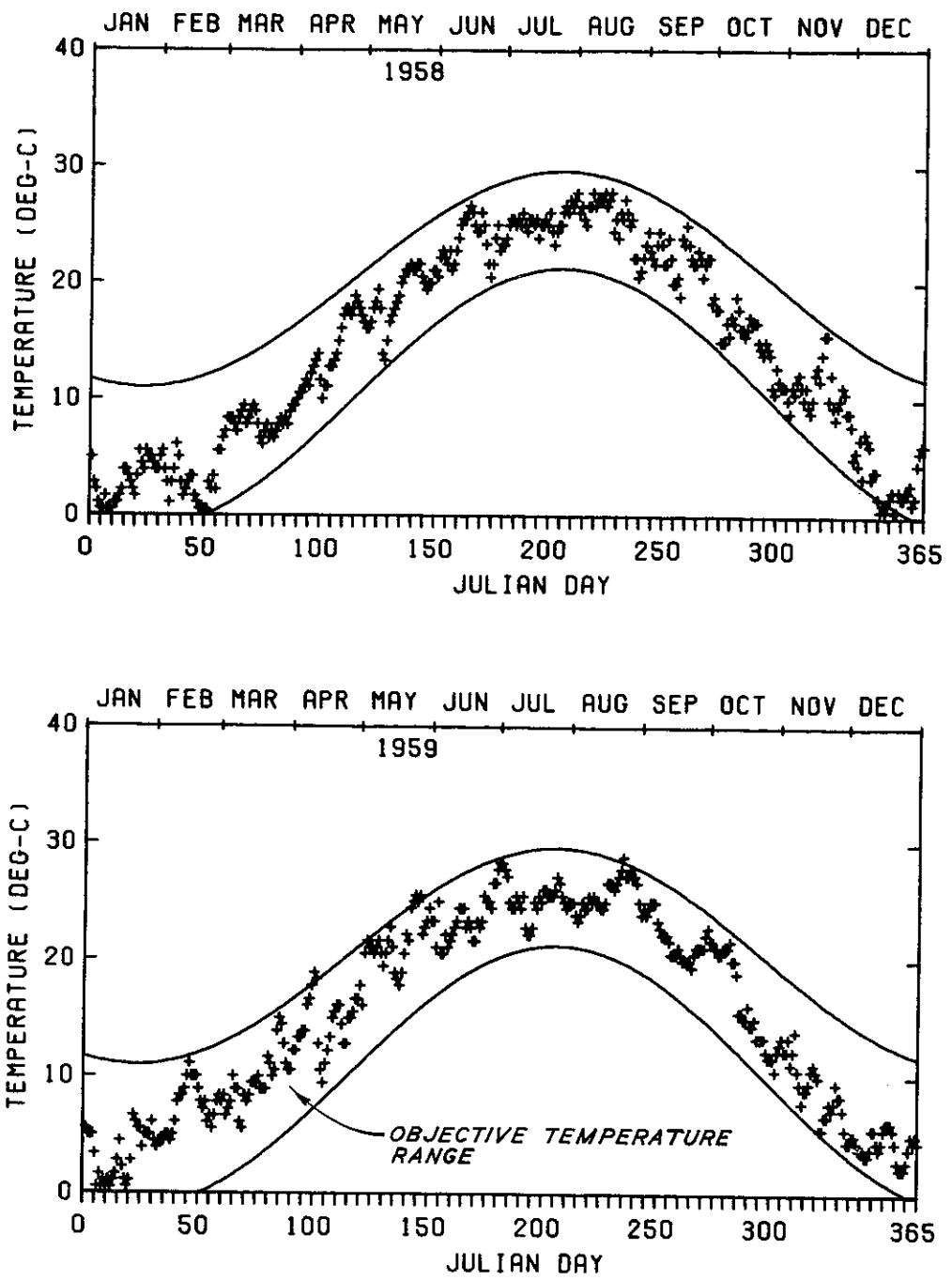
B. EVERETT JORDAN LAKE  
COMPUTED STREAM TEMPERATURE  
1952 - 1953



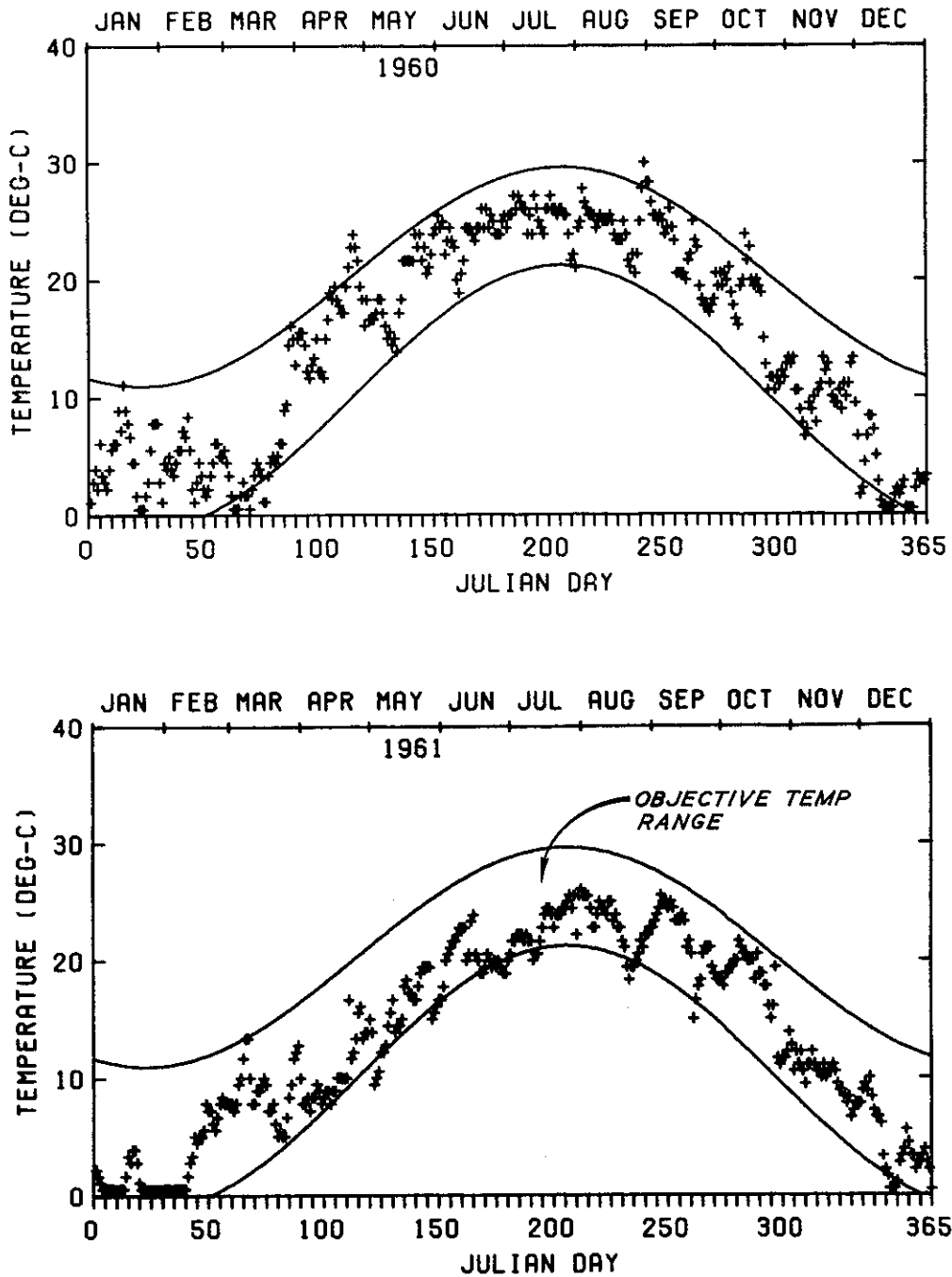
B. EVERETT JORDAN LAKE  
COMPUTED STREAM TEMPERATURE  
1954 - 1955



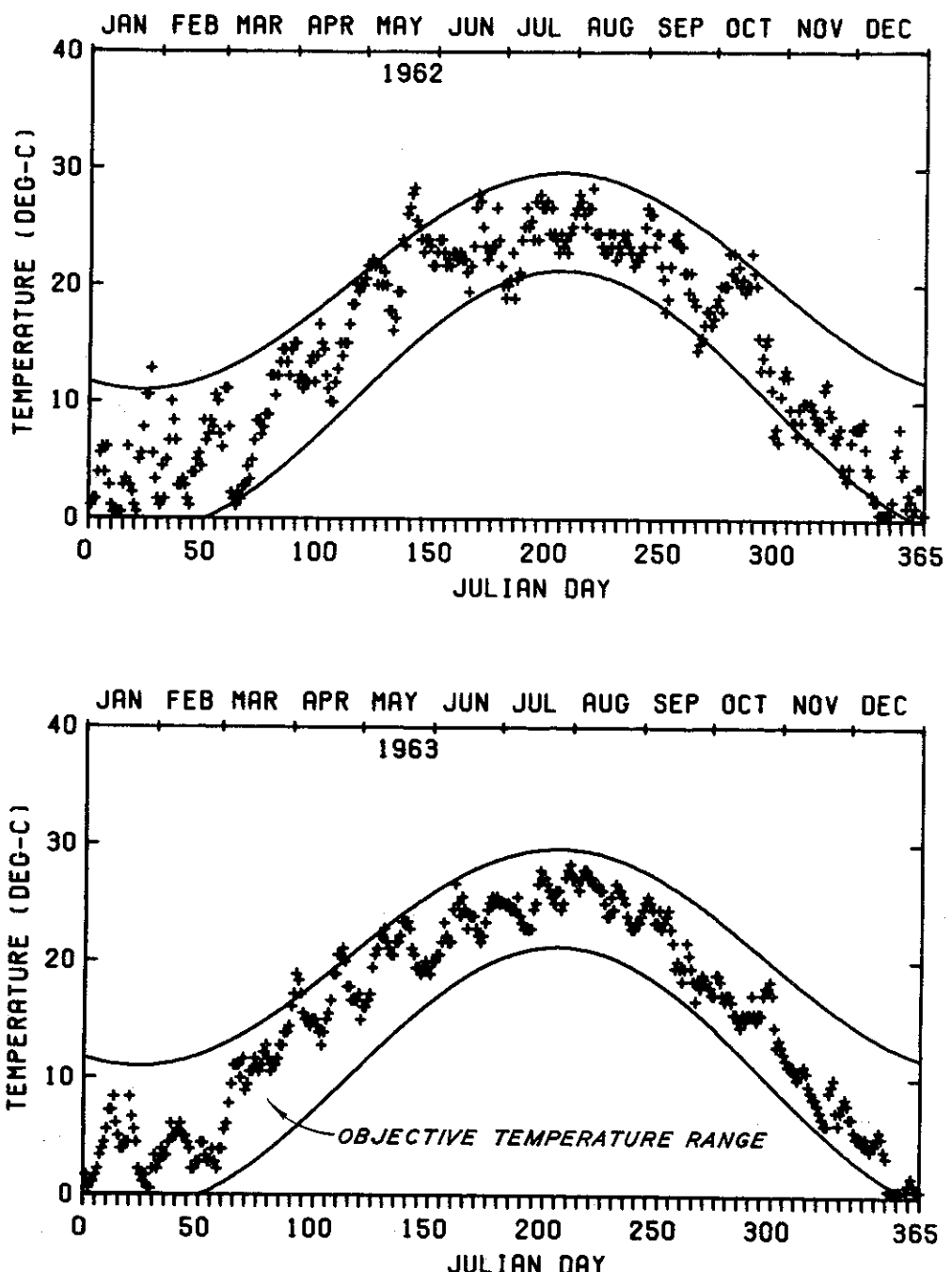
B. EVERETT JORDAN LAKE  
COMPUTED STREAM TEMPERATURE  
1956 - 1957



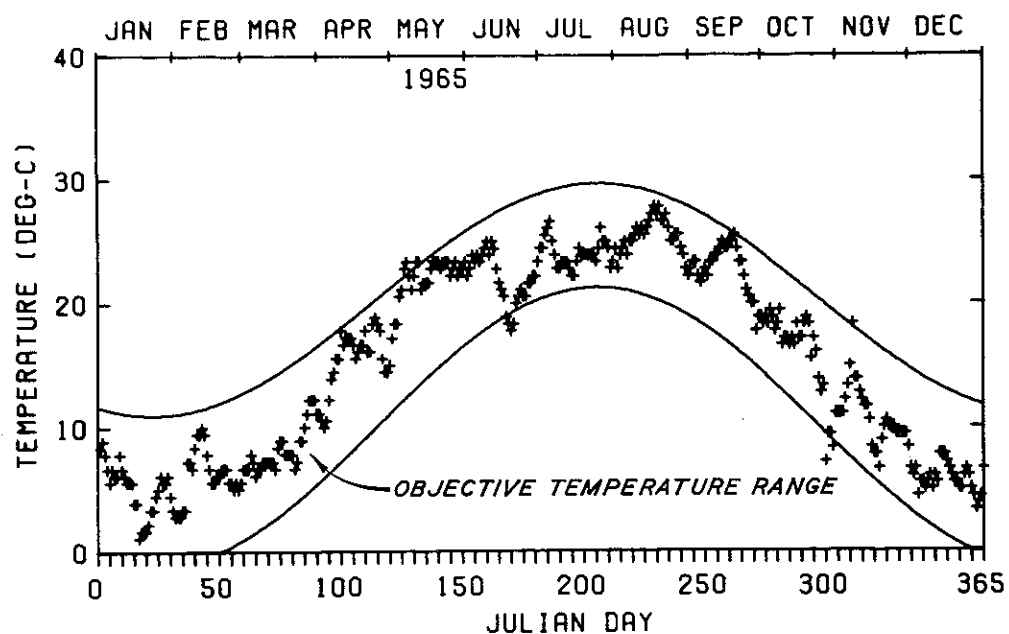
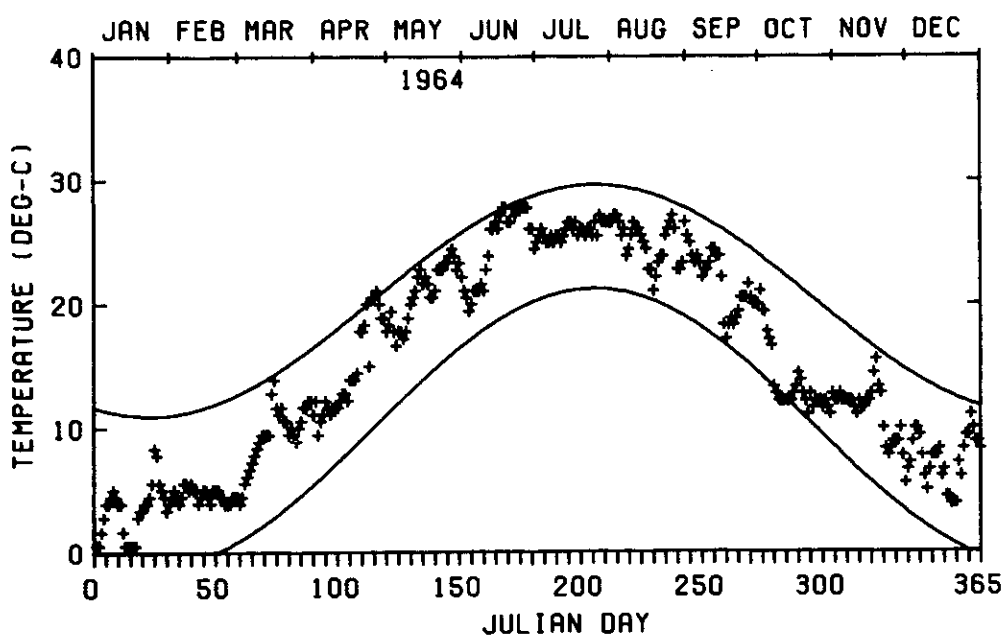
B. EVERETT JORDAN LAKE  
COMPUTED STREAM TEMPERATURE  
1958 - 1959



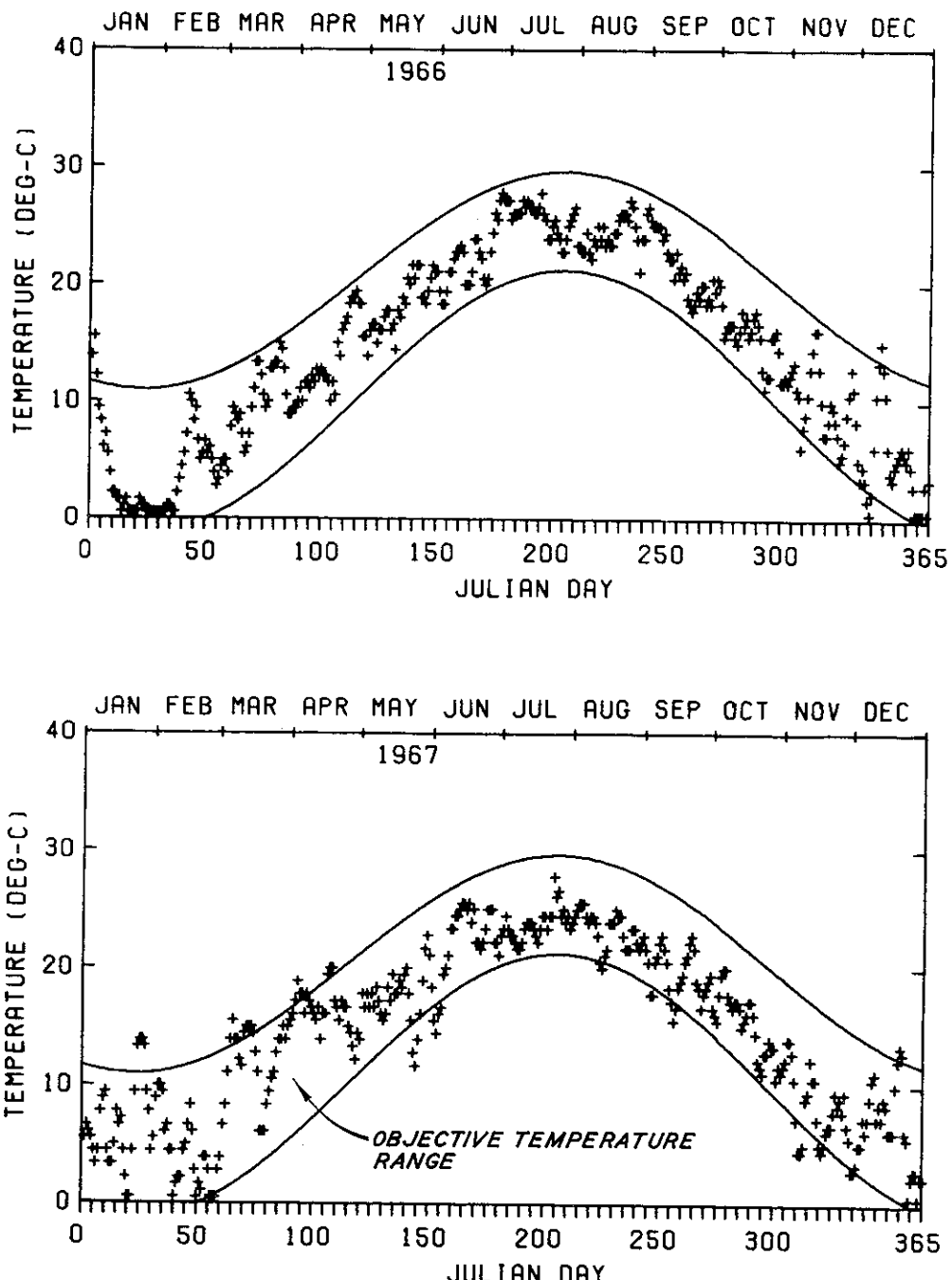
B. EVERETT JORDAN LAKE  
COMPUTED STREAM TEMPERATURE  
1960 - 1961



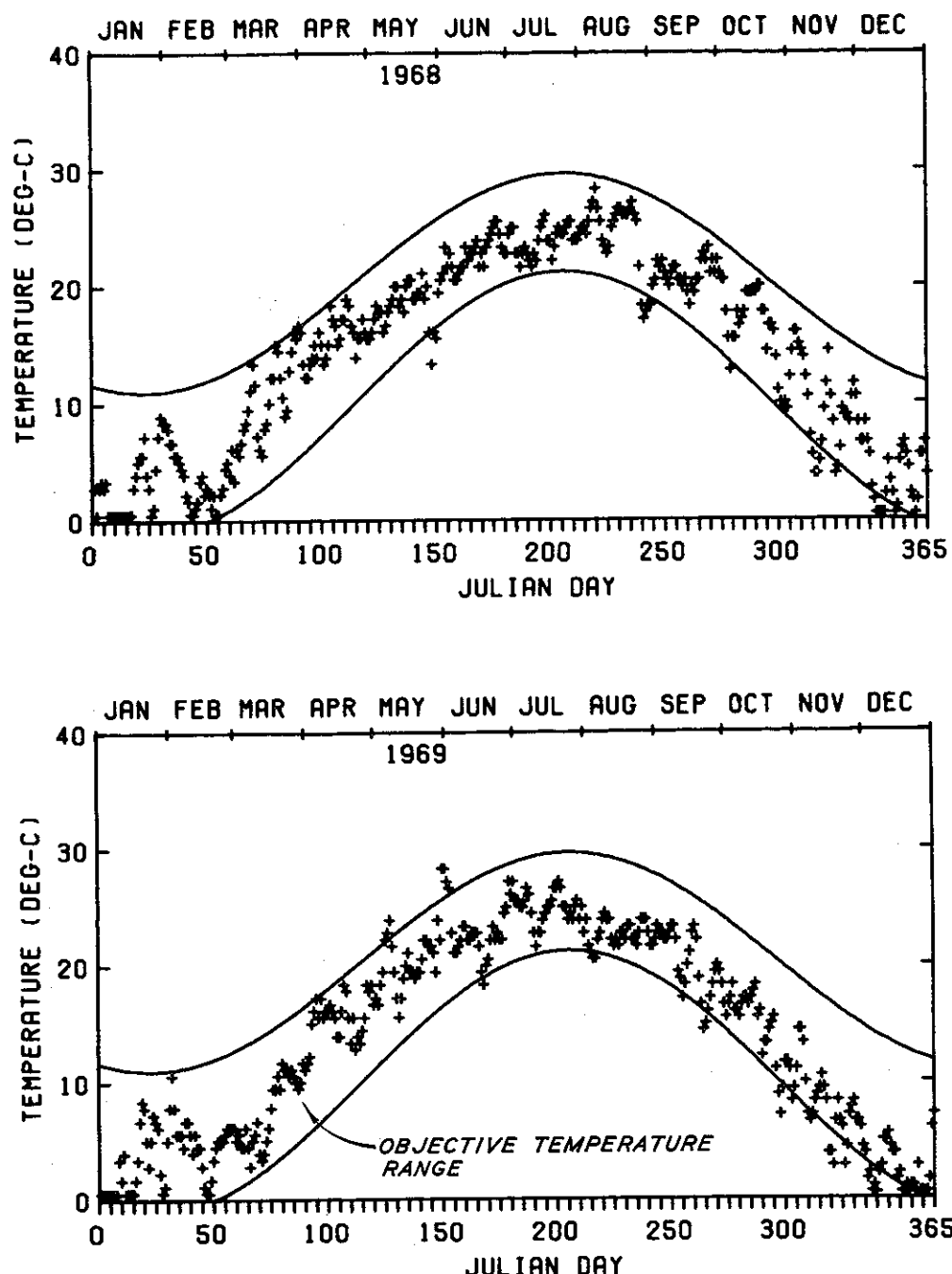
B. EVERETT JORDAN LAKE  
COMPUTED STREAM TEMPERATURE  
1962 - 1963



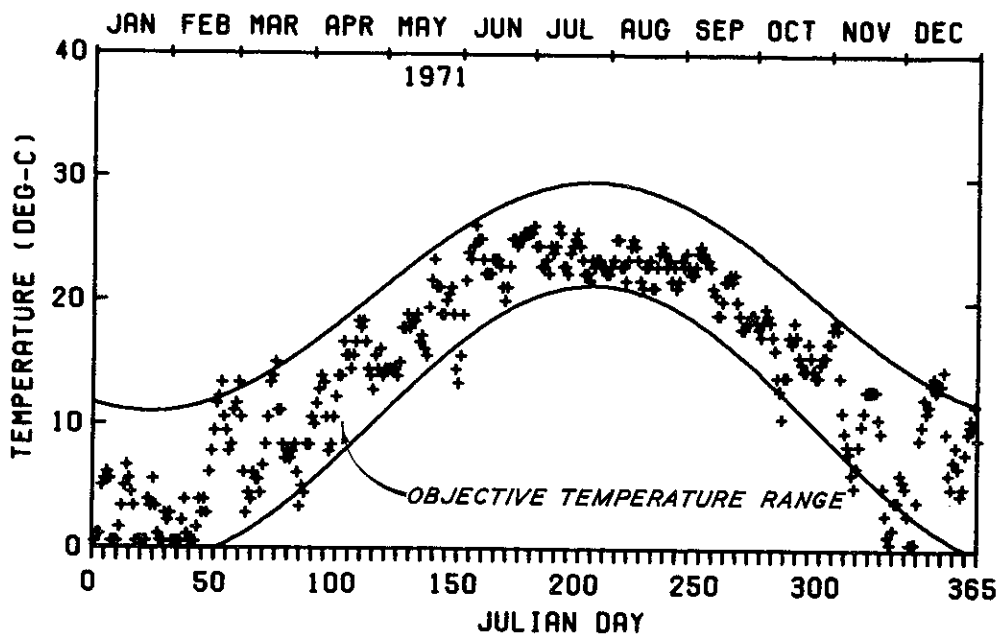
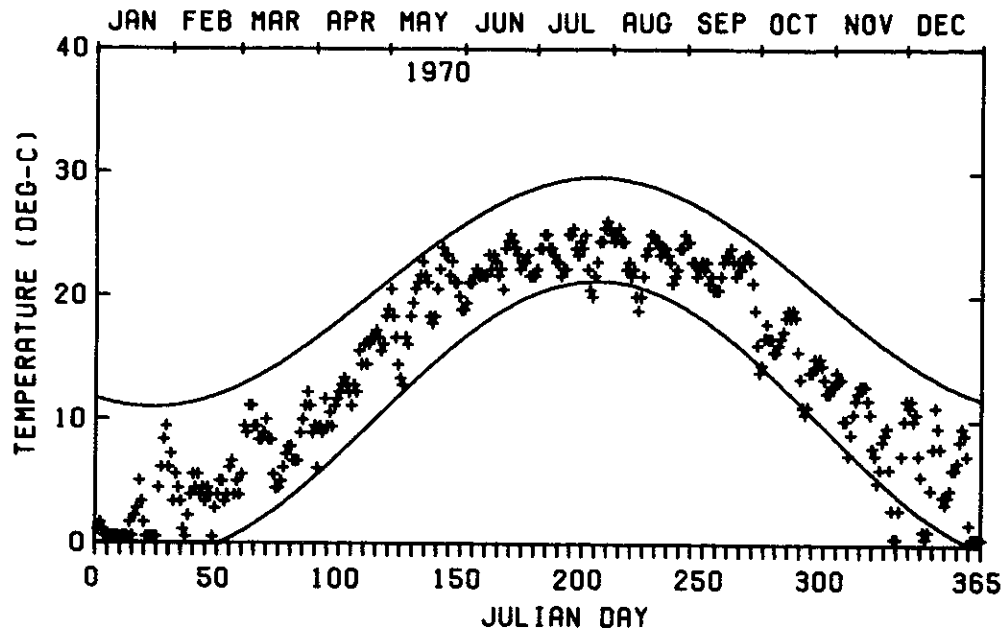
B. EVERETT JORDAN LAKE  
COMPUTED STREAM TEMPERATURE  
1964 - 1965



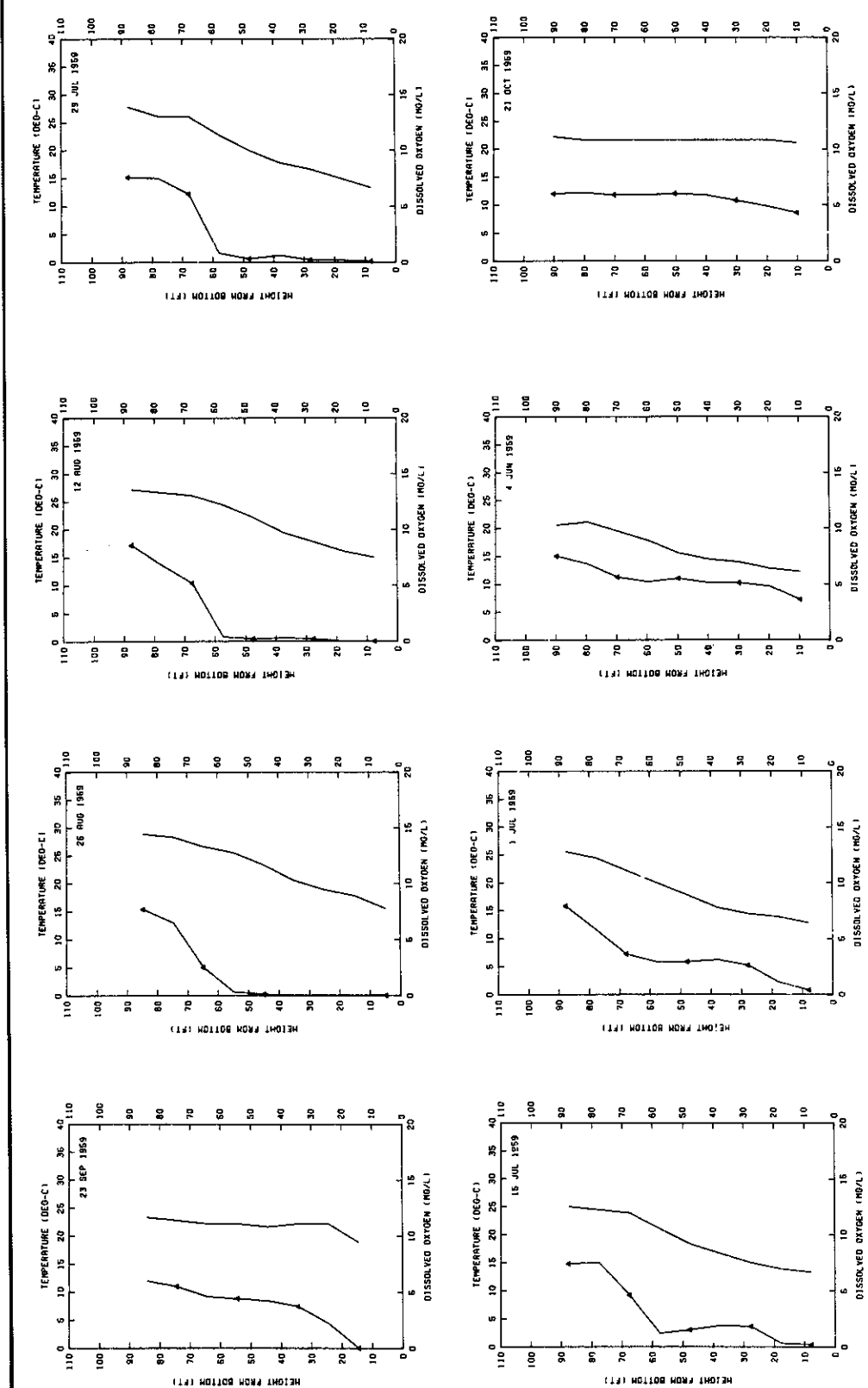
B. EVERETT JORDAN LAKE  
COMPUTED STREAM TEMPERATURE  
1966 - 1967



B. EVERETT JORDAN LAKE  
COMPUTED STREAM TEMPERATURE  
1968 - 1969

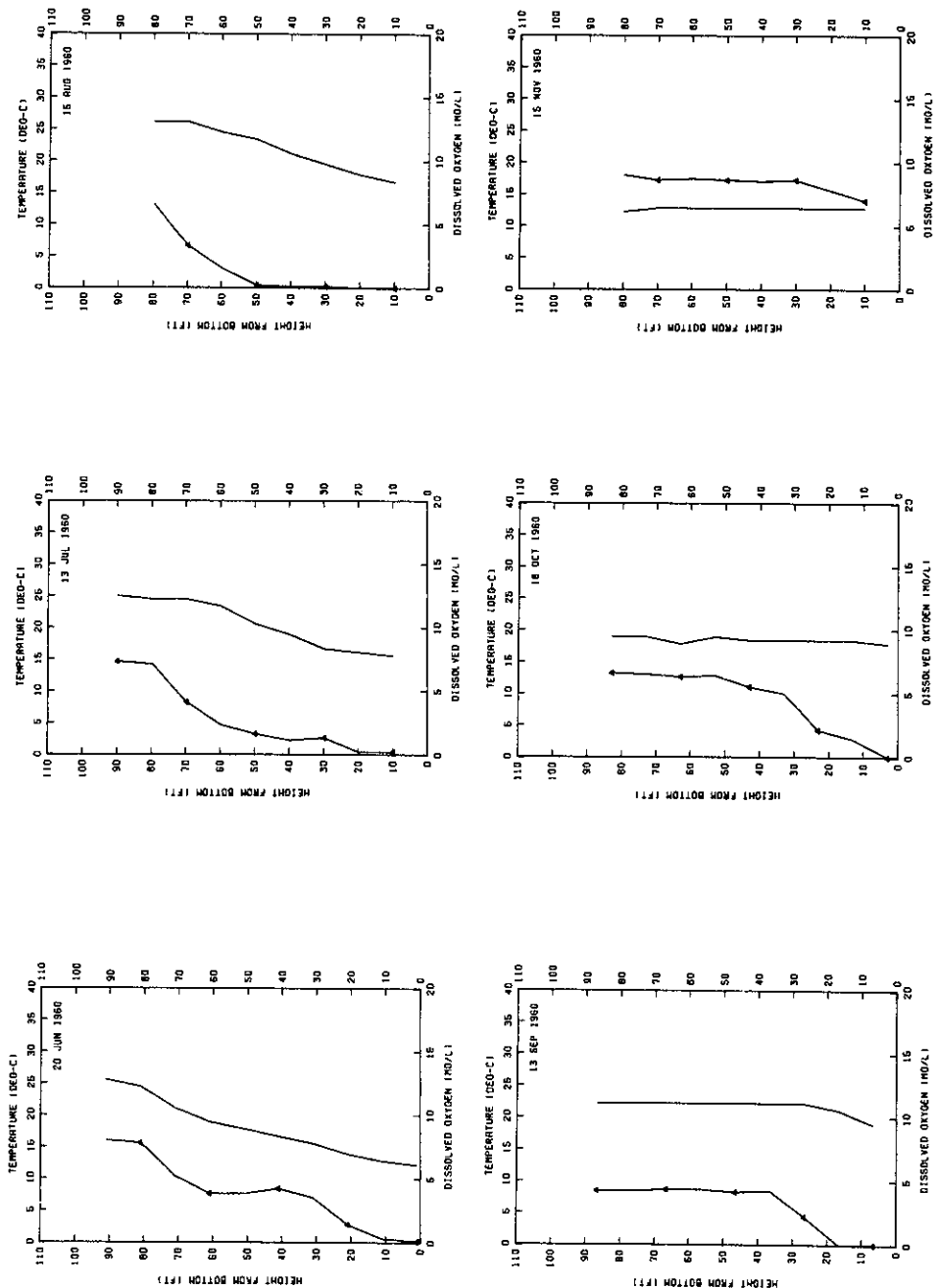


B. EVERETT JORDAN LAKE  
COMPUTED STREAM TEMPERATURE  
1970 - 1971



JOHN H KERR LAKE  
OBSERVED PROFILES  
4 JUN 1959 - 21 OCT 1959

LEGEND  
— TEMP  
← D.O.



JOHN H KERR LAKE  
OBSERVED PROFILES  
20 JUN 1960 - 15 NOV 1960

LEGEND  
 — TEMP  
 ▲ D.O.

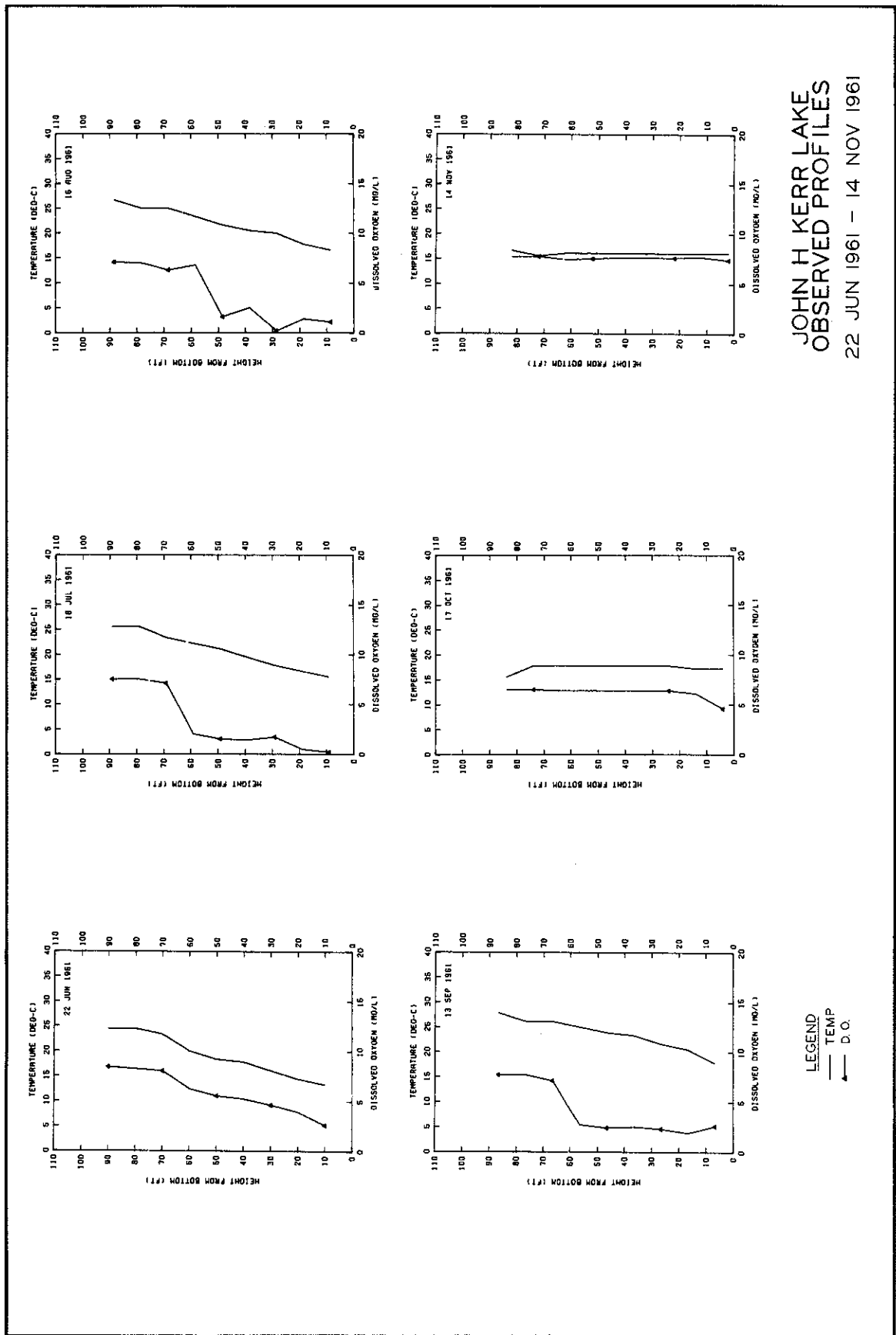
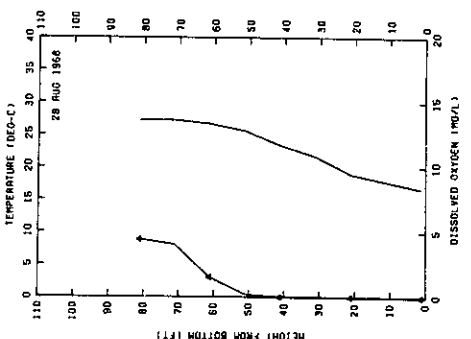
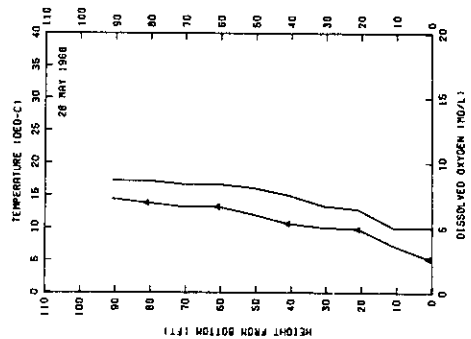
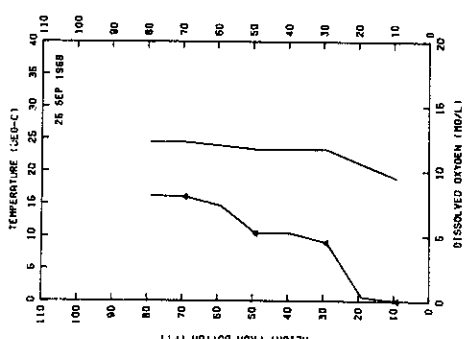
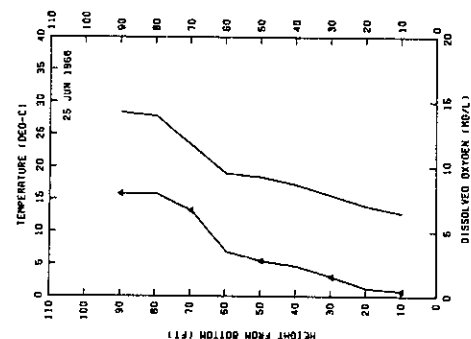
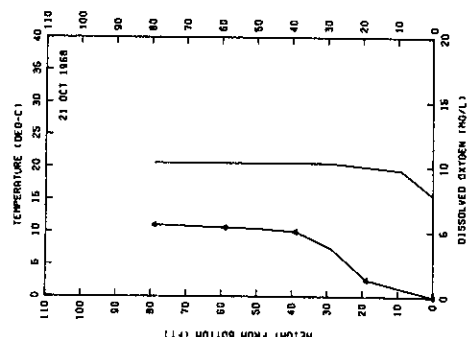
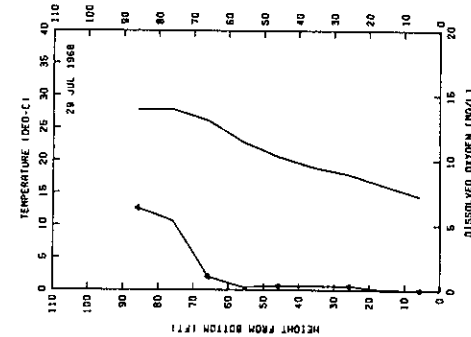


PLATE 5 (SHEET 3 OF 4)



JOHN H KERR LAKE  
OBSERVED PROFILES  
28 MAY 1968 - 21 OCT 1968

LEGEND

— TEMP

▲ D.O.

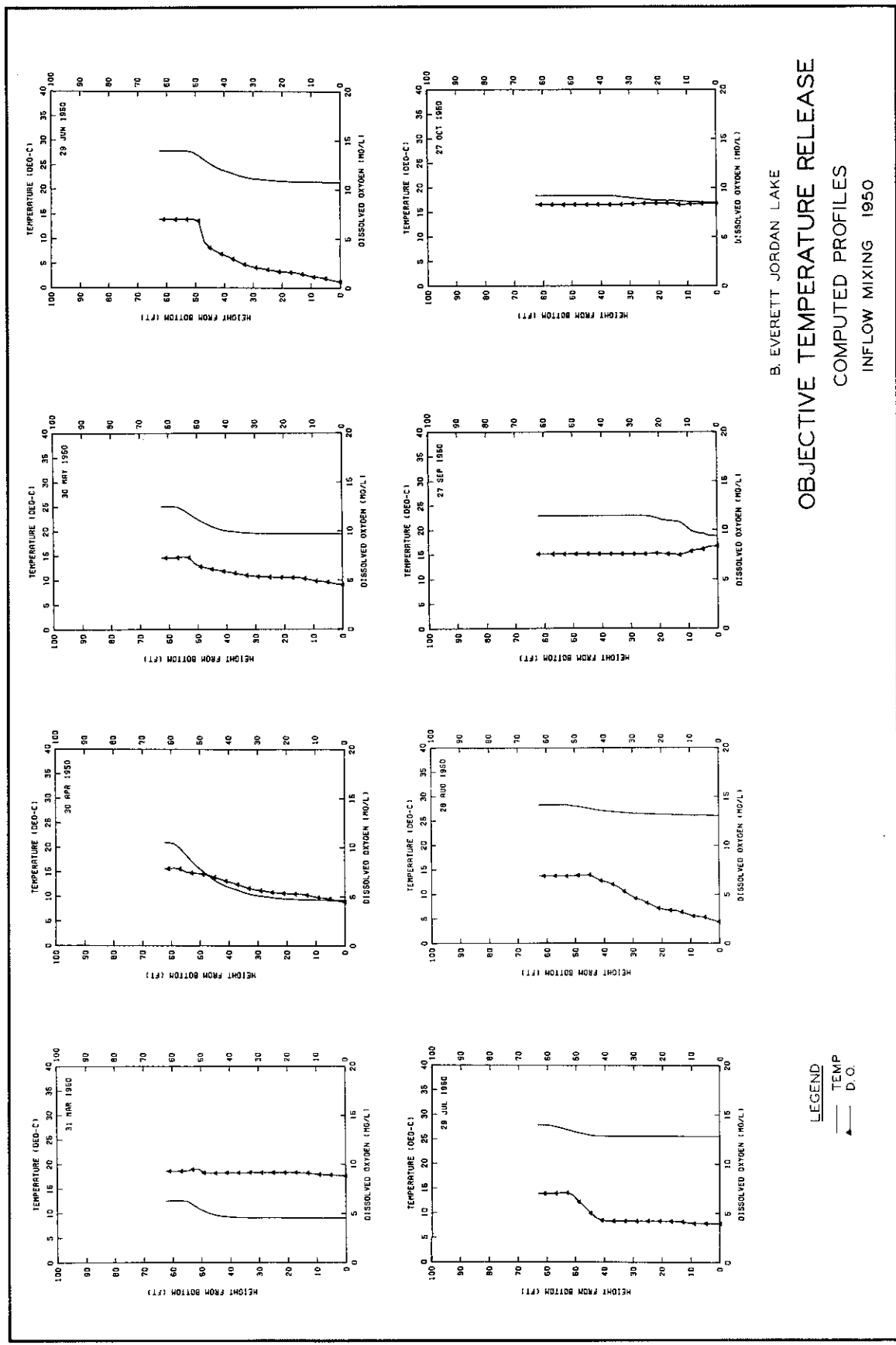
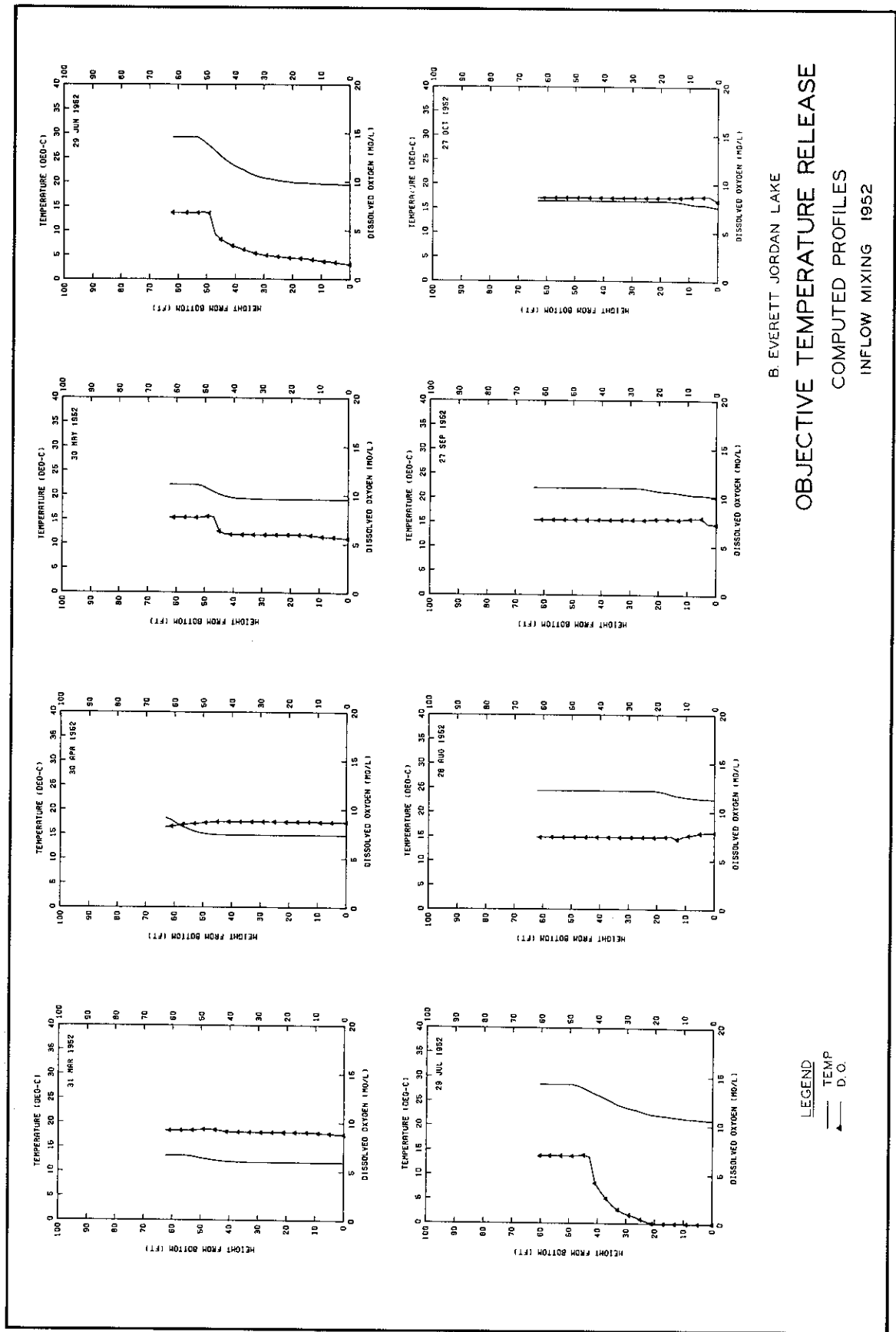
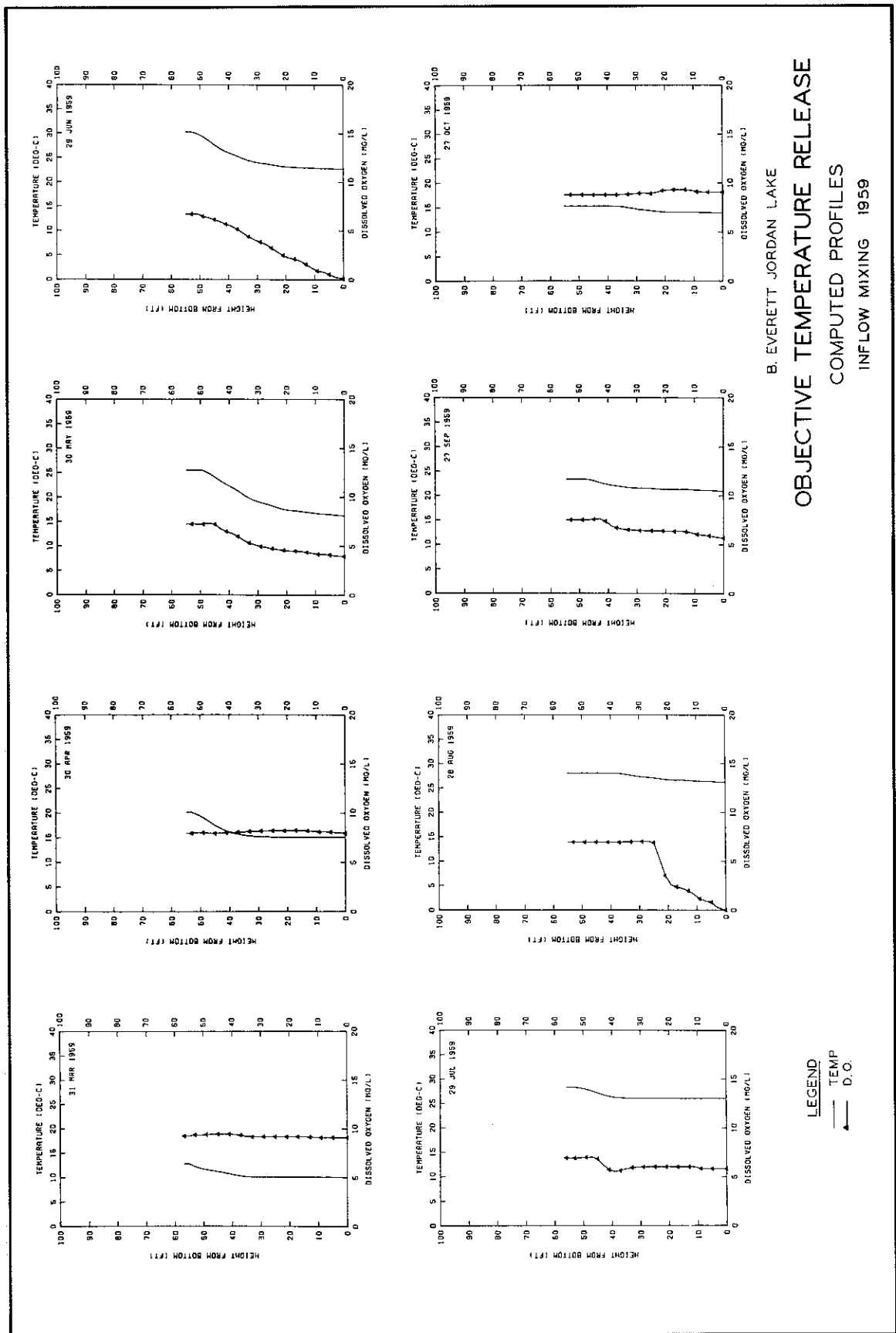
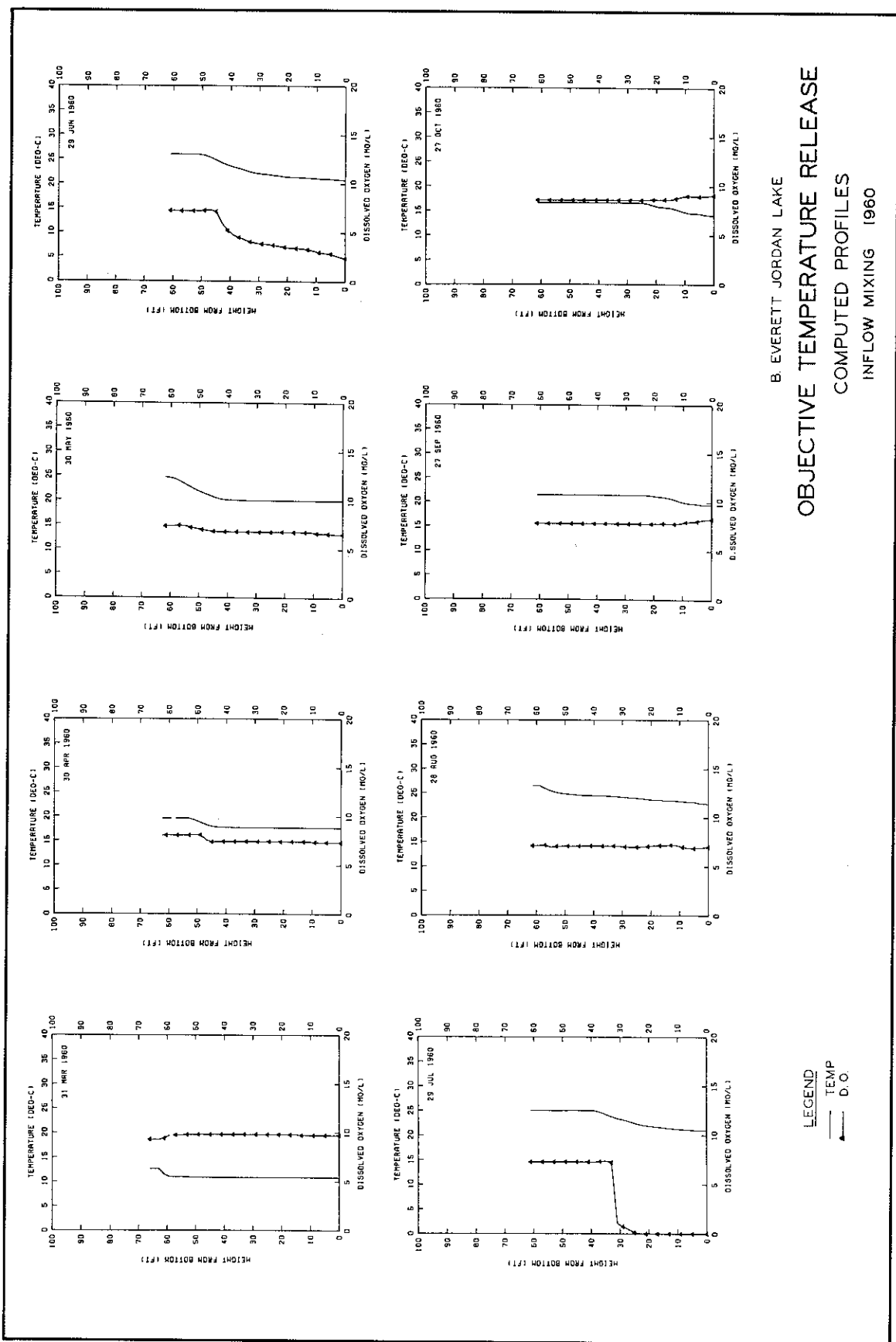
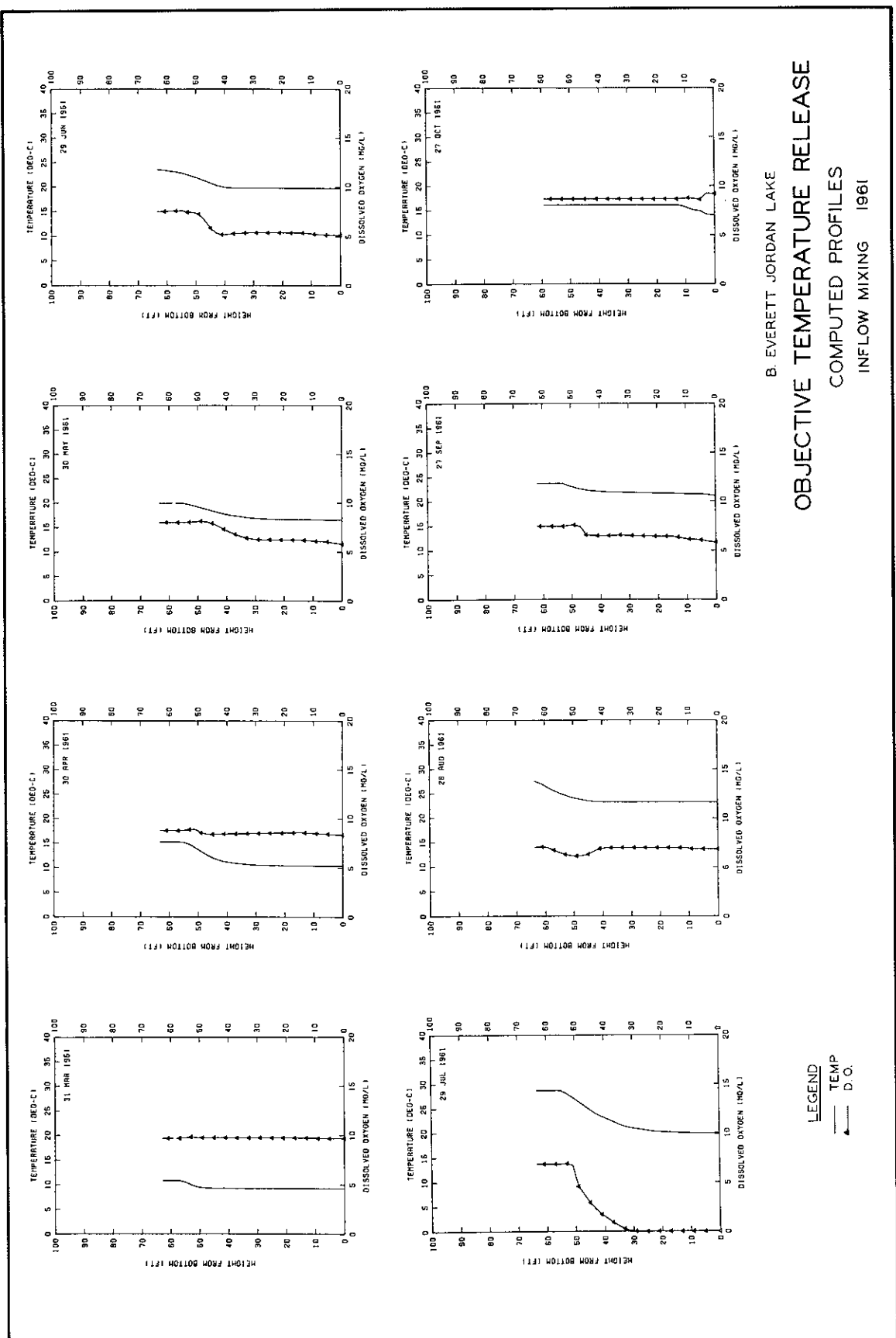


PLATE 6 (SHEET 1 OF 6)

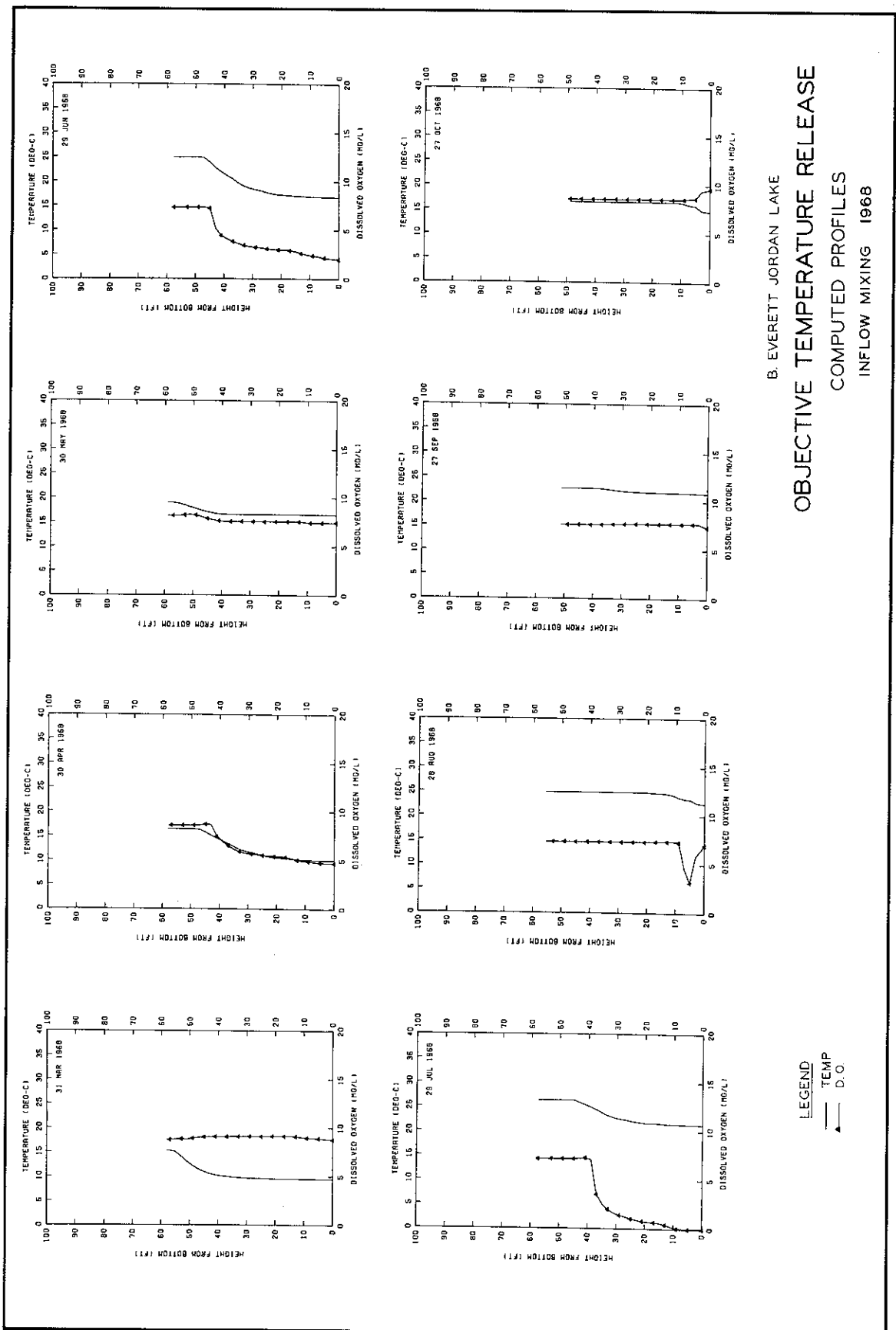


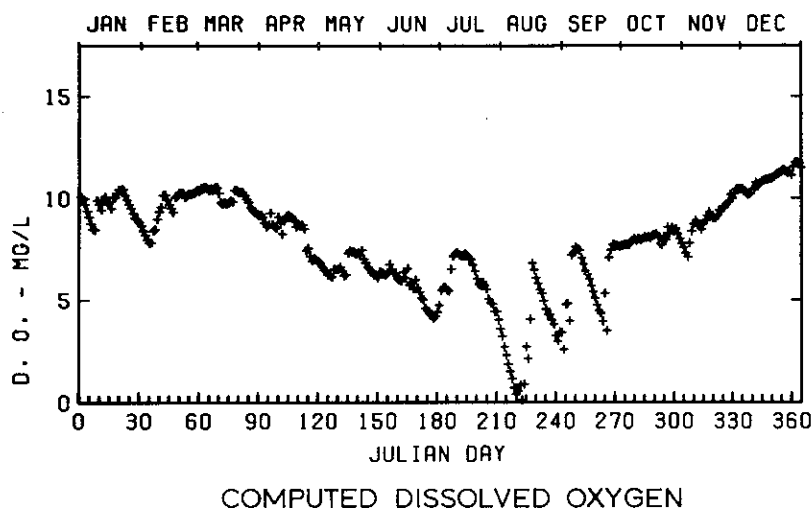
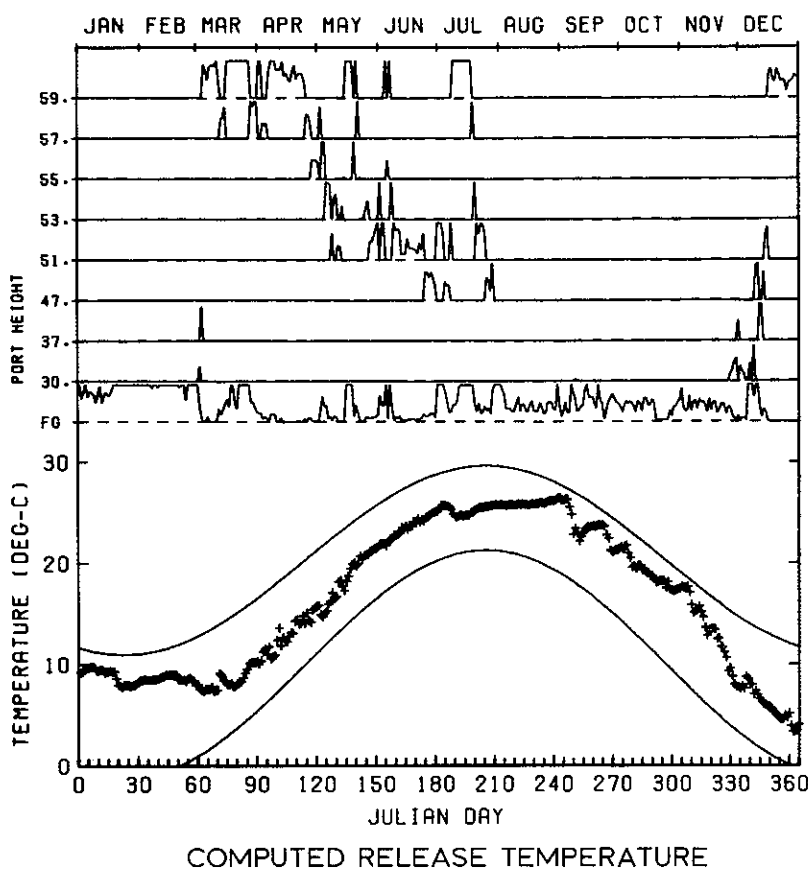




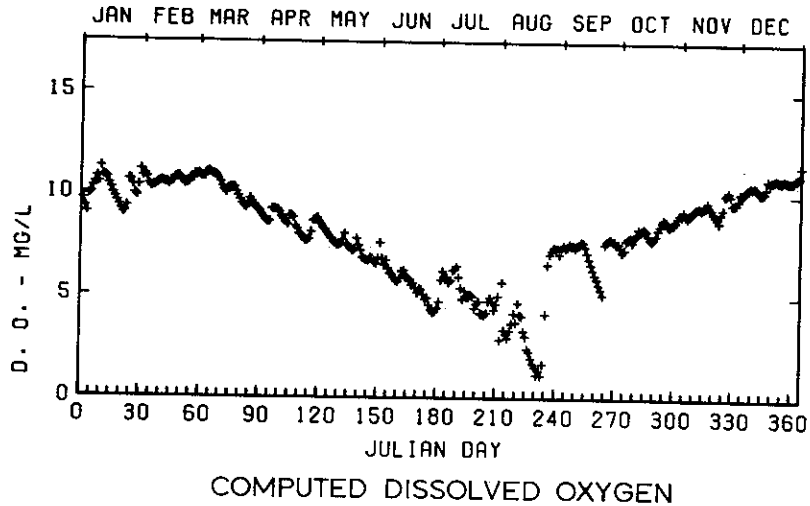
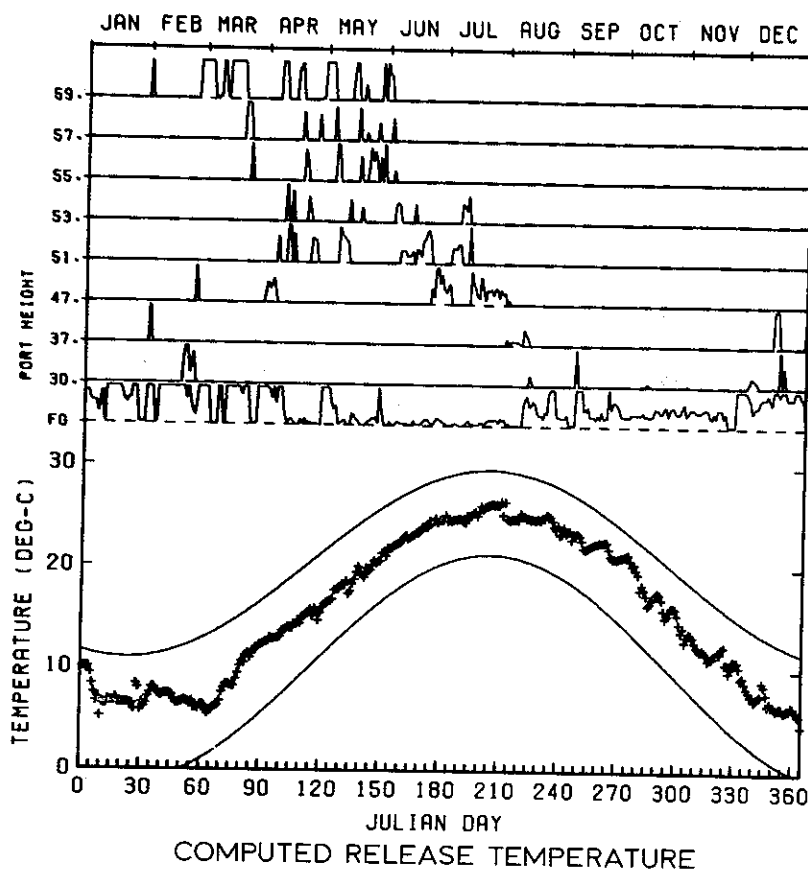


B. EVERETT JORDAN LAKE  
OBJECTIVE TEMPERATURE RELEASE  
COMPUTED PROFILES  
INFLOW MIXING 1961

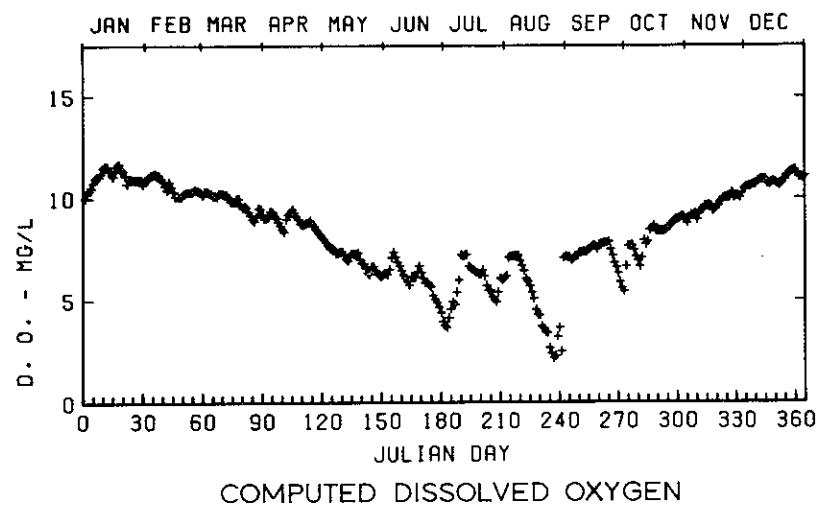
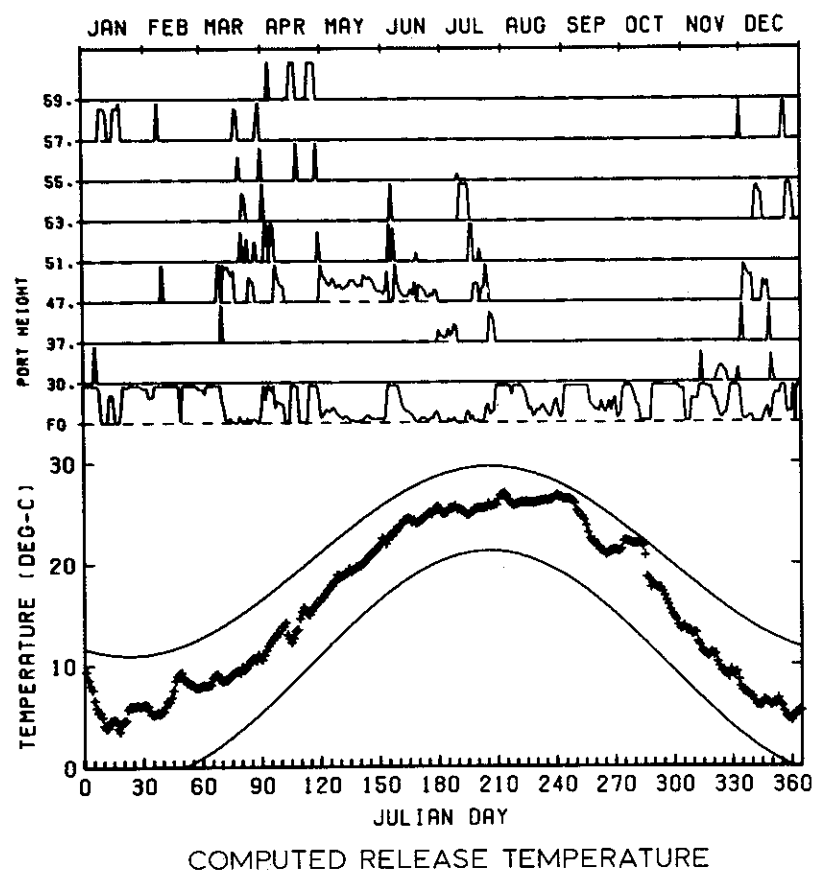




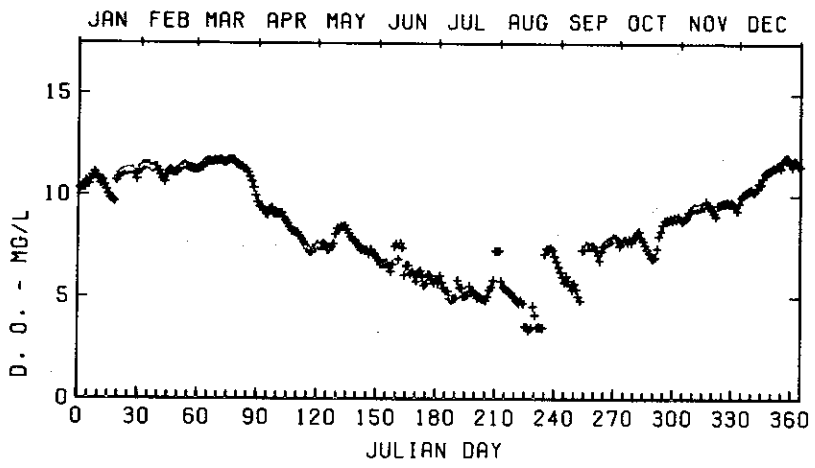
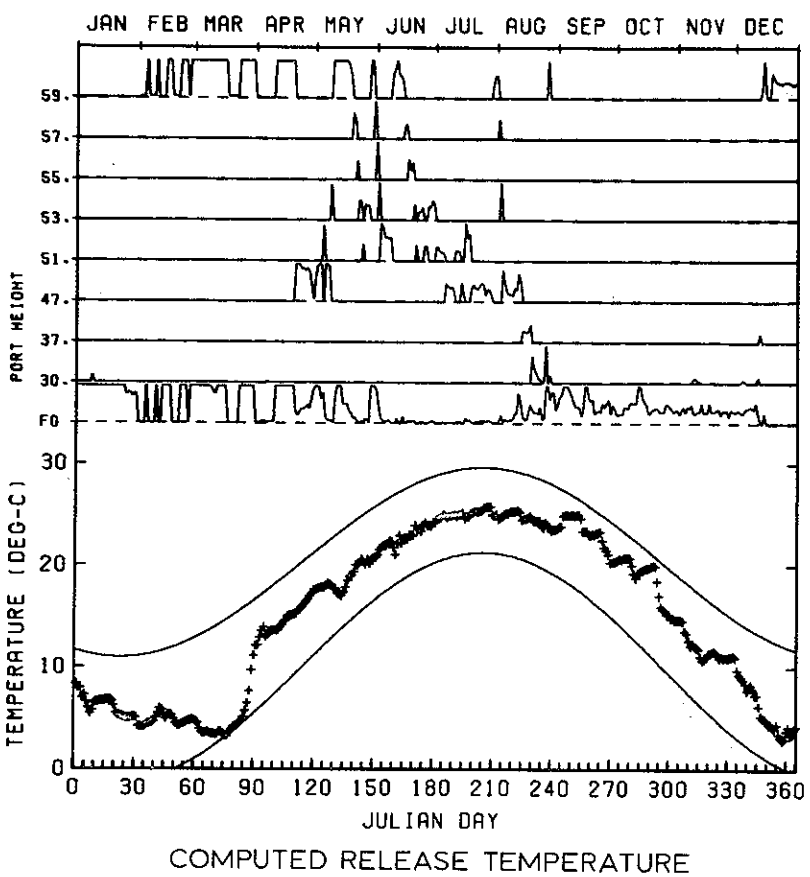
B. EVERETT JORDAN LAKE  
OBJECTIVE TEMPERATURE RELEASE  
INFLOW MIXING  
1950



B. EVERETT JORDAN LAKE  
OBJECTIVE TEMPERATURE RELEASE  
INFLOW MIXING  
1952

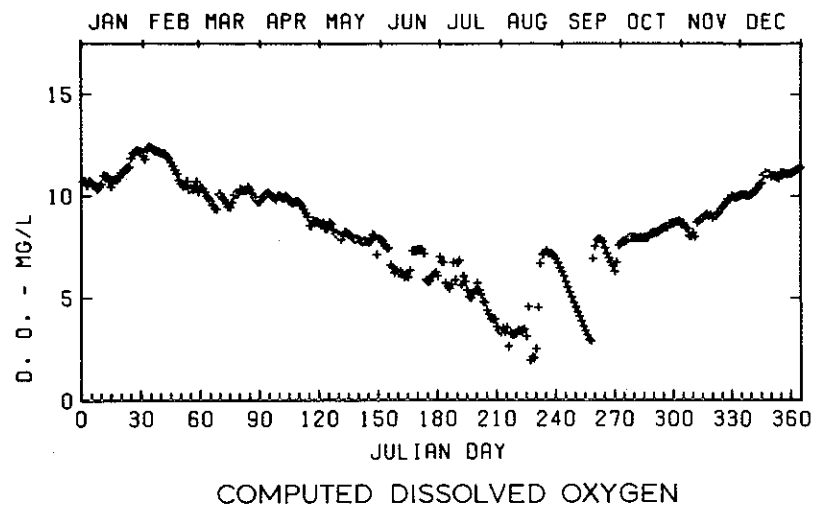
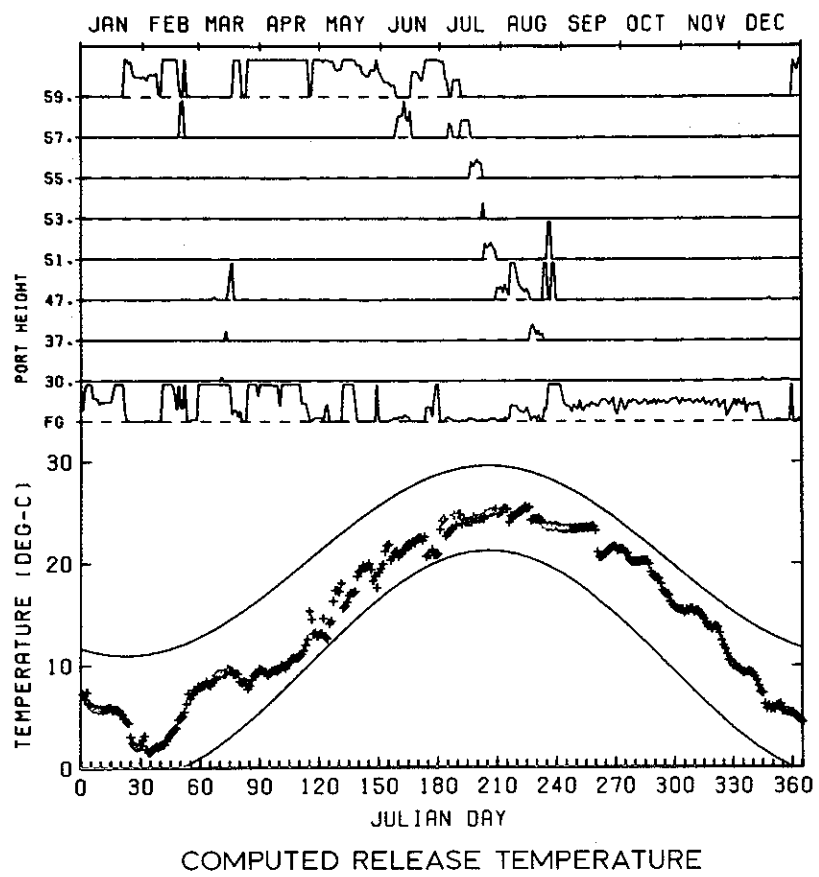


B. EVERETT JORDAN LAKE  
OBJECTIVE TEMPERATURE RELEASE  
INFLOW MIXING  
1959

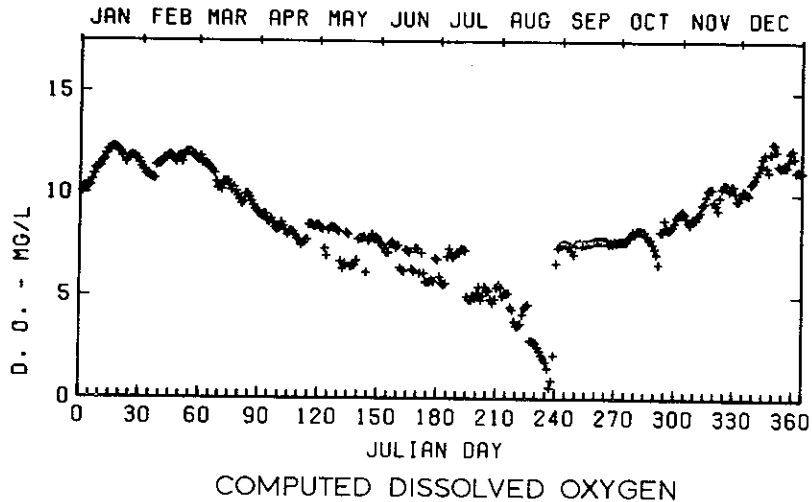
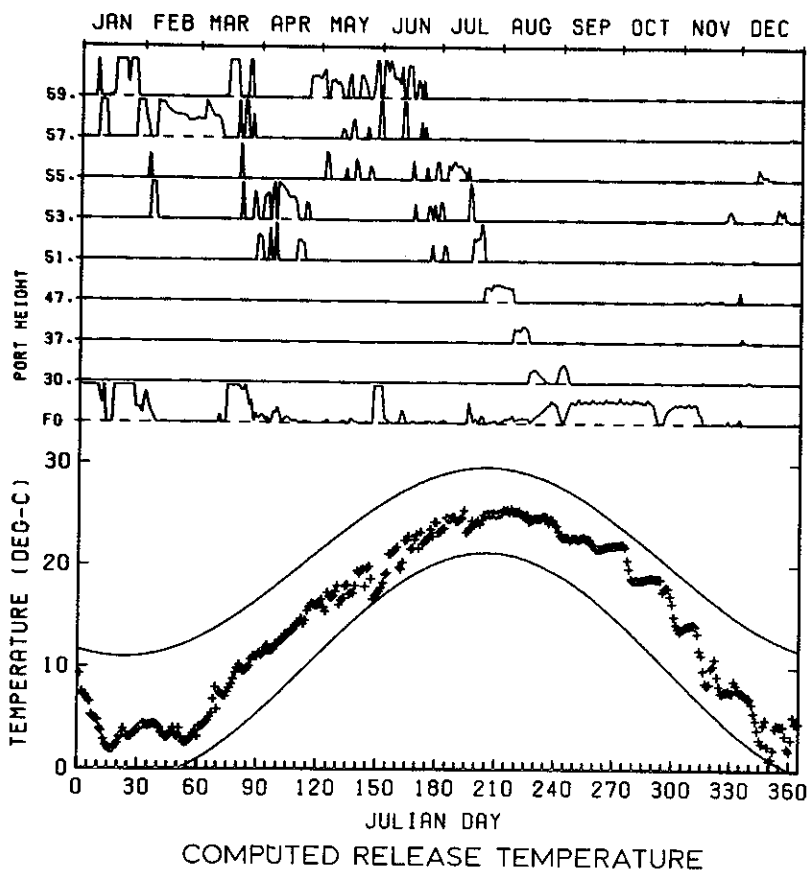


COMPUTED DISSOLVED OXYGEN

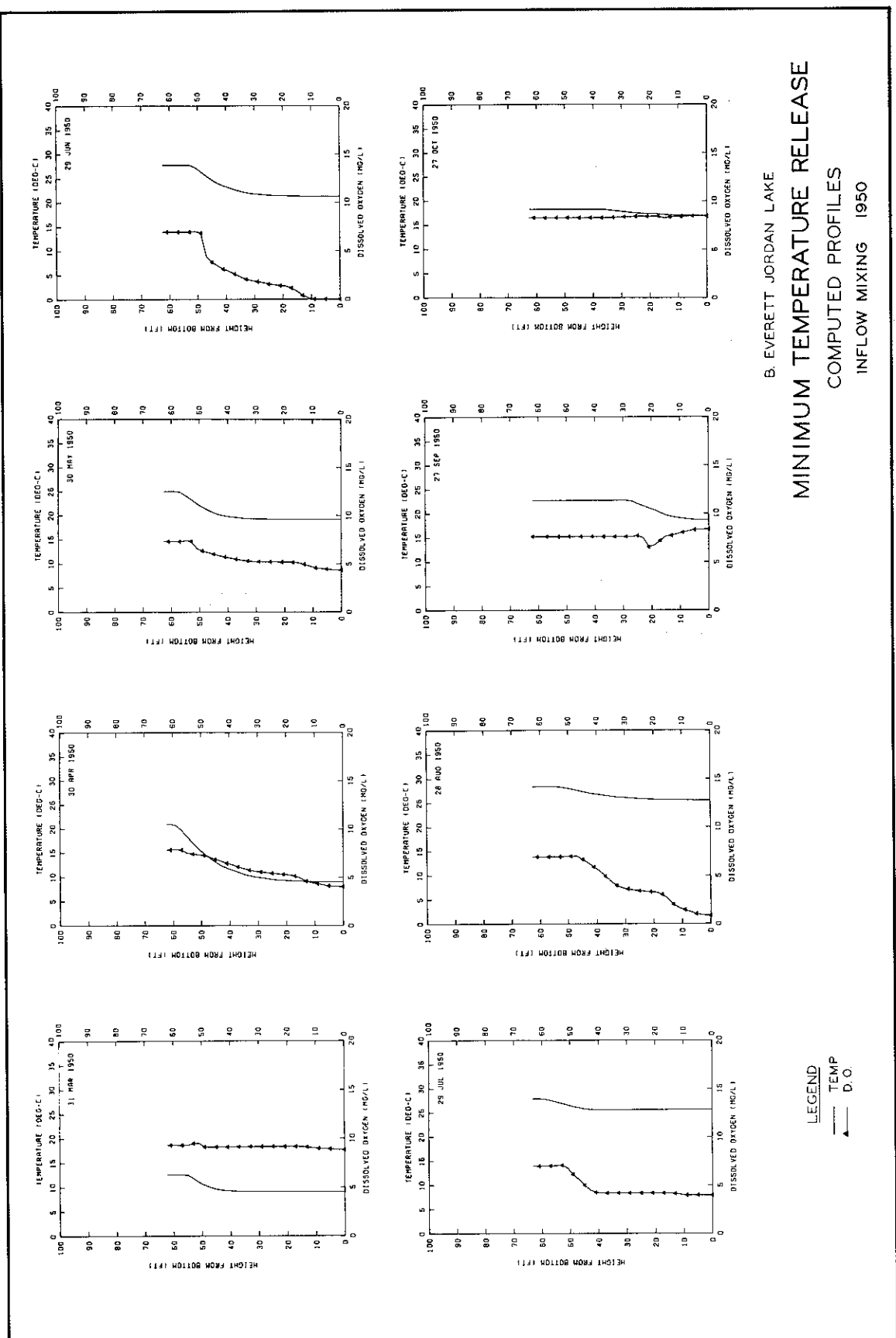
B. EVERETT JORDAN LAKE  
 OBJECTIVE TEMPERATURE RELEASE  
 INFLOW MIXING  
 1960



B. EVERETT JORDAN LAKE  
OBJECTIVE TEMPERATURE RELEASE  
INFLOW MIXING  
1961



B. EVERETT JORDAN LAKE  
OBJECTIVE TEMPERATURE RELEASE  
INFLOW MIXING  
1968



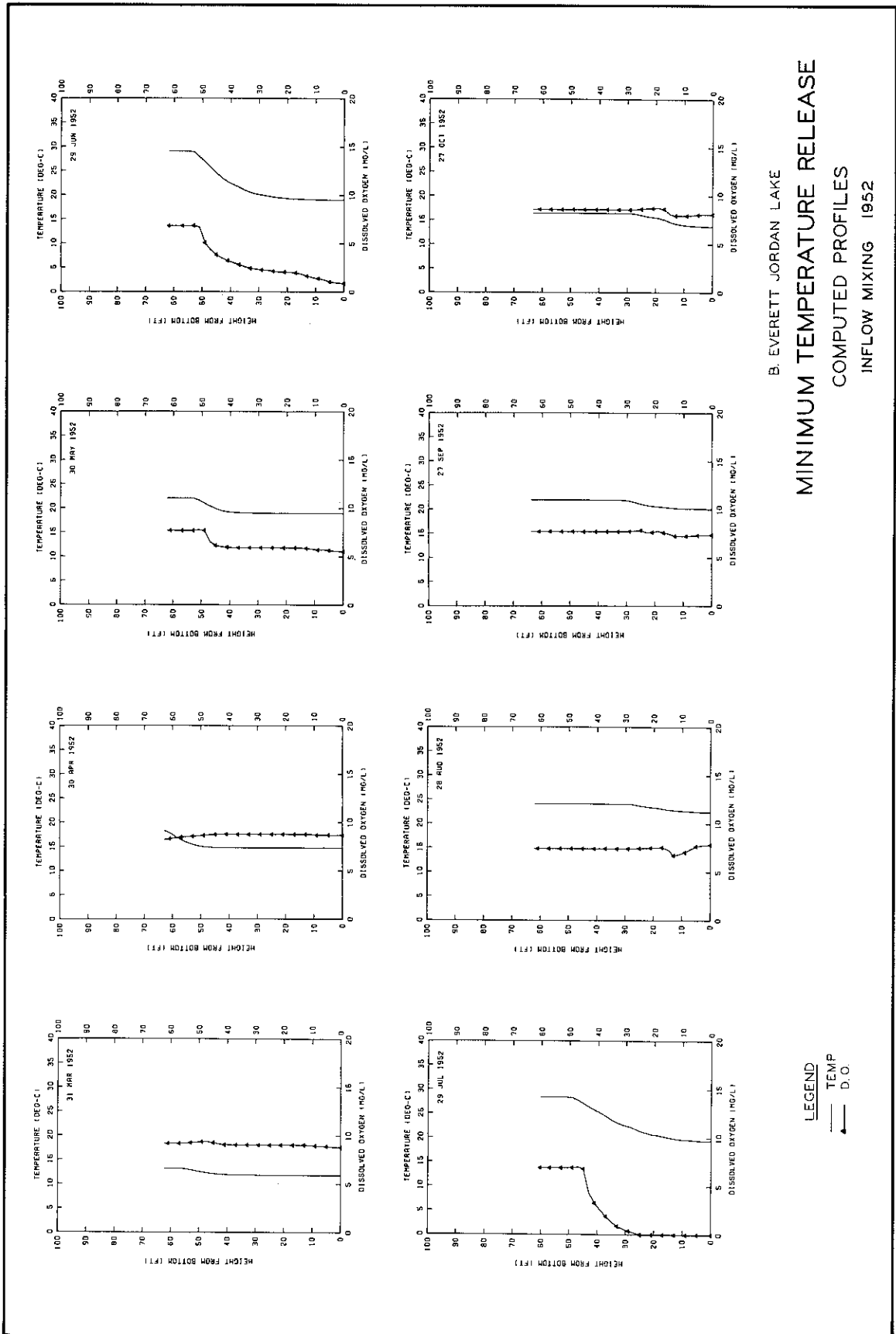
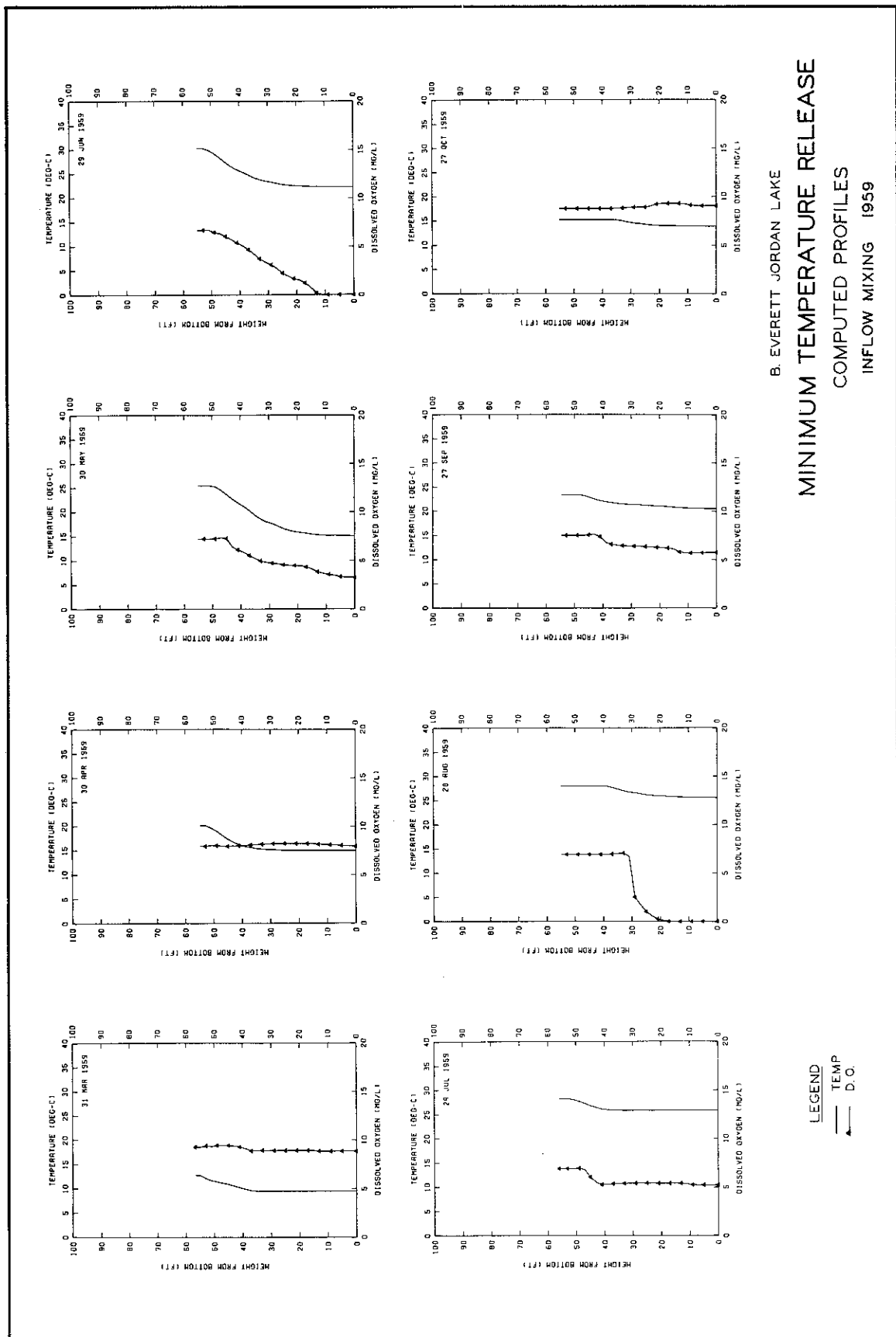
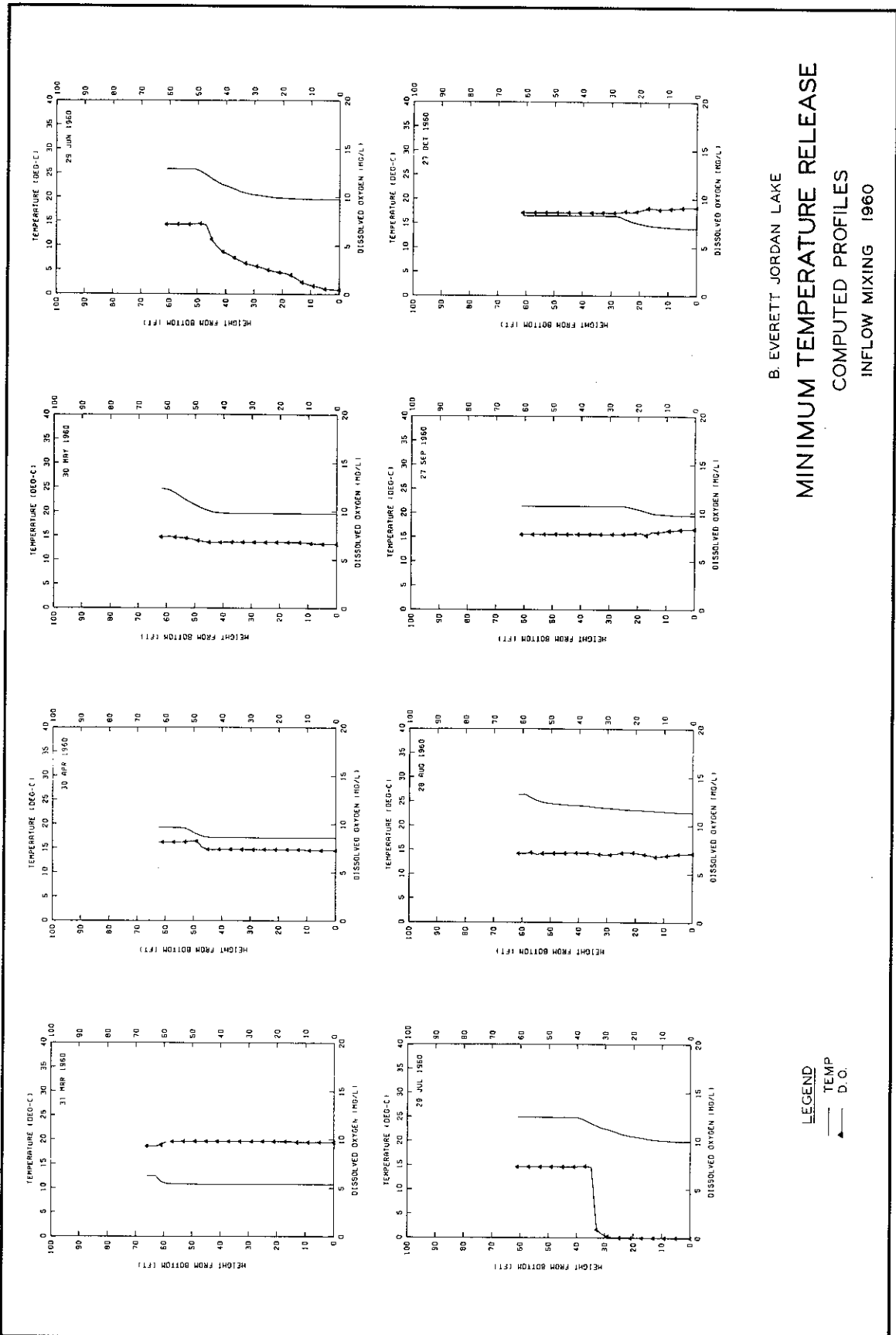
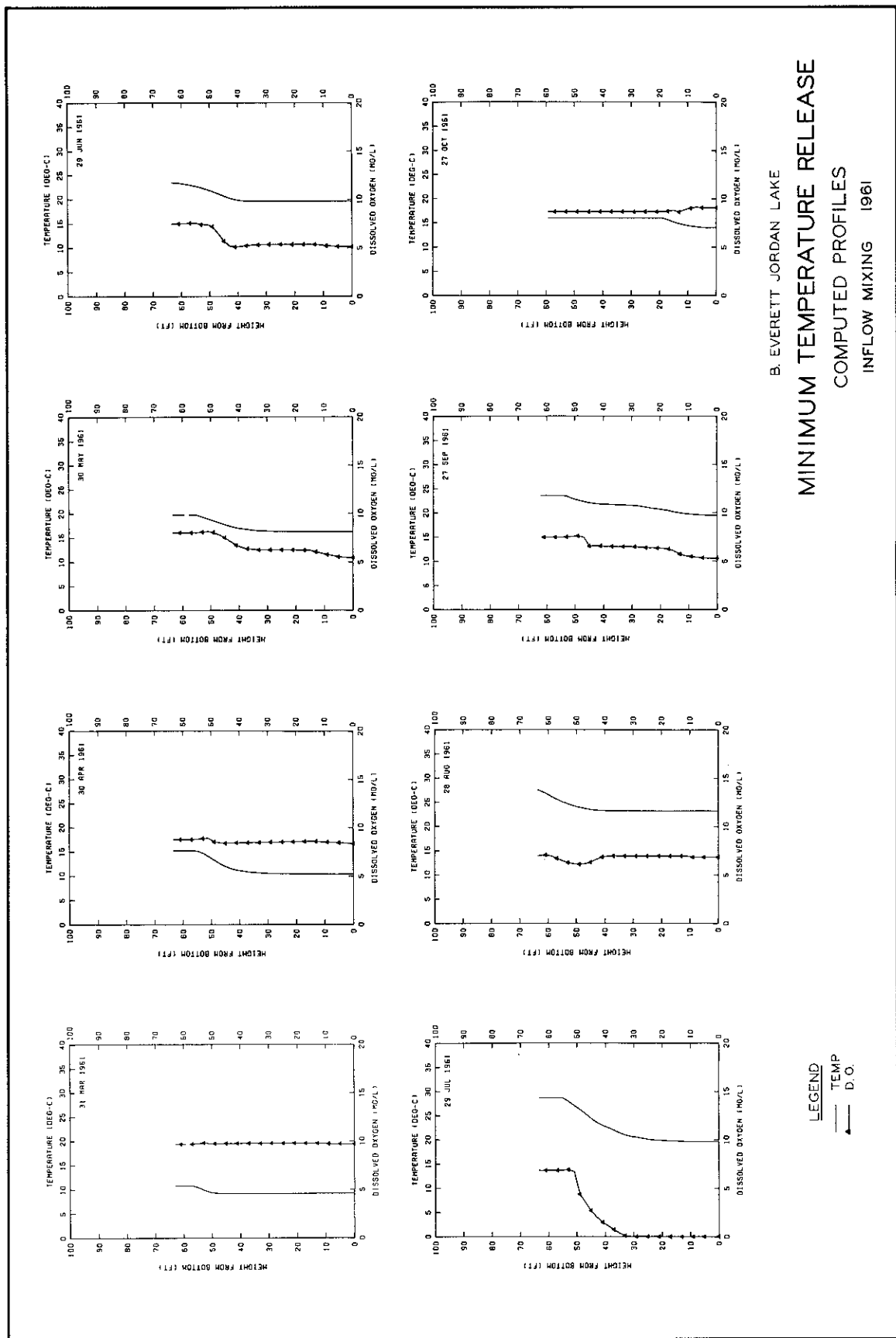


PLATE 8 (SHEET 2 OF 6)



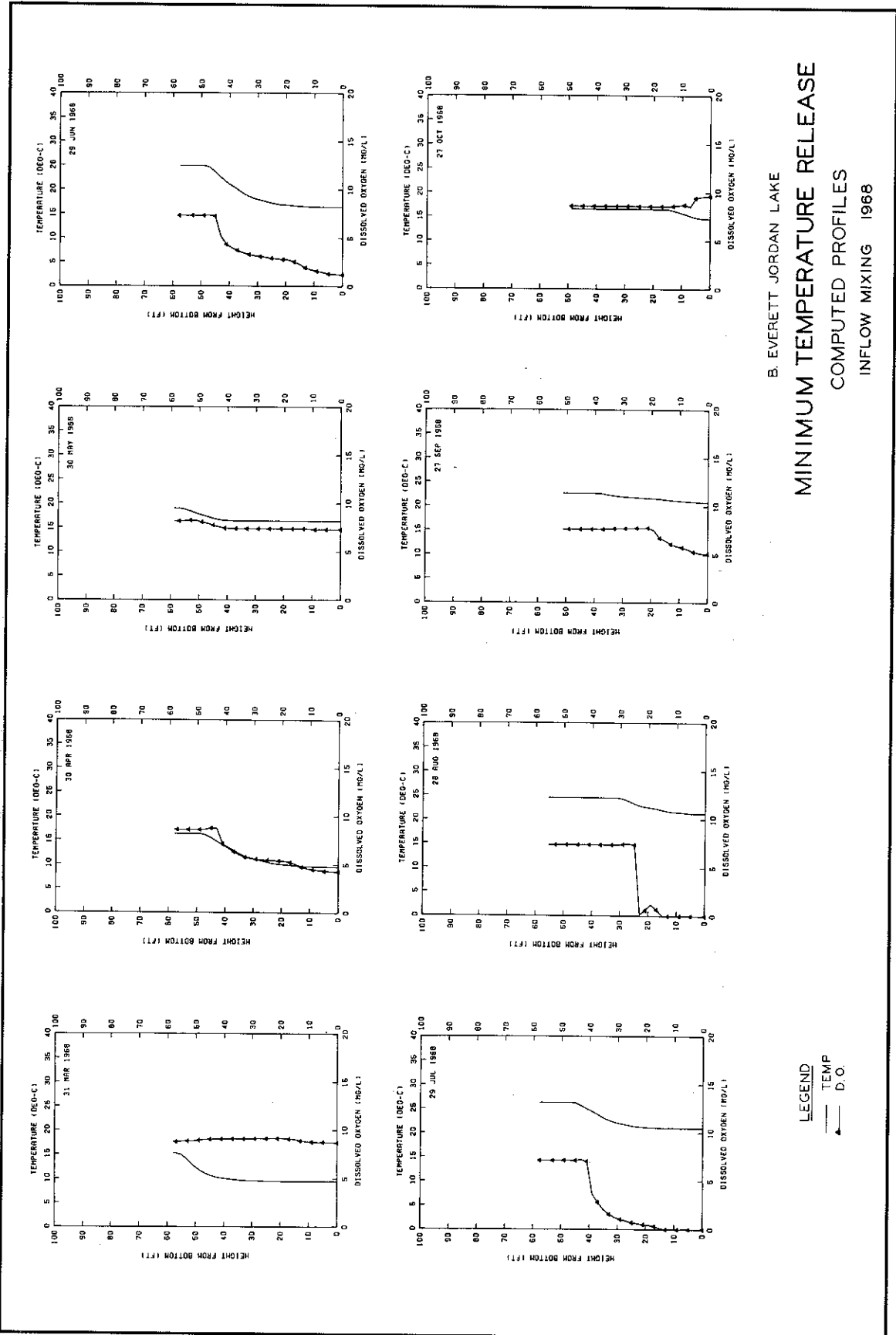


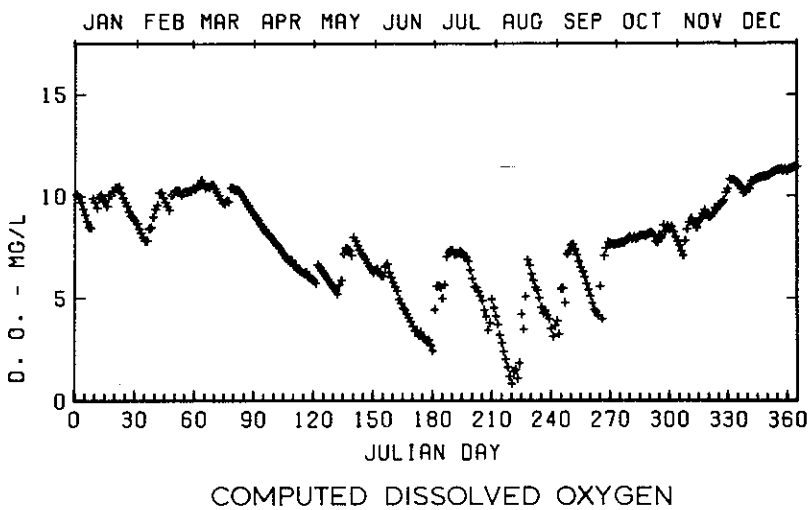
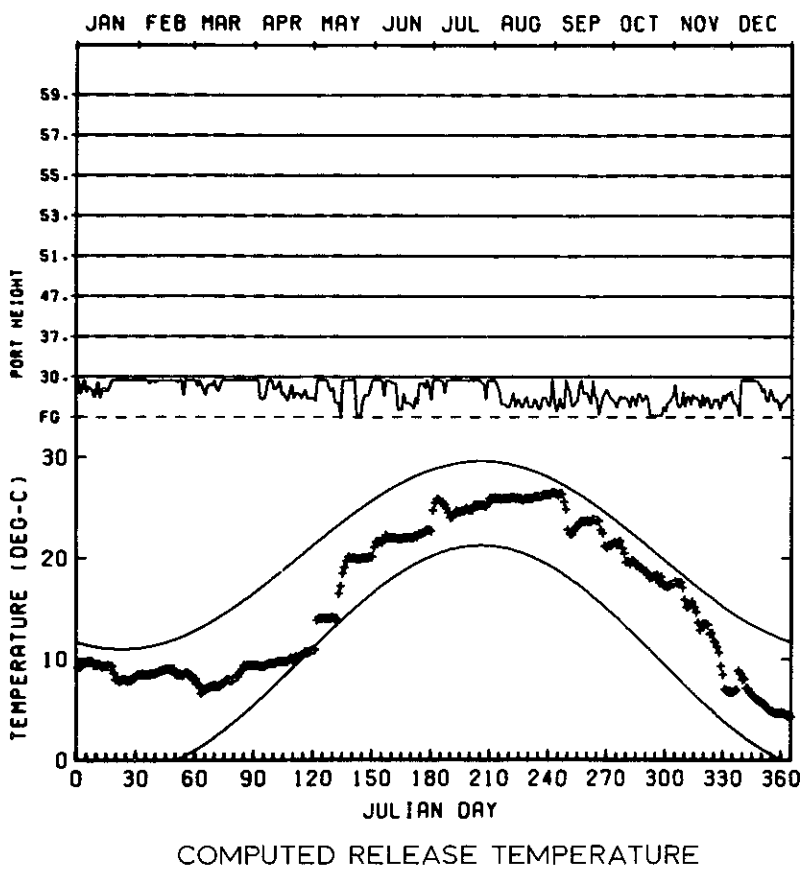


**B. EVERETT JORDAN LAKE**  
**MINIMUM TEMPERATURE RELEASE**  
**COMPUTED PROFILES**  
**INFLOW MIXING 1961**

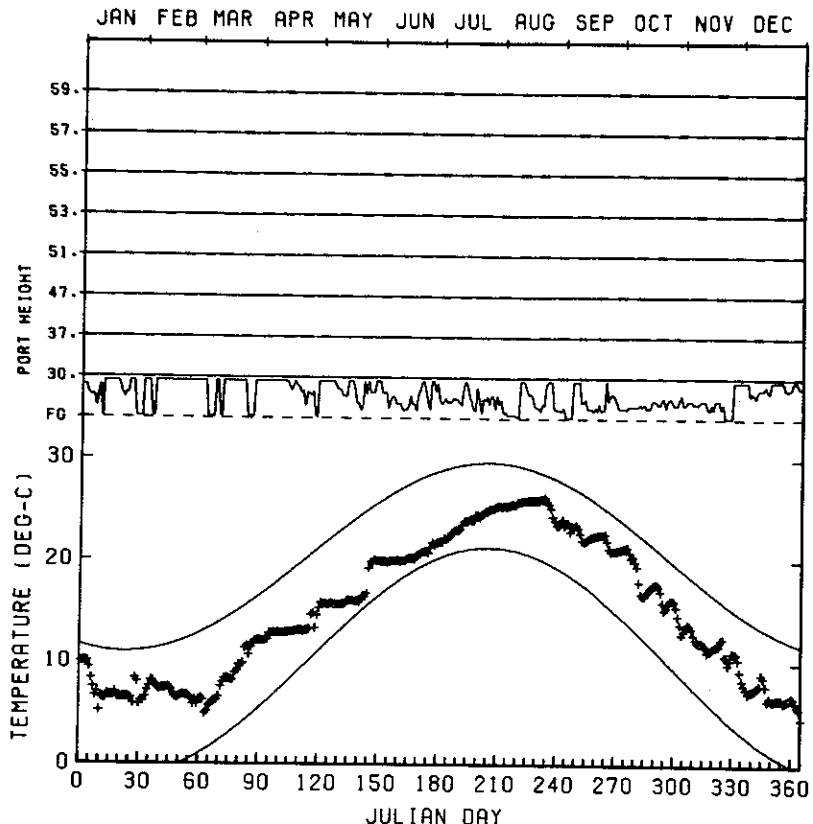
**LEGEND**

- TEMP
- ▲ D.O.

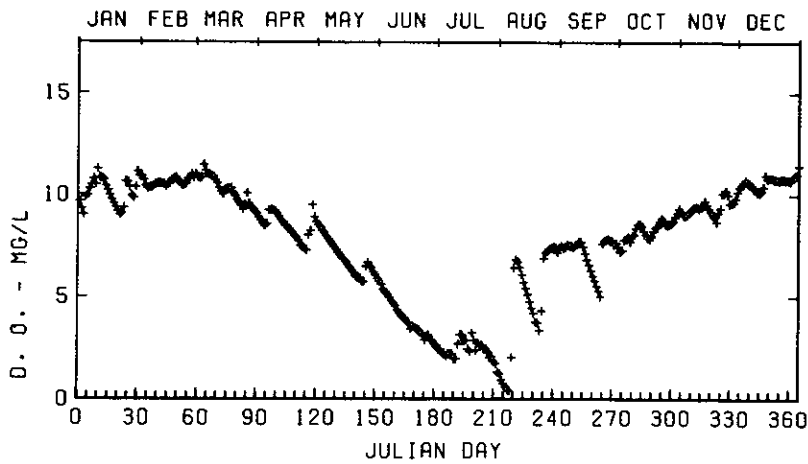




B. EVERETT JORDAN LAKE  
 MINIMUM TEMPERATURE RELEASE  
 INFLOW MIXING  
 1950

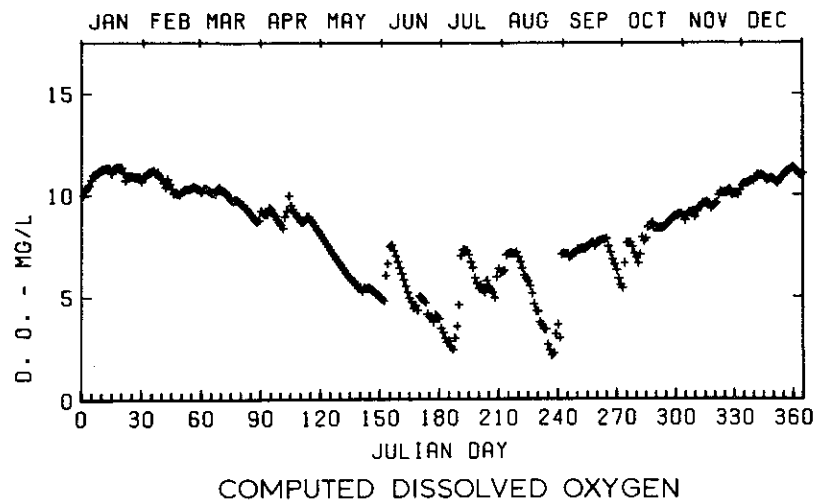
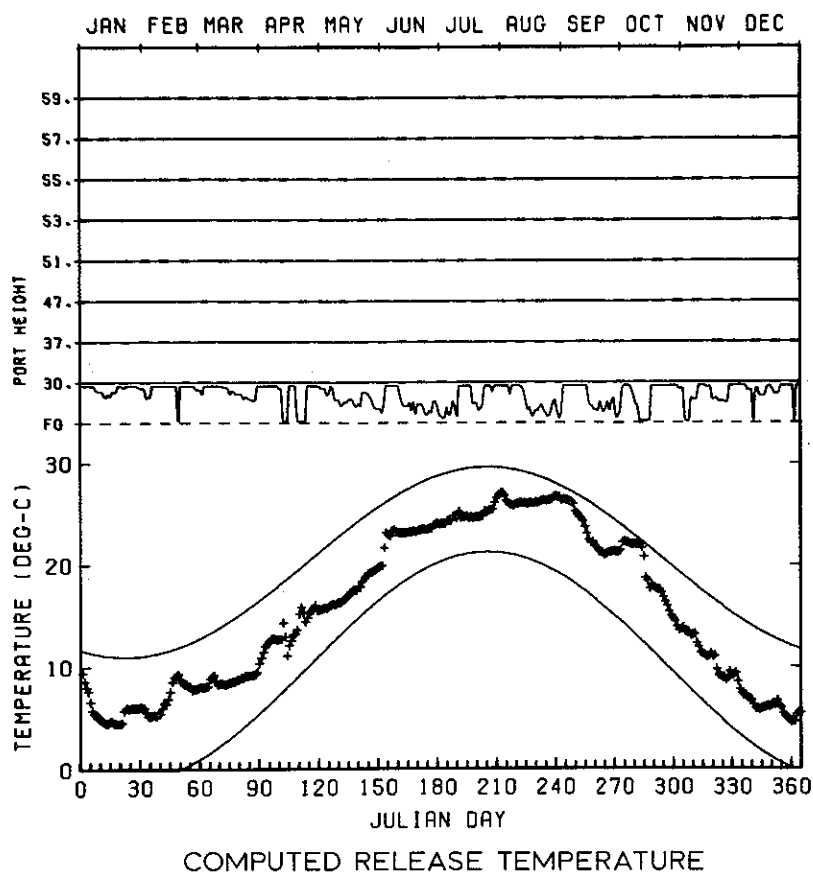


COMPUTED RELEASE TEMPERATURE

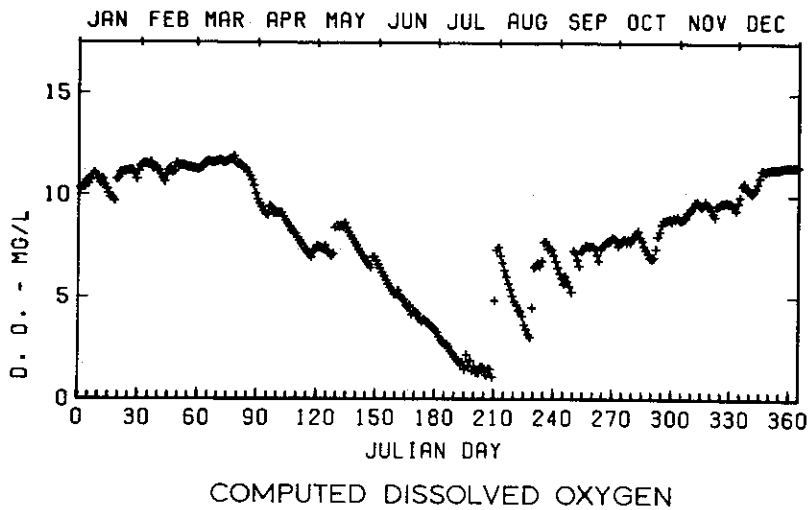
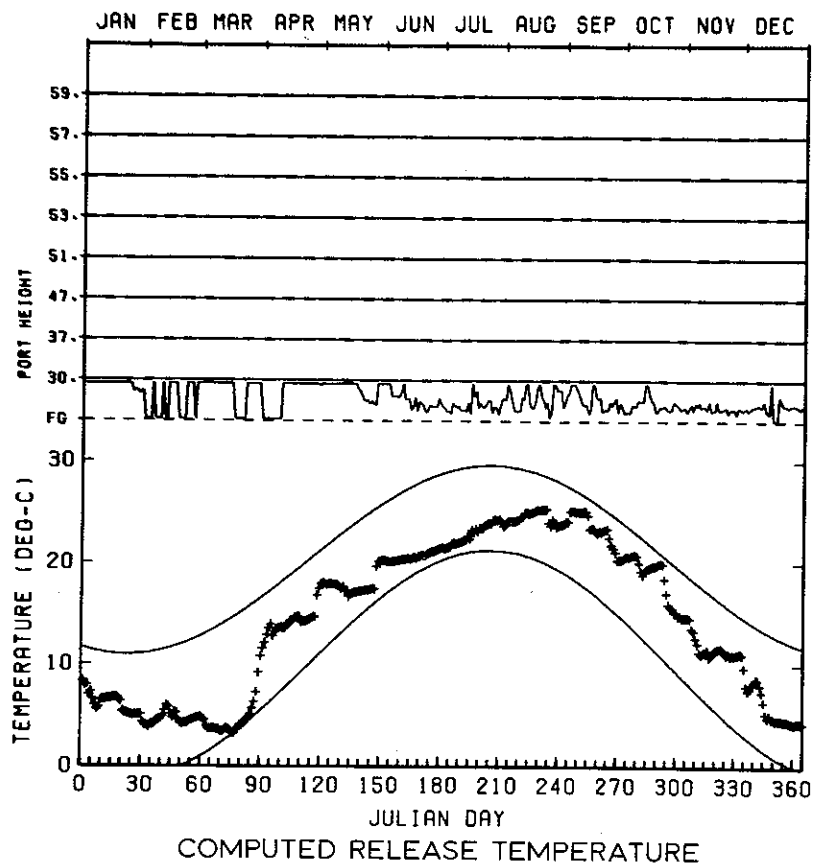


COMPUTED DISSOLVED OXYGEN

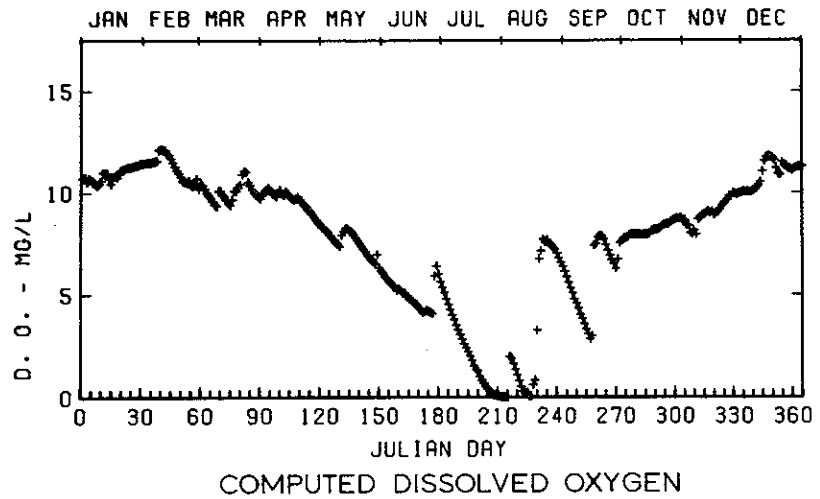
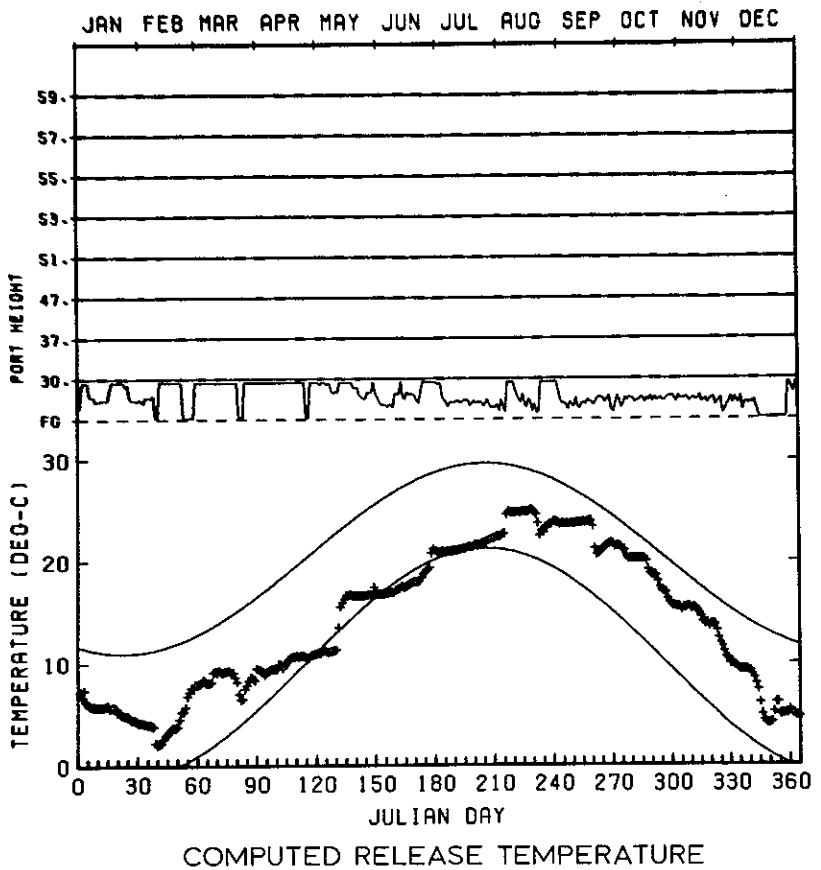
B. EVERETT JORDAN LAKE  
 MINIMUM TEMPERATURE RELEASE  
 INFLOW MIXING  
 1952



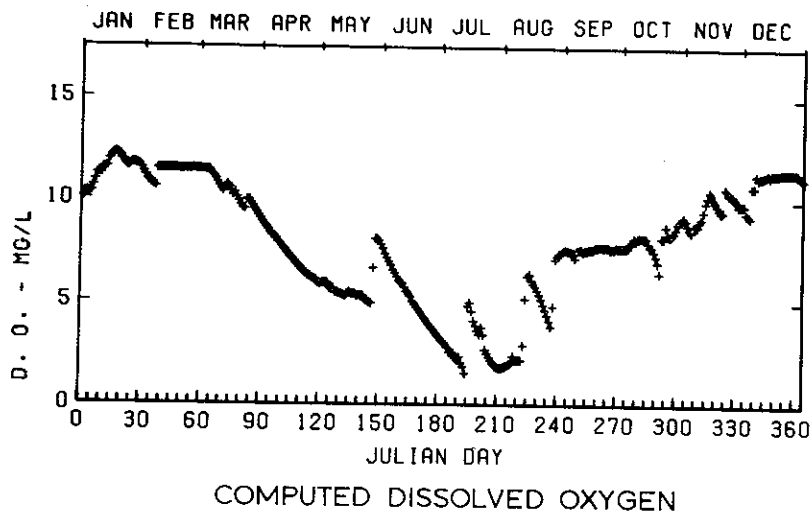
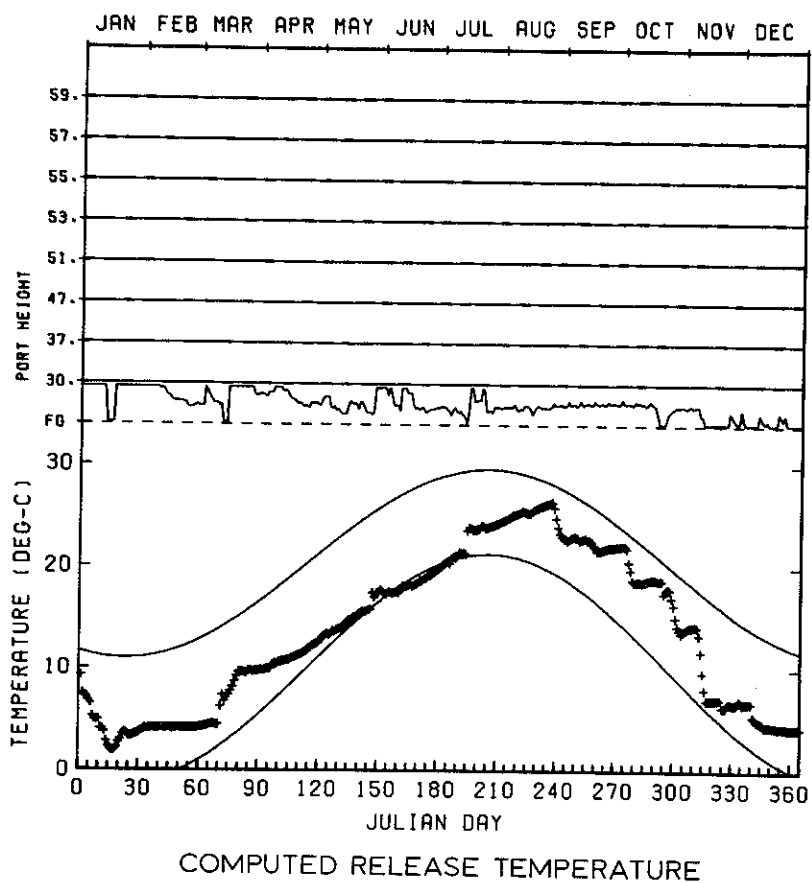
B. EVERETT JORDAN LAKE  
MINIMUM TEMPERATURE RELEASE  
INFLOW MIXING  
1959



B EVERETT JORDAN LAKE  
**MINIMUM TEMPERATURE RELEASE**  
 INFLOW MIXING  
 1960



B. EVERETT JORDAN LAKE  
**MINIMUM TEMPERATURE RELEASE**  
 INFLOW MIXING  
 1961



B. EVERETT JORDAN LAKE  
MINIMUM TEMPERATURE RELEASE  
INFLOW MIXING  
1968

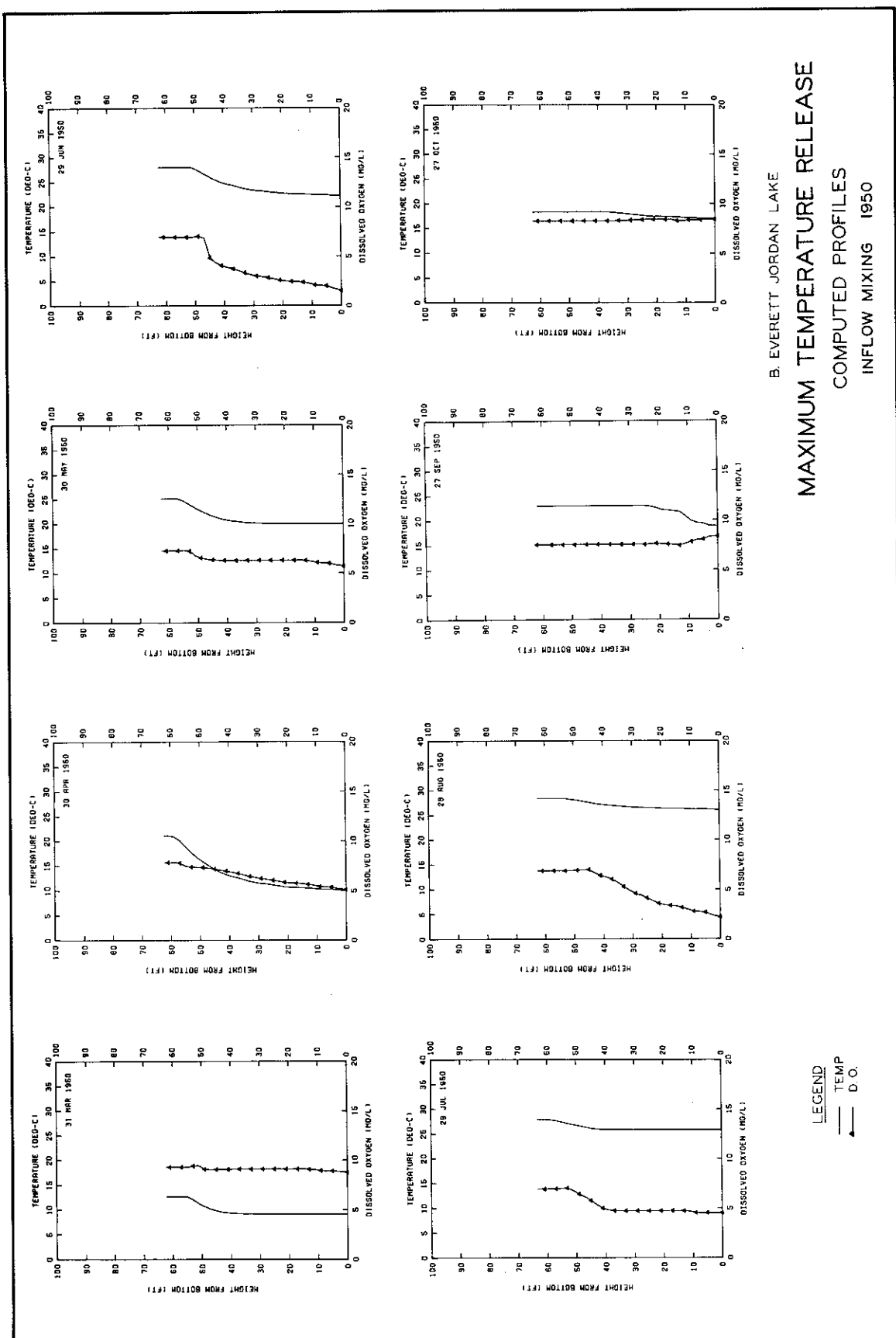
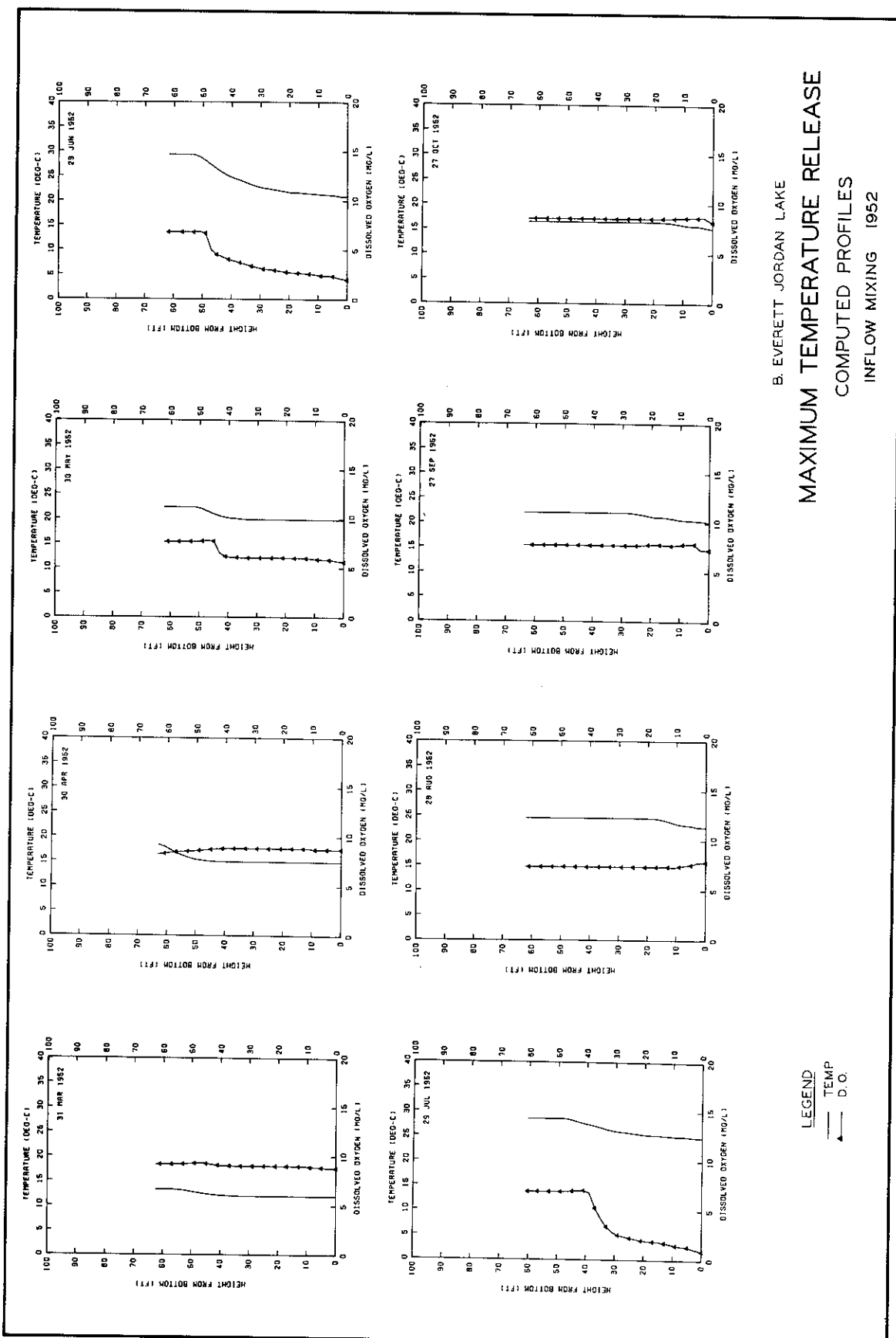
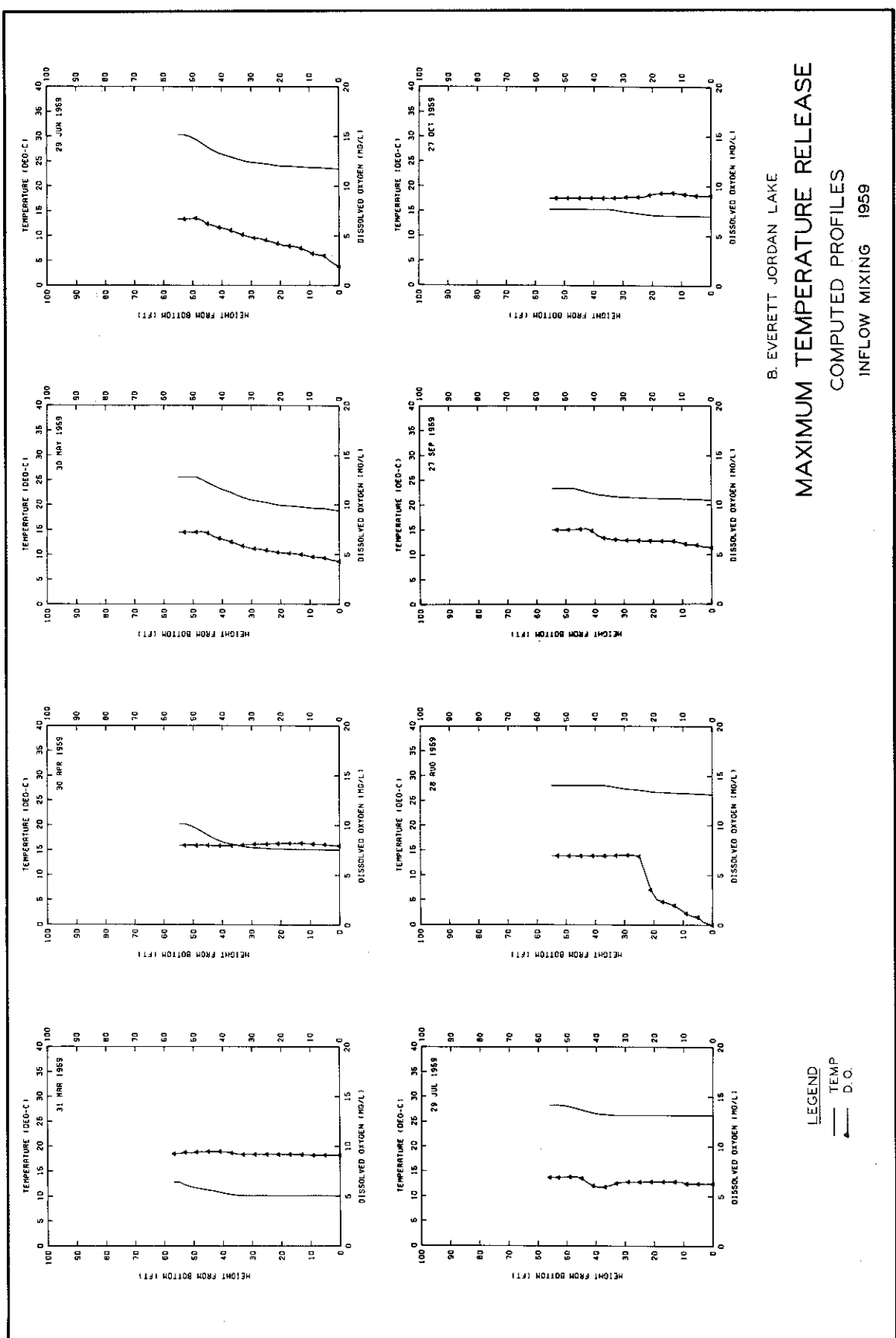
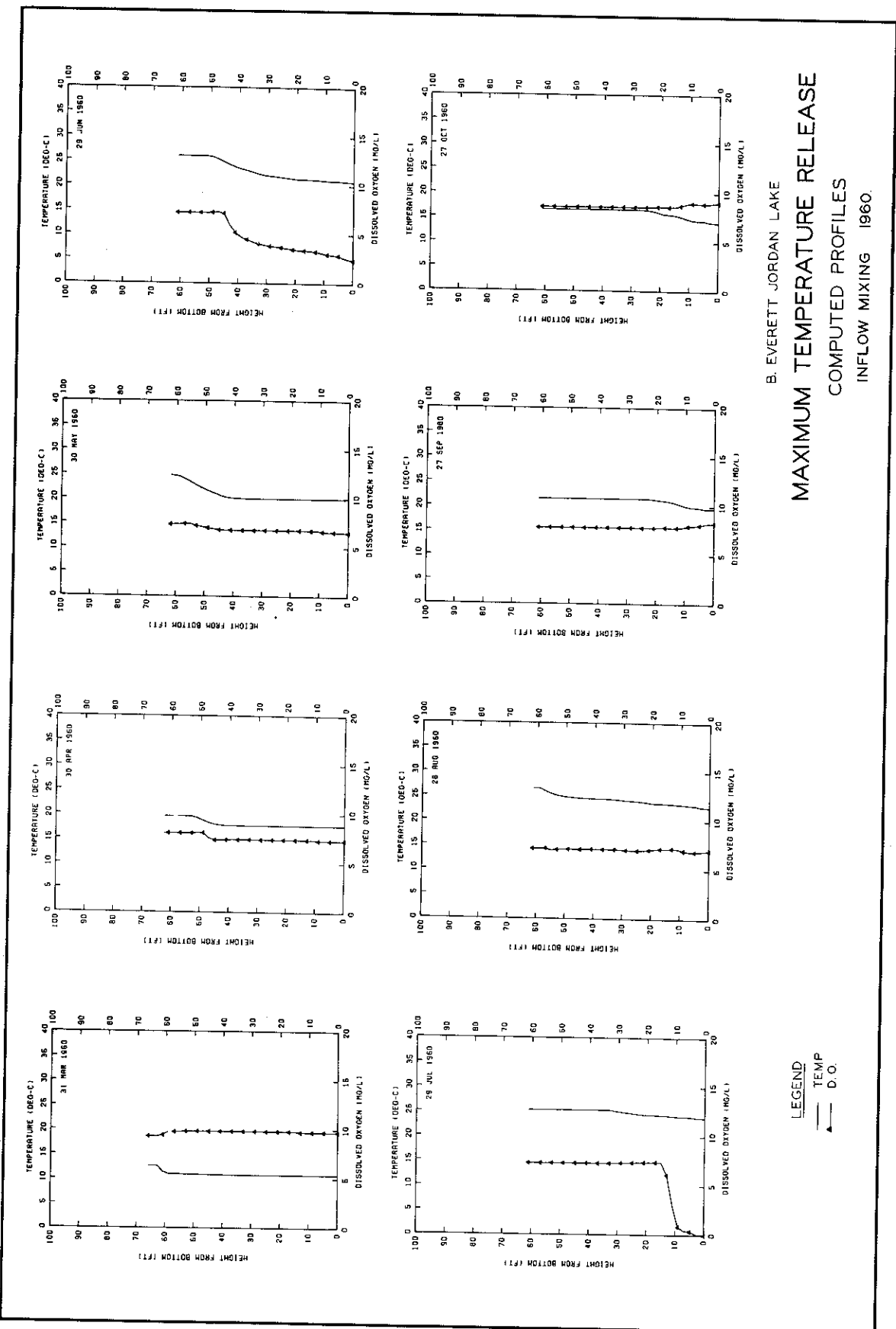


PLATE 10 (SHEET 1 OF 6)





B. EVERETT JORDAN LAKE  
MAXIMUM TEMPERATURE RELEASE  
COMPUTED PROFILES  
INFLOW MIXING 1959



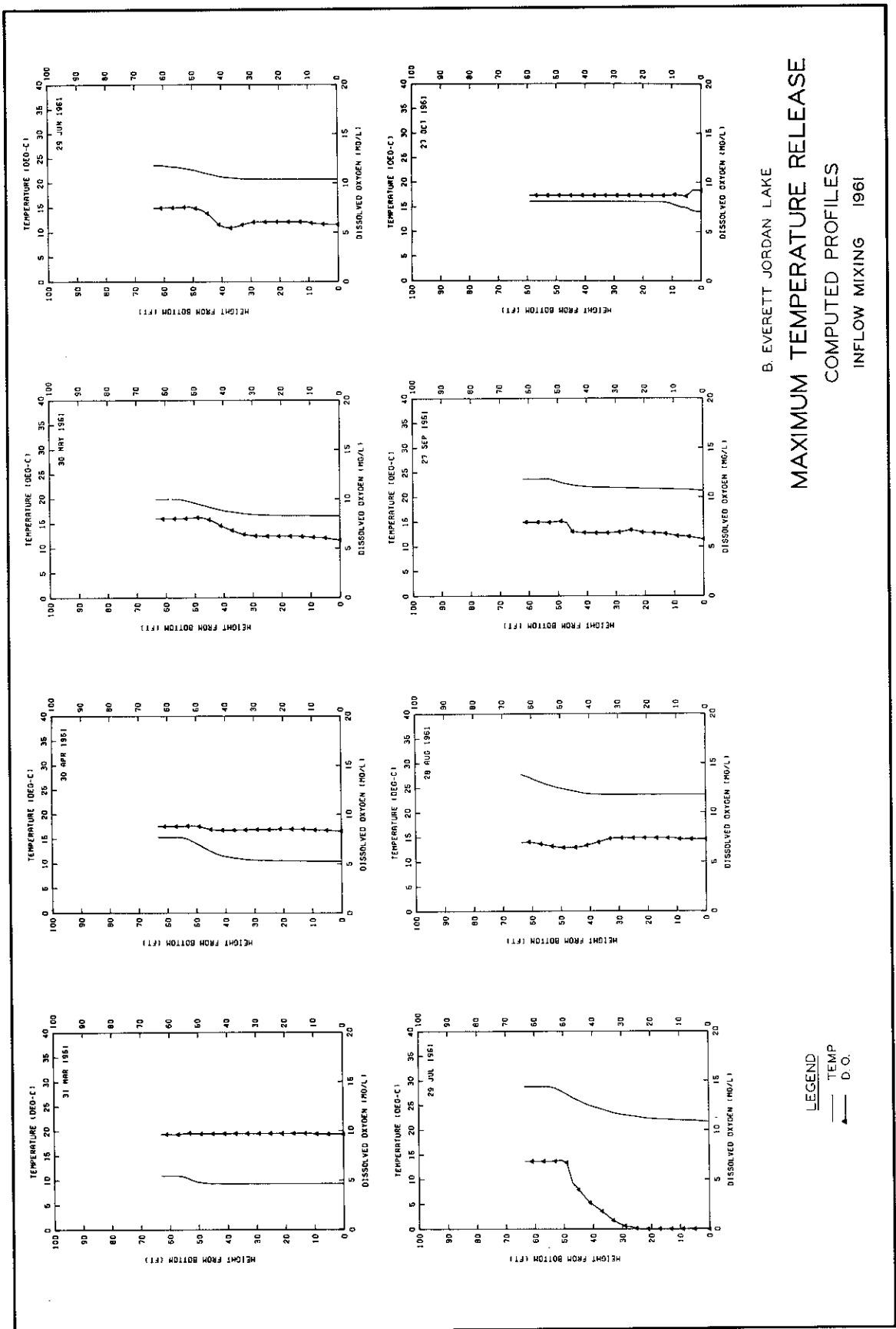
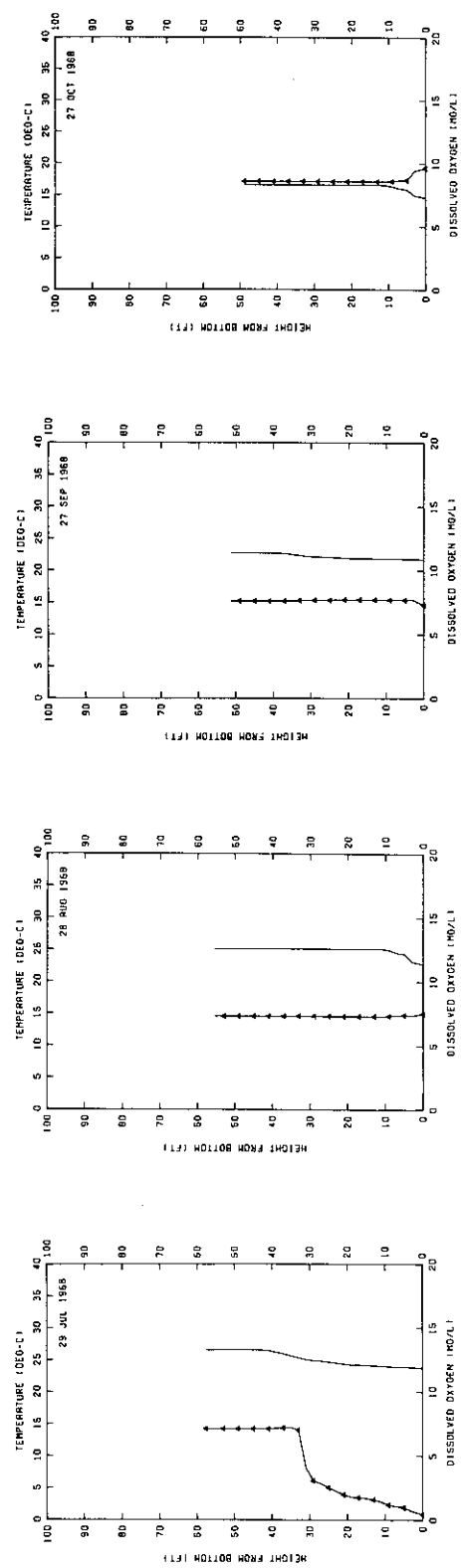
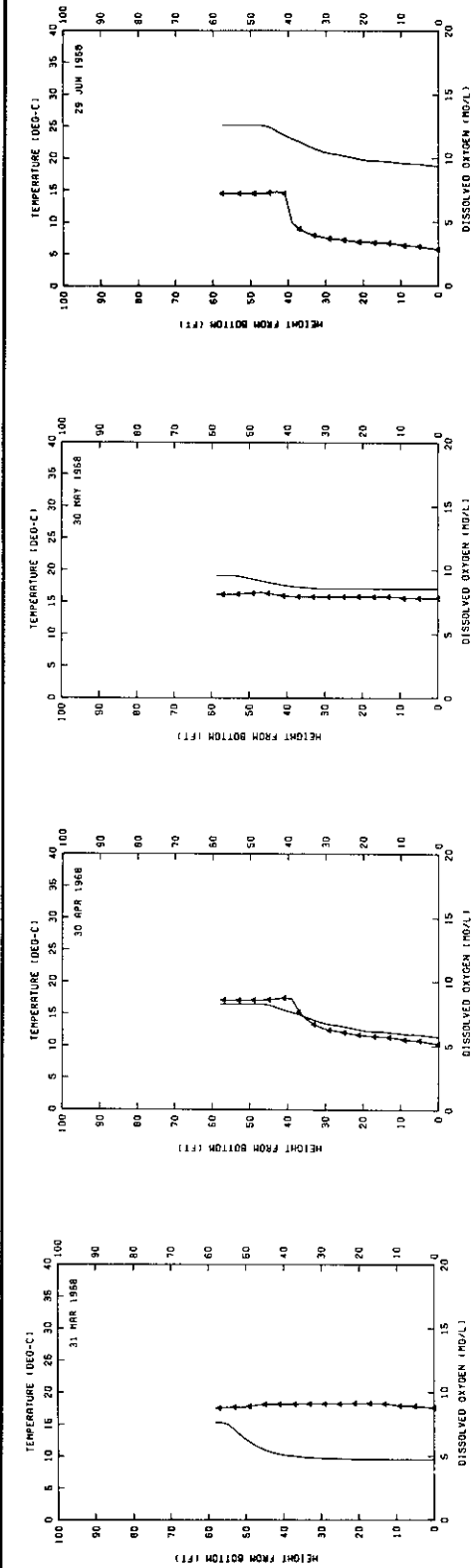


PLATE 10 (SHEET 5 OF 6)

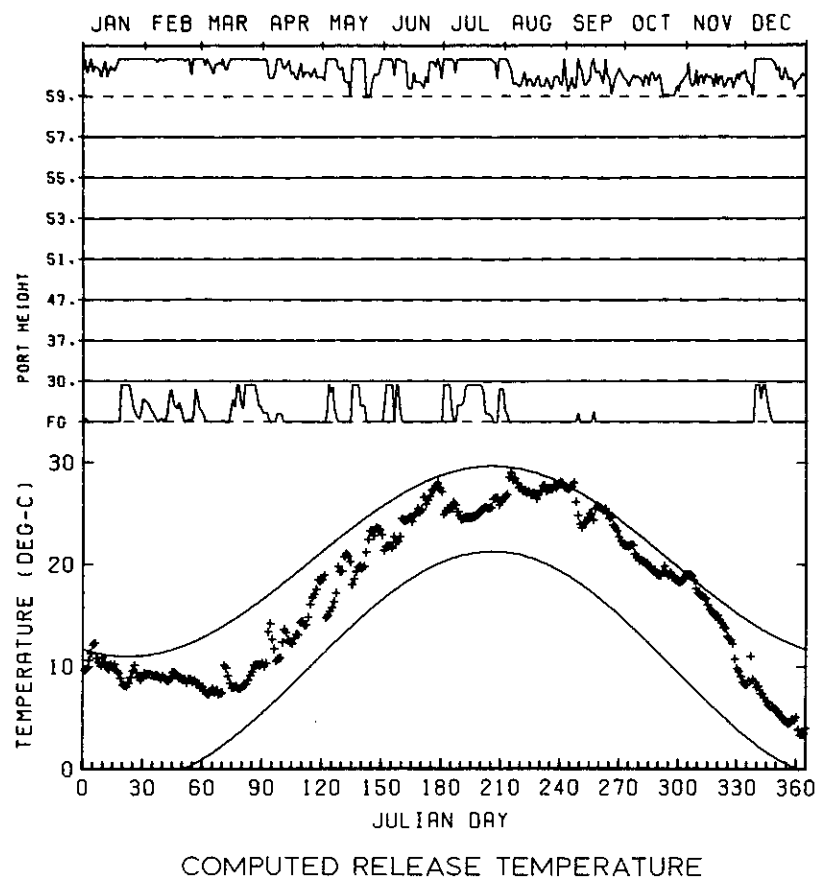


**MAXIMUM TEMPERATURE RELEASE  
COMPUTED PROFILES  
INFLOW MIXING 1968**

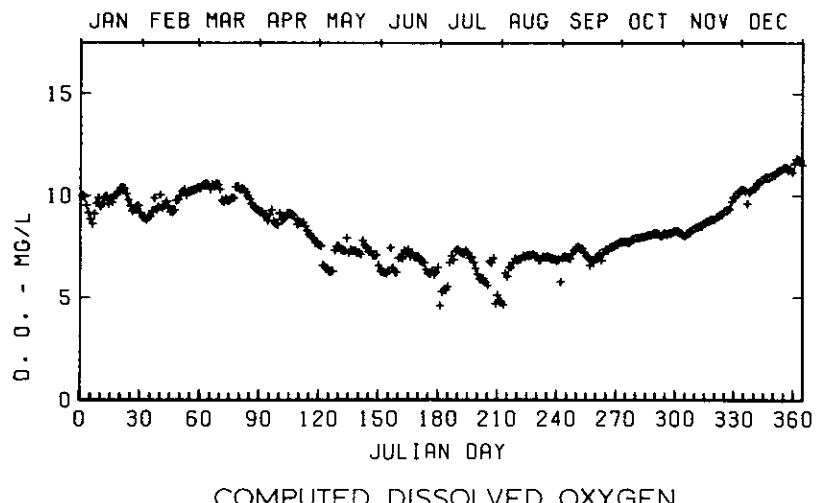
B. EVERETT JORDAN LAKE

**LEGEND**

— TEMP  
← D.O.

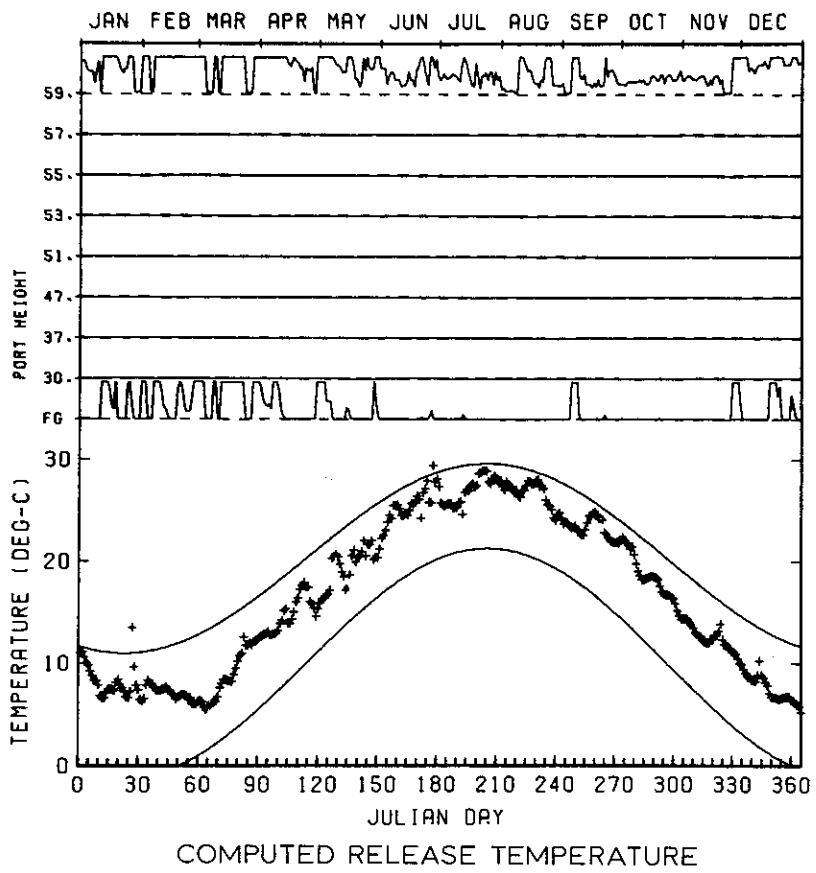


COMPUTED RELEASE TEMPERATURE

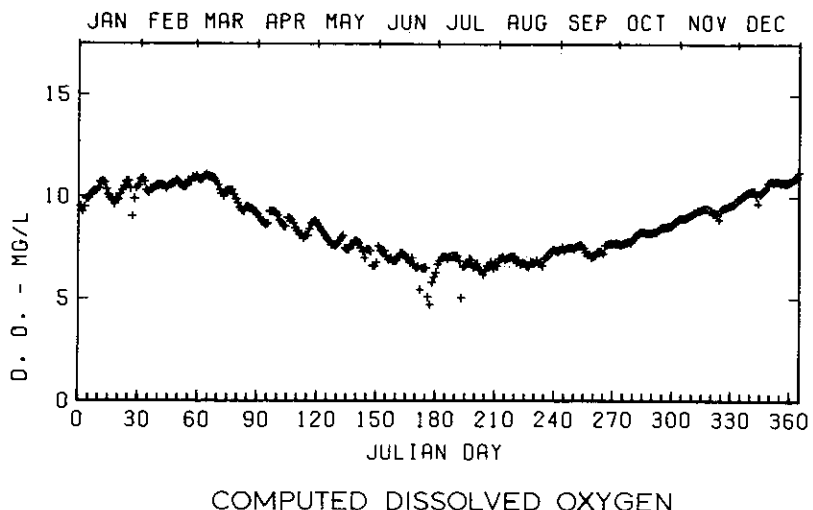


COMPUTED DISSOLVED OXYGEN

B. EVERETT JORDAN LAKE  
**MAXIMUM TEMPERATURE RELEASE**  
 INFLOW MIXING  
 1950

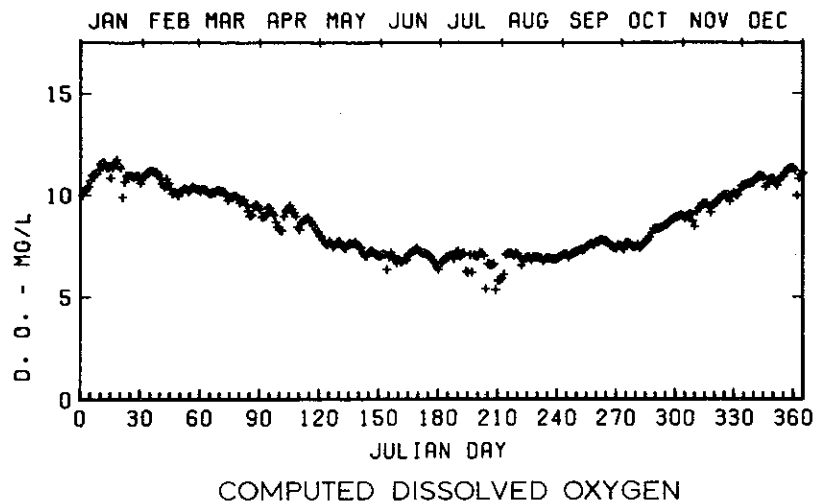
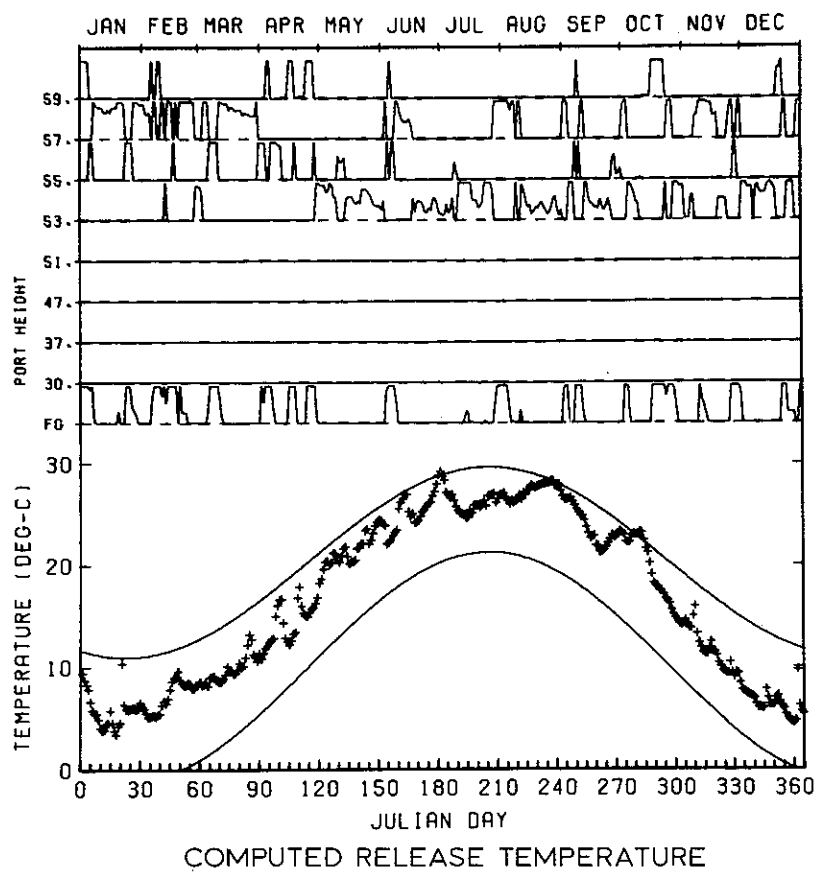


COMPUTED RELEASE TEMPERATURE

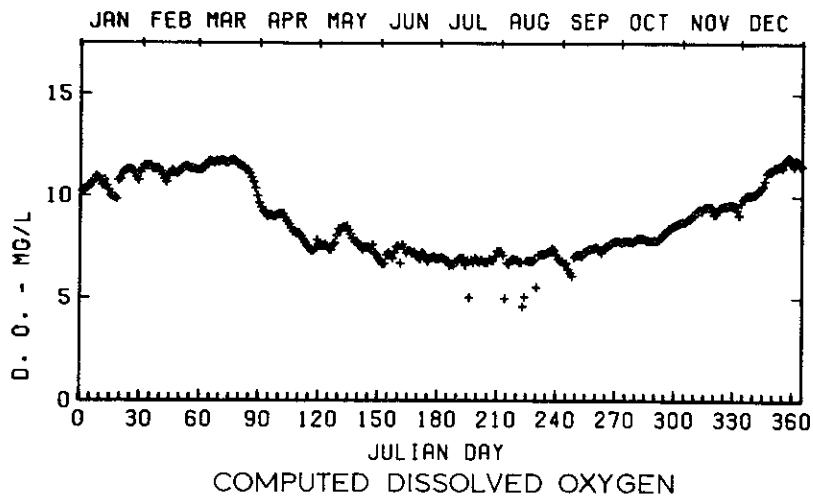
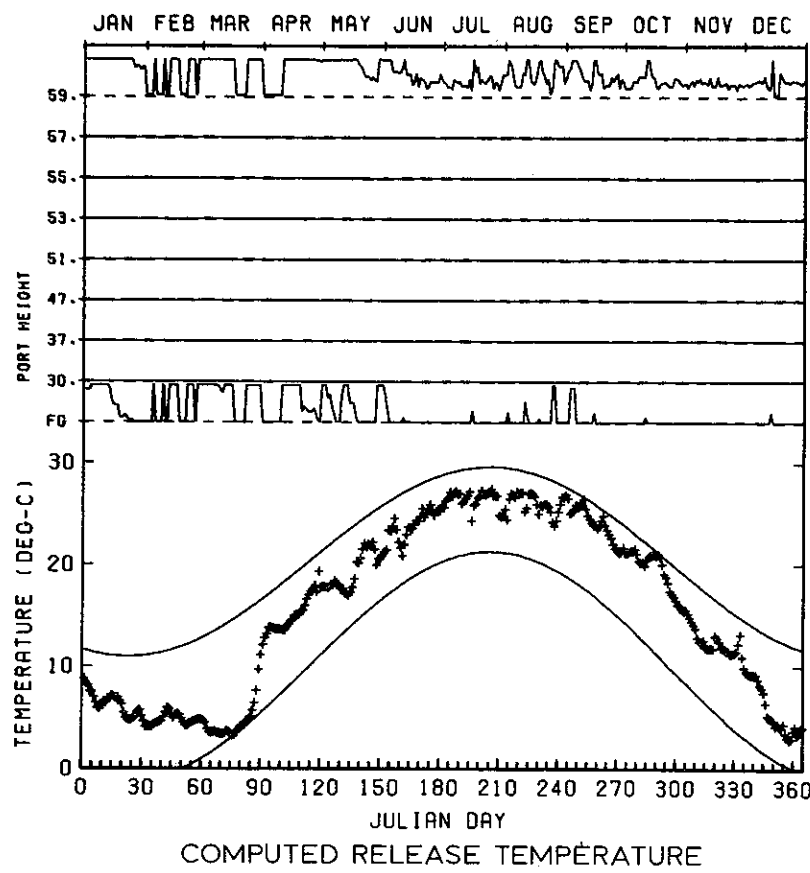


COMPUTED DISSOLVED OXYGEN

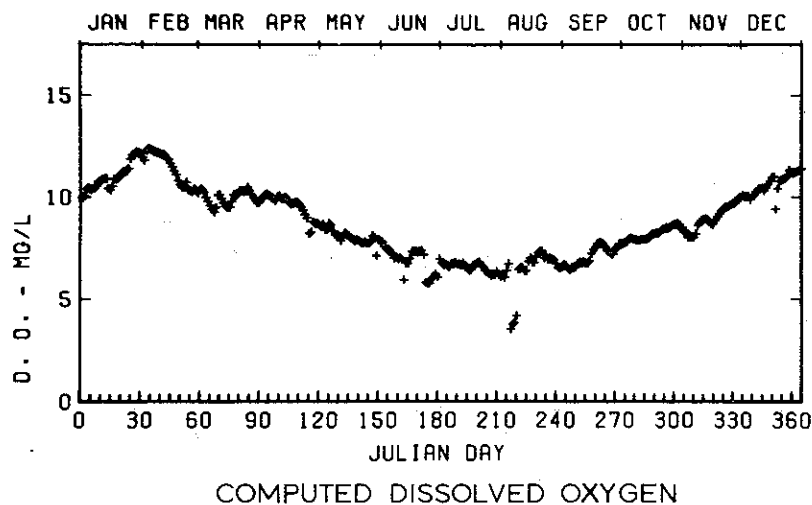
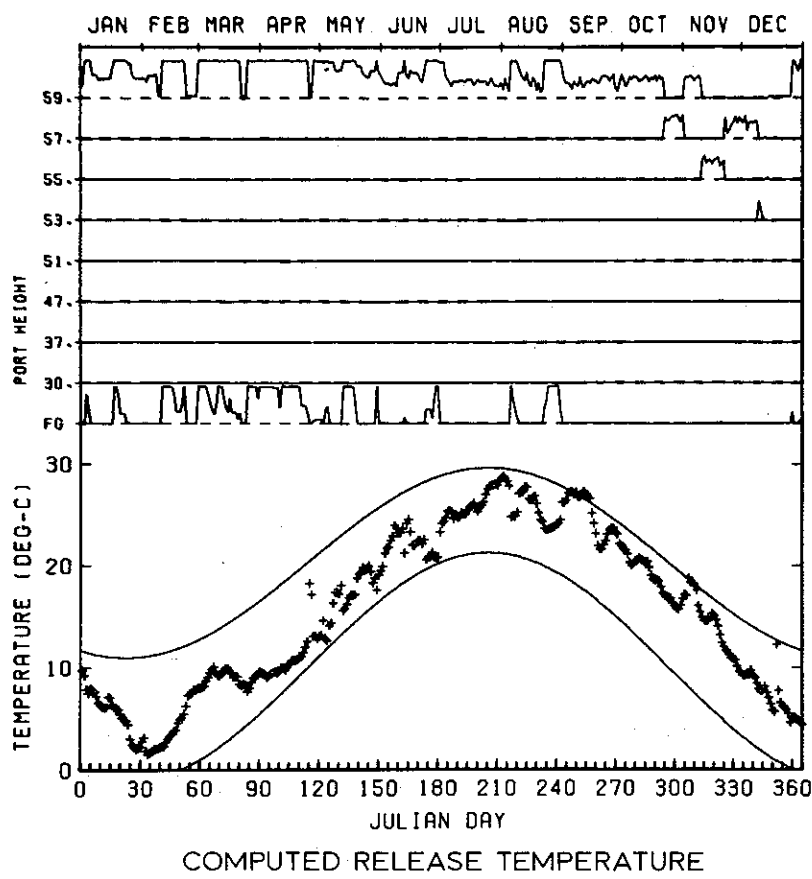
B. EVERETT JORDAN LAKE  
**MAXIMUM TEMPERATURE RELEASE**  
 INFLOW MIXING  
 1952



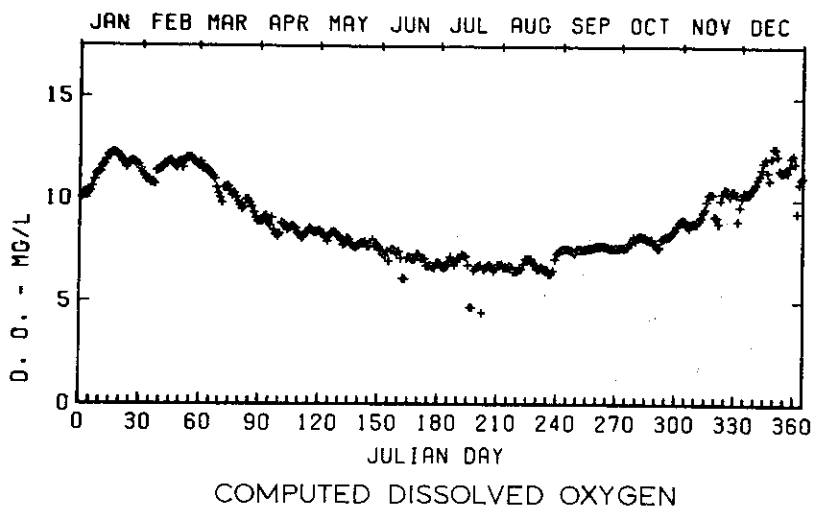
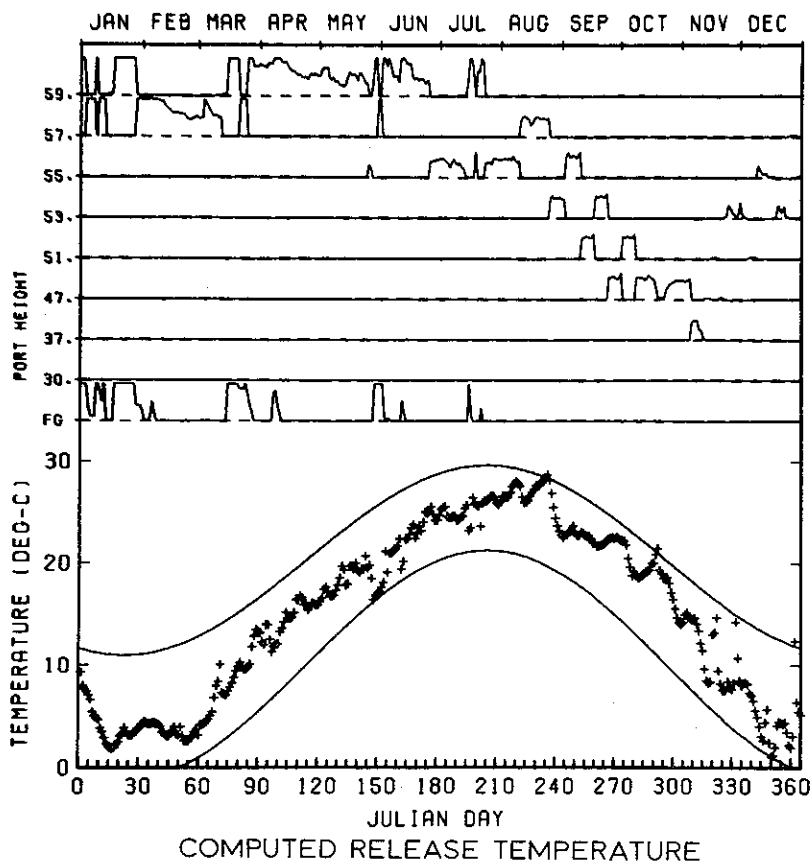
B. EVERETT JORDAN LAKE  
**MAXIMUM TEMPERATURE RELEASE**  
 INFLOW MIXING  
 1959



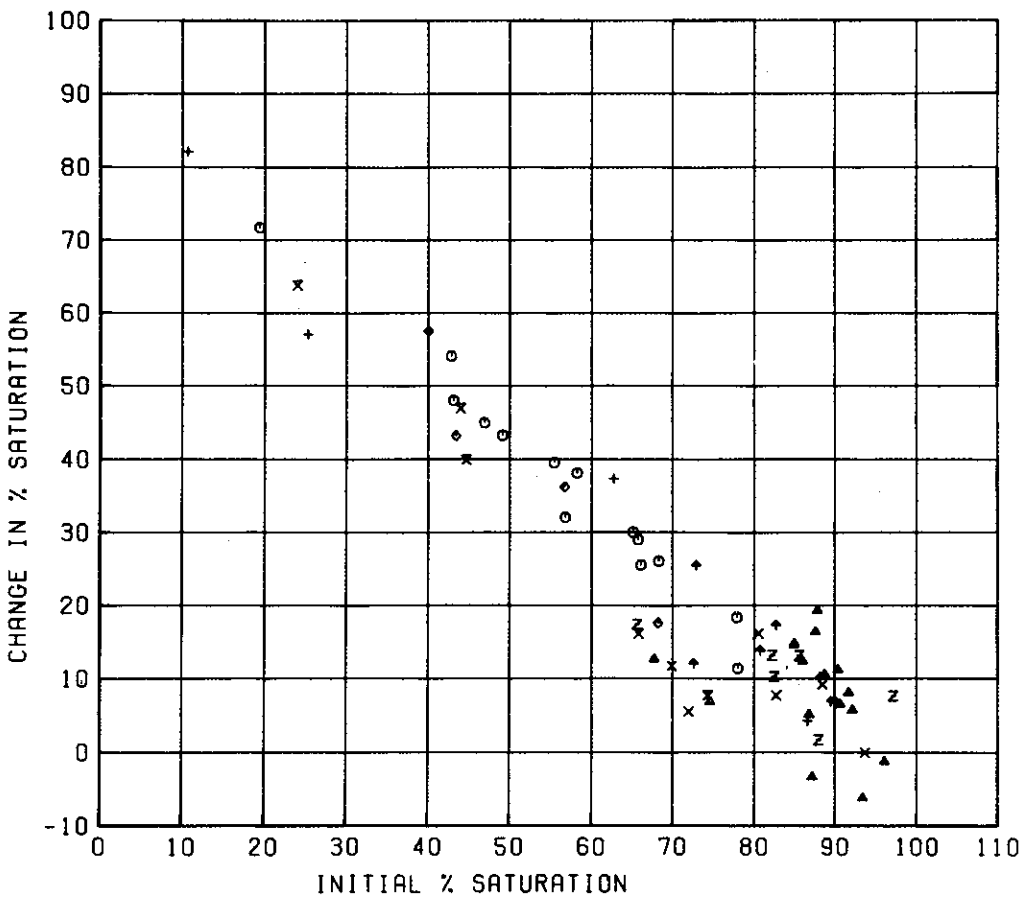
B. EVERETT JORDAN LAKE  
MAXIMUM TEMPERATURE RELEASE  
INFLOW MIXING  
1960



B. EVERETT JORDAN LAKE  
**MAXIMUM TEMPERATURE RELEASE**  
 INFLOW MIXING  
 1961



B. EVERETT JORDAN LAKE  
**MAXIMUM TEMPERATURE RELEASE**  
 INFLOW MIXING  
 1968

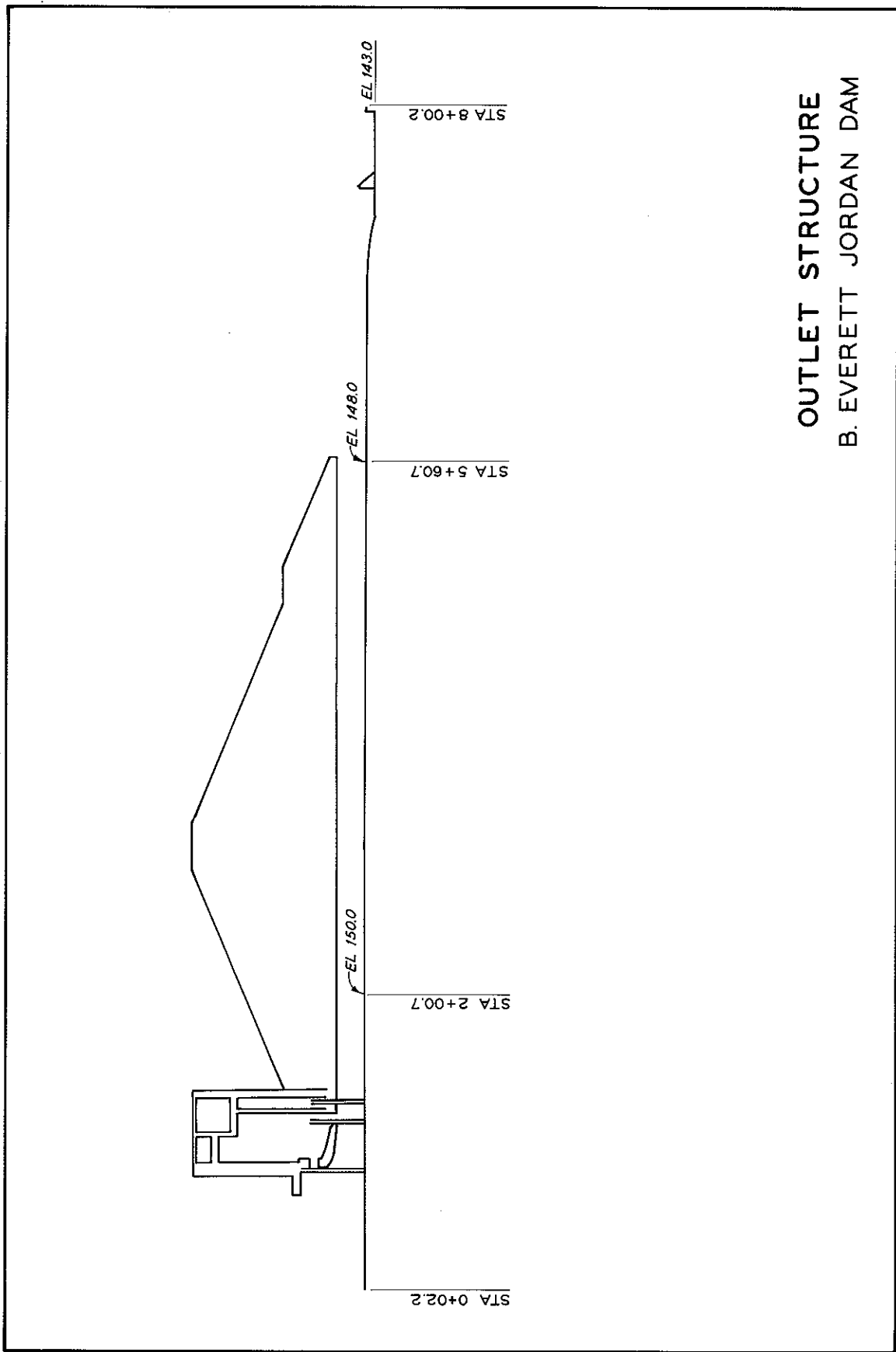


#### LEGEND

- SARDIS STRATIFIED
- △ SARDIS ISOTHERMAL
- + ENID STRATIFIED
- × ENID ISOTHERMAL
- ◊ GRENADA STRATIFIED
- ↑ GRENADA ISOTHERMAL
- ✗ ARKABUTLA STRATIFIED
- ✗ ARKABUTLA ISOTHERMAL

REAERATION THROUGH  
OUTLET STRUCTURES  
NORTHERN MISSISSIPPI

**OUTLET STRUCTURE**  
**B. EVERETT JORDAN DAM**



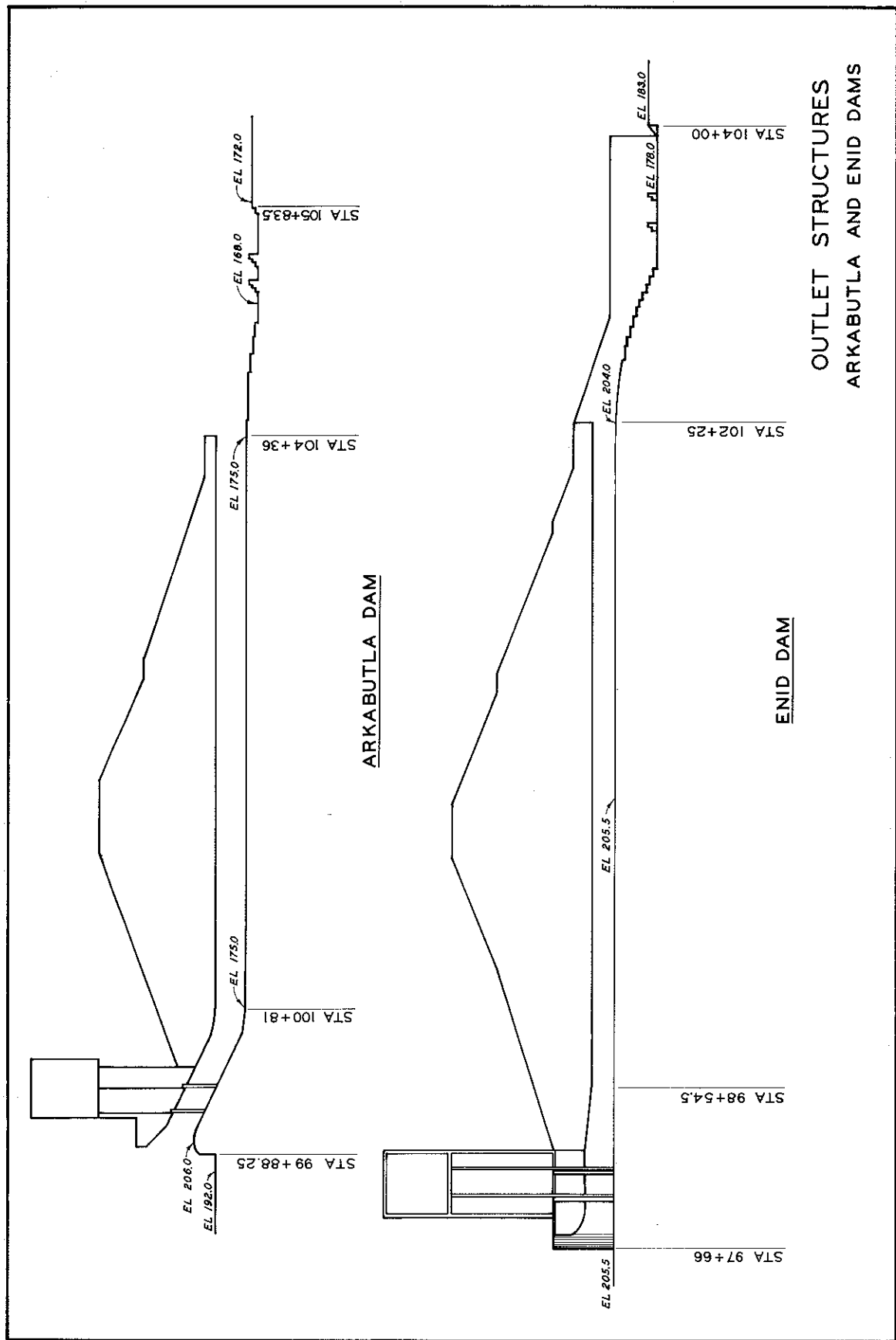


PLATE 13 (SHEET 2 OF 3)

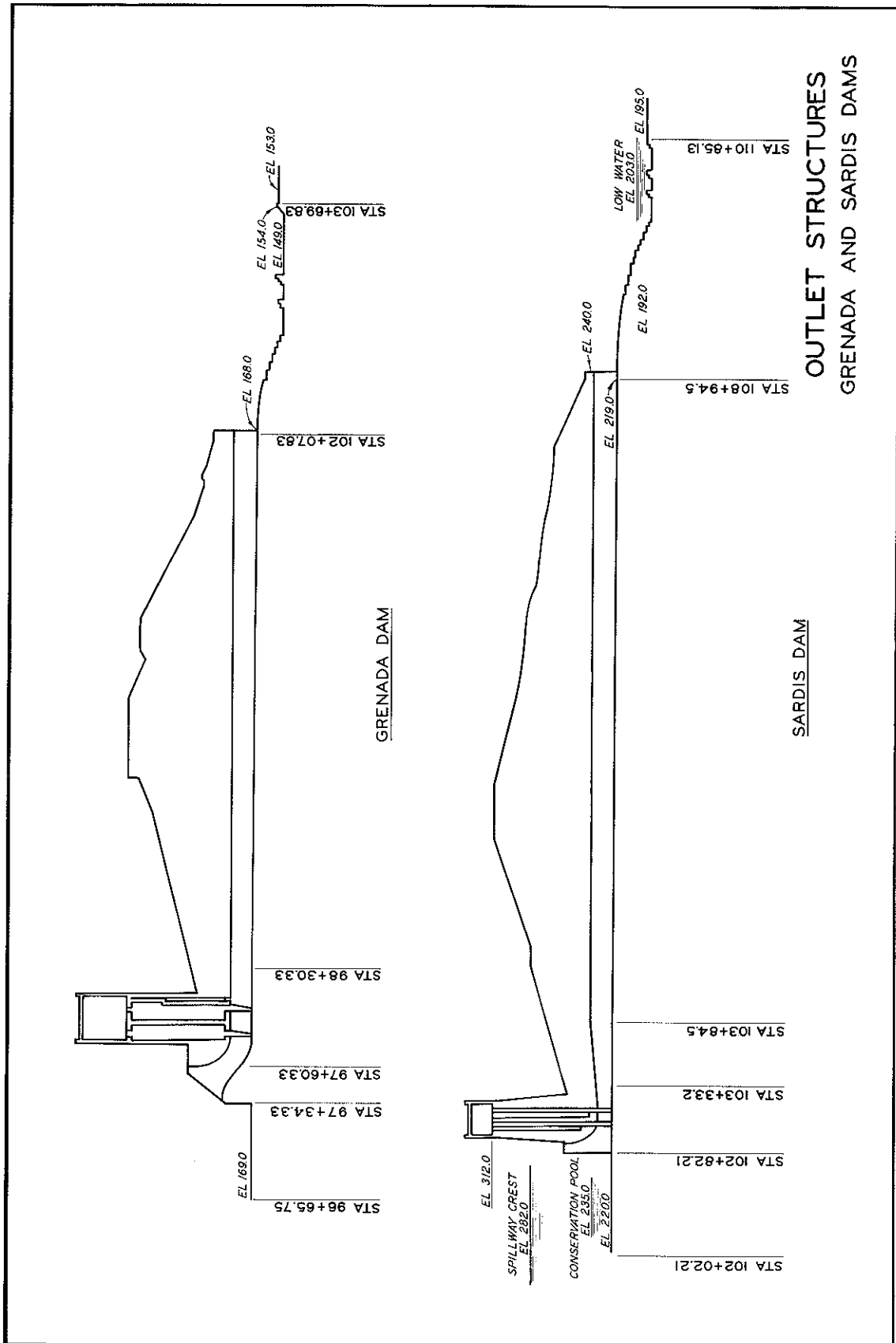


PLATE 13 (SHEET 3 OF 3)

APPENDIX A: SIMULATIONS OF B. EVERETT JORDAN  
LAKE ABOVE SR 1008

Purpose

1. Additional numerical simulations were made to predict profiles of temperature and D.O. at the bridge on secondary road (SR) 1008. These predicted profiles provide an index to the quality of water expected in the upstream pool of the New Hope River arm of B. Everett Jordan Lake.

Description

2. The shallow pool upstream of SR 1008 provides a storage volume of 21,000 acre-ft and has a surface area of 3,000 acres with the conservation pool at el 216. A maximum depth of 18 ft will exist at the bridge. The physical model indicated that Haw River inflows will have no direct influence on the upper part of the lake. Thus, the WESTEX model was applied to the upper pool with New Hope River inflow. It was assumed that submerged weir flow conditions will exist through the bridge opening and that the quantity of outflow through the bridge is equal to the New Hope River inflow. The inflow mixing modification as described in the main text was not used for these simulations.

3. Simulations were conducted for three study years: a year with average runoff (1960), a year with above average runoff (1959), and a year with below average runoff (1950). These correspond to three of the study years selected for the previous simulations.

Input Data

4. Mean daily flow into the lake was obtained by adjustment of the New Hope River streamflow records. The New Hill gaging station records were decreased by a factor of the appropriate drainage area ratio (0.916). The resultant inflows are approximately 86 percent of

those shown in Plate 3. Outflow was assumed equal to inflow for each day.

5. Daily values of B.O.D. and D.O. equal to those used in the previous simulations were input to the mathematical model. A B.O.D. decay rate,  $K_b$ , of  $0.01 \text{ day}^{-1}$ , a D.O. deoxygenation coefficient,  $K_D(20)$ , of  $0.1 \text{ mg/l/day}$ , and an average travel time of 30 days were used in the simulations.

6. The following heat transfer coefficients were used for simulations above SR 1008

$$\beta = 0.5$$

$$\lambda = 0.2$$

where

$\beta$  = percentage of incoming shortwave radiation in the surface layer

$\lambda$  = heat absorption coefficient,  $\text{ft}^{-1}$

The lack of detailed topography in the upper part of the New Hope arm reproduced in the physical model precluded accurate determination of an inflow entrainment coefficient. Thus, a range of entrainment coefficients was evaluated in order to assess the sensitivity of the simulations to variations of this parameter. The simulations indicated that the magnitudes of the inflow entrainment coefficient and the mixing coefficients at the surface and bottom of the lake had very little effect on the profiles of temperature and D.O. to be expected at the SR 1008 bridge. This is attributed to the relatively large ratio of annual inflow-outflow volume (255,500 acre-feet) to storage volume (21,000 acre-feet) in this portion of the lake.

#### D. O. Saturation Depth Sensitivity Analysis

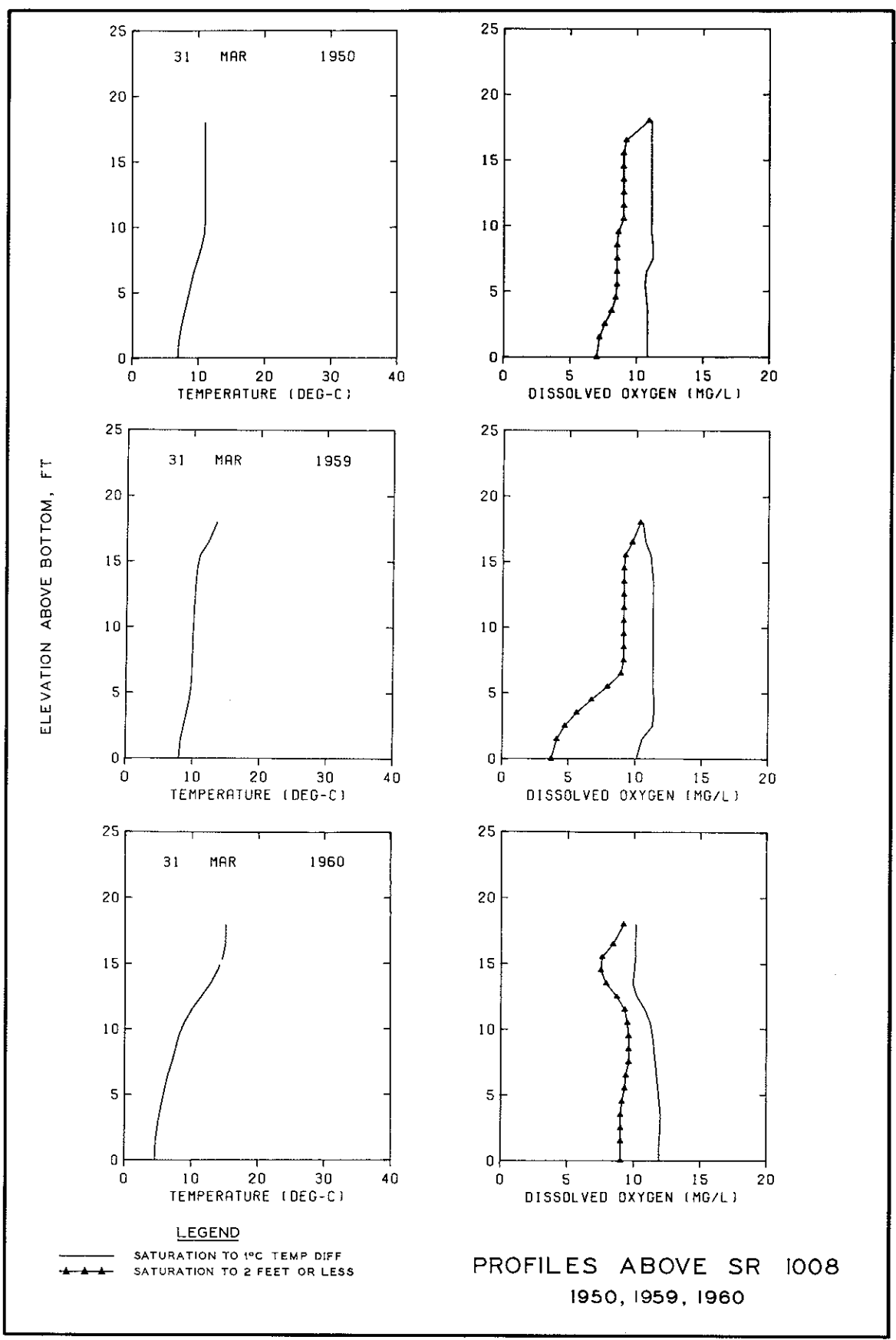
7. Simulations above SR 1008 were conducted initially with the assumption that a saturated D.O. condition will exist down to the depth

at which the temperature is 1°C less than the temperature of the surface. Results of these simulations indicated consistently high levels of D.O. from the surface to the bottom.

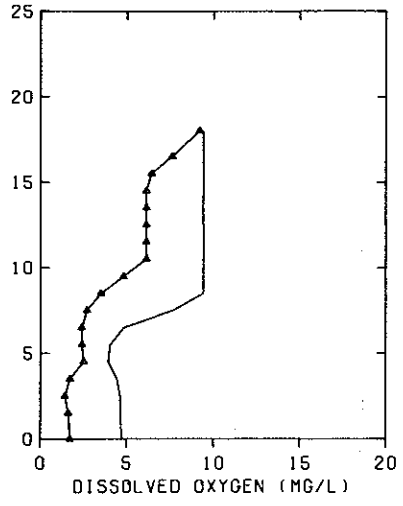
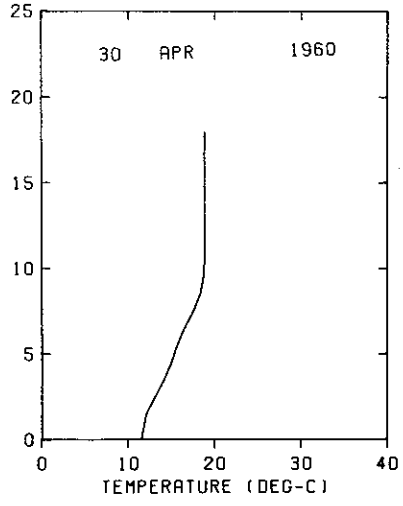
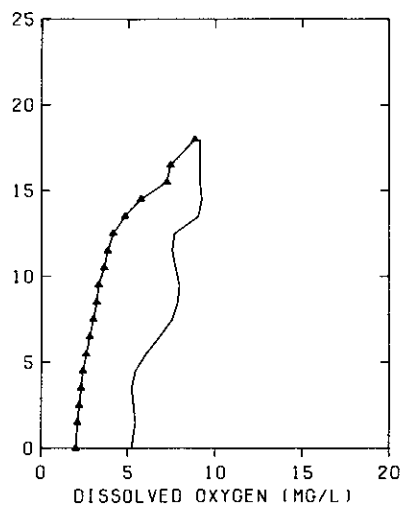
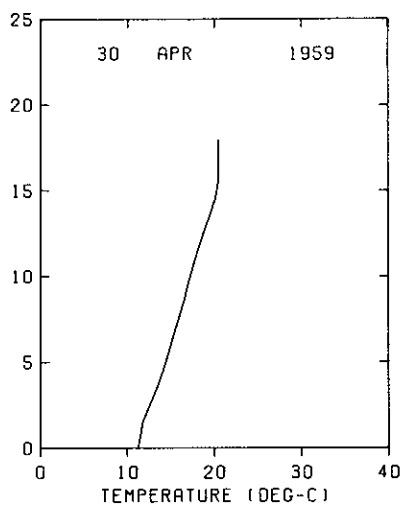
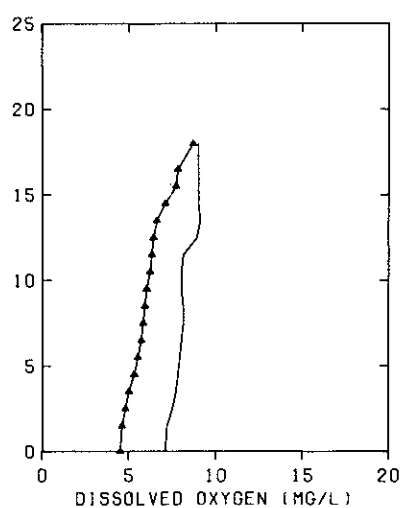
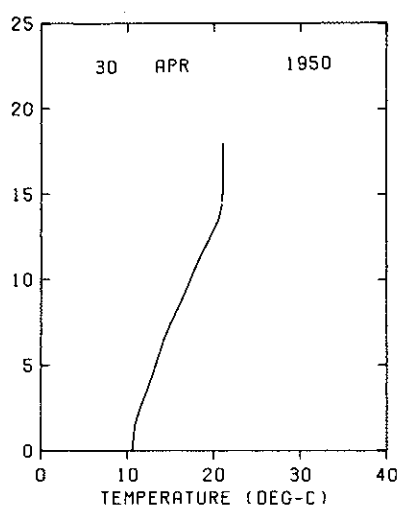
8. The New Hope River inflow contributes significant amounts of dissolved and suspended materials from point source discharges and runoff. Thus, the resulting density profile at SR 1008 may not be entirely dependent on temperature. Simulations were conducted with the assumption of shallow saturation conditions to evaluate the effect of increased stratification due to dissolved and suspended materials. For these simulations, the saturation depth was limited to 2 ft. Results of simulations with different saturation depths are presented in Plate Al.

#### Discussion

9. An attempt was made to predict profiles of temperature and D.O. at the SR 1008 bridge. A formidable difficulty arises in the extension of the WESTEX model, which was developed for application to deep lakes, to a part of a lake with only 18 ft maximum depth. The fundamental assumptions of the model, as described in the main text, may not be valid. For shallow lakes, wind forces not considered in WESTEX may significantly affect the hydrodynamics. These limitations should be considered in evaluation of the results presented in this section.



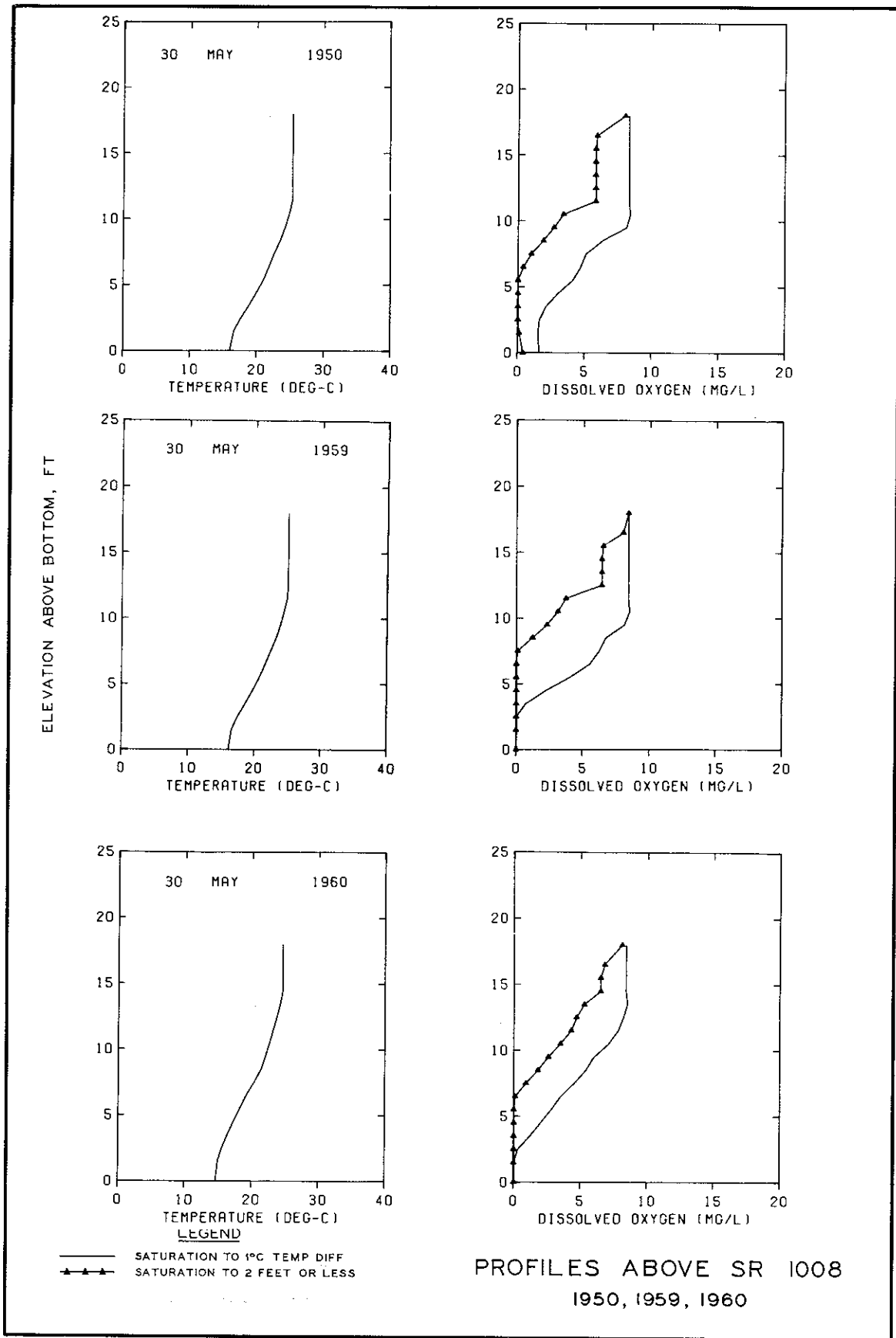
ELEVATION ABOVE BOTTOM, FT

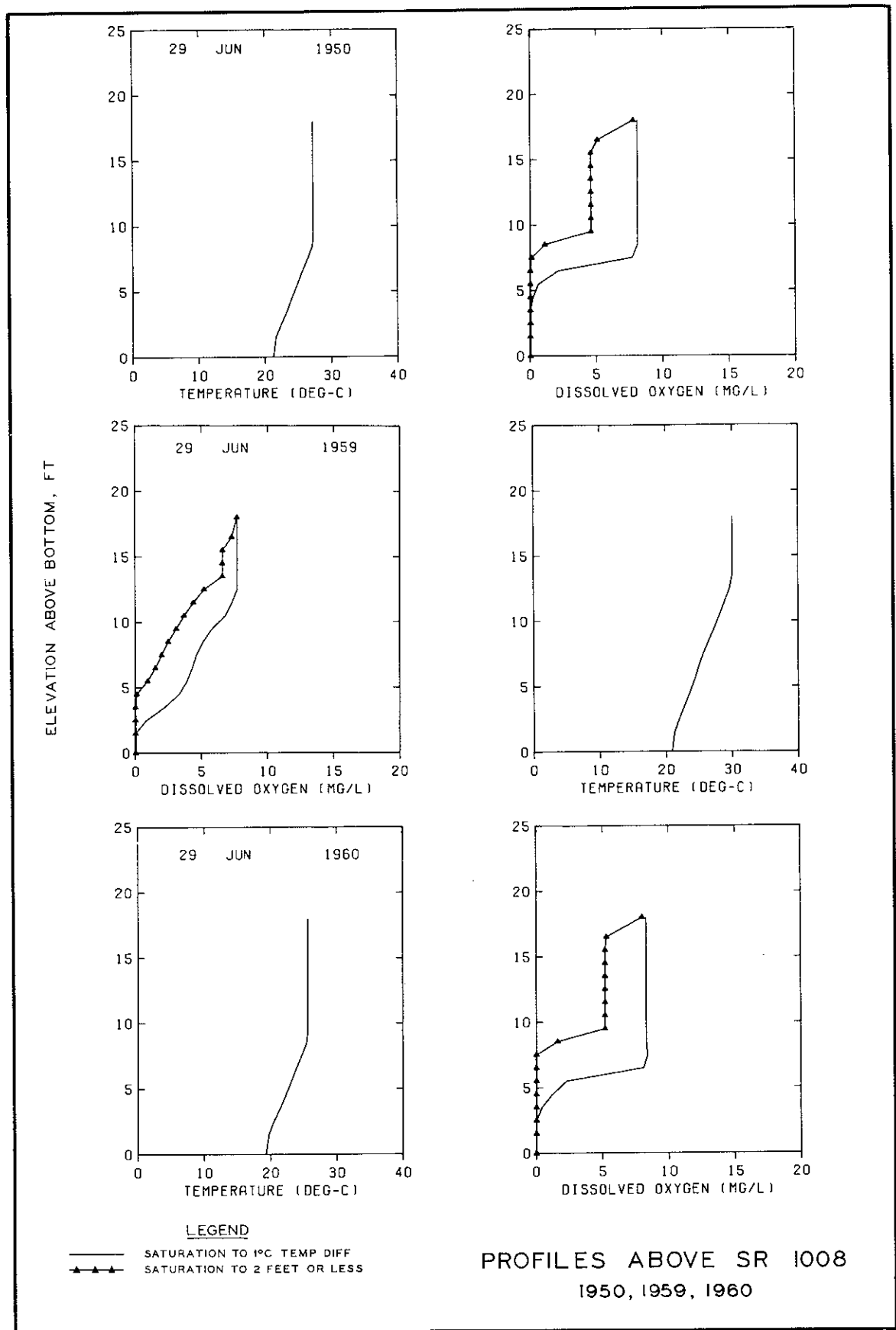


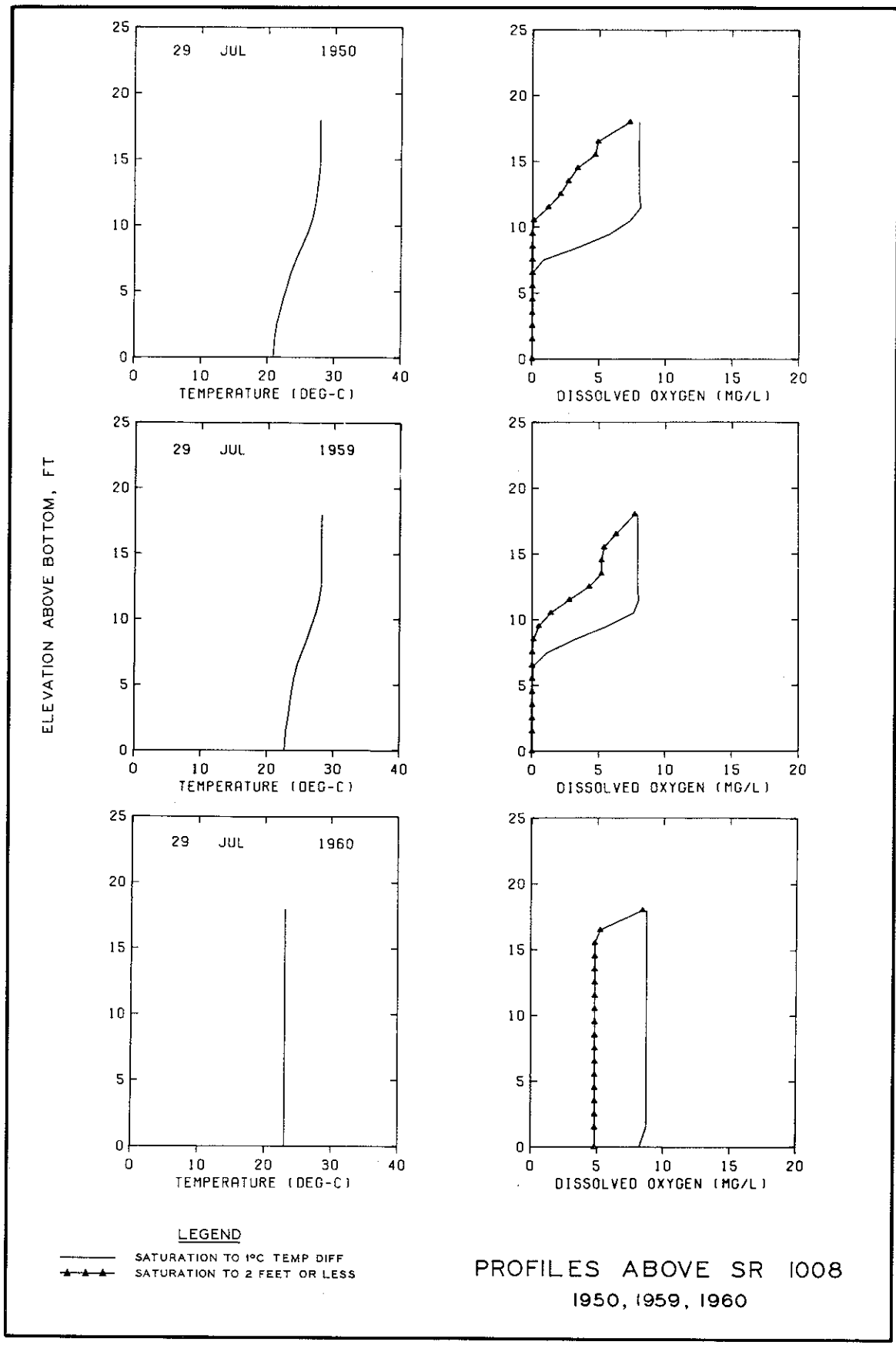
LEGEND

- SATURATION TO 1°C TEMP DIFF  
▲ SATURATION TO 2 FEET OR LESS

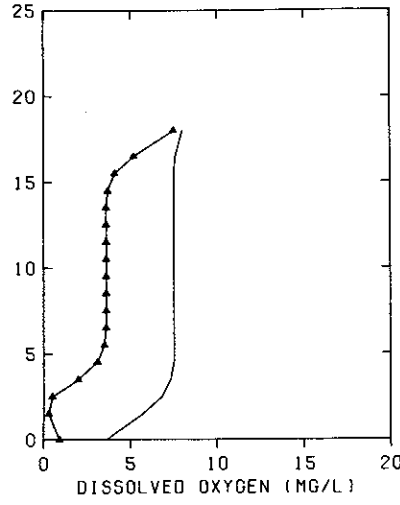
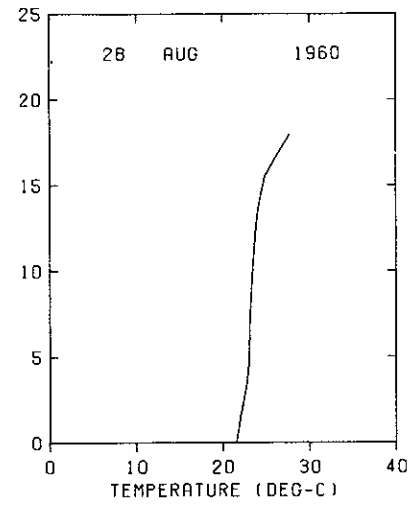
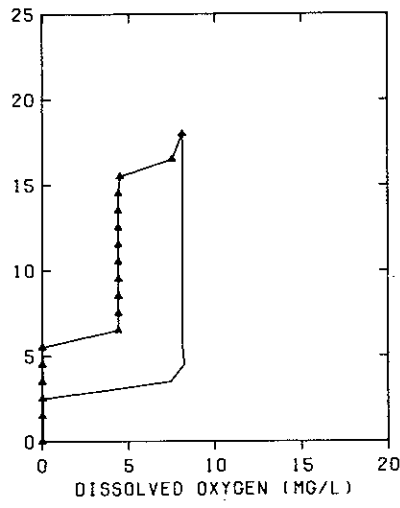
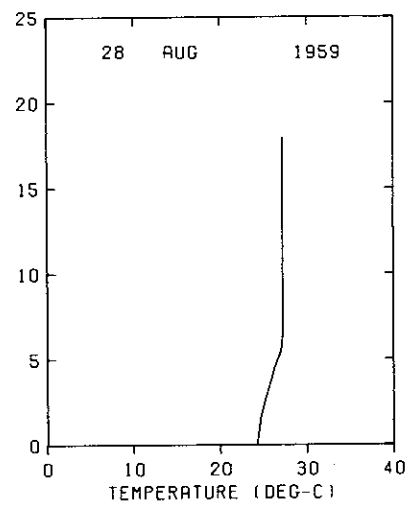
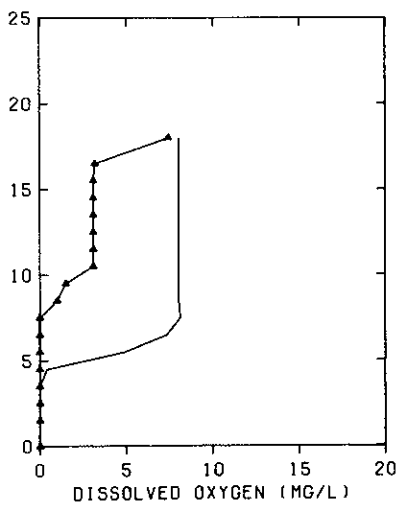
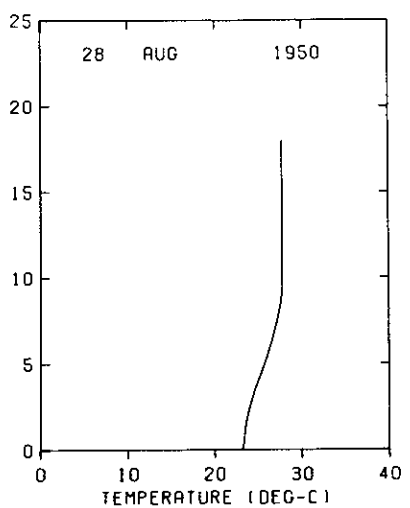
PROFILES ABOVE SR 1008  
1950, 1959, 1960







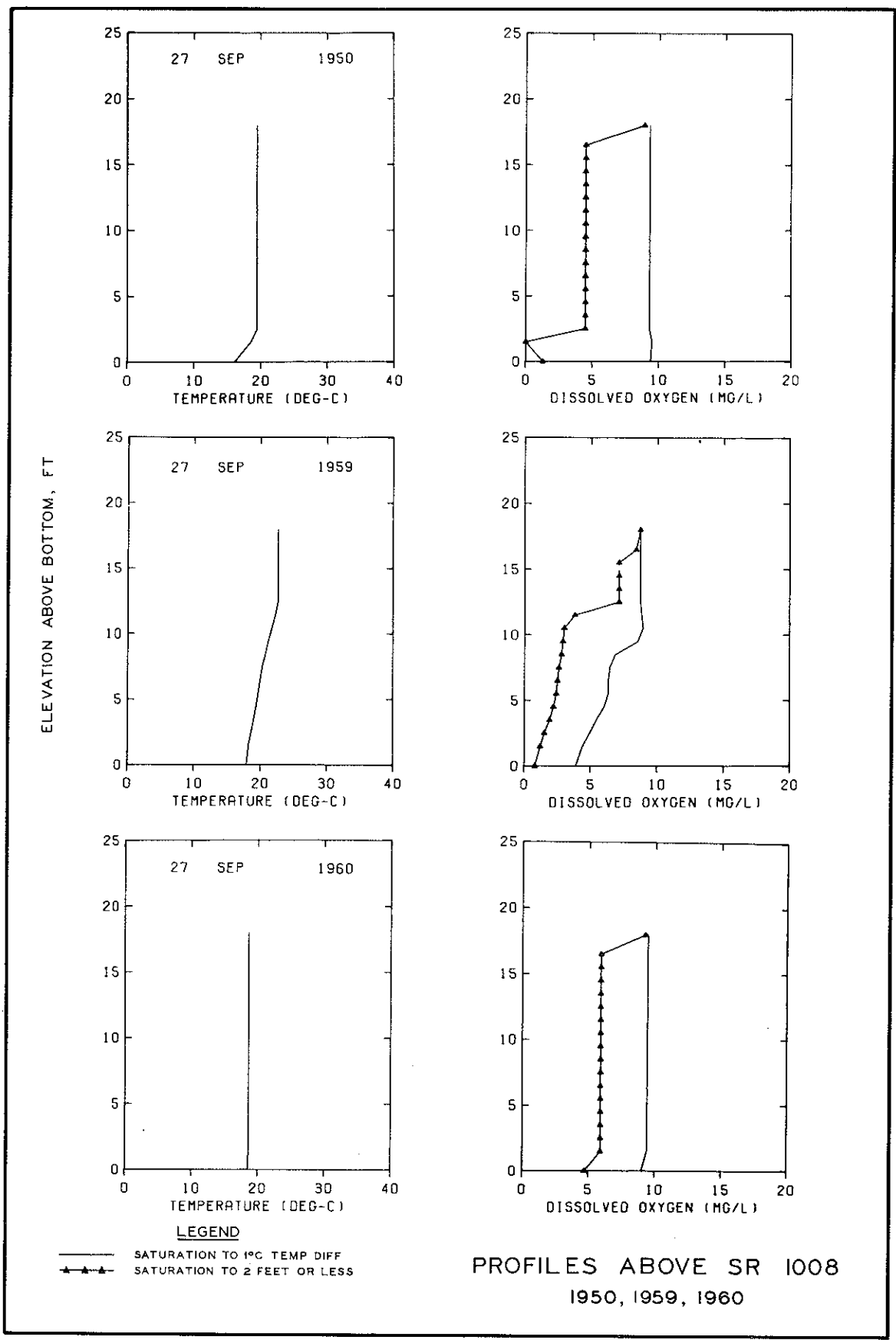
ELEVATION ABOVE BOTTOM, FT

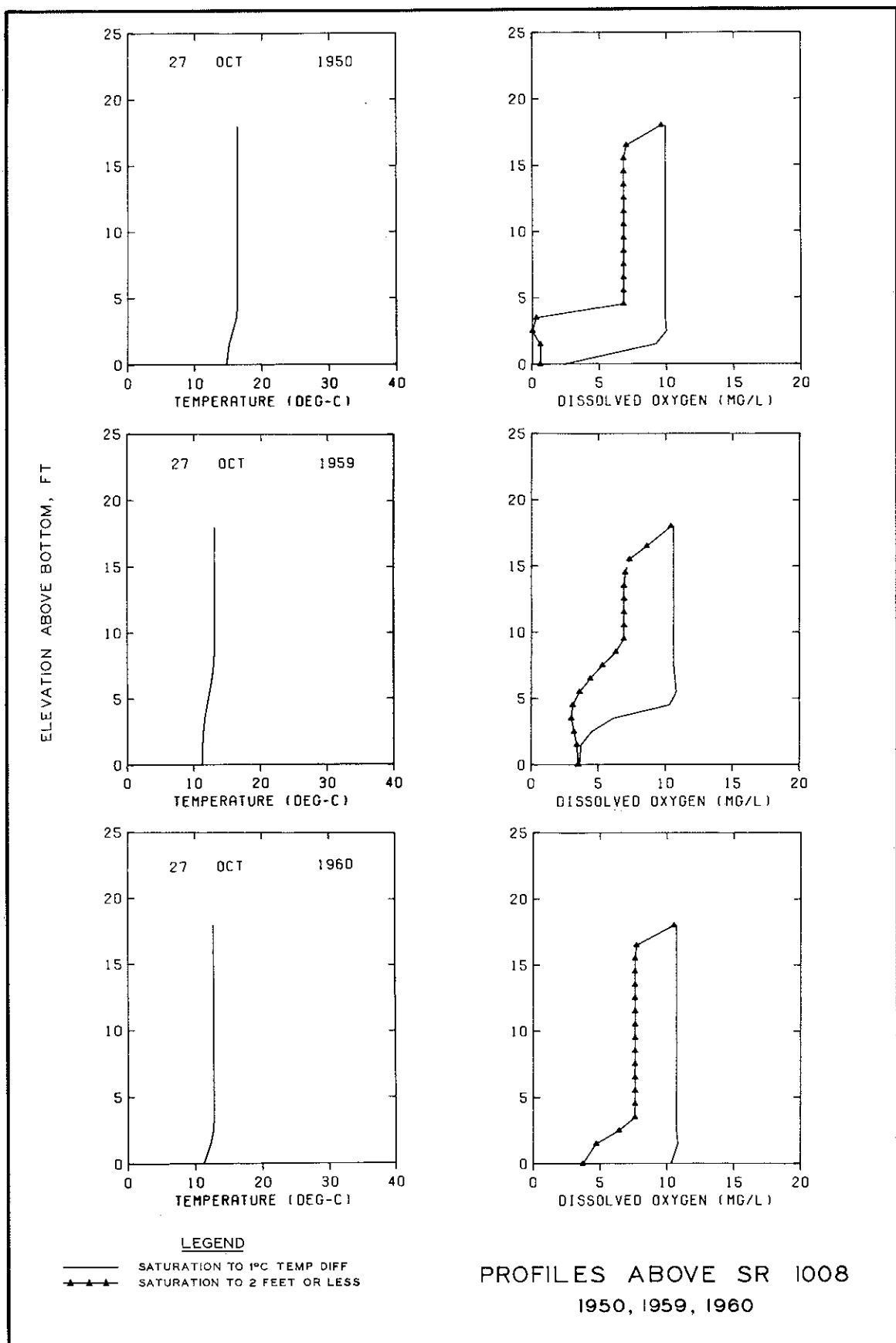


LEGEND

— Temperature profile  
▲ Dissolved oxygen profile

PROFILES ABOVE SR 1008  
1950, 1959, 1960





## APPENDIX B: RESULTS OF INITIAL SIMULATIONS

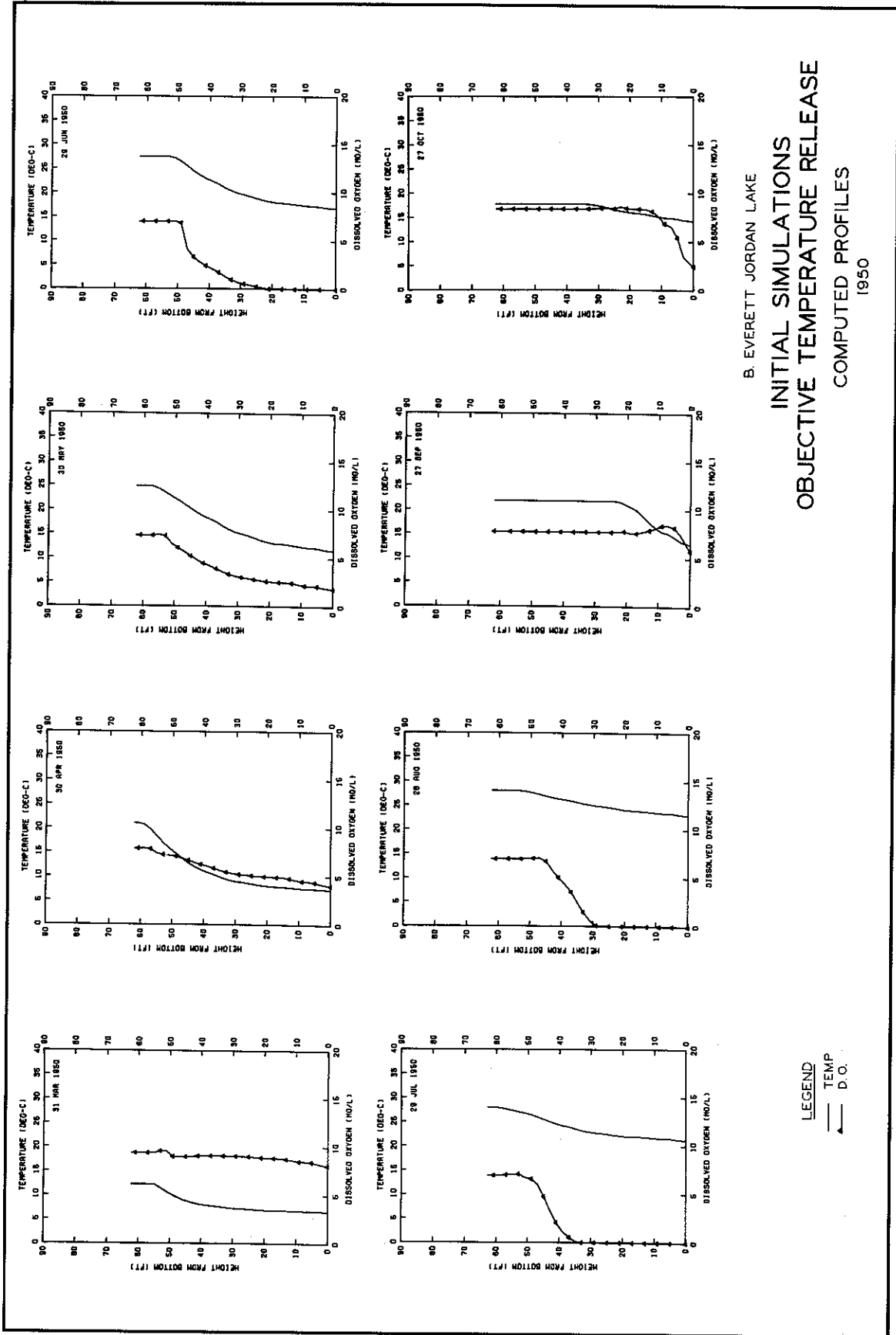
1. The results of the initial simulations, shown as thermal and D.O. profiles and release plots, are presented in this appendix. Plate B1 shows temperature and D.O. profiles; Plate B2 shows temperature and D.O. release plots based on an operation for achieving an objective temperature. Plate B3 shows profiles; Plate B4 shows release plots based on a minimum release temperature operation. Plate B5 shows profiles; and Plate B6 shows release plots based on a maximum release temperature operation. All of the results in these plates are based on a deoxygenation coefficient,  $K_D(20)$ , of  $0.15 \text{ day}^{-1}$  in the lower 14 ft of the lake and  $0.1 \text{ day}^{-1}$  elsewhere, and a B.O.D. decay coefficient,  $K_b$ , of  $0.01 \text{ day}^{-1}$ . Plate B7 shows profiles based on a maximum release temperature operation with  $K_D(20)$  unchanged but with the B.O.D. decay coefficient,  $K_b$ , equal to  $0.1 \text{ day}^{-1}$ .

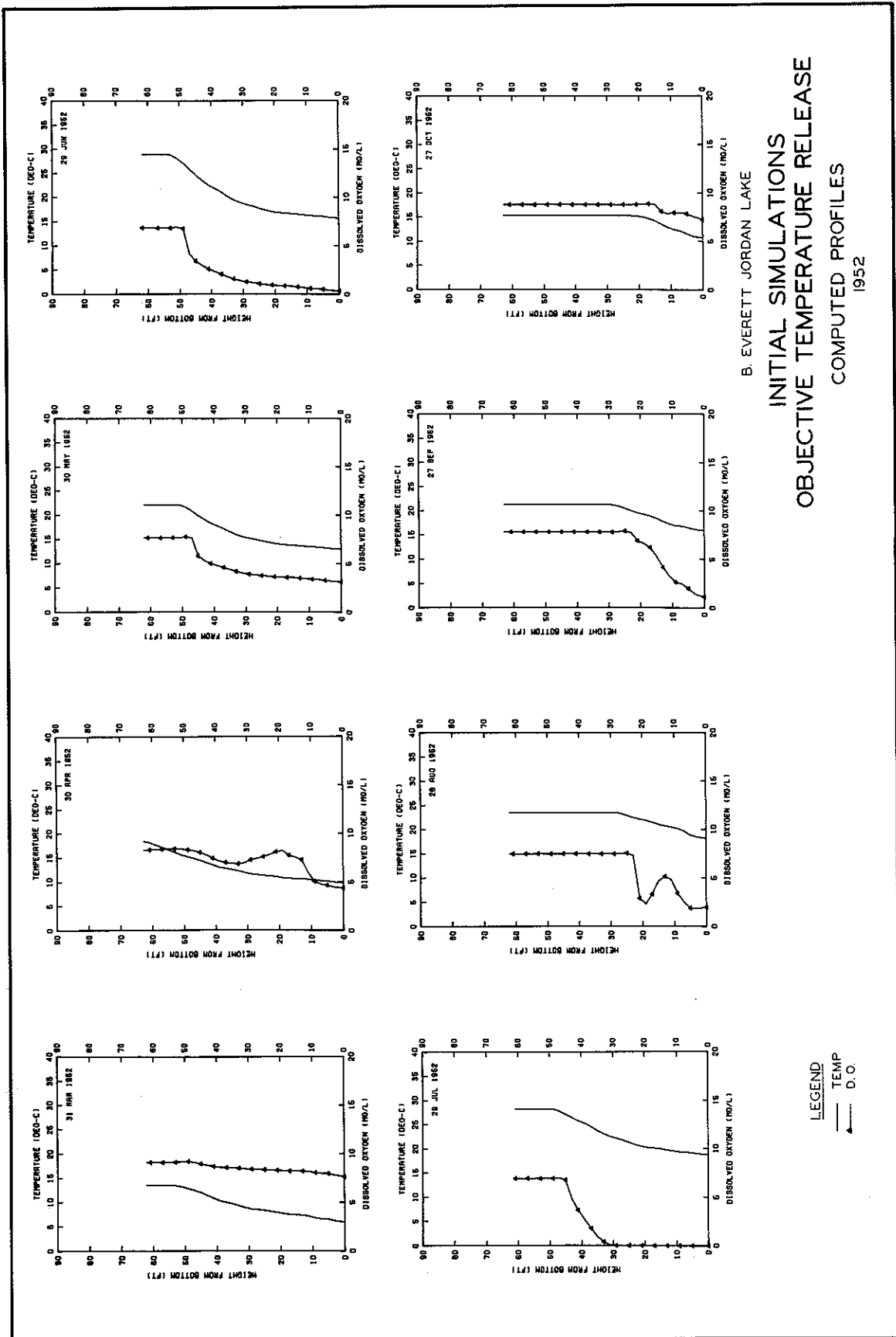
2. As discussed previously, these results can be compared with the results shown in Plate 5 to evaluate the calibration of the WESTEX model. Additionally, the results of the initial simulations can be compared with the results shown in Plates 6-11 to assess the effect of the modifications made to the numerical simulation model based on the physical model tests.

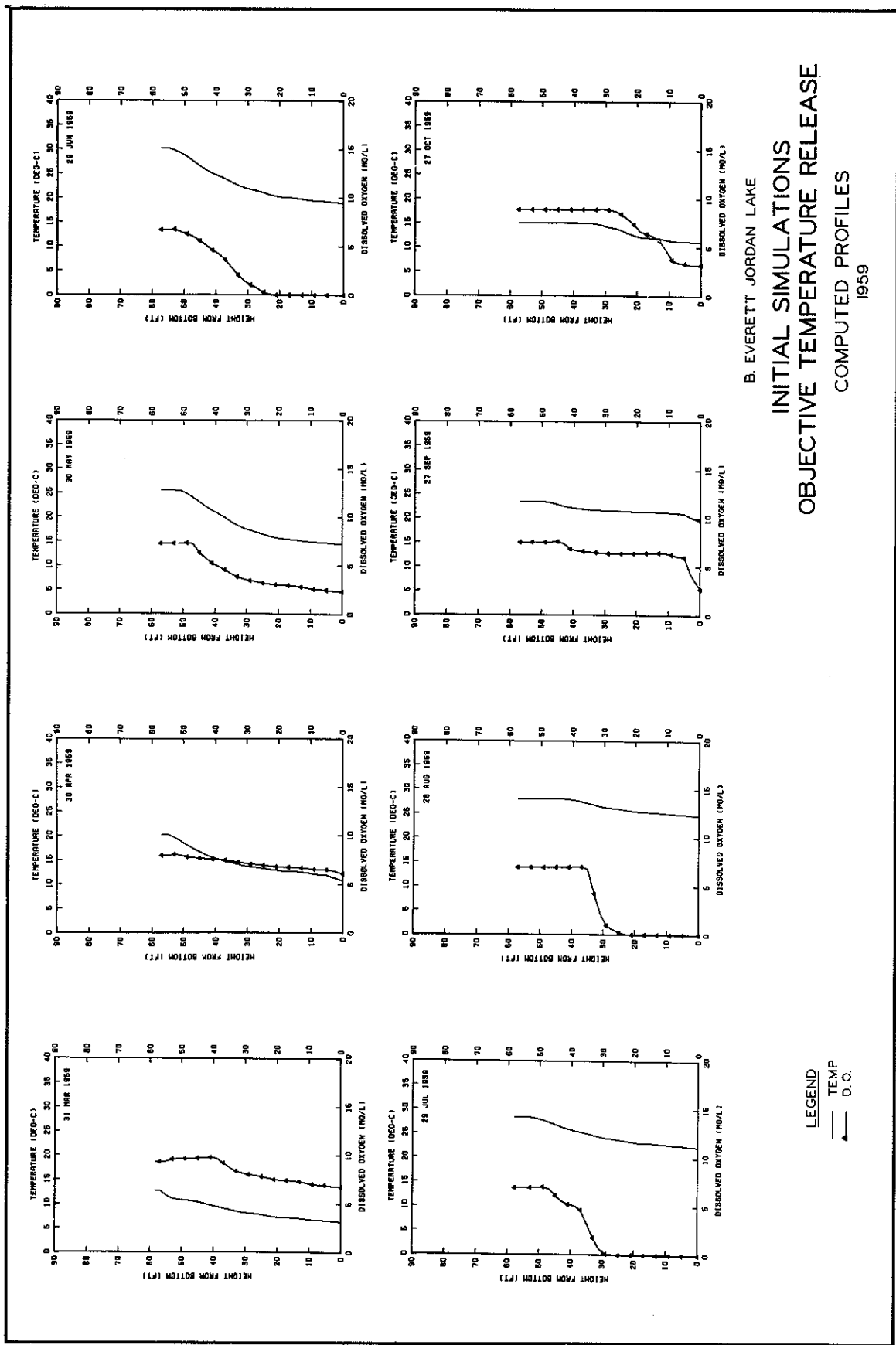
3. The modifications made to the WESTEX model were the incorporation of inflow mixing, entrainment by the inflow current, reduction of the effective storage, elimination of the D.O. contributed by the New Hope inflow, and travel time. Comparison of results shows the effects of these modifications are most apparent in the predicted thermal and D.O. profiles. The modified WESTEX predictions show B. Everett Jordan Lake to be less stratified (temperature and D.O.) than predicted by the initial simulations.

4. The value of the physical model was to identify and quantify the modifications that were required in the numerical simulation model to represent the hydrodynamics of B. Everett Jordan Lake. This improved hydrodynamic description yields increased confidence in the simulation

results. It should be noted that more information was contained in the physical model than could be used in the WESTEX model. The WESTEX model predicts conditions immediately upstream of the dam. Hydrodynamic conditions at other locations may also be important. This was particularly well illustrated by the important circulation characteristics of the New Hope arm of B. Everett Jordan Lake.







B. EVERETT JORDAN LAKE  
INITIAL SIMULATIONS  
OBJECTIVE TEMPERATURE RELEASE  
COMPUTED PROFILES  
1959

LEGEND  
 TEMP  
 D.O.

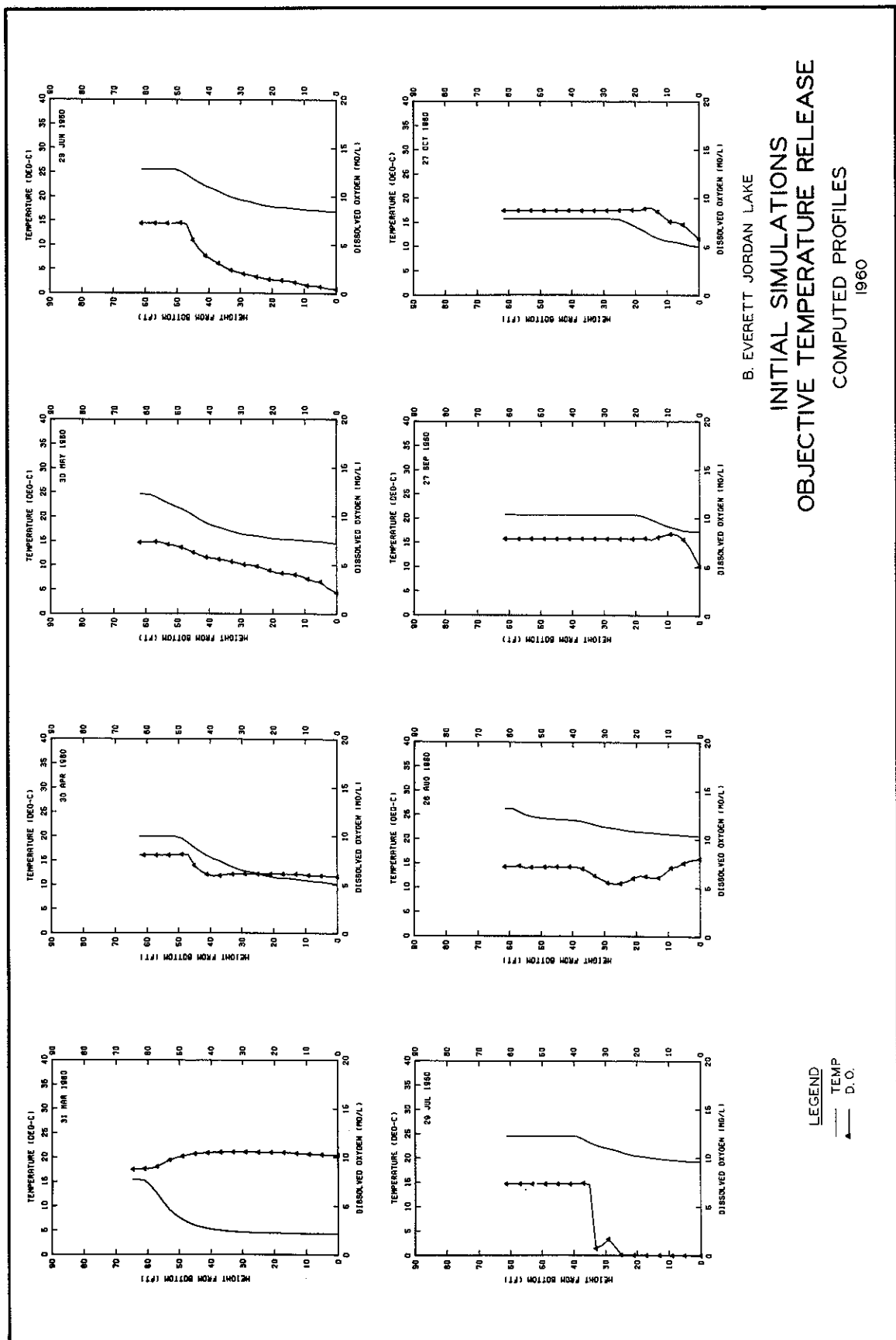
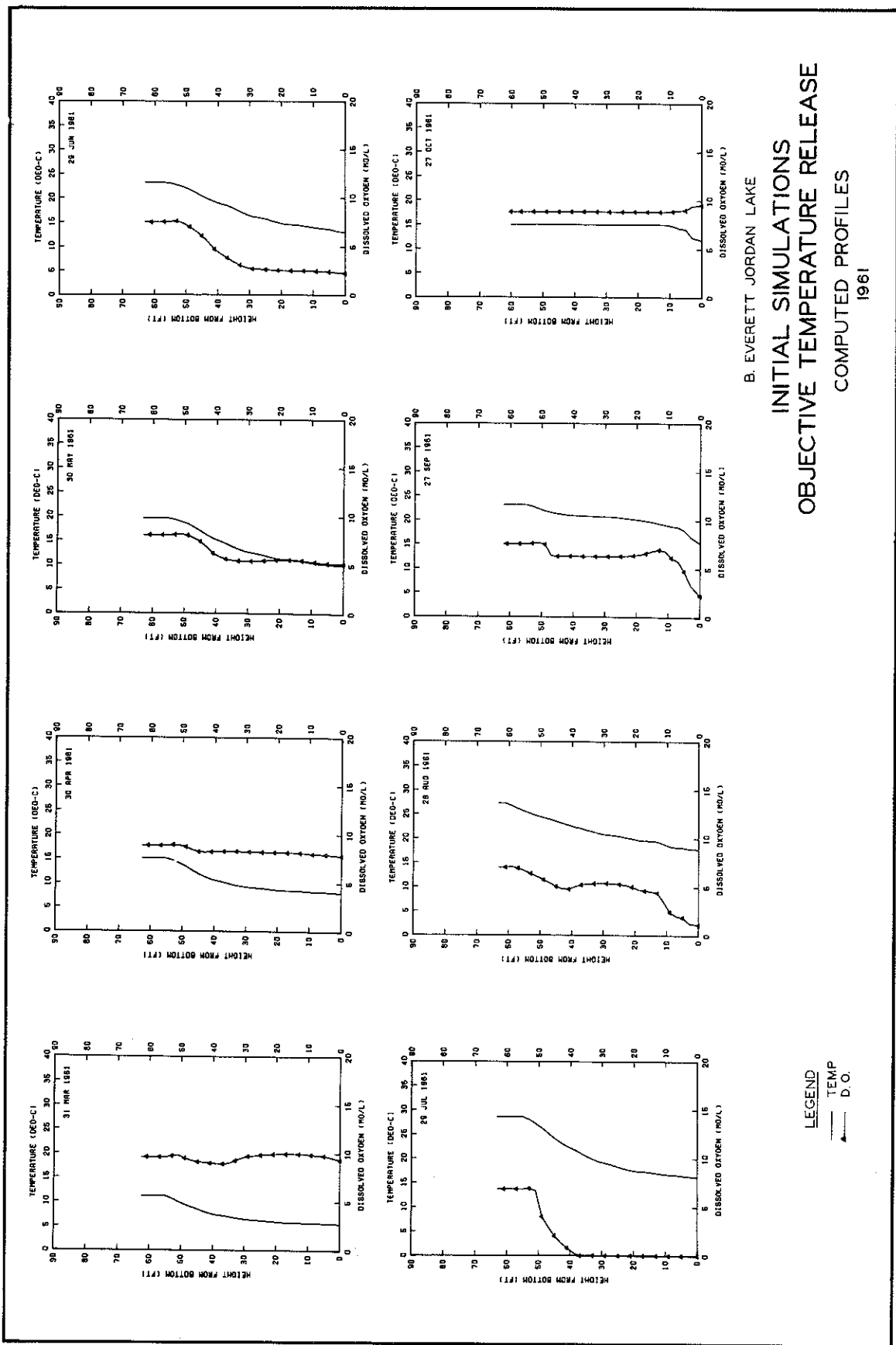
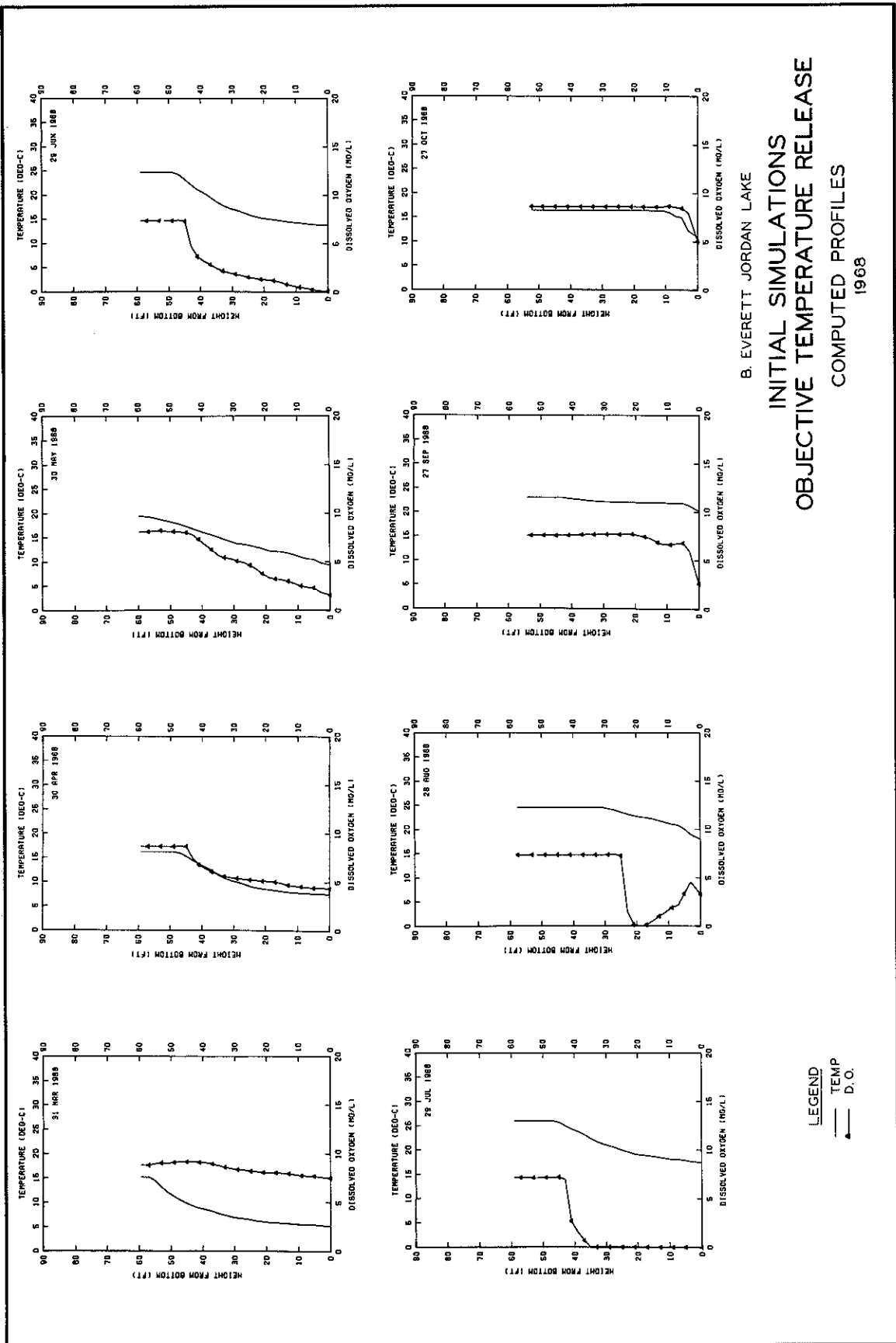
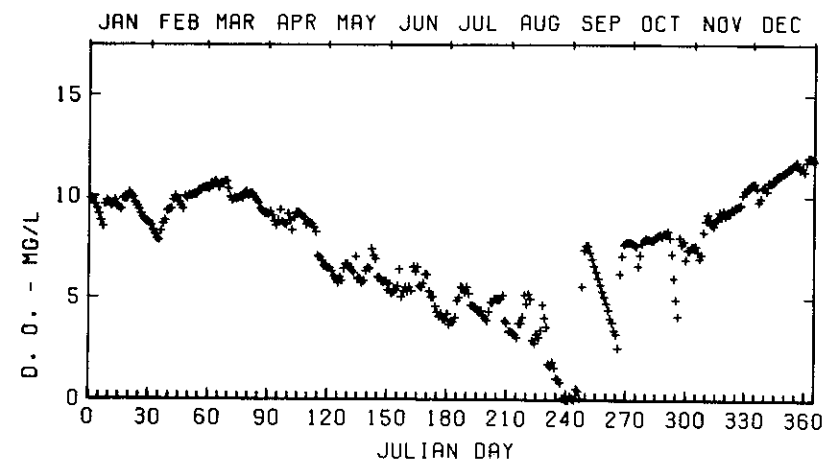
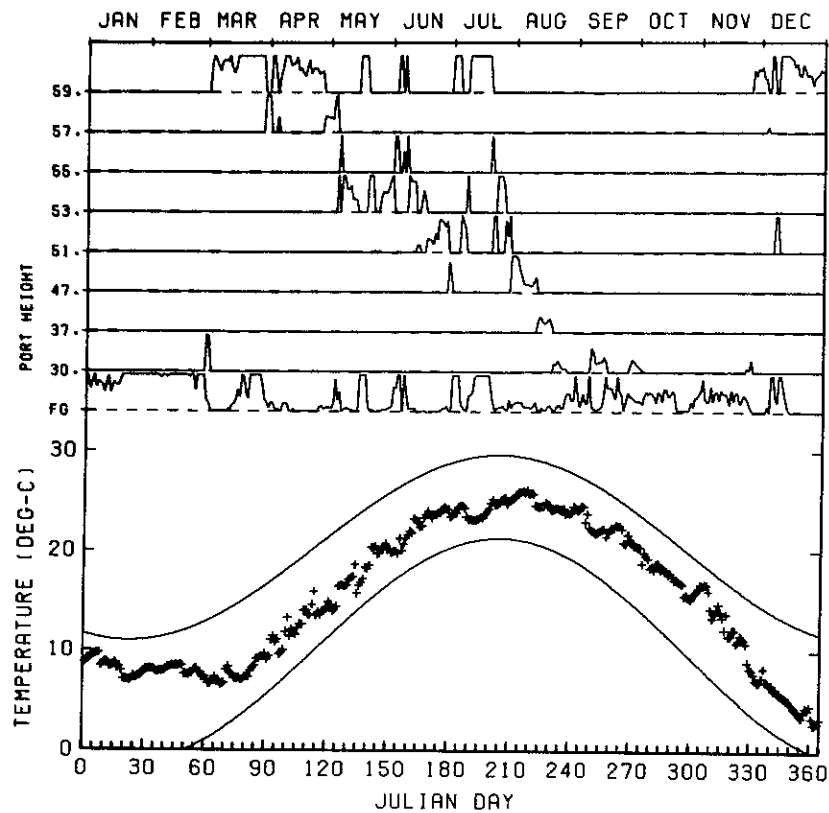


PLATE B1 (SHEET 4 OF 6)

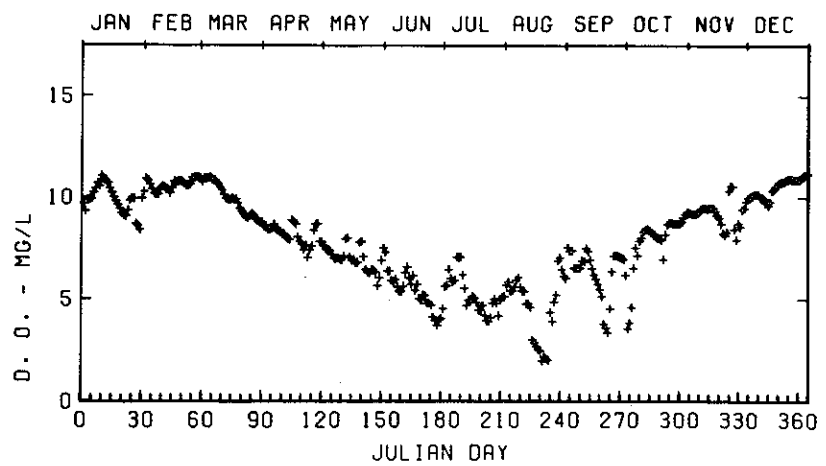
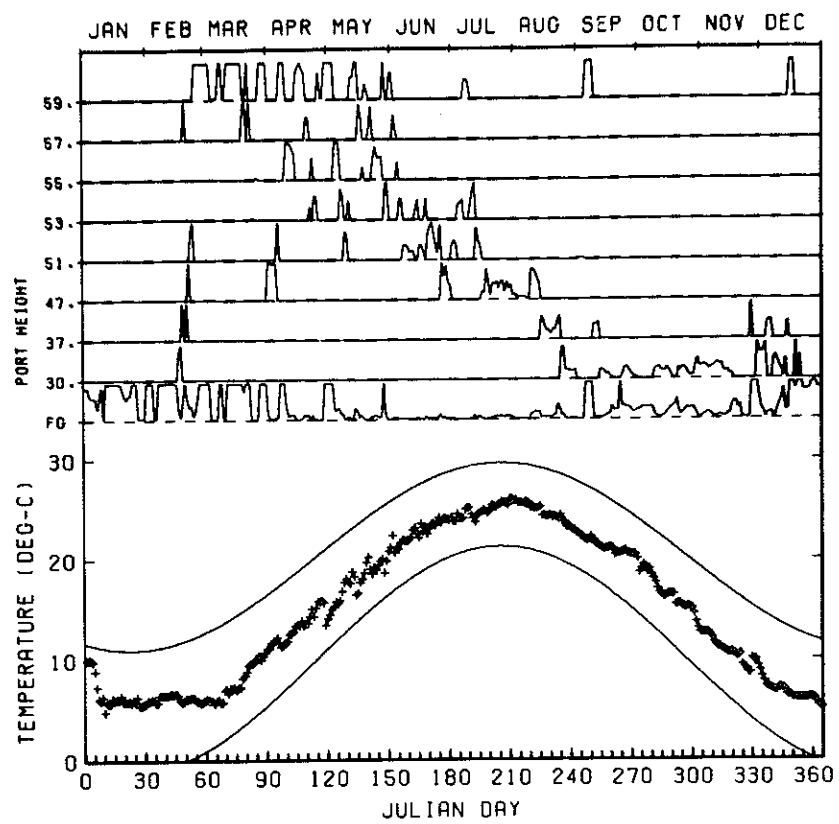
B. EVERETT JORDAN LAKE  
INITIAL SIMULATIONS  
OBJECTIVE TEMPERATURE RELEASE  
COMPUTED PROFILES  
1960



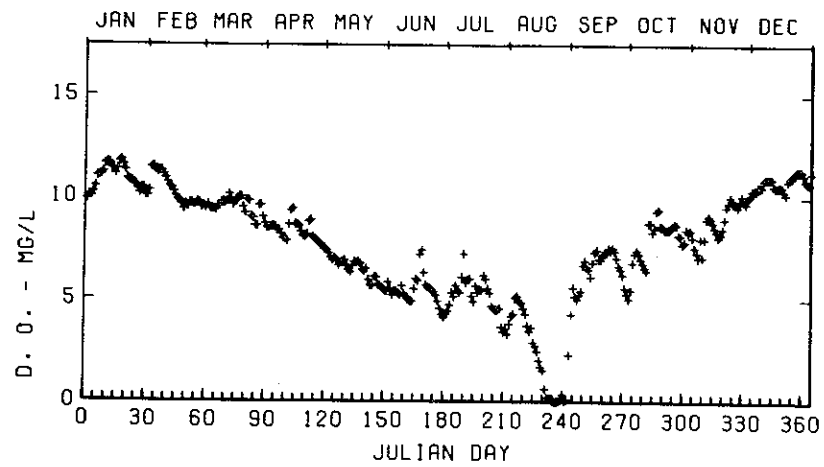
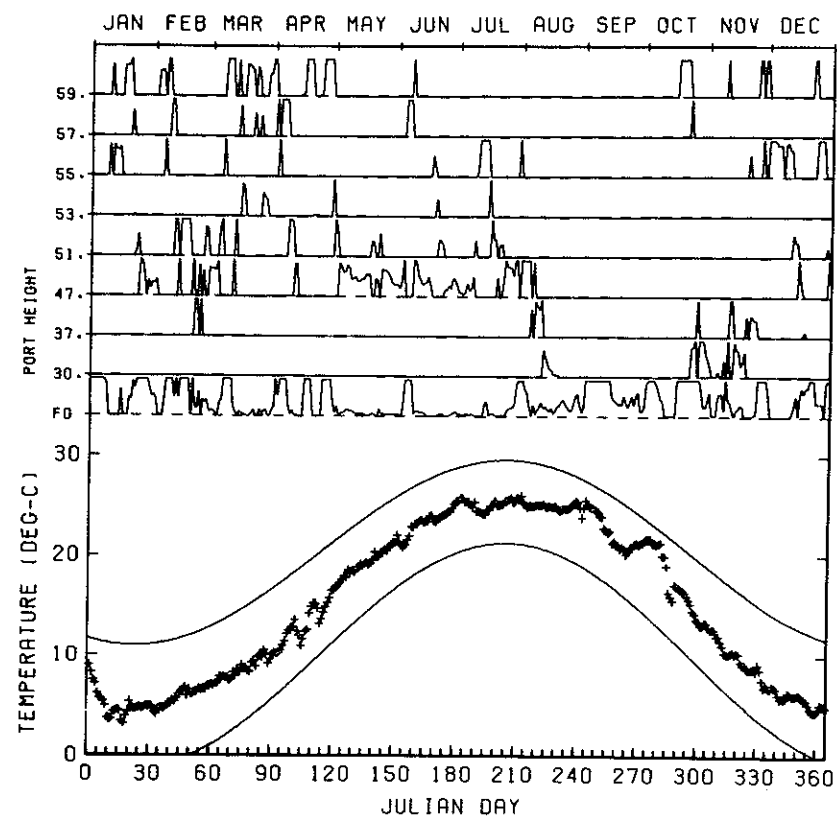




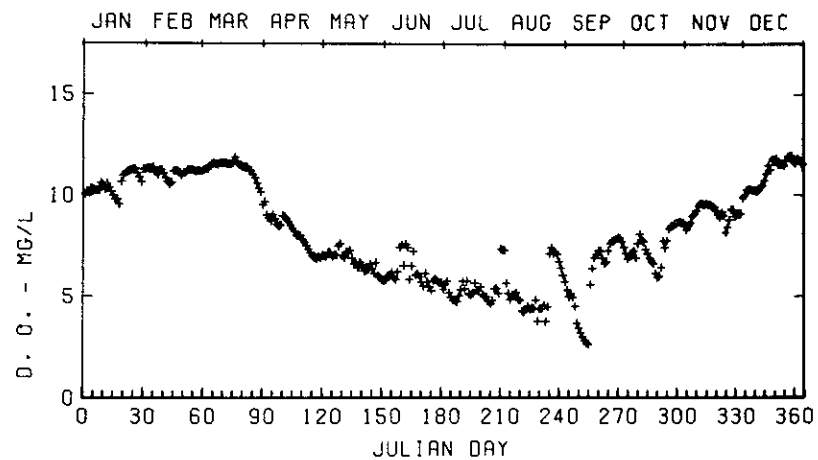
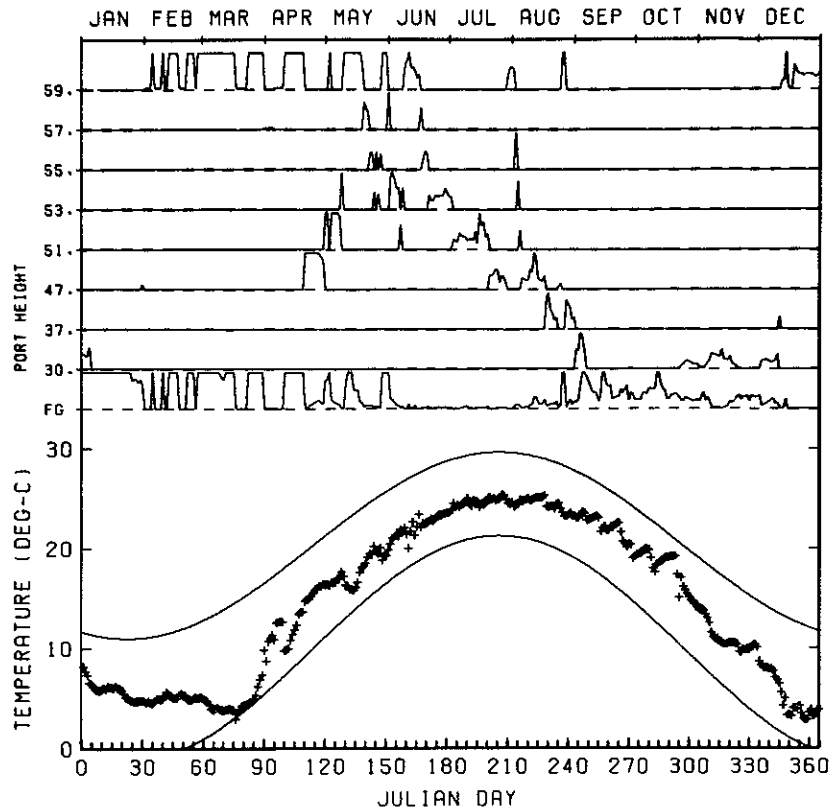
B. EVERETT JORDAN LAKE  
 INITIAL SIMULATIONS  
 TEMPERATURE OBJECTIVE  
 1950



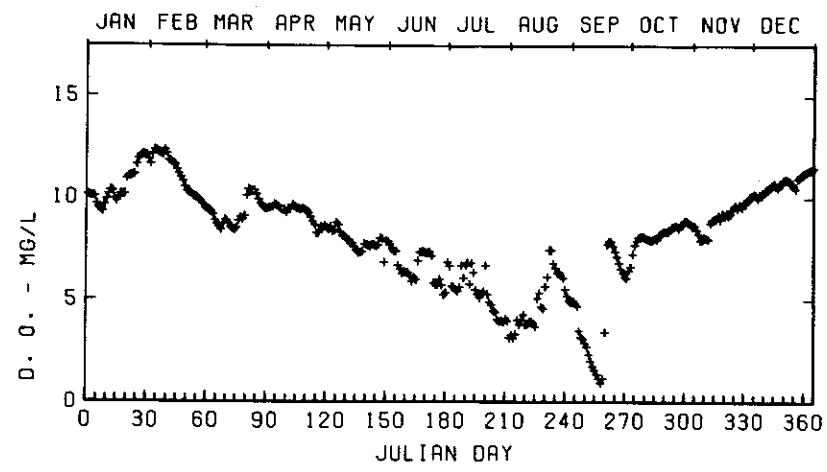
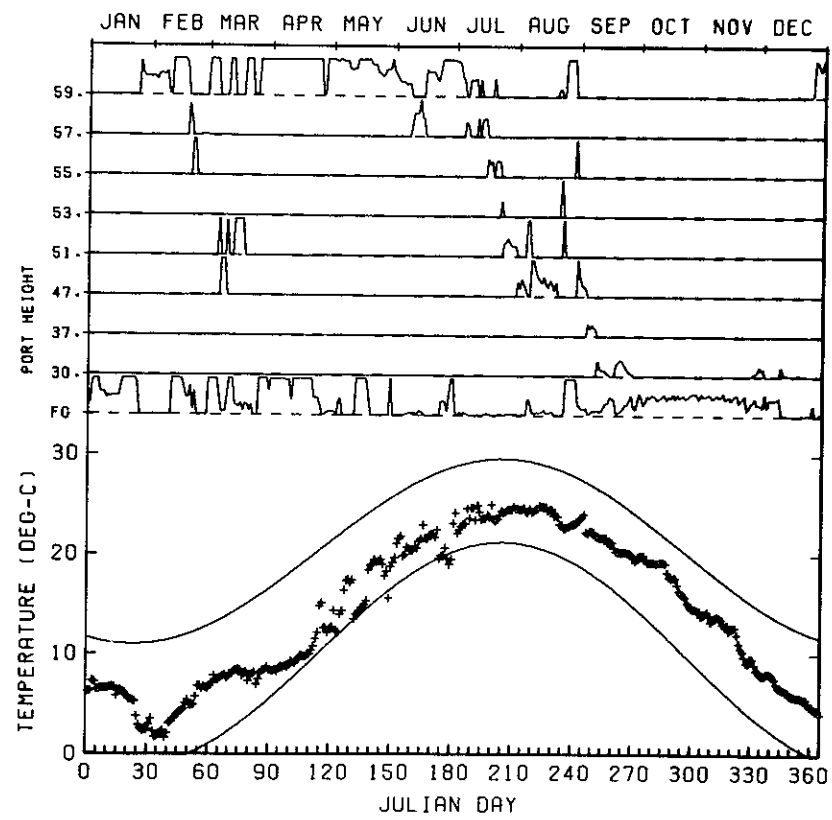
B. EVERETT JORDAN LAKE  
INITIAL SIMULATIONS  
TEMPERATURE OBJECTIVE  
1952



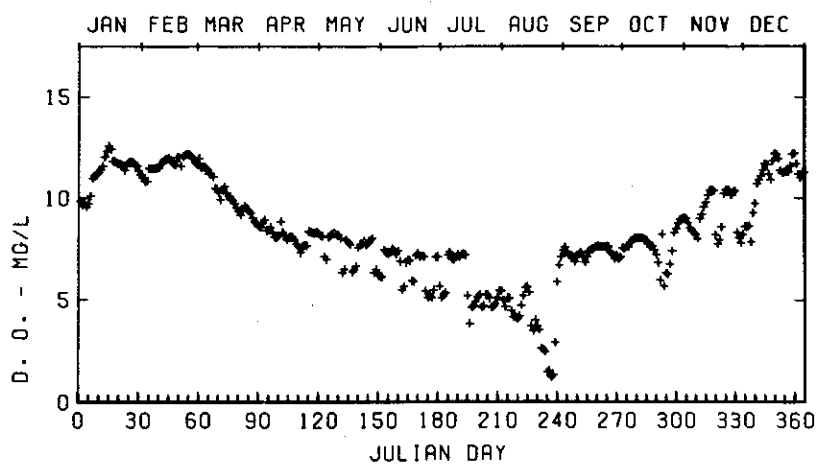
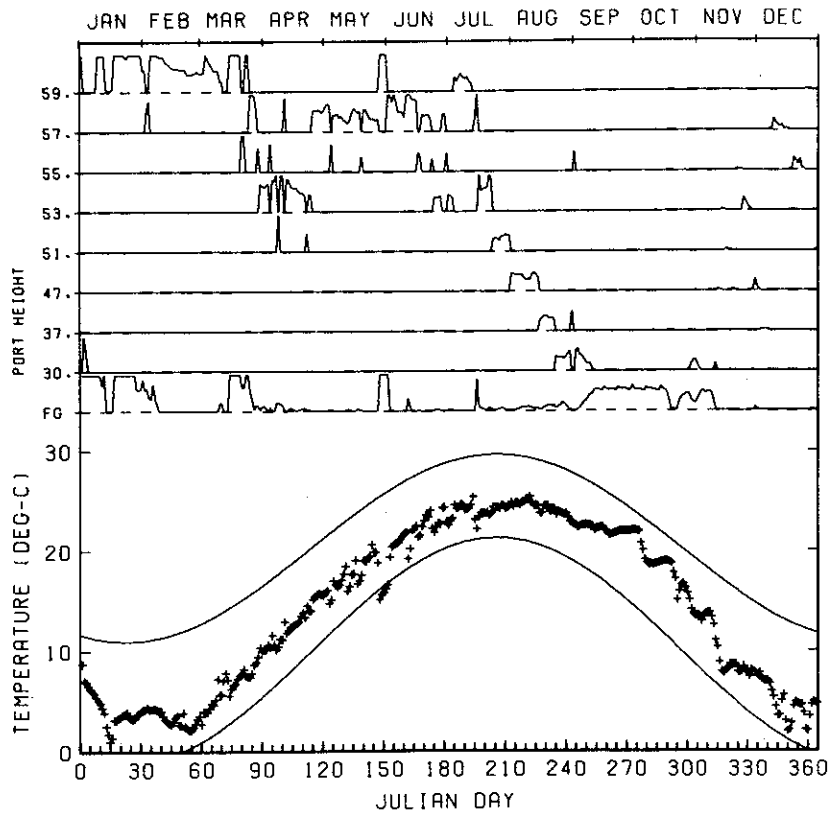
B. EVERETT JORDAN LAKE  
INITIAL SIMULATIONS  
TEMPERATURE OBJECTIVE  
1959



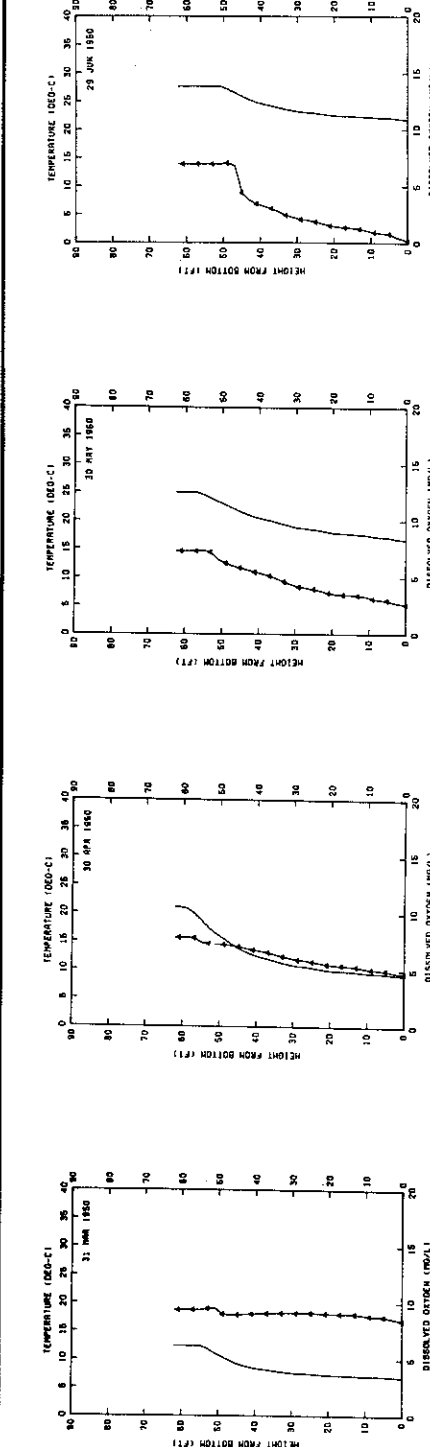
B. EVERETT JORDAN LAKE  
INITIAL SIMULATIONS  
TEMPERATURE OBJECTIVE  
1960



B. EVERETT JORDAN LAKE  
INITIAL SIMULATIONS  
TEMPERATURE OBJECTIVE  
1961



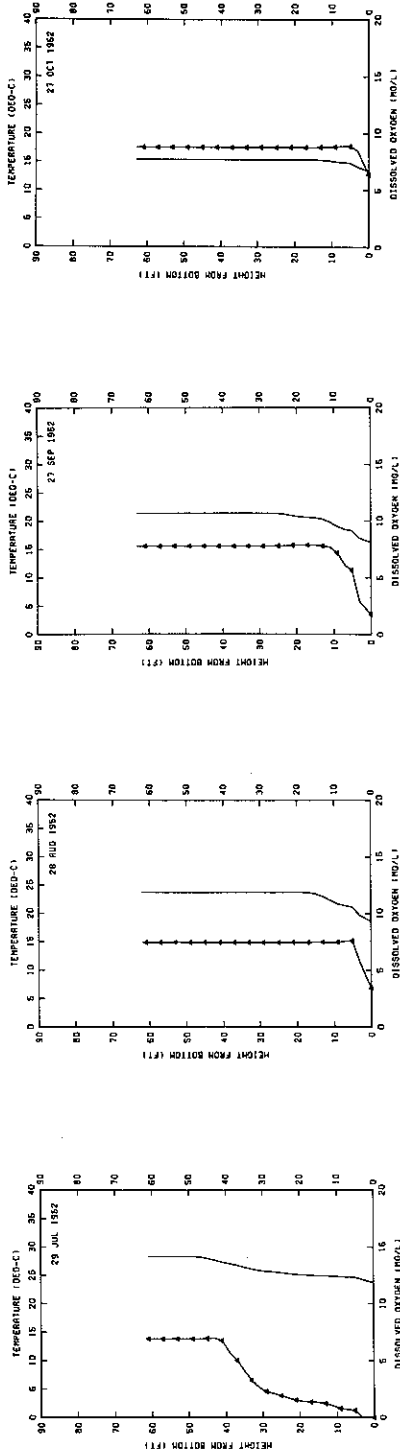
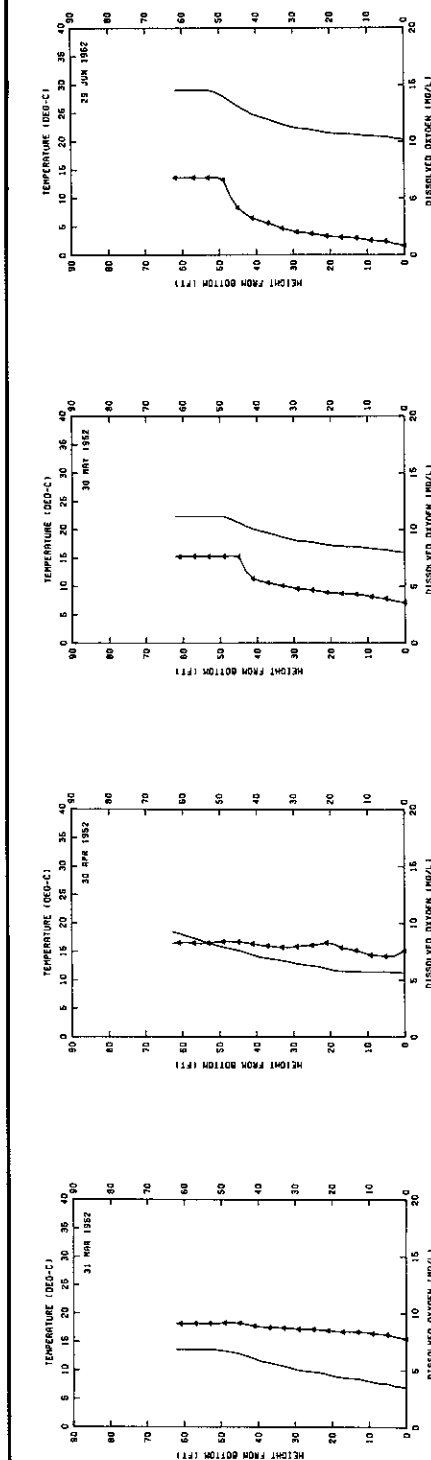
B. EVERETT JORDAN LAKE  
INITIAL SIMULATIONS  
TEMPERATURE OBJECTIVE  
1968



B. EVERETT JORDAN LAKE  
INITIAL SIMULATIONS  
MINIMUM RELEASE TEMPERATURE  
COMPUTED PROFILES

[950]

LEGEND  
— TEMP  
↔ D.O.

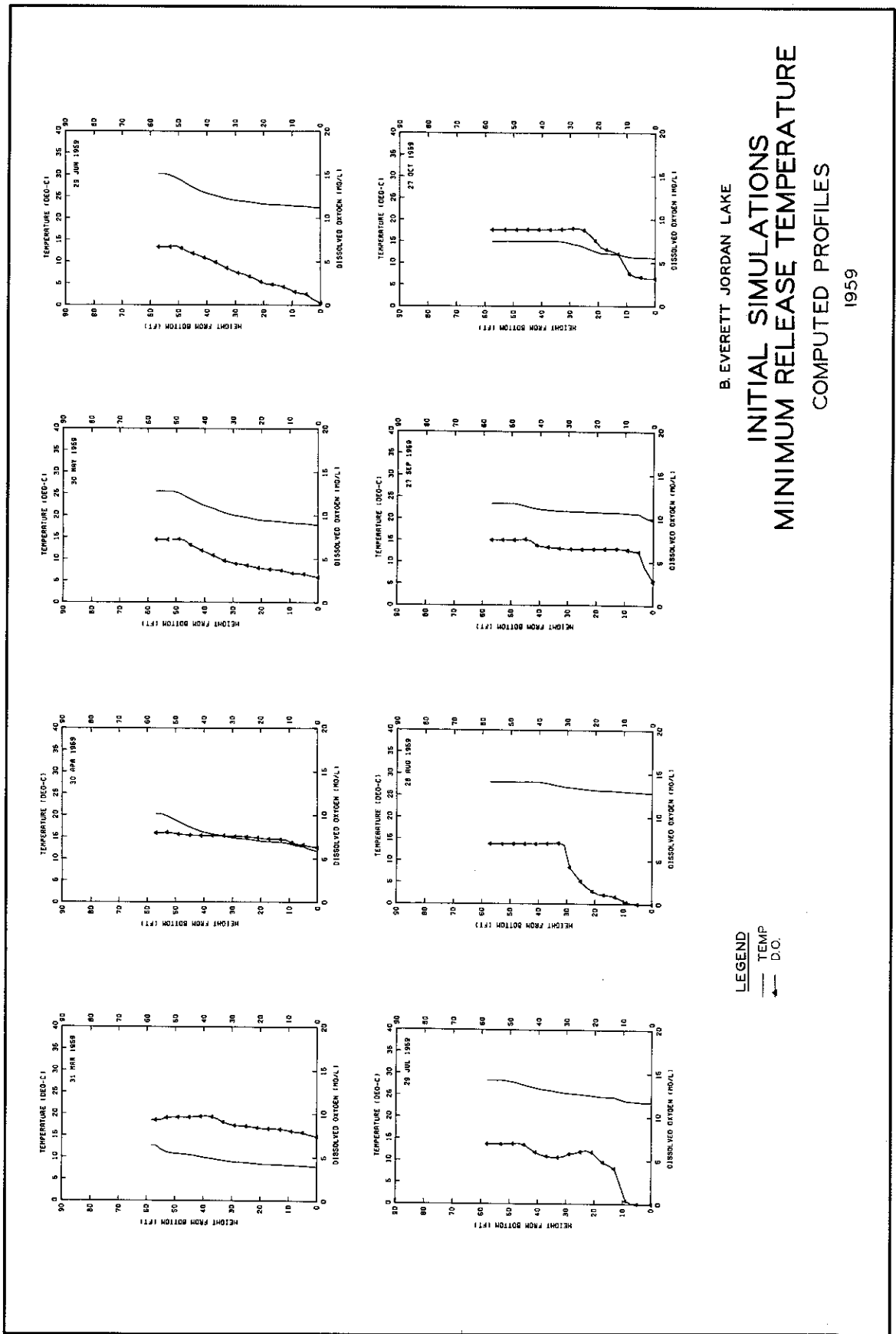


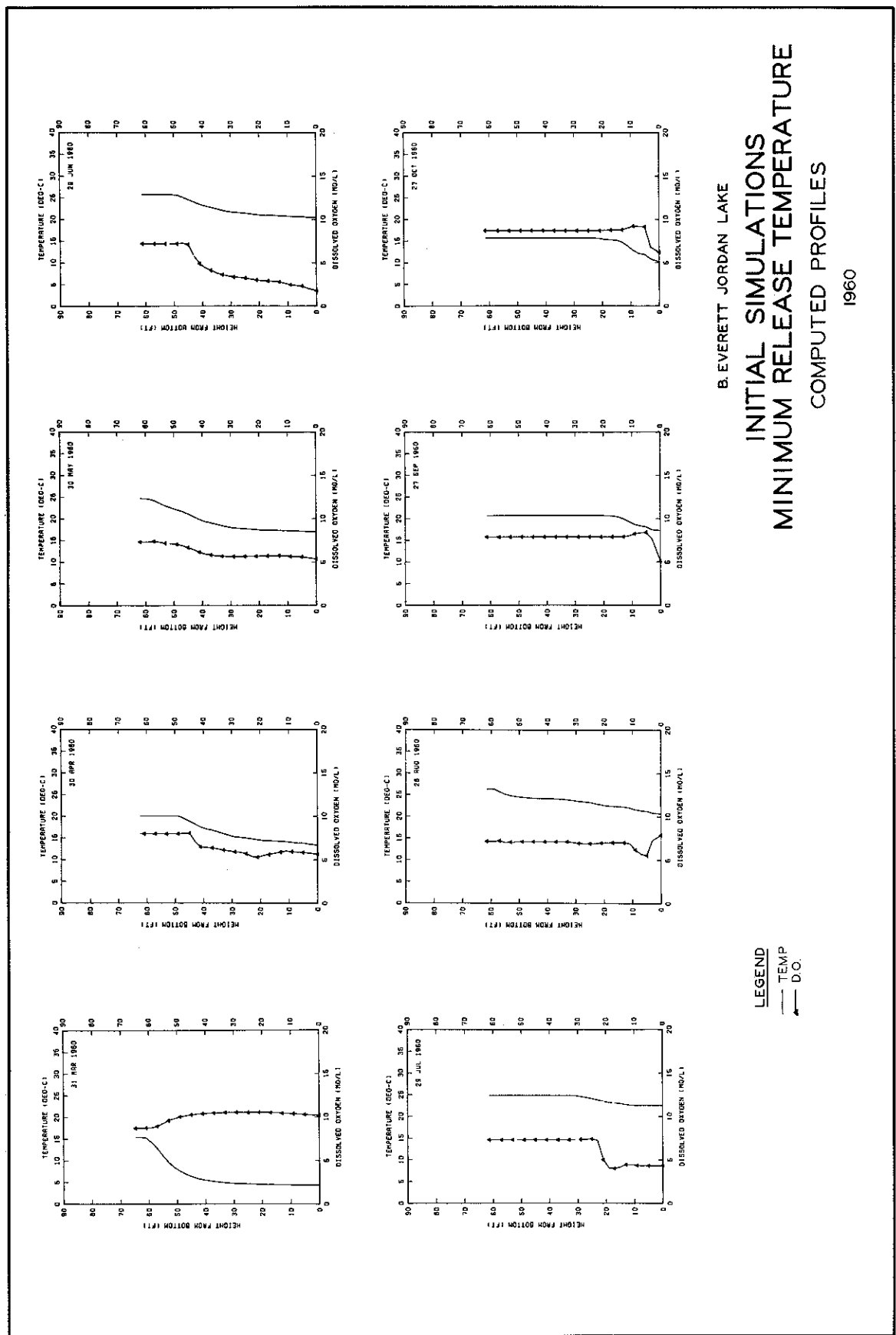
B. EVERETT JORDAN LAKE  
INITIAL SIMULATIONS  
MINIMUM RELEASE TEMPERATURE  
COMPUTED PROFILES  
1952

LEGEND

— TEMP

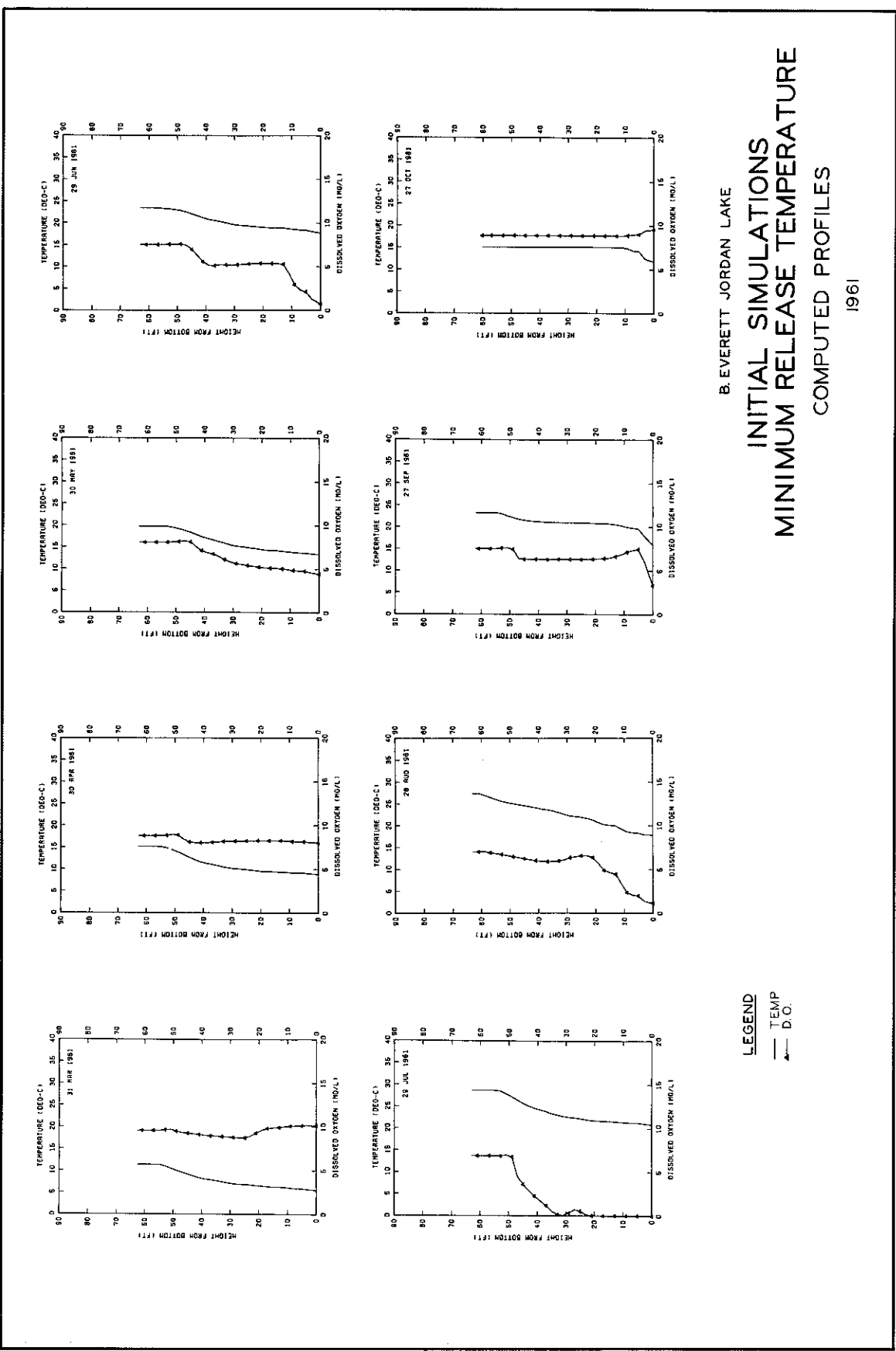
↔ D.O.

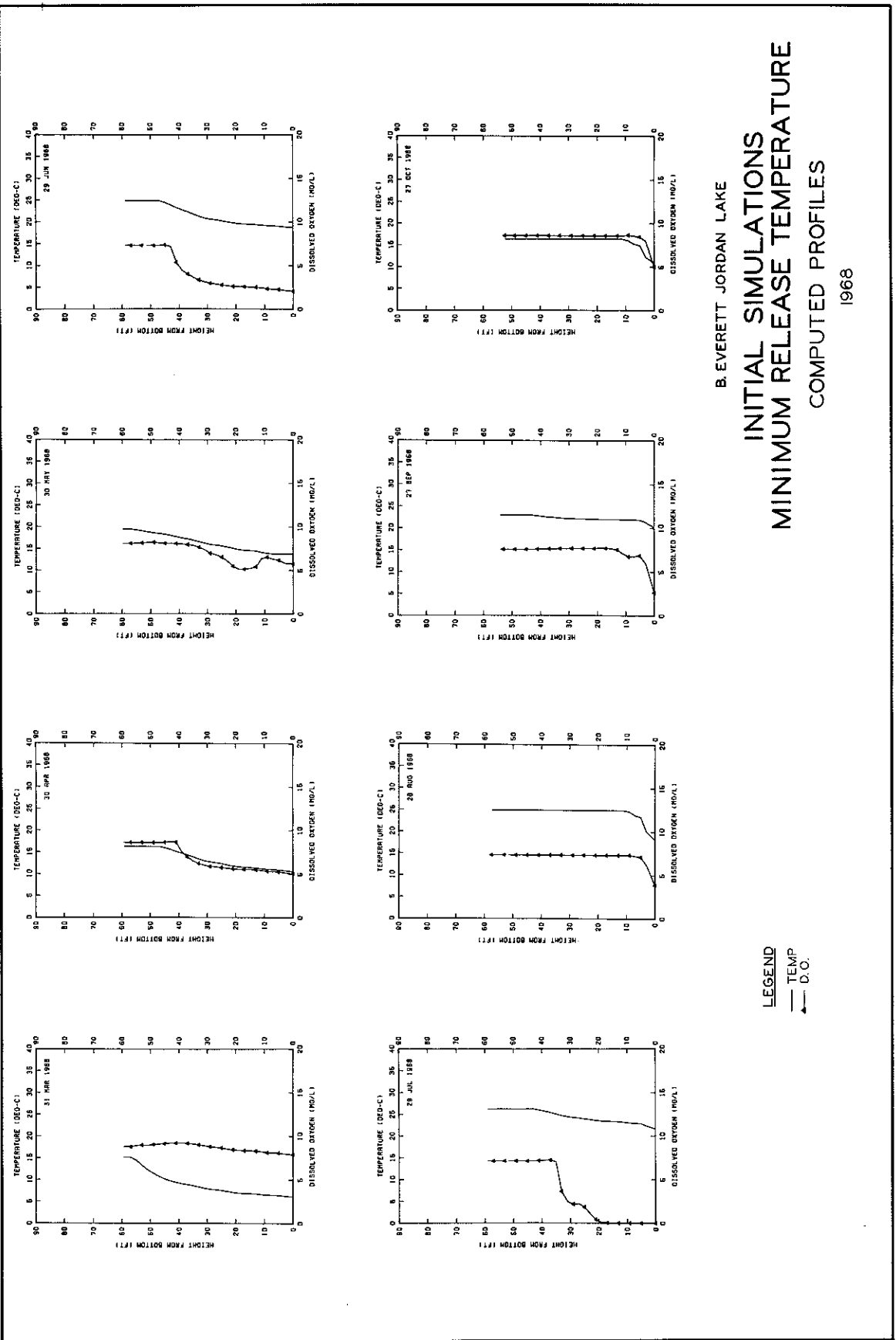




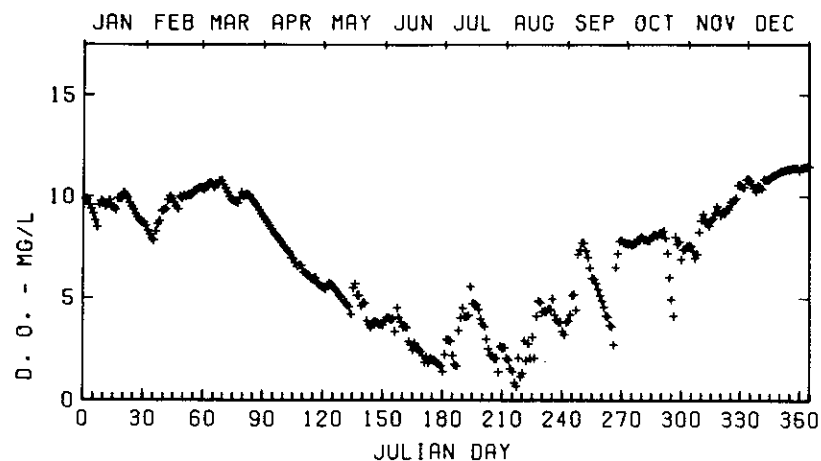
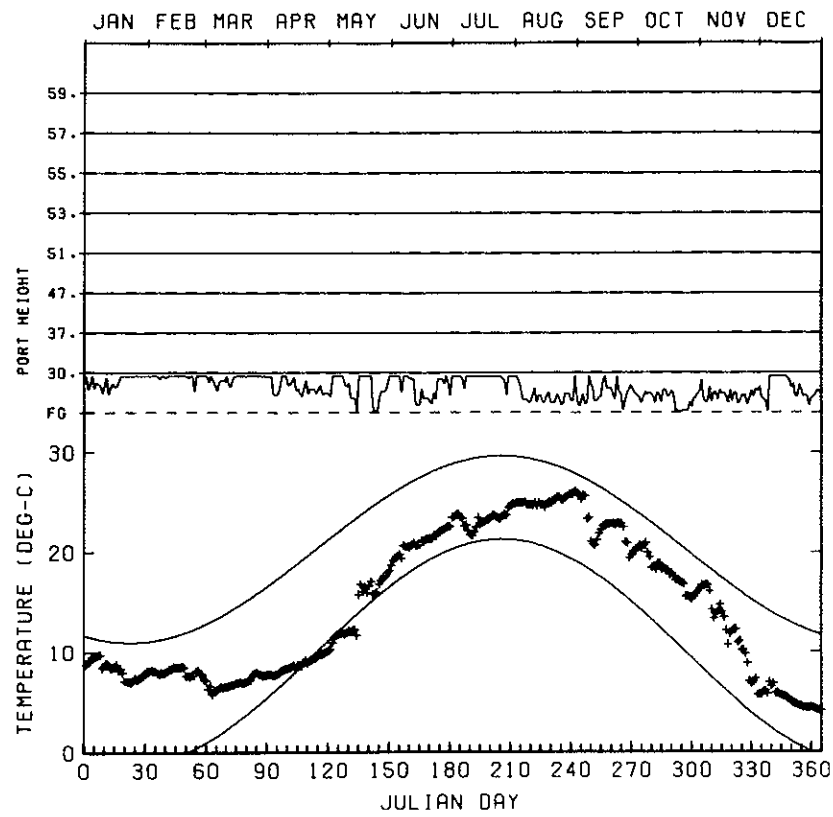
B. EVERETT JORDAN LAKE  
INITIAL SIMULATIONS  
MINIMUM RELEASE TEMPERATURE  
COMPUTED PROFILES  
1960

LEGEND  
— Temp  
— D.O.

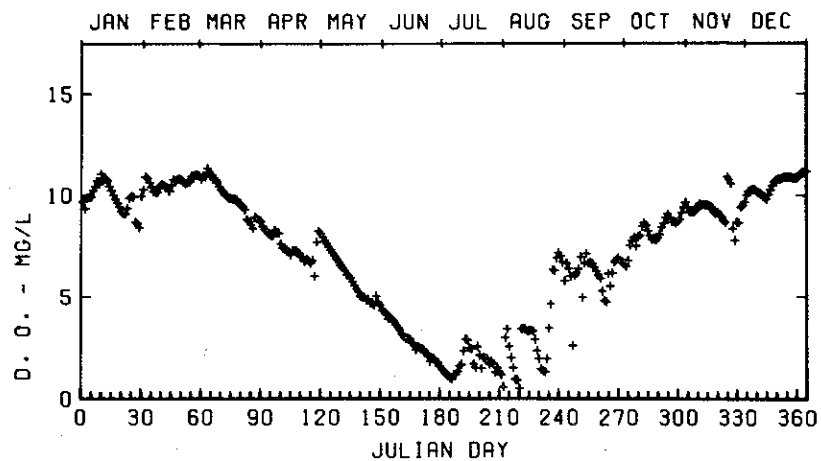
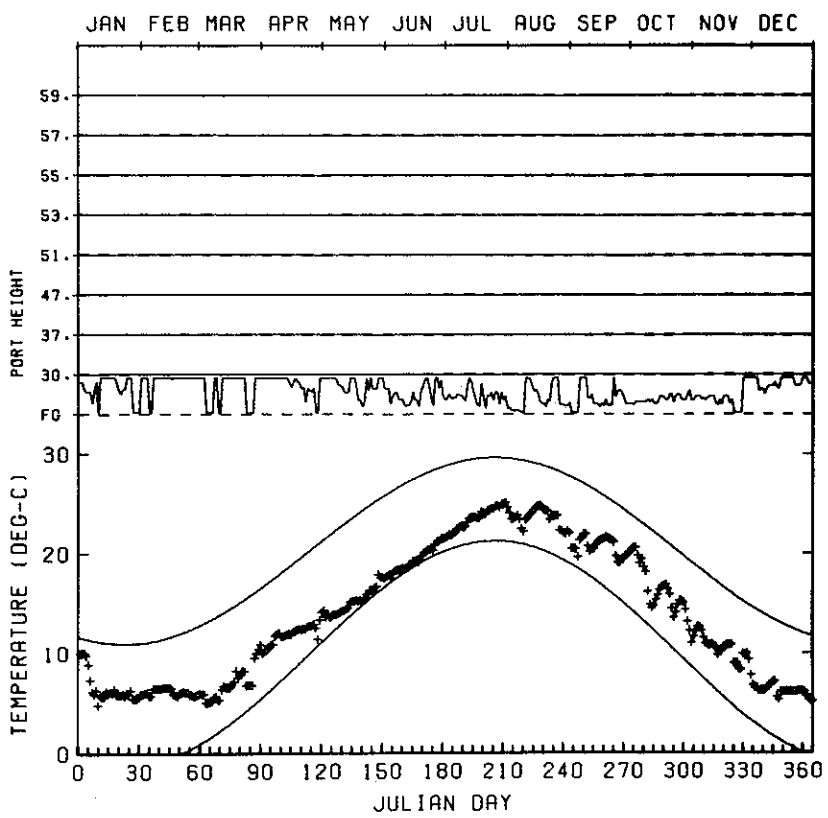




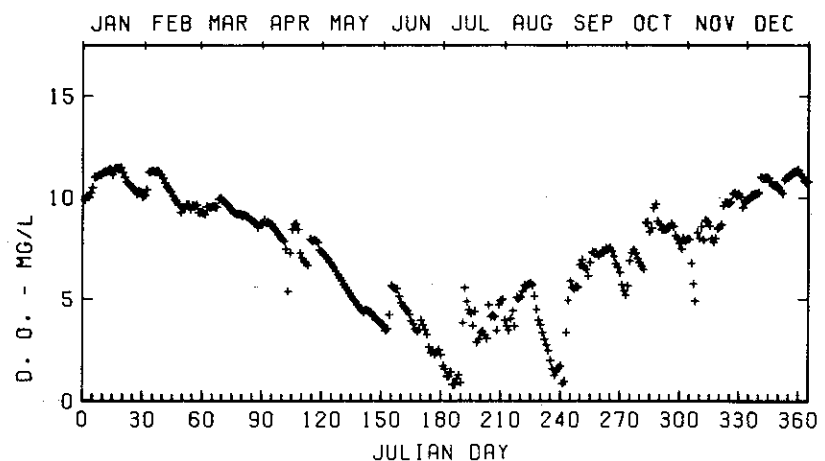
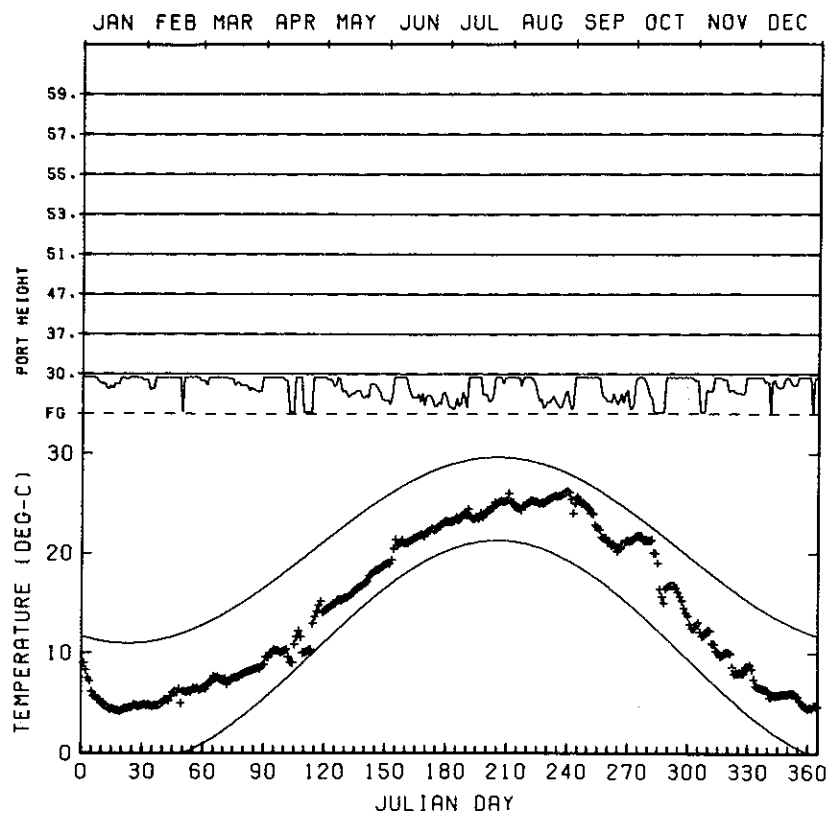
B. EVERETT JORDAN LAKE  
**INITIAL SIMULATIONS  
 MINIMUM RELEASE TEMPERATURE  
 COMPUTED PROFILES**  
 1968



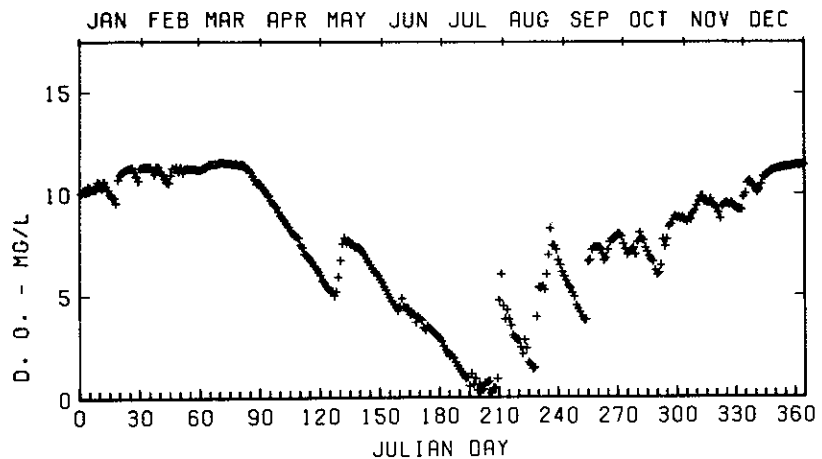
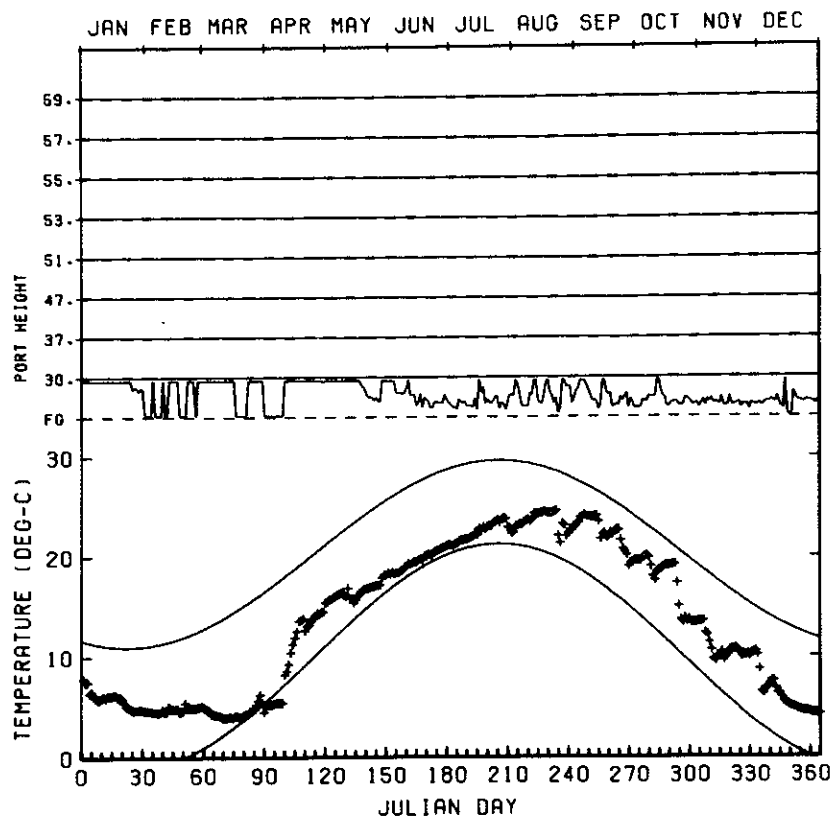
B. EVERETT JORDAN LAKE  
 INITIAL SIMULATIONS  
 MINIMUM RELEASE TEMPERATURE  
 1950



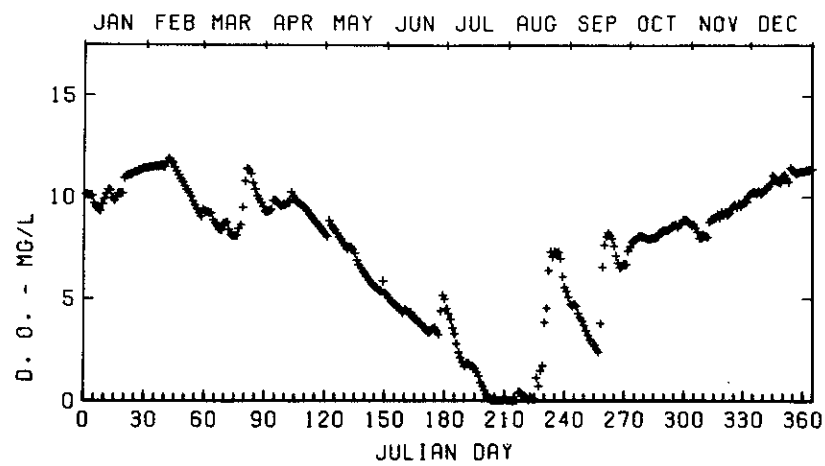
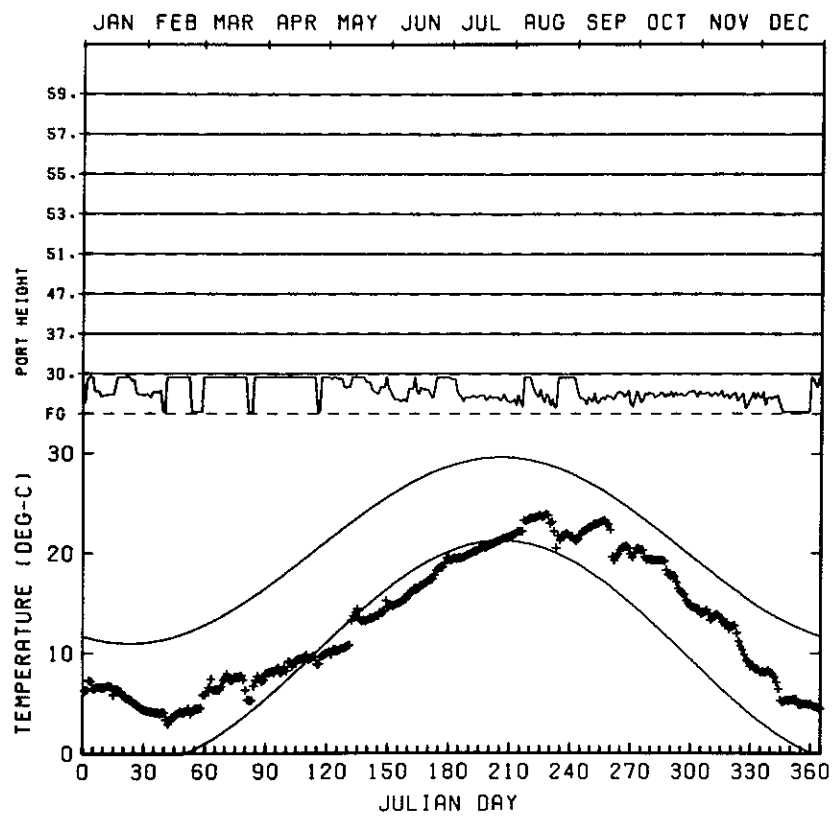
B. EVERETT JORDAN LAKE  
 INITIAL SIMULATIONS  
 MINIMUM RELEASE TEMPERATURE  
 1952



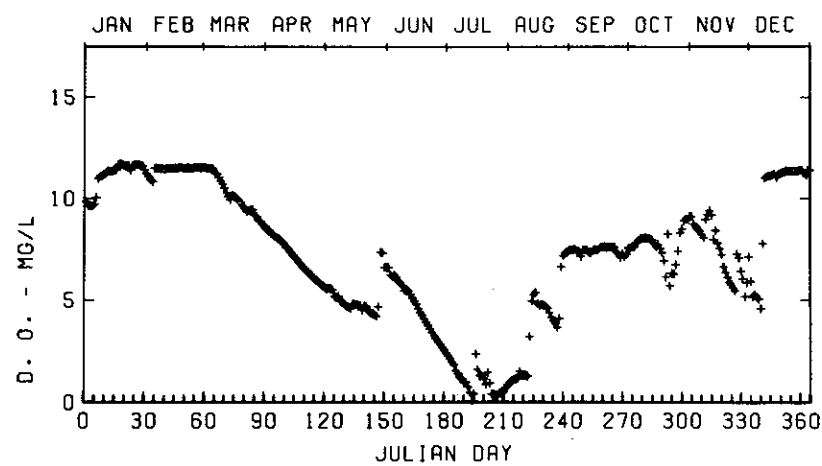
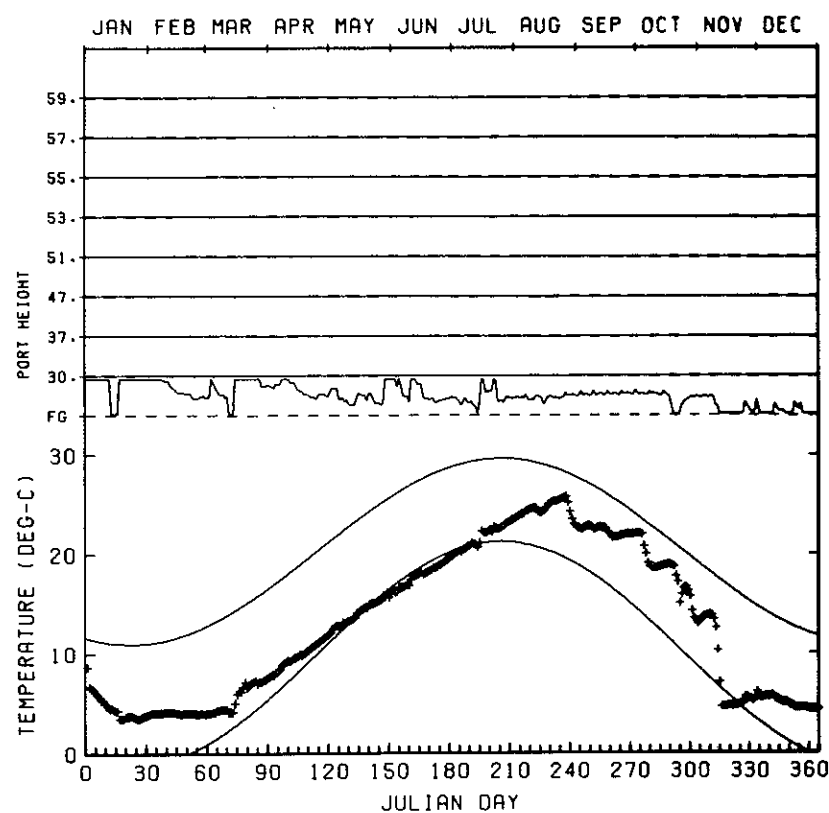
B. EVERETT JORDAN LAKE  
INITIAL SIMULATIONS  
MINIMUM RELEASE TEMPERATURE  
1959



B. EVERETT JORDAN LAKE  
INITIAL SIMULATIONS  
MINIMUM RELEASE TEMPERATURE  
1960



B. EVERETT JORDAN LAKE  
INITIAL SIMULATIONS  
MINIMUM RELEASE TEMPERATURE  
1961



B. EVERETT JORDAN LAKE  
INITIAL SIMULATIONS  
MINIMUM RELEASE TEMPERATURE  
1968

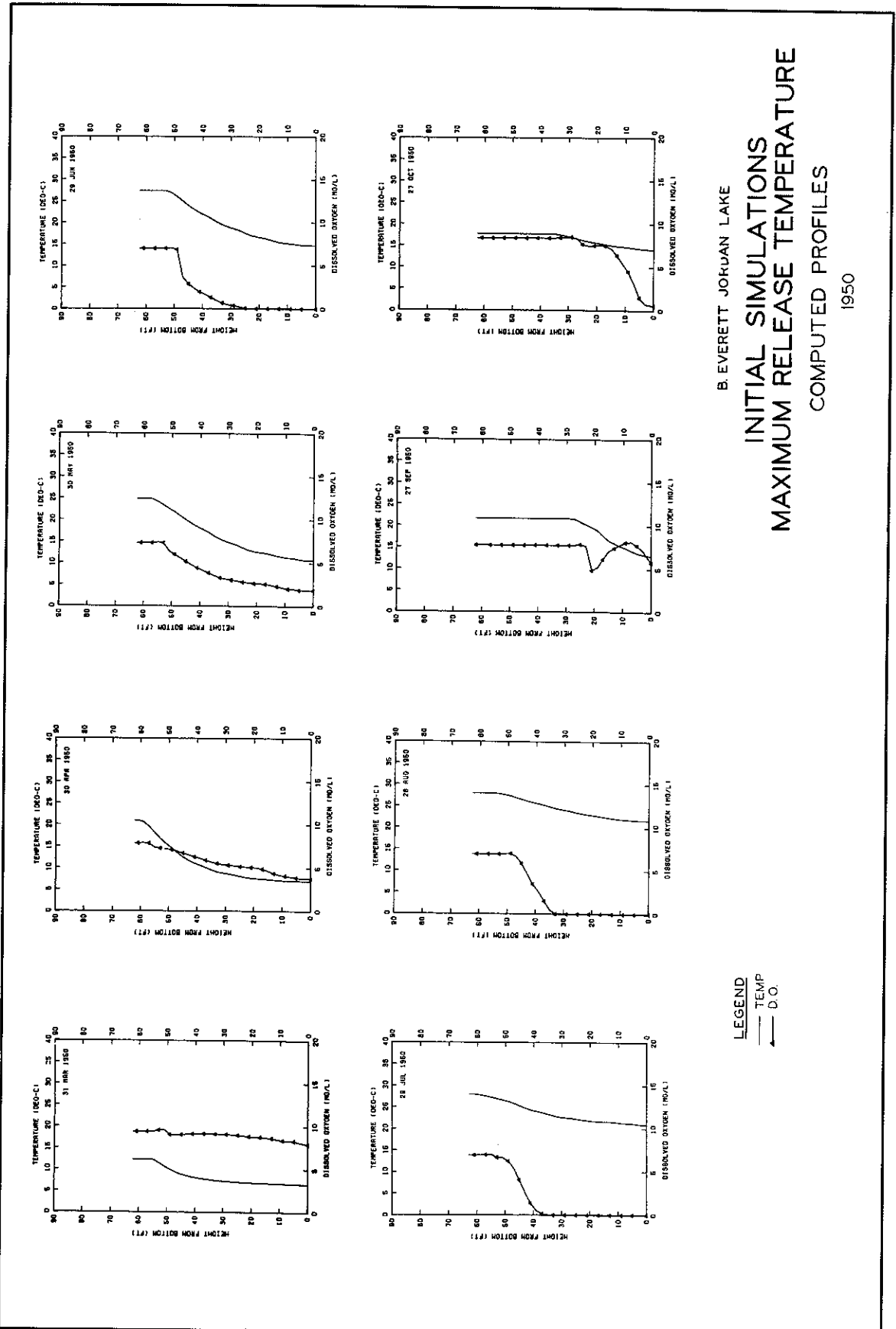
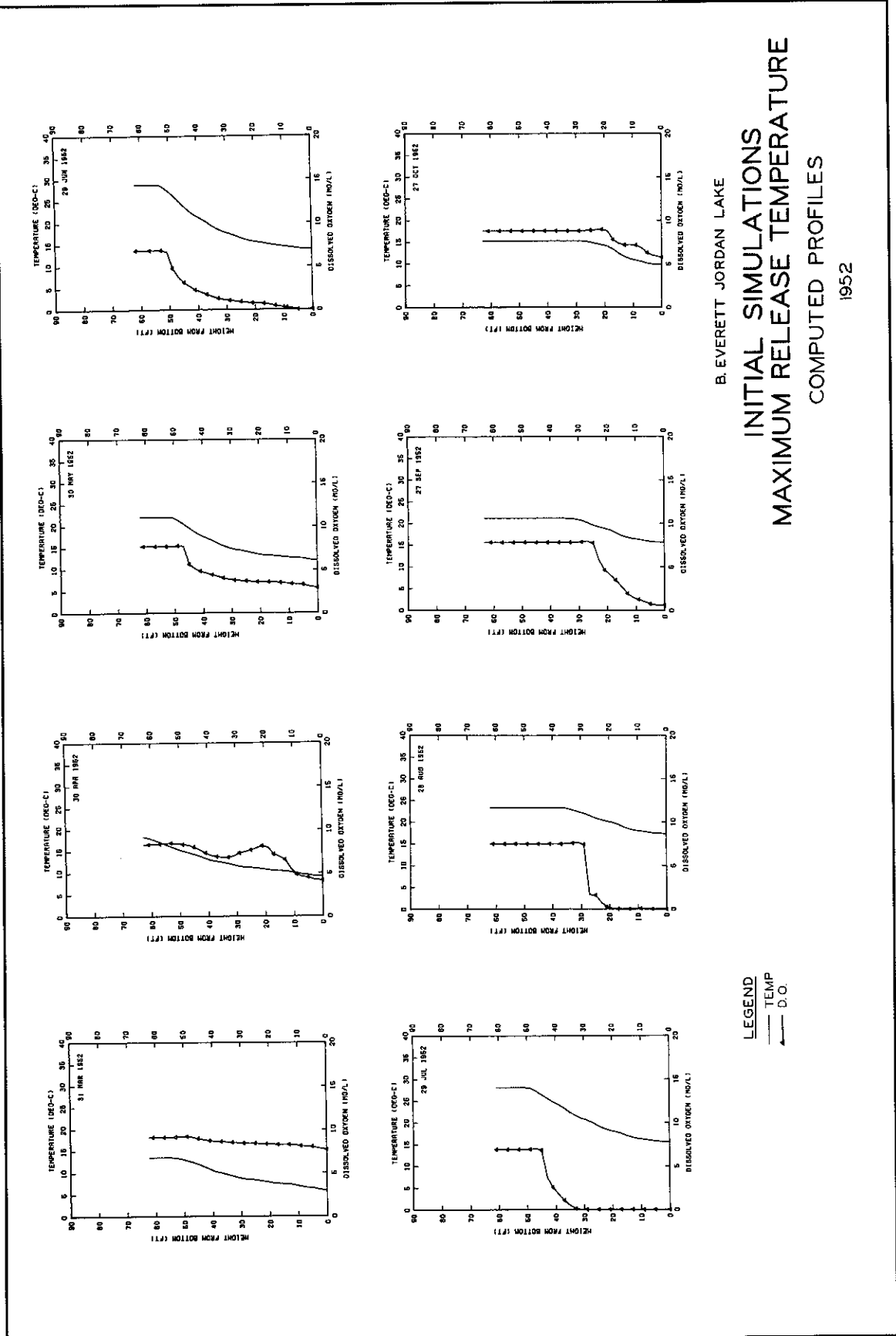
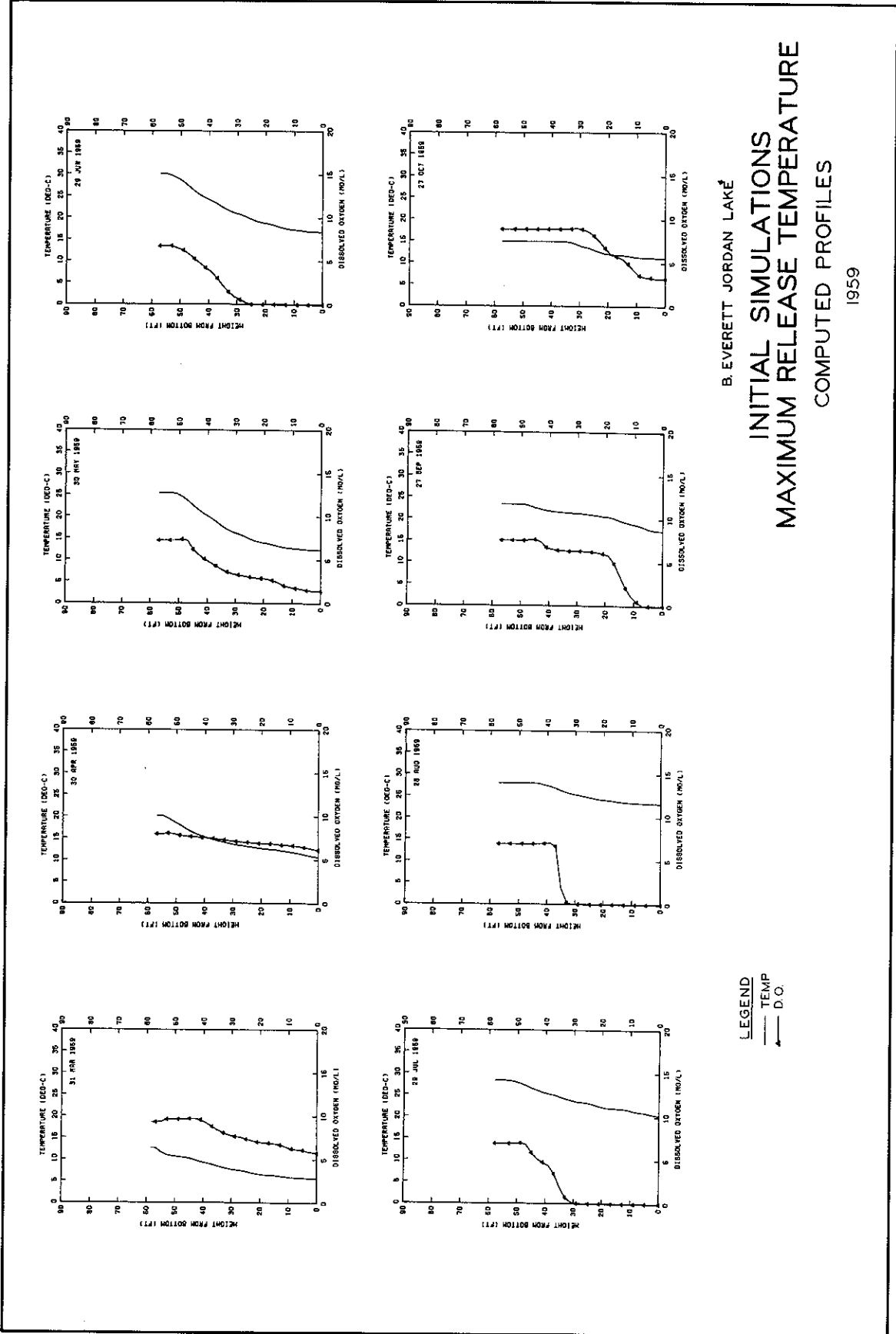


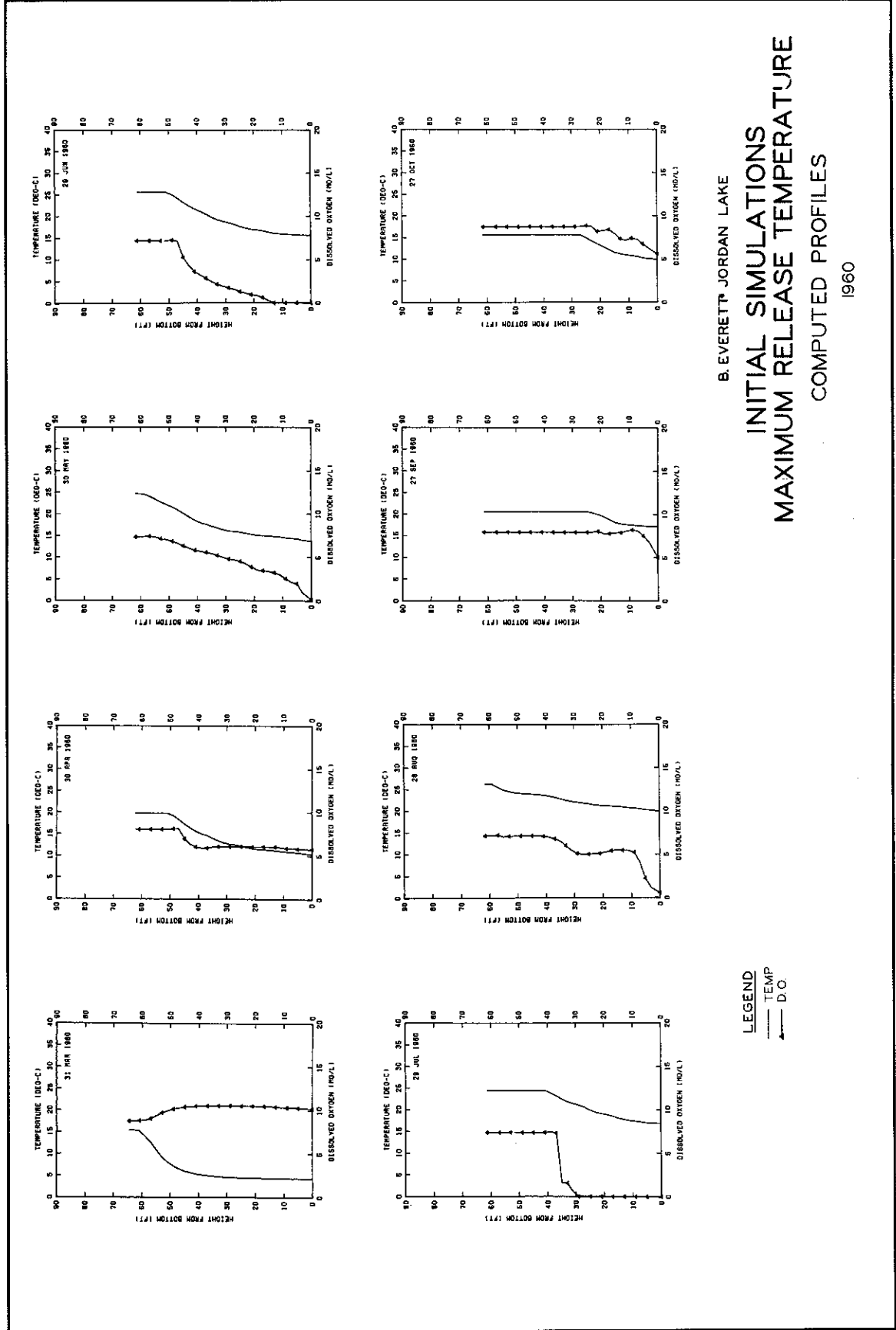
PLATE B5 (SHEET 1 OF 6)

B. EVERETT JORUAN LAKE  
**INITIAL SIMULATIONS**  
**MAXIMUM RELEASE TEMPERATURE**  
**COMPUTED PROFILES**  
 1950



B. EVERETT JORDAN LAKE  
INITIAL SIMULATIONS  
MAXIMUM RELEASE TEMPERATURE  
COMPUTED PROFILES  
1952





B. EVERETT JORDAN LAKE  
INITIAL SIMULATIONS  
MAXIMUM RELEASE TEMPERATURE  
COMPUTED PROFILES  
1960

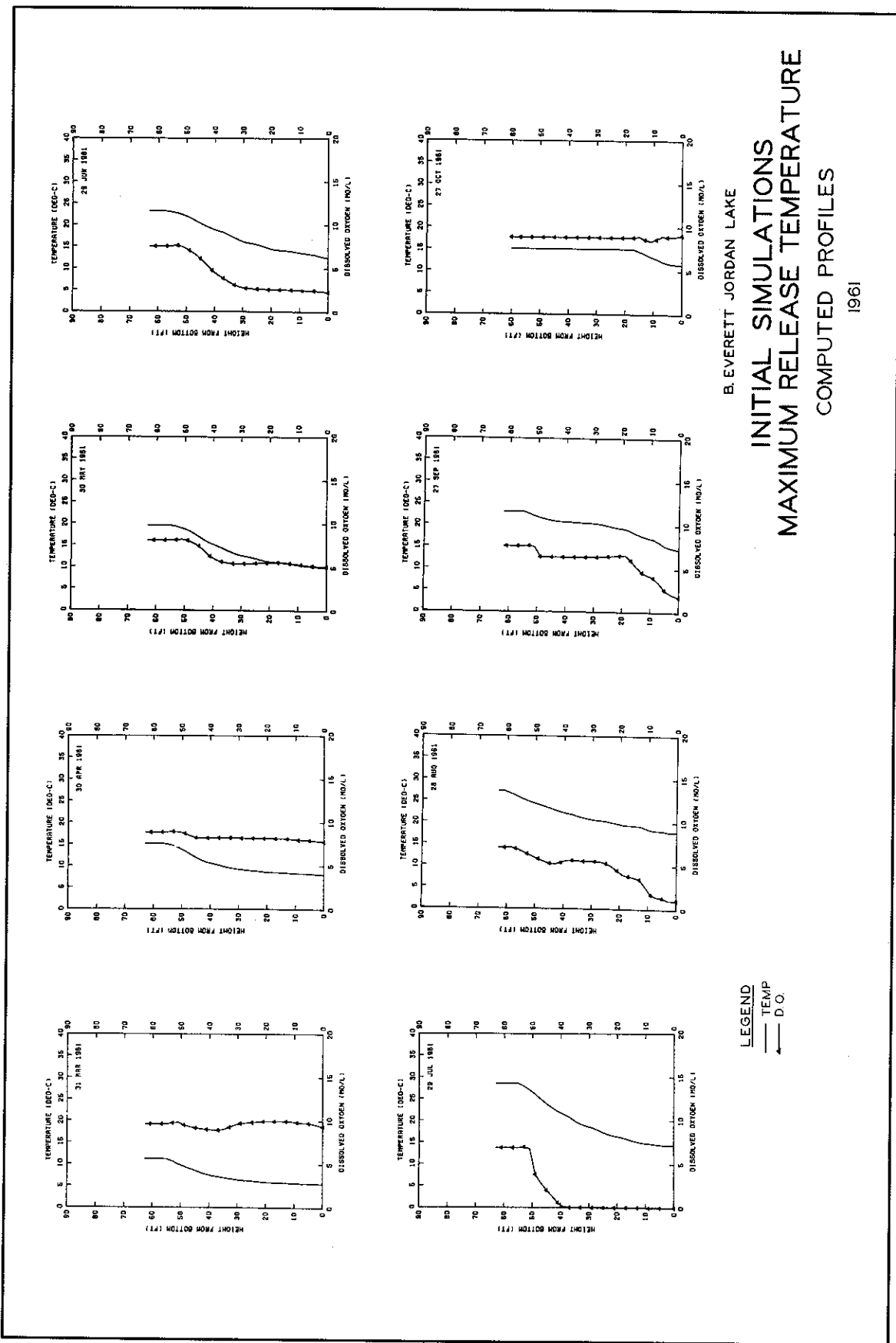
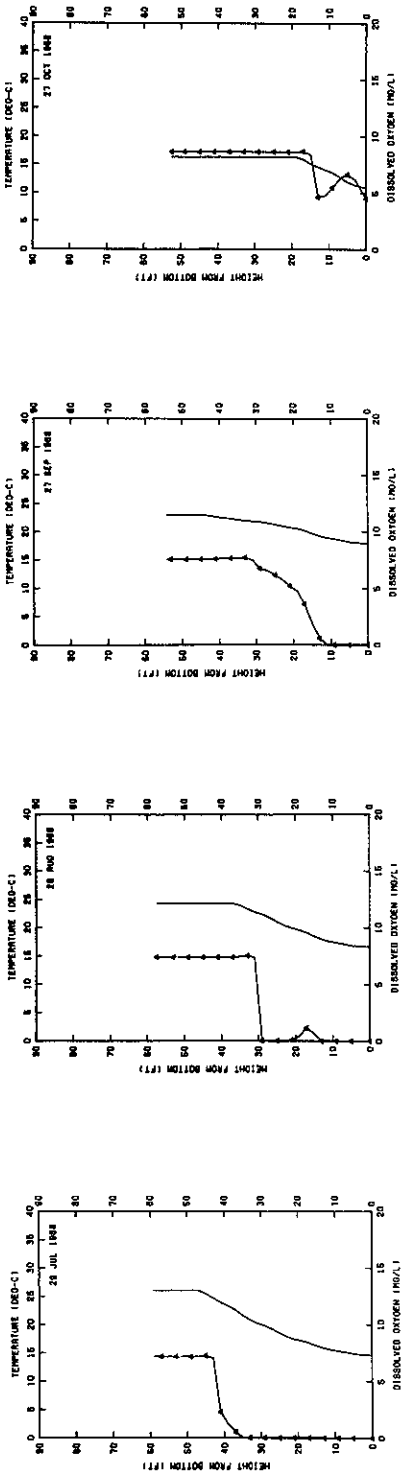
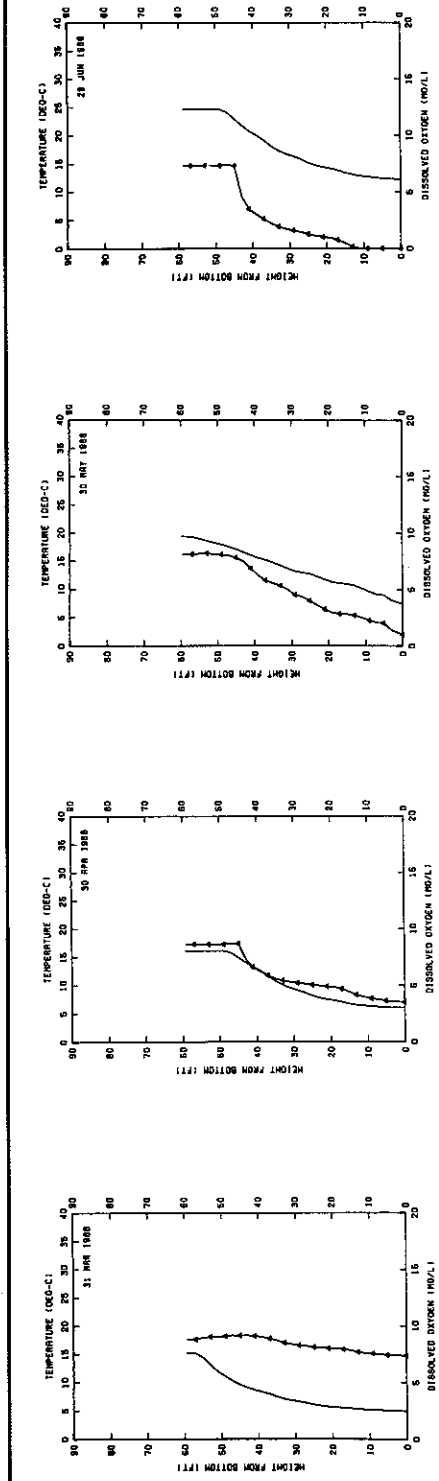


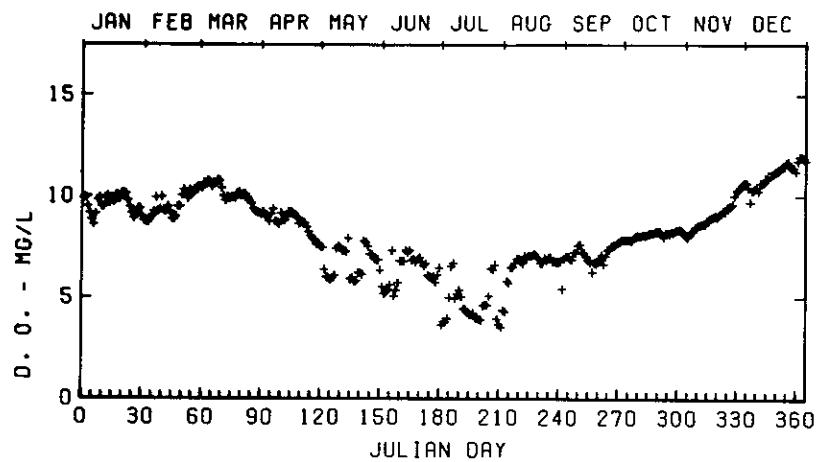
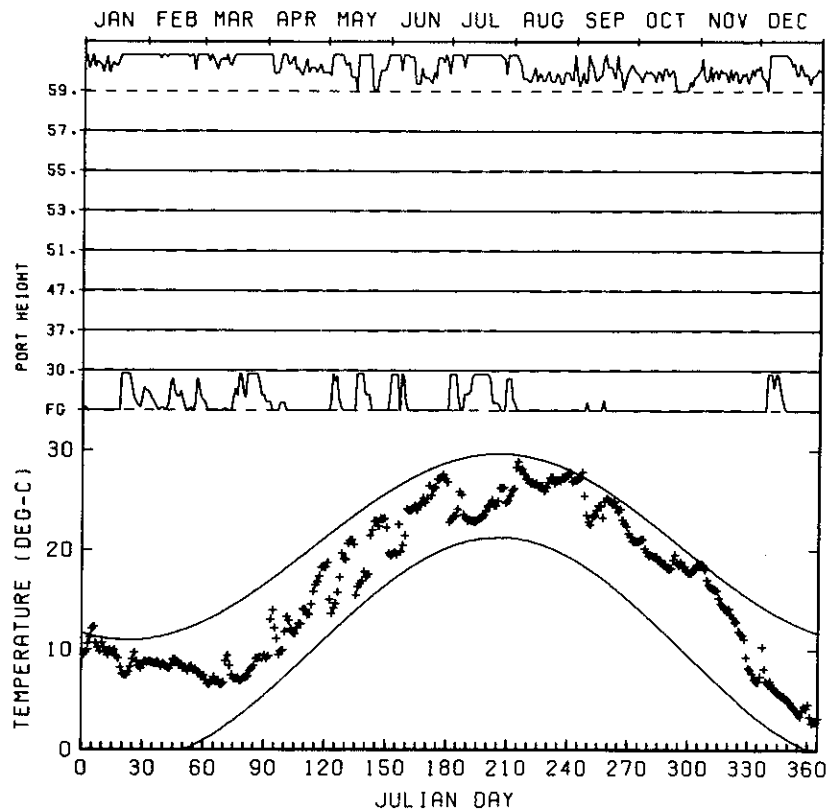
PLATE B5 (SHEET 5 OF 6)

B. EVERETT JORDAN LAKE  
**INITIAL SIMULATIONS  
 MAXIMUM RELEASE TEMPERATURE  
 COMPUTED PROFILES**  
 1961

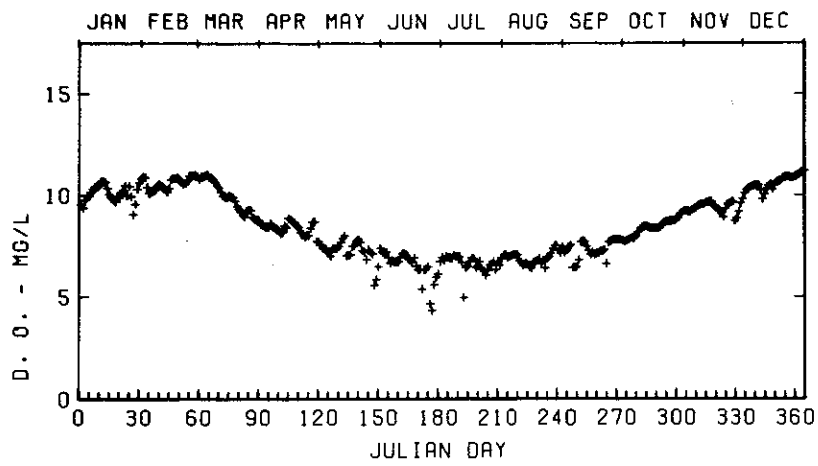
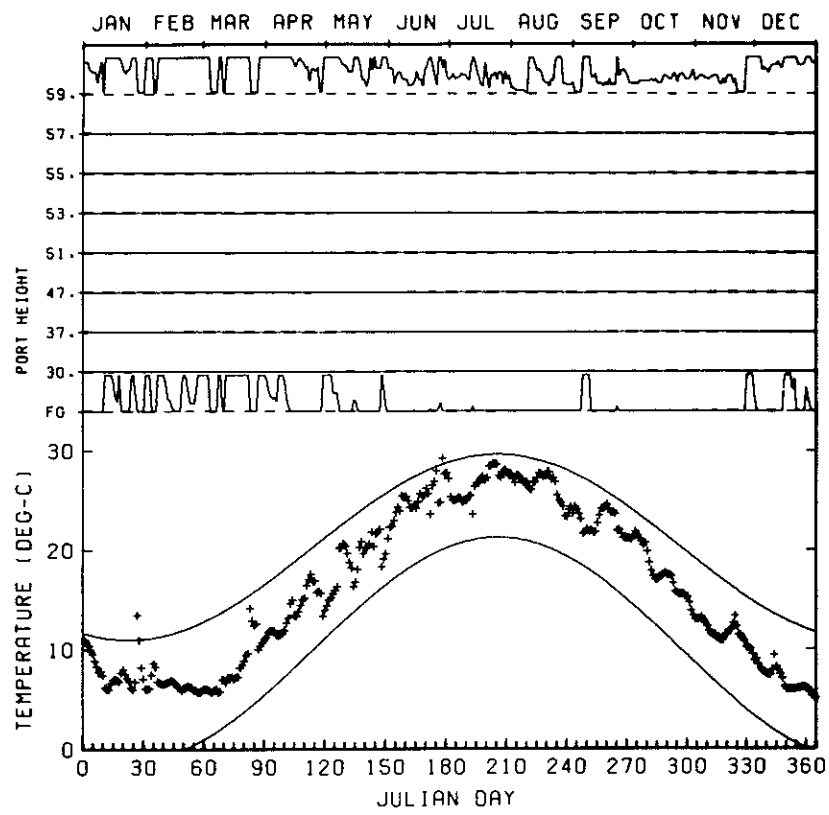


B. EVERETT JORDAN LAKE  
INITIAL SIMULATIONS  
MAXIMUM RELEASE TEMPERATURE  
COMPUTED PROFILES  
1968

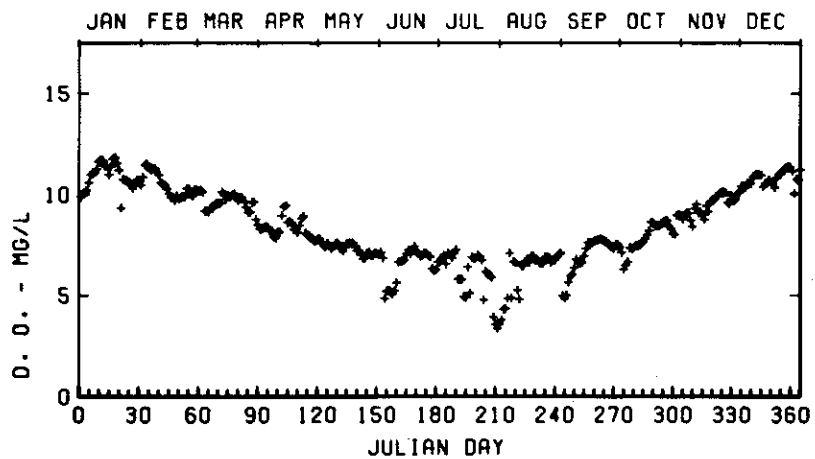
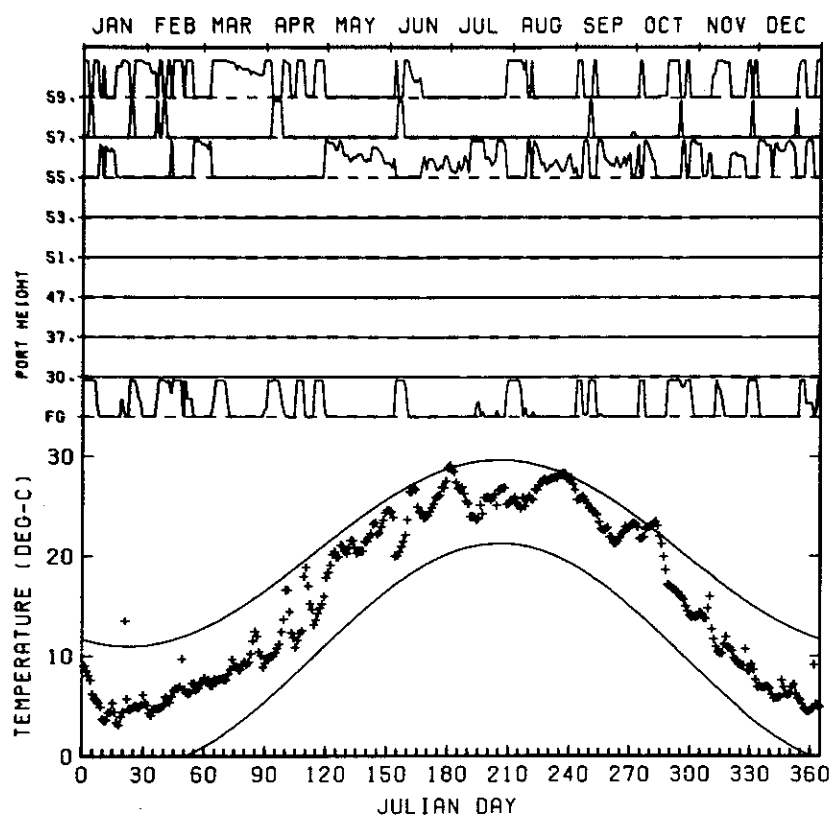
LEGEND  
— TEMP  
← D.O.



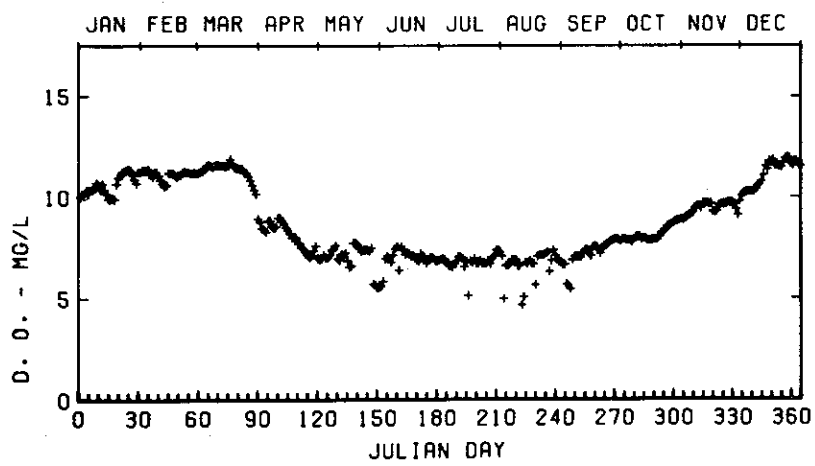
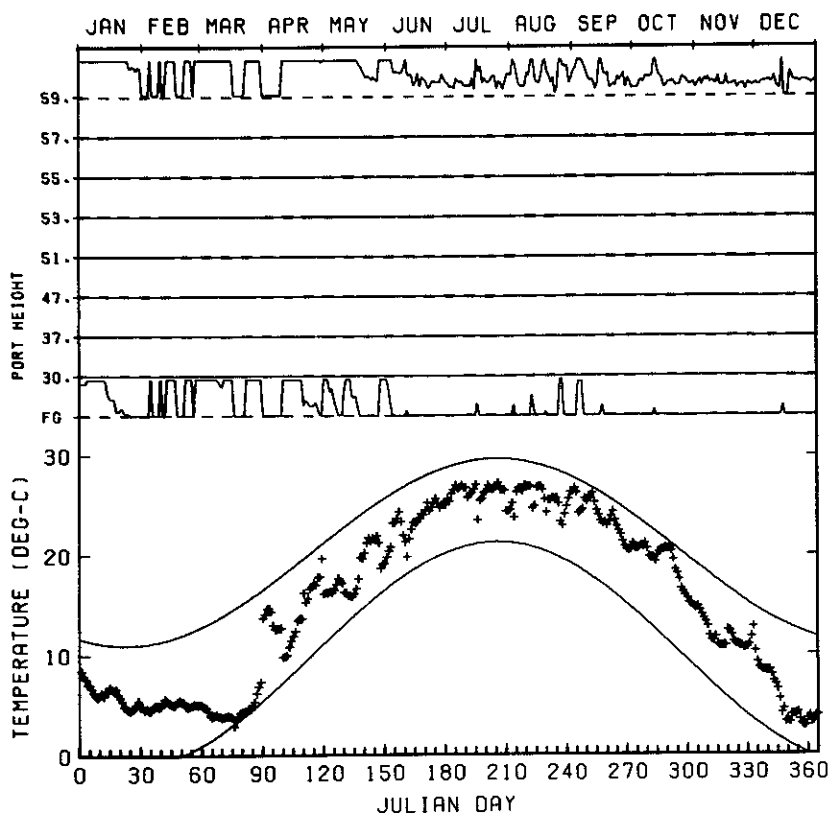
B. EVERETT JORDAN LAKE  
INITIAL SIMULATIONS  
MAXIMUM RELEASE TEMPERATURE  
1950



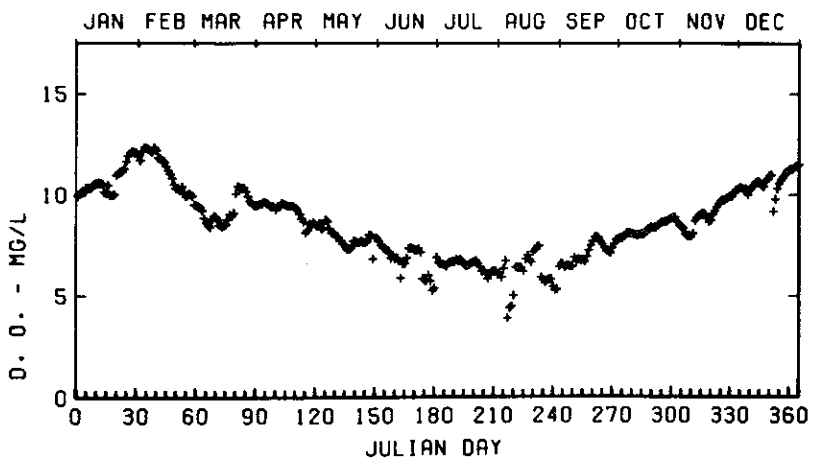
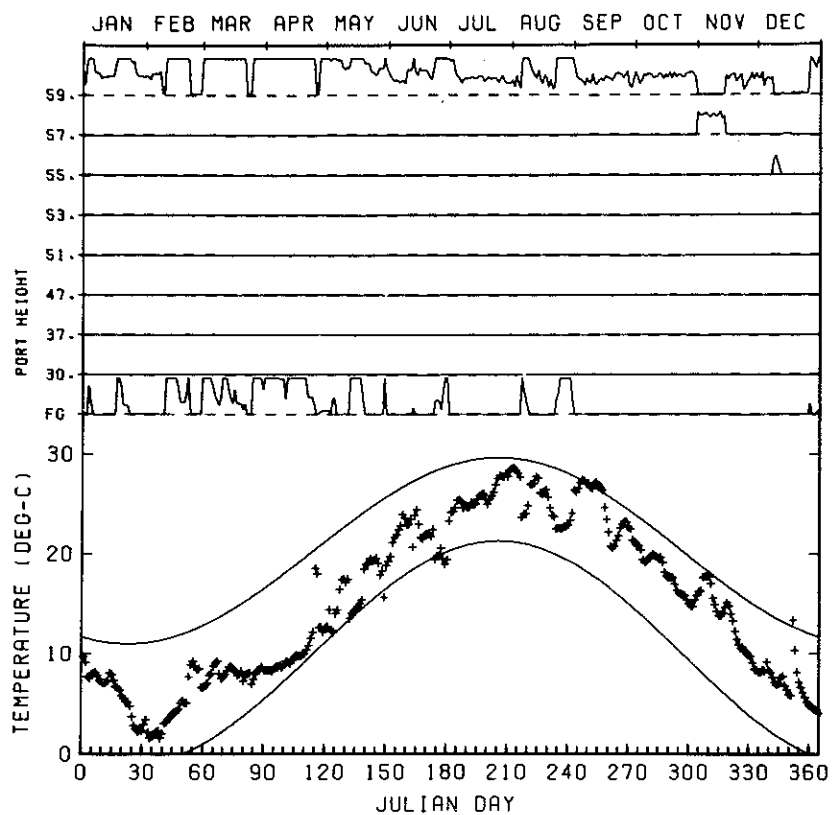
B. EVERETT JORDAN LAKE  
INITIAL SIMULATIONS  
MAXIMUM RELEASE TEMPERATURE  
1952



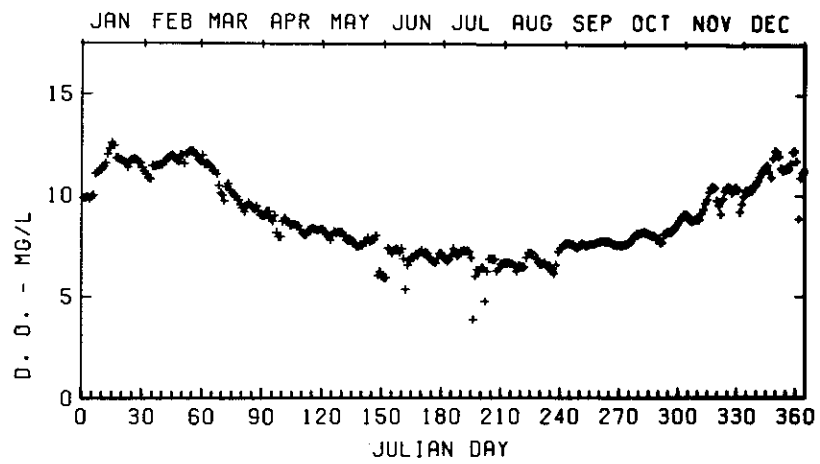
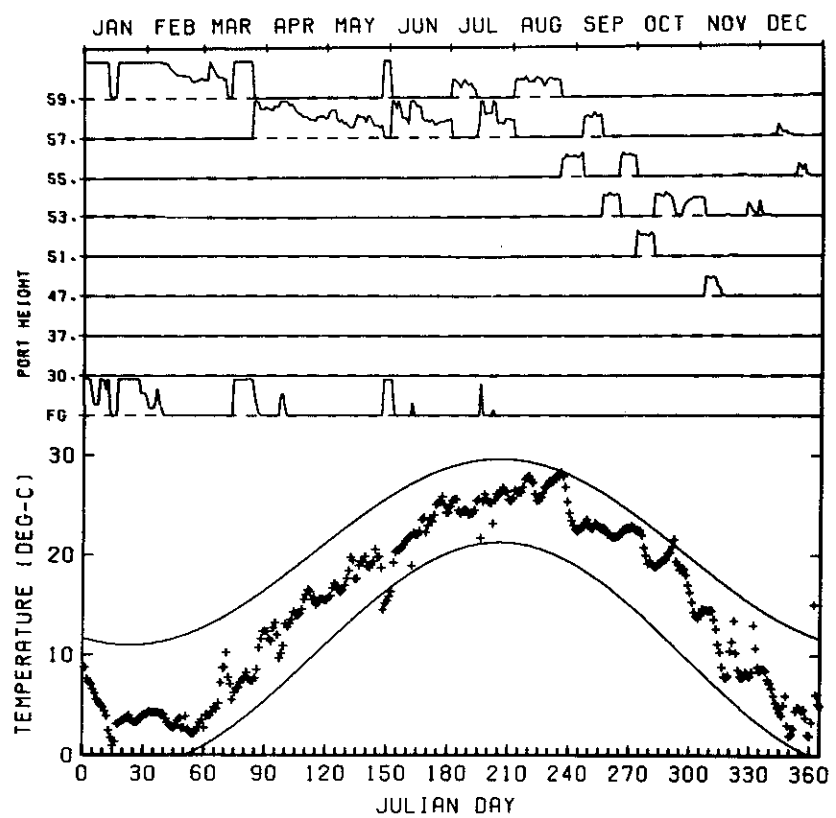
B. EVERETT JORDAN LAKE  
INITIAL SIMULATIONS  
MAXIMUM RELEASE TEMPERATURE  
1959



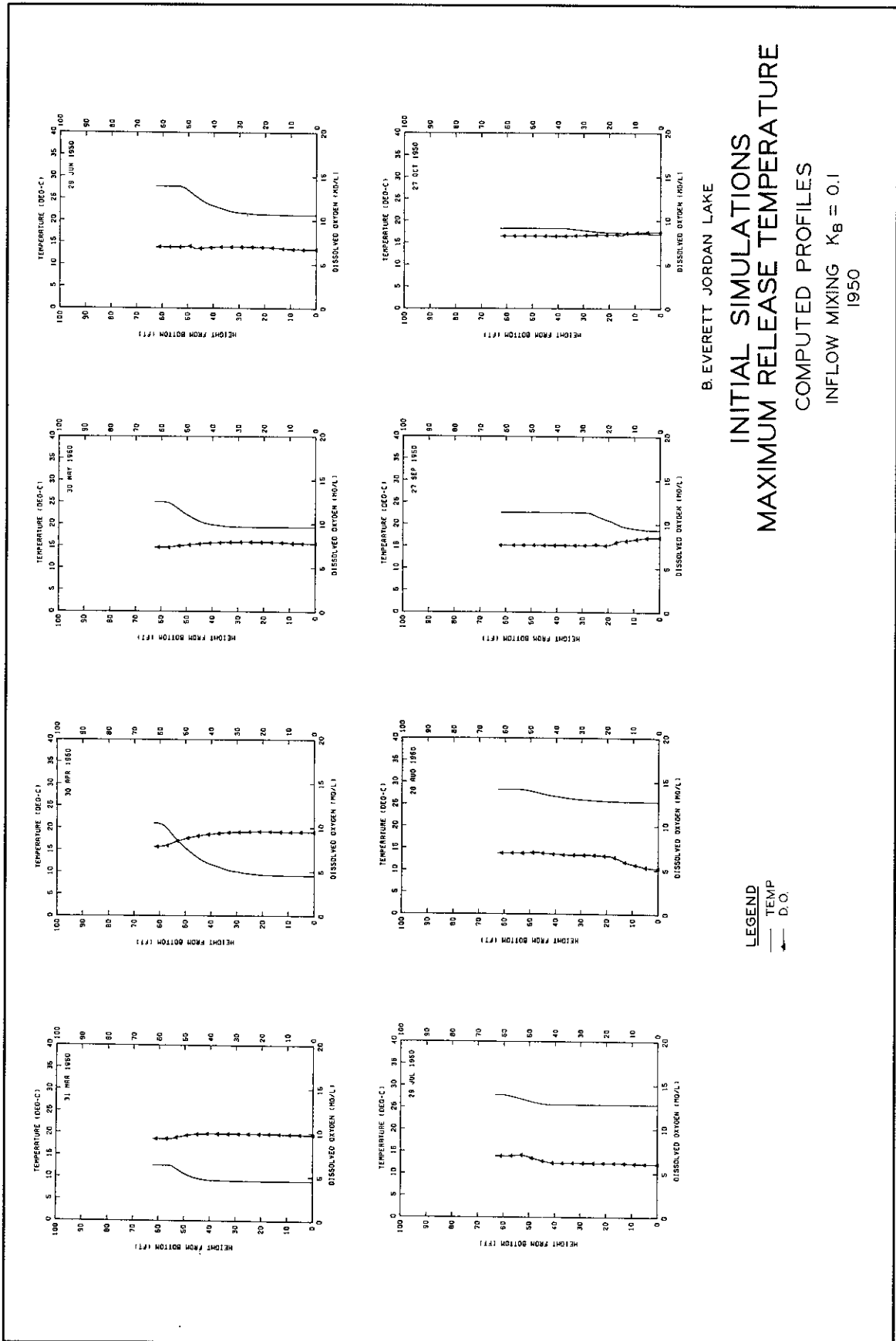
B. EVERETT JORDAN LAKE  
 INITIAL SIMULATIONS  
 MAXIMUM RELEASE TEMPERATURE  
 1960



B. EVERETT JORDAN LAKE  
INITIAL SIMULATIONS  
MAXIMUM RELEASE TEMPERATURE  
1961



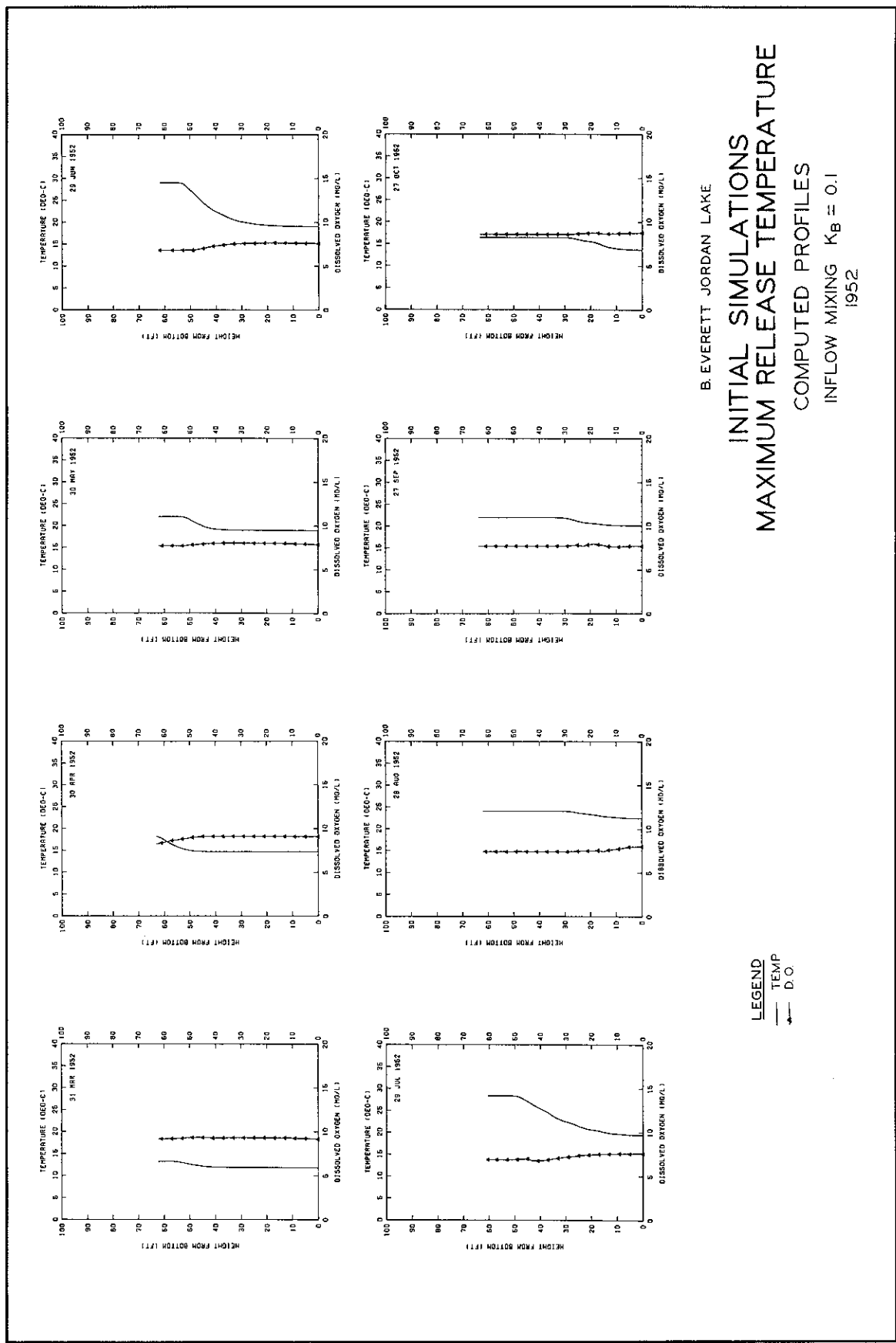
B. EVERETT JORDAN LAKE  
 INITIAL SIMULATIONS  
 MAXIMUM RELEASE TEMPERATURE  
 1968



B. EVERETT JORDAN LAKE  
**INITIAL SIMULATIONS**  
**MAXIMUM RELEASE TEMPERATURE**  
**COMPUTED PROFILES**  
 INFLOW MIXING  $K_B = 0.1$   
 1950

**LEGEND**

— TEMP  
↔ D.O.

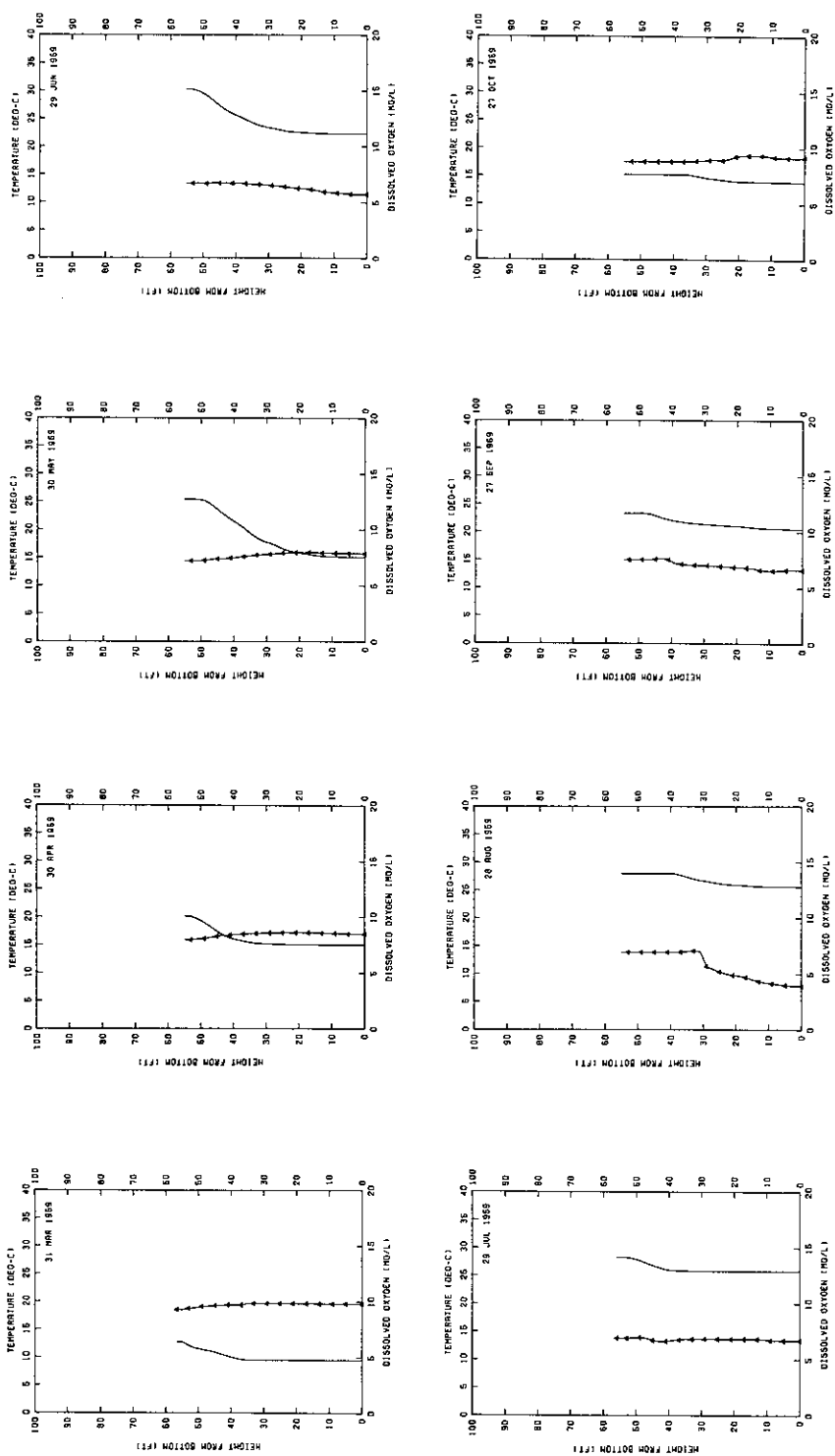


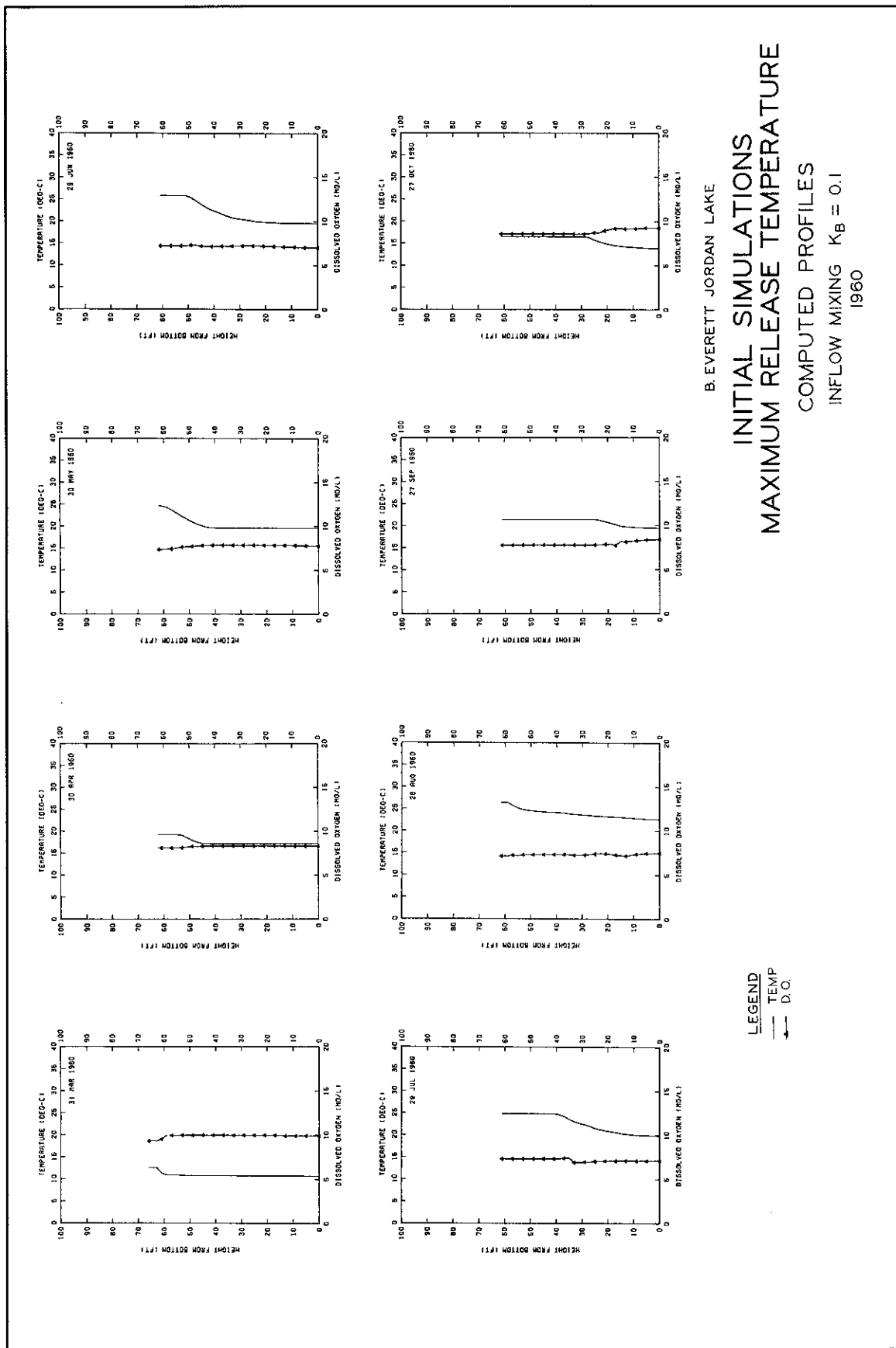
**INITIAL SIMULATIONS  
MAXIMUM RELEASE TEMPERATURE  
COMPUTED PROFILES**

1959

B. EVERETT JORDAN LAKE

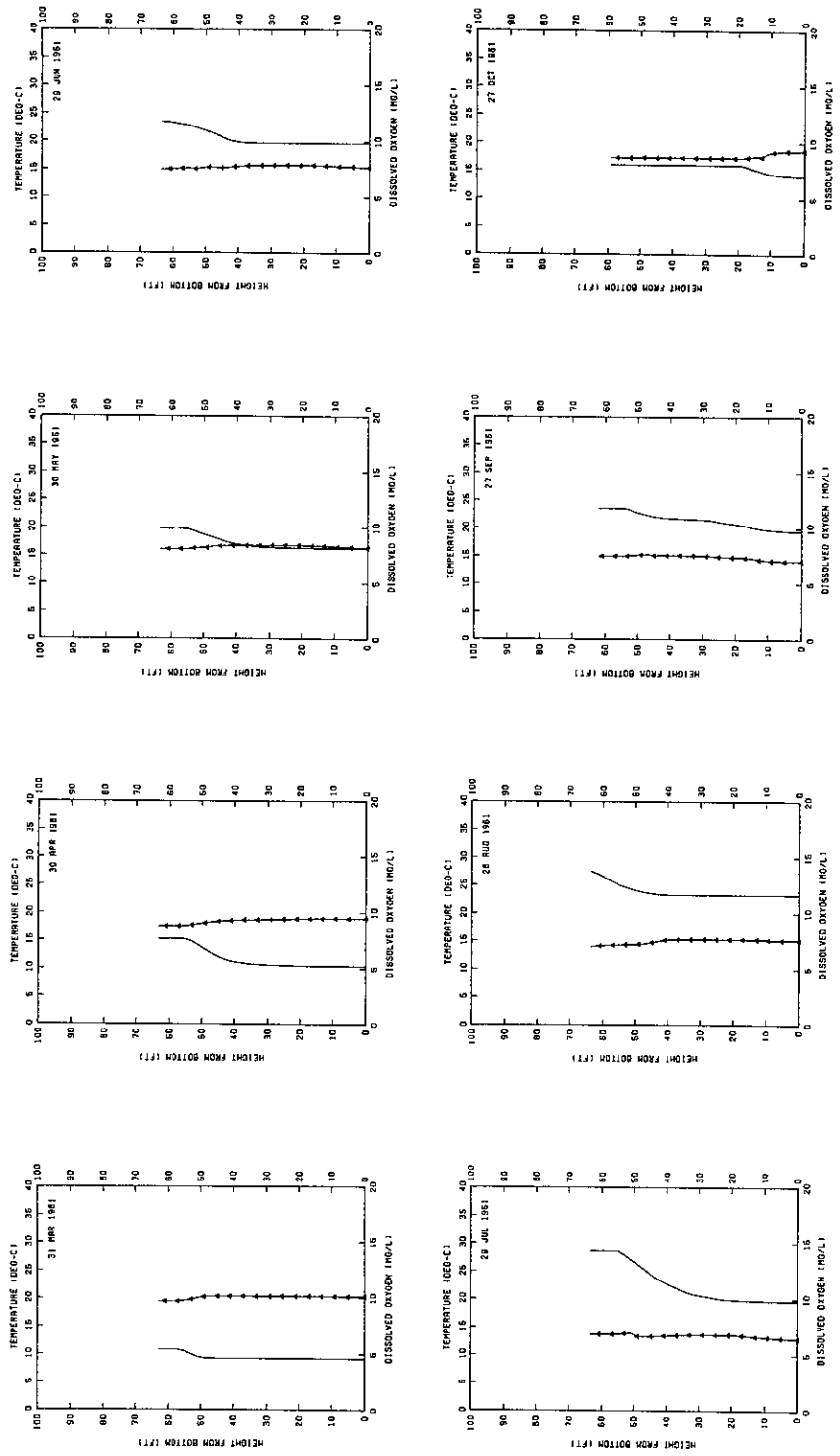
**LEGEND**





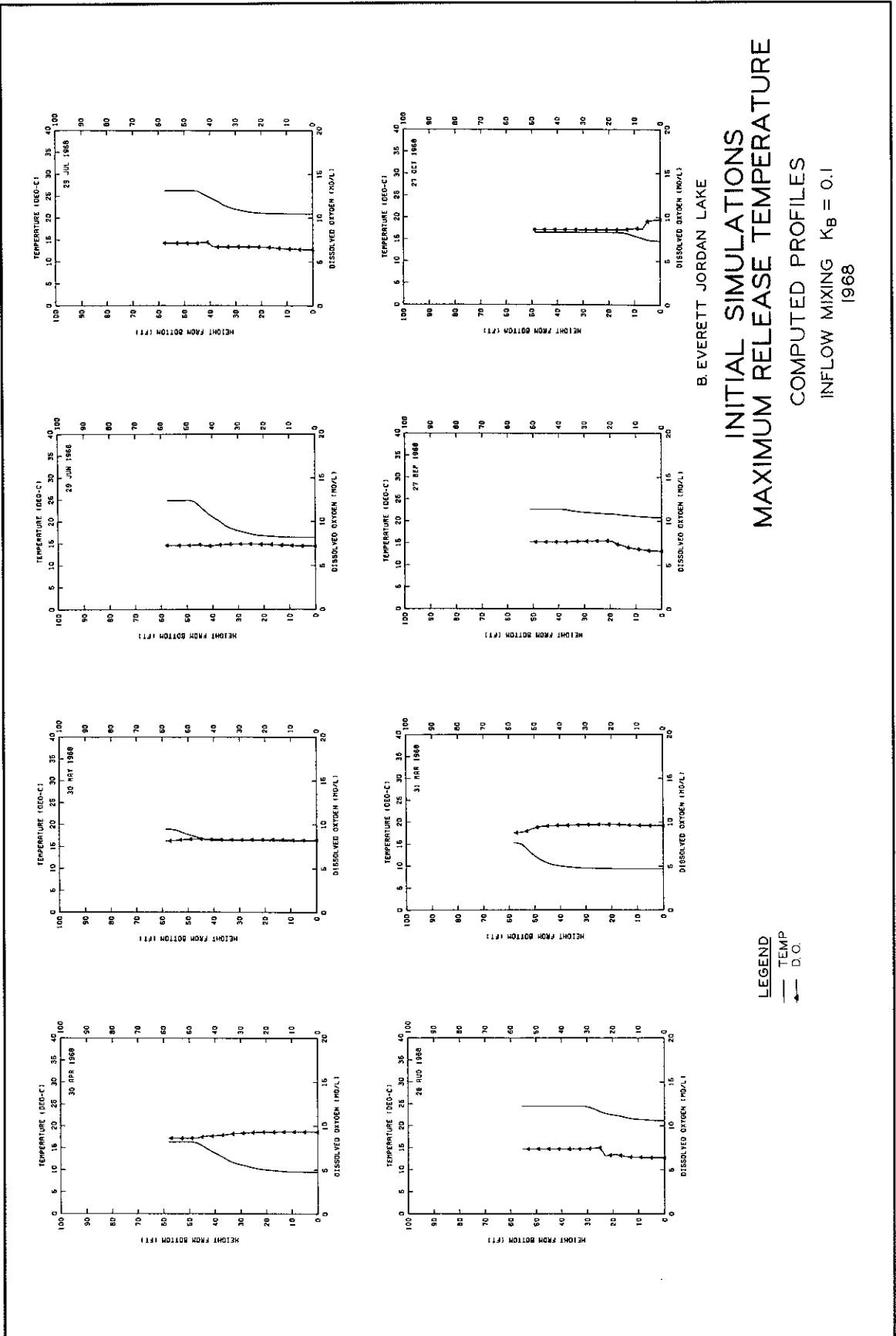
B. EVERETT JORDAN LAKE  
INITIAL SIMULATIONS  
MAXIMUM RELEASE TEMPERATURE  
COMPUTED PROFILES  
INFLOW MIXING  $K_B = 0.1$   
1960

LEGEND  
— TEMP  
↔ D.O.

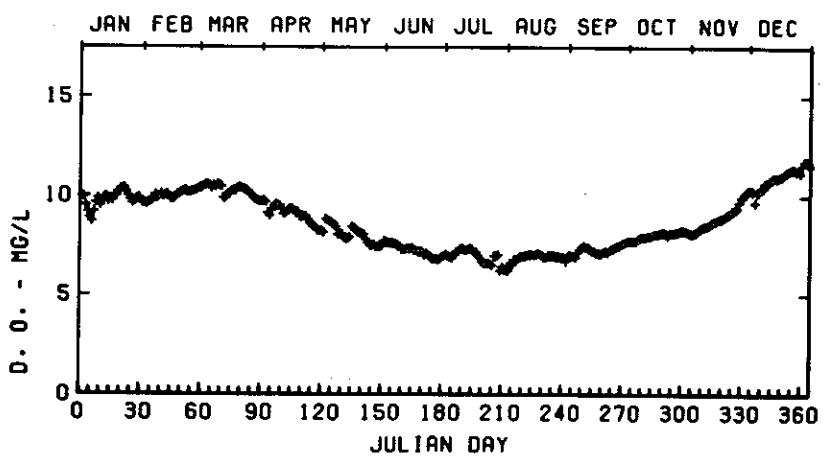
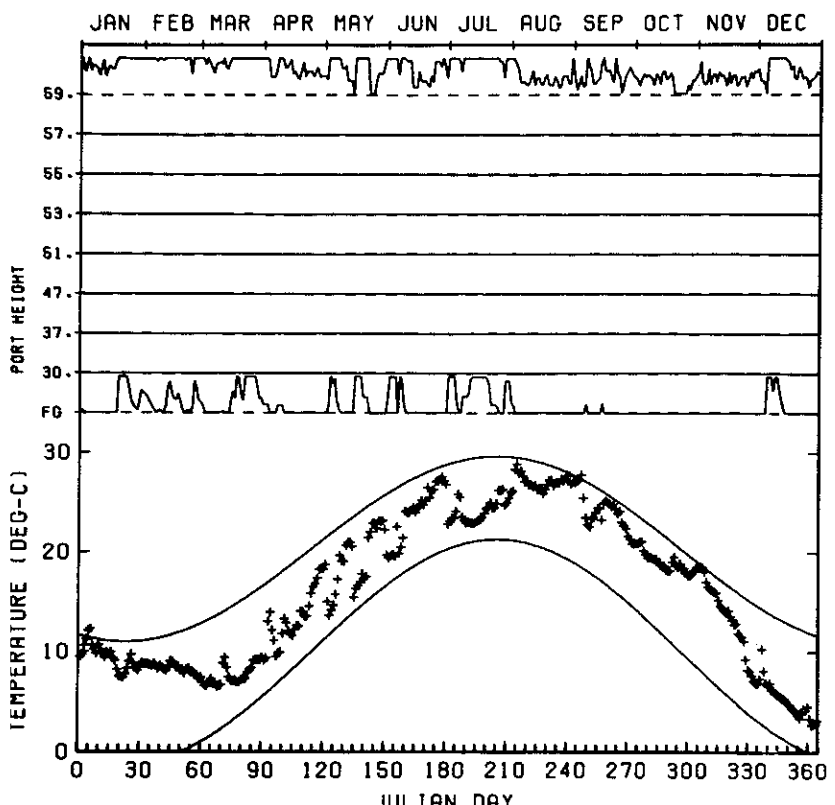


B. EVERETT JORDAN LAKE  
INITIAL SIMULATIONS  
MAXIMUM RELEASE TEMPERATURE  
COMPUTED PROFILES  
INFLOW MIXING  $K_B = 0.1$   
961

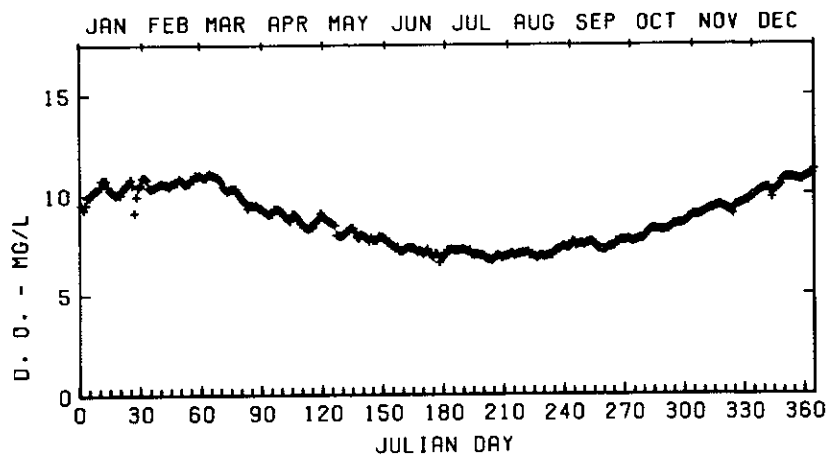
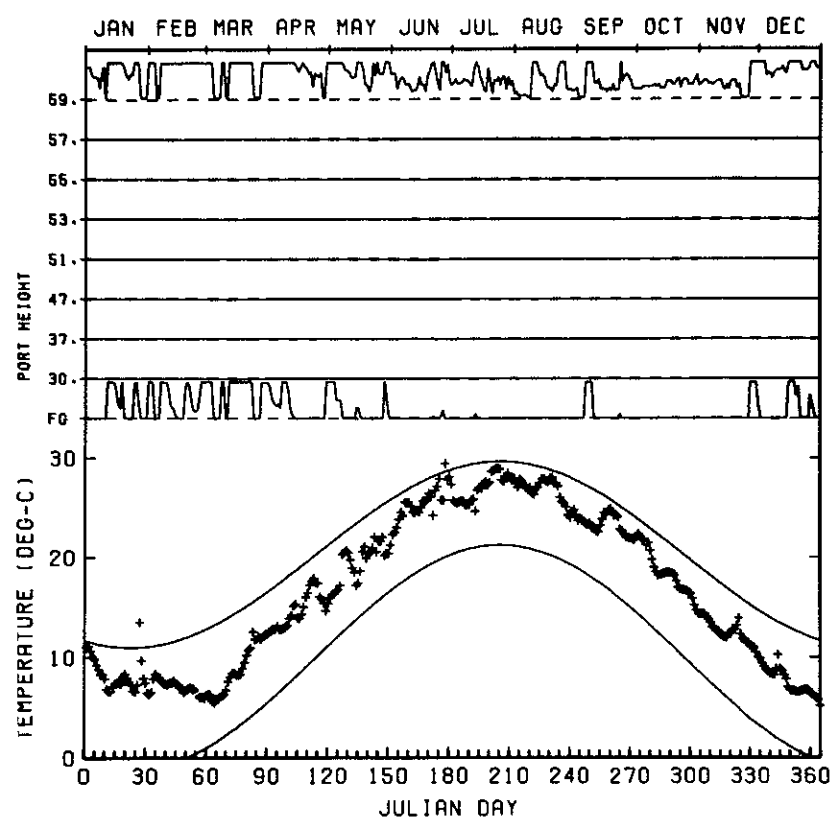
LEGEND  
— TEMP  
— D.O.



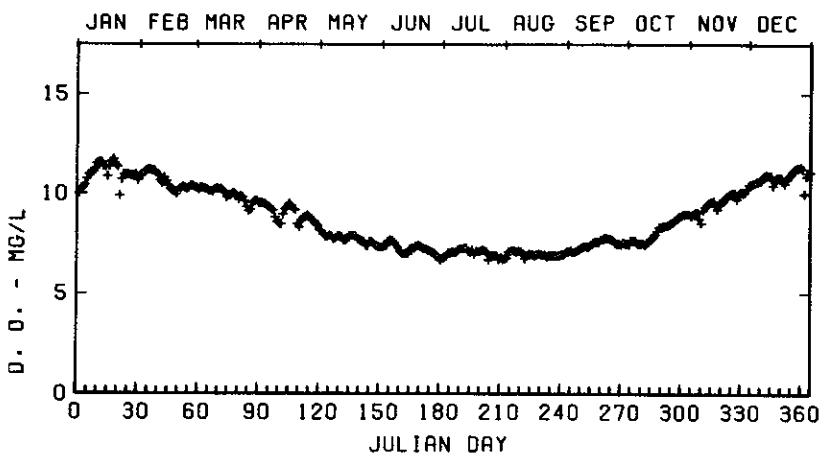
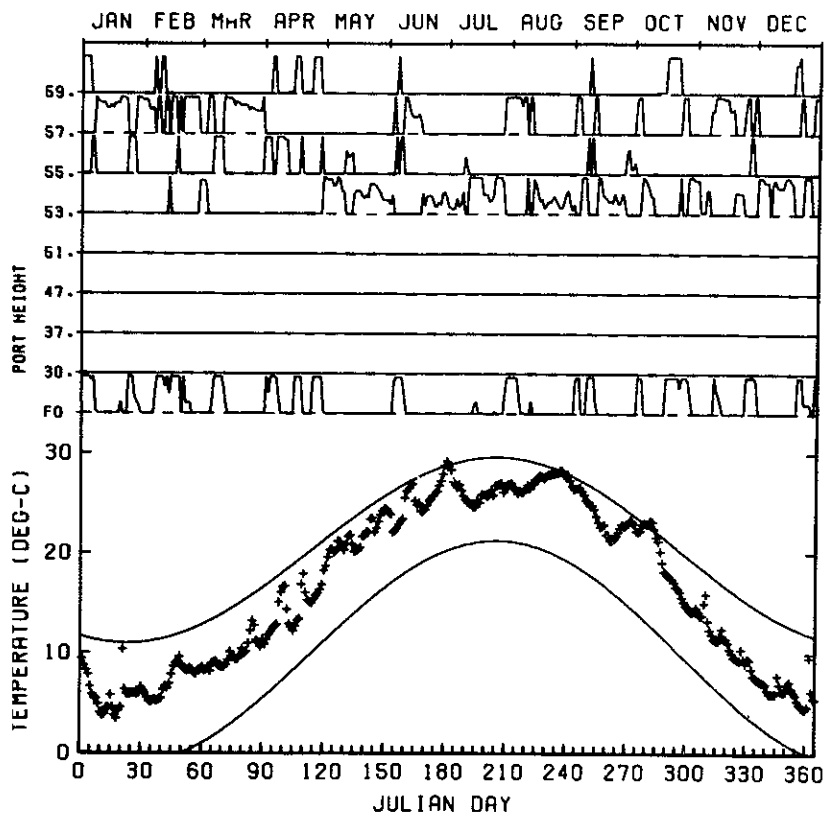
**B. EVERETT JORDAN LAKE**  
**INITIAL SIMULATIONS**  
**MAXIMUM RELEASE TEMPERATURE**  
**COMPUTED PROFILES**  
**INFLOW MIXING  $K_B = 0.1$**   
**1968**



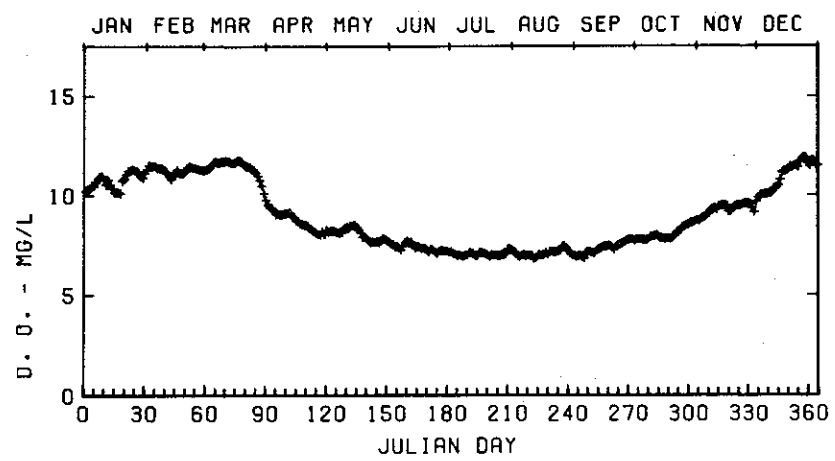
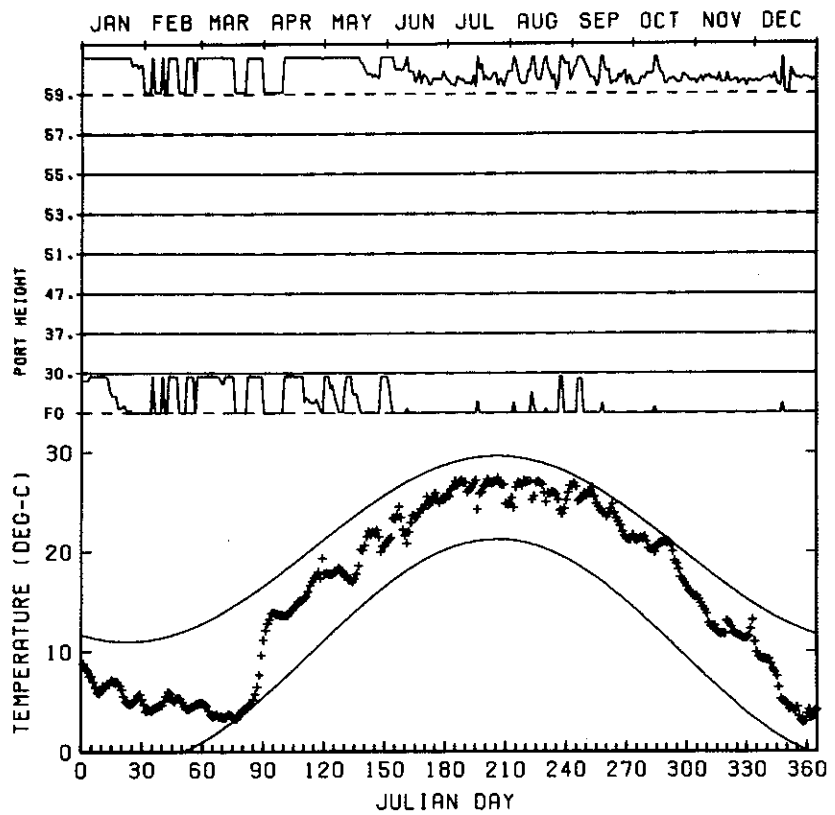
B. EVERETT JORDAN LAKE  
 INITIAL SIMULATIONS  
 MAXIMUM RELEASE TEMPERATURE  
 INFLOW MIXING  $K_B = 0.1$   
 1950



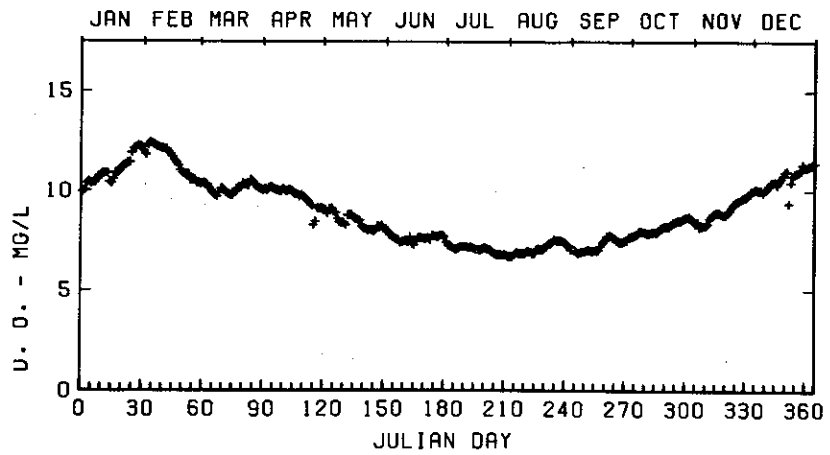
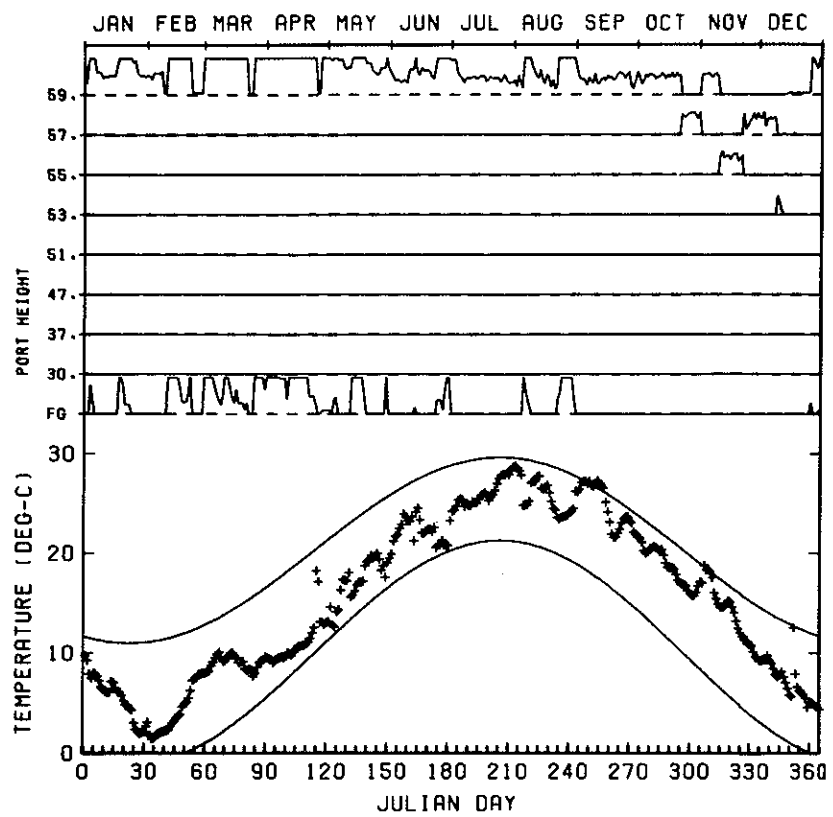
B. EVERETT JORDAN LAKE  
 INITIAL SIMULATIONS  
 MAXIMUM RELEASE TEMPERATURE  
 INFLOW MIXING  $K_B = 0.1$   
 1952



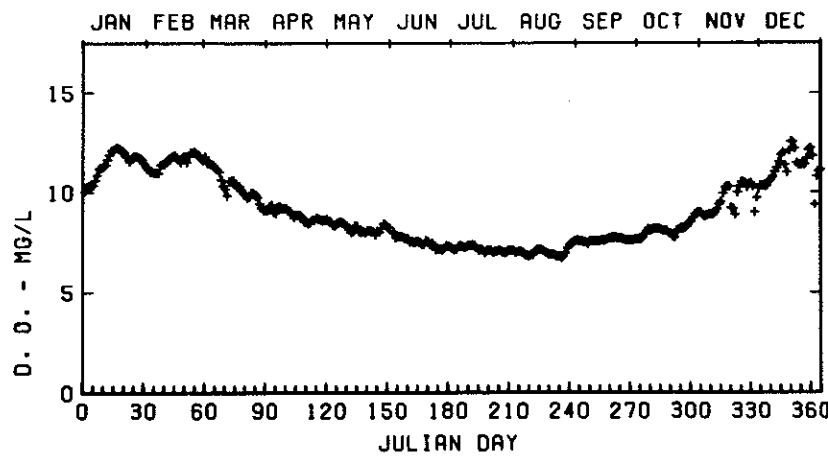
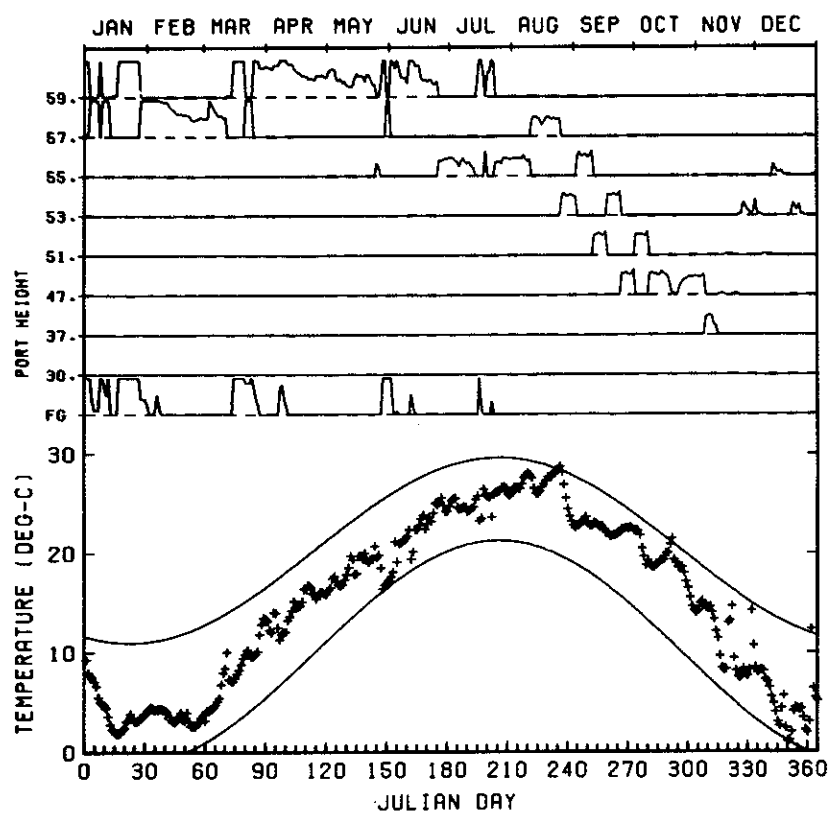
B. EVERETT JORDAN LAKE  
 INITIAL SIMULATIONS  
 MAXIMUM RELEASE TEMPERATURE  
 INFLOW MIXING  $K_B = 0.1$   
 1959



B. EVERETT JORDAN LAKE  
**INITIAL SIMULATIONS**  
**MAXIMUM RELEASE TEMPERATURE**  
 INFLOW MIXING  $K_B = 0.1$   
 1960



B. EVERETT JORDAN LAKE  
 INITIAL SIMULATIONS  
 MAXIMUM RELEASE TEMPERATURE  
 INFLOW MIXING  $K_B = 0.1$   
 1961



B. EVERETT JORDAN LAKE  
 INITIAL SIMULATIONS  
 MAXIMUM RELEASE TEMPERATURE  
 INFLOW MIXING  $K_B = 0.1$   
 1968

## APPENDIX C: NOTATION

$D.O.$ <sub>net</sub>	Net D.O. content due to inflow, mg/l; applied to D.O. profile at dam
$D.O.$ <sub>in</sub>	D.O. content of inflowing stream, mg/l
E	Equilibrium temperature, °F
F	Mean daily streamflow, cfs
H	Net rate of surface heat transfer, Btu/ft <sup>2</sup> /day
$H_i$	Heat absorbed in layer (i), Btu/ft <sup>2</sup> /day
$H_s$	Heat transfer into or out of surface layer, Btu/ft <sup>2</sup> /day
K	Coefficient of surface heat exchange, Btu/ft <sup>2</sup> /day/°F
$K_b$	Decay coefficient, day <sup>-1</sup>
$K_D(T)$	Temperature-dependent deoxygenation coefficient, day <sup>-1</sup>
$K_D(20)$	Deoxygenation coefficient at 20°C, day <sup>-1</sup>
L	Existing B.O.D., mg/l
$L_{in}$	B.O.D. content of the inflowing stream, mg/l
Q	Mean daily streamflow, cfs
S	Total incoming shortwave radiation, Btu/ft <sup>2</sup> /day
t	Julian day
T	Temperature within layer, °C
$z_i$	Depth below surface, ft
$\alpha$	Regression coefficient
$\alpha_1$	Mixing coefficient at surface
$\alpha_2$	Mixing coefficient at bottom
$\beta$	Shortwave radiation absorbed in the surface layer, percent
$\beta_1$	Regression coefficient
$\Delta B$	B.O.D. depletion, mg/l
$\Delta D$	D.O. depletion, mg/l/day
$\theta$	Surface or stream temperature, °F
$\lambda$	Heat absorption coefficient, ft <sup>-1</sup>
$\psi$	Travel time, or time required for the inflow current to reach the outlet structure, days

In accordance with ER 70-2-3, paragraph 6c(1)(b),  
dated 15 February 1973, a facsimile catalog card  
in Library of Congress format is reproduced below.

Loftis, Bruce

B. Everett Jordan Lake water-quality study, by Bruce  
Loftis, Peter E. Saunders, [and] John L. Grace, Jr.  
Vicksburg, U. S. Army Engineer Waterways Experiment  
Station, 1976.

1 v. (various pagings) illus. 27 cm. (U. S. Water-  
ways Experiment Station. Technical report H-76-3)  
Prepared for U. S. Army Engineer District, Wilmington,  
Wilmington, North Carolina.  
Includes bibliography.

1. B. Everett Jordan Lake. 2. Hydraulic models. 3. Math-  
ematical models. 4. Stratified flow. 5. Water quality.  
I. Saunders, Peter E., joint author. II. Grace, John Linson,  
joint author. III. U. S. Army Engineer District,  
Wilmington. (Series: U. S. Waterways Experiment Station,  
Vicksburg, Miss. Technical report H-76-3)  
TA7.W34 no.H-76-3